Electron transfer in deep eutectic solvents : from kinetics to the hydrogen-bonding and ion pairing effects

Fangchen Zhen

UNIVERSITÉ DE RENNES 1

THESE DE DOCTORAT DE

L'UNIVERSITE DE RENNES 1

ECOLE DOCTORALE N° 596
Matière, Molécules, Matériaux
Spécialité : Chimie-Physique, Chimie Théorique

Par
Fangchen ZHEN

Transfert d'Électrons dans les Eutectiques Profonds. De la Cinétique aux Effets de Liaisons Hydrogène et de Paires d'Ions.

Electron Transfer in Deep Eutectic Solvents: from Kinetics to the Hydrogen-bonding and Ion Pairing Effects.

Thèse présentée et soutenue à Rennes, le 18 juillet 2022
Unité de recherche : Institut des Sciences Chimiques de Rennes (ISCR), UMR 6226
Thèse N° :

Rapporteurs avant soutenance :

Jalal GHILANE	Directeur de Recherche CNRS, ITODYS, Université Paris-Cité
Grégoire HERZOG	Chargé de Recherche CNRS, LCPME, Université de Lorraine

Composition du Jury :

Examinateurs :	Mireille TURMINE	Maitre de Conférences, Sorbonne Université
	Florence GENESTE	Directrice de Recherche CNRS, ISCR, Université de Rennes 1
Dir. de thèse :	Philippe HAPIOT	Directeur de Recherche CNRS, ISCR, Université de Rennes 1

Ph.D. Thesis Title

Electron Transfer in Deep Eutectic Solvents: from Kinetics to the Hydrogen-bonding and Ion Pairing Effects

By Fangchen Zhen （甄方臣）

Supervisor: Philippe Hapiot

Rennes, France

July 2022

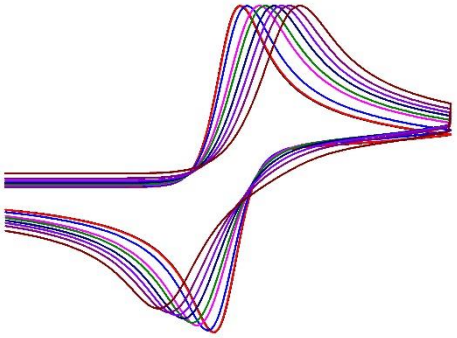

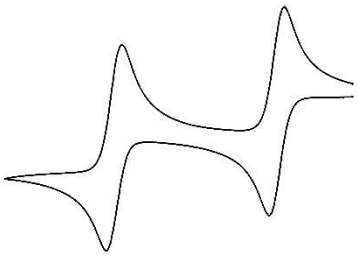

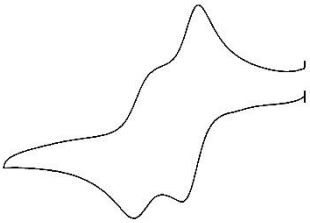

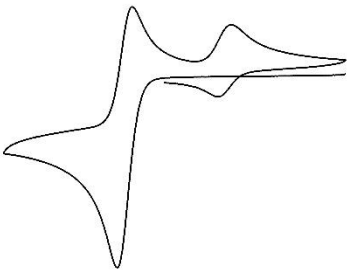

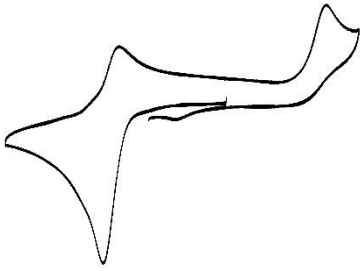

Contents

Chapter 1 Introduction

1.1 Deep eutectic solvents

The term of deep eutectic solvents (DESs) has been proposed in 2002 by Abbot and co-workers who initially wanted to improve the properties of ionic liquids.[1, 2] The past two decades have seen the incredible development of DESs and their applications. Several reviews have been published in this field.[3-5] As all the studies will be conducted in DESs, making a general review and understanding of DES is significantly necessary.

1.1.1 Definition, classification, preparation

Definition Deep eutectic solvents (DESs) are a mixture of two or more components, usually a molecular hydrogen bond donor (HBD) and a hydrogen bond acceptor (HBA), which form a eutectic liquid with a significantly depressed melting point.[6] DESs contain large, nonsymmetrical ions that have low lattice energy and hence low melting points. They are usually obtained by the complexation of a quaternary ammonium salt with a metal salt or hydrogen bond donor (HBD). The charge delocalization occurring through hydrogen bonding between for example, a halide ion and the hydrogen-donor moiety is responsible for the decrease in the melting point of the mixture relative to the melting points of the individual components.

Two recent publications[7, 8] have provided some more profound insights into the definition of DESs, based on investigations of the phase diagrams of DESs, which correlated the phase behavior and the deepness of the eutectic point to the definition of DESs. Kollau et al.[8] used regular solution theory to predict the phase diagrams and showed that some combinations of two solid components could be predicted with ideal phase behavior, while some have a clear deep eutectic. It is stated that a eutectic mixture

could only be considered as a DES when the melting point of the mixture is significantly lower than the one of the ideal predictions. Martins et al.[7] states that it becomes necessary to find a stricter definition of what a DES is.

Several points are still the subject of debates concerning the definition of a DES. A first aspect of high importance is the fact that DESs are mixtures of two or more components and not pure salt consisting of ions. Thus, treating DES as a new class of ionic liquid analogues makes no sense due to the large differences with these media. DESs are usually noted as hydrogen bond complexes but, the presence of a hydrogen bond between two components of a mixture is not a sufficient condition to define a DES. For example, an ideal mixture of hydrogen bonding compounds, such as fatty acids with alcohols, must not be defined as a DES. Moreover, one could wonder if a combination of a solid and a liquid component, like Ethaline, is actually a DES[9]; it might be a solvolysis instead. Some authors also emphase that a fixed stoichiometric proportion should not define a DES but a wider composition range which below operating temperature. Finally, the biggest debate is about the eutectic composition of a DES, the deepness of the eutectic point and how to define it. In their paper, Martins et al.[7] provide a more general and acceptable definition: "*A deep eutectic solvent is a mixture of two or more pure compounds for which the eutectic point temperature is below that of an ideal liquid mixture, presenting significant negative deviations from ideality (ΔT2>0). Additionally, the temperature depression should be such that the mixture is liquid at operating the temperature for a certain composition range. Otherwise, a simpler term 'eutectic solvent' could be used to describe mixtures that do not fulfill these criteria*."

This general definition of DES provides a solid start and a critical perspective to further discuss DESs and offers a reasonable and correct conduct to the future study of DESs and their applications.

Classification, different types of DES. As described [4], deep eutectic solvents can be defined by the following general formula:

$$Cat^{+}\,[X^{-}\,zY]$$

Where Cat^{+} is any ammonium, phosphonium, or sulfonium cation, and X is a Lewis base, generally a halide anion. The complex anionic species in square brackets are formed between X- and either a Lewis or Brønsted acid Y, z refers to the number of Y molecules that interact with the anion. Classical cations are quaternary ammoniums and imidazolium with a particular emphasis on choline chloride (ChCl) for practical applications.

DESs are classified depending on the nature of the complexing agent used, as shown in Table 1.1.

Table 1.1 General formula for the Classification of deep eutectic solvents

Type	General formula	terms
Type I	$Cat^{+}\,[X^{-}\,zMCl_x]$	M = Zn, Sn, Fe, Al, Ga, In
Type II	$Cat^{+}\,[X^{-}\,zMCl_x{\bullet}yH_2O]$	M = Cr, Co, Cu, Ni, Fe
Type III	$Cat^{+}\,[X^{-}\,zRZ]$	Z = $CONH_2$, COOH, OH
Type IV	$MCl_x + RZ = MCl_{x-1}^{+}{\bullet}\,RZ + MCl_{x+1}^{-}$	M = Al, Zn and Z = $CONH_2$, OH
Type V	RZ+R'Z	Z = COOH, OH

- Type I DESs are formed from MClx and quaternary ammonium salts. Examples of type I DESs include the common one chloroaluminate-imidazolium salt melts and less studied ionic liquids formed with imidazolium salts and various metal halides.[10]

- Type II DESs are similar to type I and formed between hydrated metal halides MClx and quaternary ammonium salts with particular emphasis on choline chloride. The range of non-hydrated metal halides which formed type I DESs is limited. However, the scope of DESs can be widen by replacing non-hydrated metal halides with hydrated one. Furthermore, hydrated metal halides which with inherent air or moisture insensitivity makes their use in large scale industrial processes possible.

- Type III DESs are formed from mixture of choline chloride and different hydrogen bond donors. They are the most studied because their ability to solvate a wide range of transition metal species which included chlorides[2] and oxides.[2, 11] A large range of hydrogen bond donors have been studied to date, such as alcohols, amides, and

carboxylic acids (Figure 1.1). These DESs are easy to prepare by mixing and heating two components, and relatively not sensitive to water. Many are biodegradable and are relatively low cost.

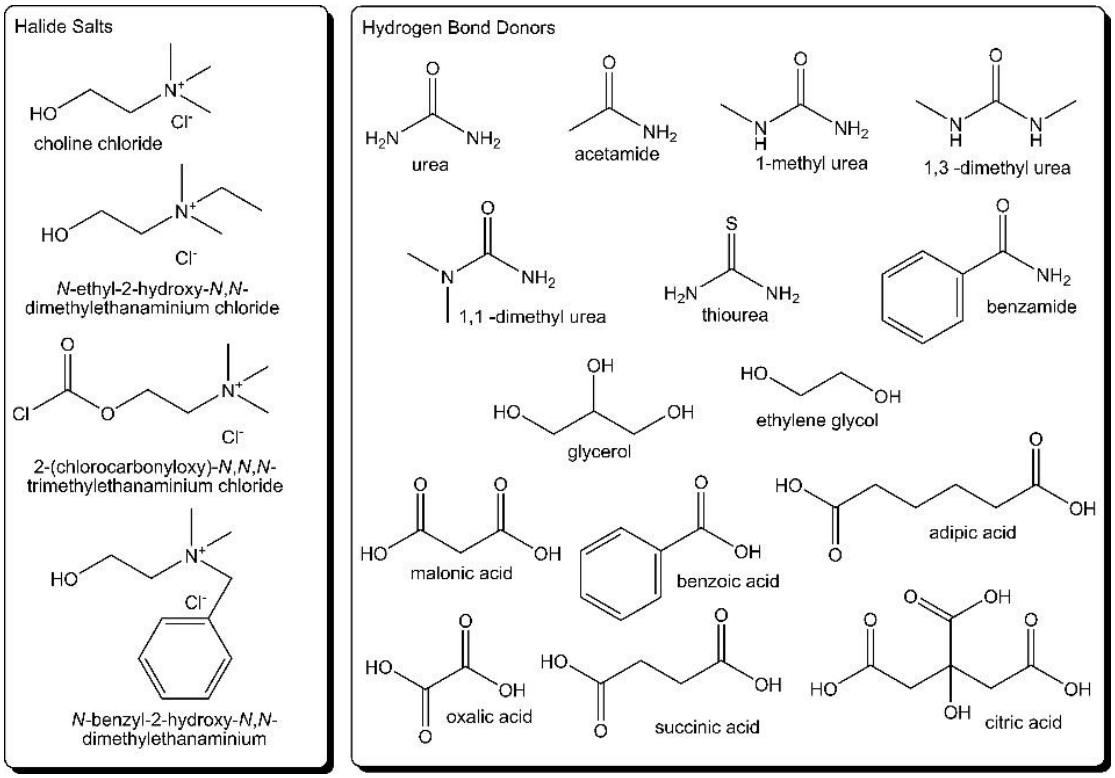

Figure 1.1. Structures of some halide salts and hydrogen bond donors used in the formation of deep eutectic solvents.[4]

Thanks to the wide available range of hydrogen bond donors, this class of DESs is particularly adaptable. DESs considered in this thesis are all from that type. They are based on the quaternary ammonium salt: choline chloride. It is classified as a provitamin in Europe and is produced on the megaton scale as animal feed supplement. It is produced by a one-step gas phase reaction between HCl, ethylene oxide, and trimethylamine that leads to negligible ancillary waste. The physical properties, such as density, viscosity, and conductivity, of type III DESs could easily be tailored for specific applications by simply adjusting the hydrogen bond donor. The electrochemical windows have been examined on different material electrodes and are sufficiently wide to allow the electrochemical measurement of redox reactions in DESs. This class of DESs has been shown to be particularly versatile, with a wide range of possible applications.

- Type IV DESs are formed from mixtures of inorganic cations, for example metal halides, with urea, acetamide, ethylene glycol, and 1,6-hexanediol et al. Inorganic cations generally do not form low melting point eutectics due to their high charge density. However, previous studies have shown that mixtures of metal halides with urea can form eutectics with melting points of <150 °C.[12] Abbott et al. have shown that a large range of transition metals could be incorporated into ambient temperature eutectics.[13]

- Type V DESs is a class of novel non-ionic DES that are composed only of molecular substances and form hydrogen bond between its components. Abranches and Coutinho et al.[14] first defines the type V DESs in 2019. They considered the thymol-menthol system as an example with an abnormal strong interaction that was identified from the acidity differences of phenolic and hydroxyl groups. They described solid-liquid equilibrium phase diagrams with eutectic temperature much lower than that predicted by assuming a thermodynamic ideal behavior. However, most studies on type V DES focus only on investigating the melting temperature of specific stoichiometric mixtures of substances and do not study their phase behavior.[15]

Besides the structural classification, DESs could also be considered by composition or properties. For examples, two commonly terms appeared in literature: natural deep eutectic solvents and hydrophobic deep eutectic solvents. Natural deep eutectic solvents (NADES)[16] are a special type of DES for which the components are primary metabolites, namely, amino acids, organic acids, sugars, or choline derivatives. NADES have a lot of applications such as bio-catalysis, electrochemistry, extraction, and natural products[17]. Hydrophobic deep eutectic solvents are a new generation of water immiscible solvents that have been presented in the literature for the first time in 2015.[18] They are hydrophobic DESs that were far from ideal at that moment with high viscosities and large amounts of DES components that leached to the water phase. The second publication concerning menthol-based eutectic mixtures show hydrophobic low viscosity solvents.[19] Most of these type of eutectic mixtures are not real DES[14]. The year 2017 saw an increase of the hydrophobic DES field. Interesting applications such

as the extraction of Artemisinin from Artemisia annua leaves[20], the first micro-extraction[21], photon up conversion[22] and the use of hydrophobic DESs in membranes[23]. In 2018, a great growth of the field was observed with series of publications related to theoretical approaches[8] and the introduction of the type V DES[14], specifically introduced for hydrophobic DESs.

The physicochemical properties are essential for solvent design and applications. the density of present reported hydrophobic DESs are range from 0.88 to 1.5 g•cm-3 which provide a broad chosen range both upper and lower than water. The viscosity of hydrophobic DESs have a large range from 7 to 86800 mPa•s. Low viscosity is rewarded because this could expand DESs' industrial application. Several low viscosity DESs have been reported, such as, dodecanoic acid: octanoic acid (1:3), dodecanoic acid: nonanoic acid (1:3)[24], and menthol: acetic acid (1:1)[25], which have viscosity of 7 or 8 mPa•s.

General conditions of preparation of DES. DESs are generally easy to prepare and the methods of preparation are often determined by personal preference, equipment available and the ability to minimize water content. The most commonly used preparation method involves heating and stirring the constituents of the DES together under and inert atmosphere until a homogeneous liquid is formed.[2] No additional solvent is needed and no reaction in the traditional sense occurs. Consequently, no purification steps are needed, contributing to their promise as economically viable alternatives to conventional organic solvents and ionic liquids (ILs). Other methods of preparation of DESs[26] include vacuum evaporation, grinding[27] and freeze-drying. In the grinding method, the two solid components are added to a mortar, after which they are solid components are added to a mortar, after which they are ground until a clear, homogeneous liquid is formed, again typically under a nitrogen atmosphere or inside a glovebox.

Besides the above mentioned method, to get a very dry DES, it is generally required to dry each component individually before mixing them together.[28, 29] For anhydrous reline,[29] the water mass fraction of these batches, determined by Coulometric Karl

Fischer titration, was always w (H_2O) < 350 × 10^{-6} wt%.

1.1.2 Comparison of ionic liquids to DESs

Some general properties and definitions of ILs. Ionic liquid is a class of fluid which consists of ions and are liquid at temperatures <100 °C. Figure 1.2 shows the commonly used cations and inions of ionic liquids.

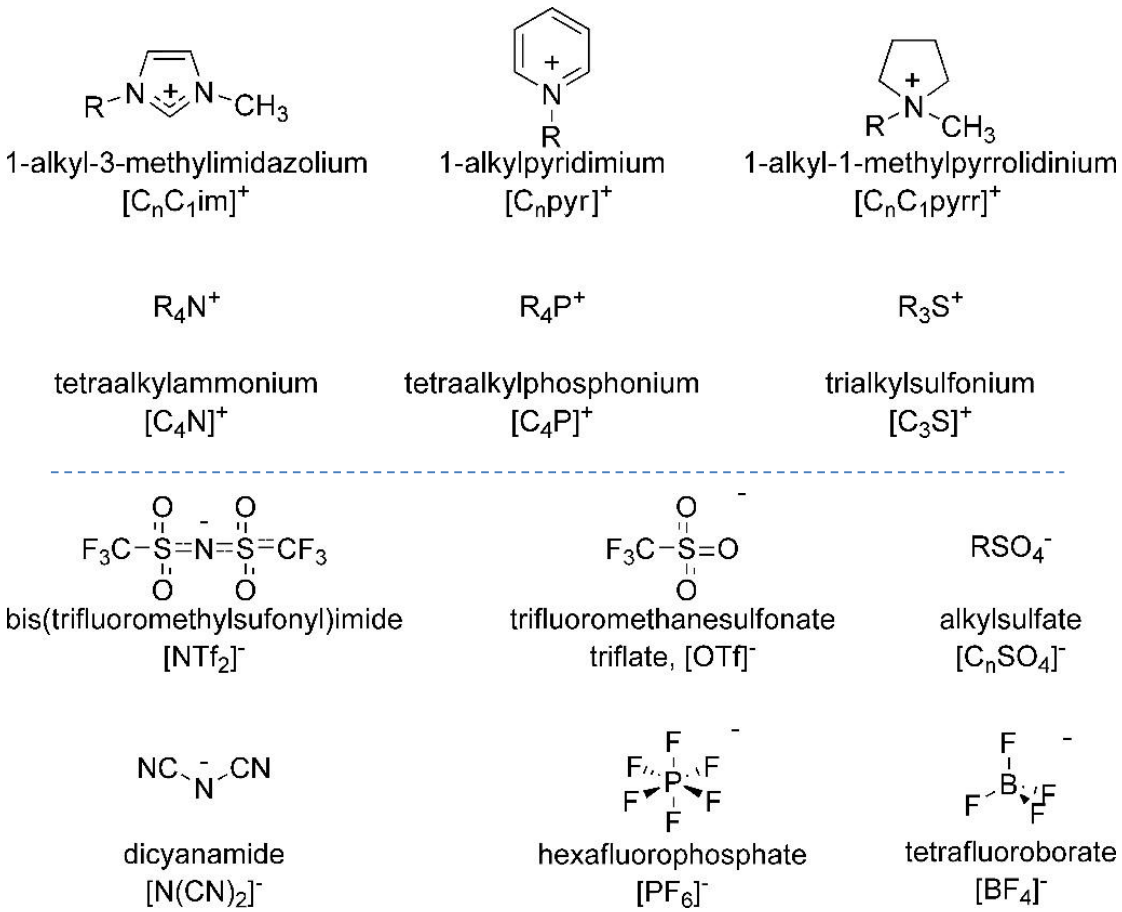

Figure 1.2. Common cations and inions of ionic liquids

In the past 30 years, ionic liquids (ILs) have drawn a wide range of attention, such as in the field of synthesis, catalysis[30, 31], electrochemistry,[32] materials science, separations and more recently for the pre-treatment of biomass. At its early stages, scientists mainly focused on the formation of ionic liquids by mixing metal salts, mostly zinc, aluminum, tin and iron chlorides, with quaternary ammonium salts.[31] Although both salts have very high melting points, their proper mixing leads to the formation of a liquid phase as an eutectic mixture. These eutectic mixtures are generally

characterized by a very large depression of freezing point. A major limitation of the chloroaluminate ILs is their inherent air and moisture sensitivity, due to the rapid hydrolysis of $AlCl_3$ upon contact with moisture. The moisture sensitivity of these systems could be somewhat reduced by the replacement of $AlCl_3$ with more stable metal halides such as $ZnCl_2$ to form eutectic based ionic liquids. The ionic liquids formed from organic cations with $AlCl_3$ and $ZnCl_2$ are often termed first generation ionic liquids. With the introduction of green chemistry concept in the early 1990's, the search for metal-free ILs has become of growing interest. In this context, a lot of works were dedicated to the design of ILs by combining an organic cation (usually imidazolium-based cations) with a large variety of anions.

The second generation of ionic liquids are those that are entirely composed of separate ions, rather than the eutectic mixture of complex ions found in the first-generation ionic liquids. To improve the stability of the metal halides ionic liquids, a lot of works have dedicated to the design of ILs by combining an organic cation with a large variety of anions. Wilkes et al.[33] synthesized moisture stable liquids stable ionic liquids by replacing metal halide, $AlCl_3$, to discrete anions such as the tetrafluoroborate and acetate moieties. Furthermore, later research found that this class of ILs can be improved by using more hydrophobic anions such as trifluoromethanesulfonate ($CF_3SO_3^-$), bis(trifluoromethanesulphonyl)imide [$(CF_3SO_2)_2N^-$] and tris(trifluoromethanesulphonyl)methide [$(CF_3SO_2)_2C^-$].[34-36] These systems have the additional benefit of large electrochemical windows, allowing less noble metals, inaccessible from the chloroaluminate liquids, to be electrodeposited.

Although for their improving evolution and wide range applications, ionic liquids still have many drawbacks.[37] Many reports have pointed out the hazardous toxicity and the very poor biodegradability of most ILs. ILs with high purity are also required since impurities, even in trace amounts, affect their physical properties. Additionally, their synthesis is far to be environmentally friendly since it generally requires a large amount of salts and solvents in to completely exchange the anions. These drawbacks together with the high price of common ILs unfortunately have hampered their industrial

emergence and new concepts are now strongly needed in order to utilize these systems in a more rational way.

Interest of DES versus ILs. Although ILs and DESs have similar physicochemical properties, there are different solvents.[4] The definitions of DES and IL are totally different. Moreover, DESs are not entirely composed of ionic species and could also be obtained from non-ionic species or totally composed of nonionic molecules, for example, the type 5 DESs.[14] DESs are easier to prepare than ionic liquids because they can be formed by simply mixing together two components and heating at a relatively low temperature, 60~80 °C. Furthermore, the components which formed DESs are cheap, renewable and biodegradable and non-toxicity, for instance, the most widely spread component choline chloride. Other advantages of DESs are their chemical inertness with water. With these advantageous properties, DESs have a very promising future for practice applications.

1.1.3 Properties of DESs

Physicochemical properties of a solvent are basic and fundamental parameters that are required for their use. The careful measurements and collection of fundamental properties is thus paramount in the development of relatively new field of DESs. Hereafter, we have gathered some of the reported properties, such as freezing point, viscosity, density, conductivity, and surface tension, of DESs.

1.1.3.1 Phase behavior

The difference in the freezing point (T_f) at the eutectic composition of a binary mixture of A + B compared to that of a theoretical ideal mixture, ΔT_f, is related to the magnitude of the interaction between A and B. The larger the interaction is, the larger ΔT_f is. This is shown schematically in Figure 1.3. For the Type I eutectics, the interactions between different metal halides and the halide anion from the quaternary ammonium salt produce all the similar halometallate species with similar enthalpies of formation. This suggests that ΔT_f values should be between 200 °C and 300 °C. It has been proved by

producing room temperature eutectics of metal halides such as $AlCl_3$ (m.p. = 193 °C), $FeCl_3$ (mp = 308 °C), $ZnCl_2$ (m.p. = 290 °C). Type II eutectics were developed in an attempt to include other metals into the DES formulations. It was found that metal halide hydrates have lower melting points than the corresponding anhydrous salt. The Type III DESs are related to the formation of hydrogen bonds between the halide anion of the salt and the hydrogen bonding donor (HBD). This type of DESs also show the depression of freezing point that depends on the mass fraction of HBD in the mixture. While in another study,[7] their defined the temperature depression should be the difference (ΔT_2) between the ideal and the real eutectic point and not the difference (ΔT_1) between the linear combination of the melting points of the pure components and the real eutectic, see Figure 1.4. This definition is more reasonable. Type IV and type V can also form hydrogen bonds between its two components and their phase behavior is similar to type III DES.

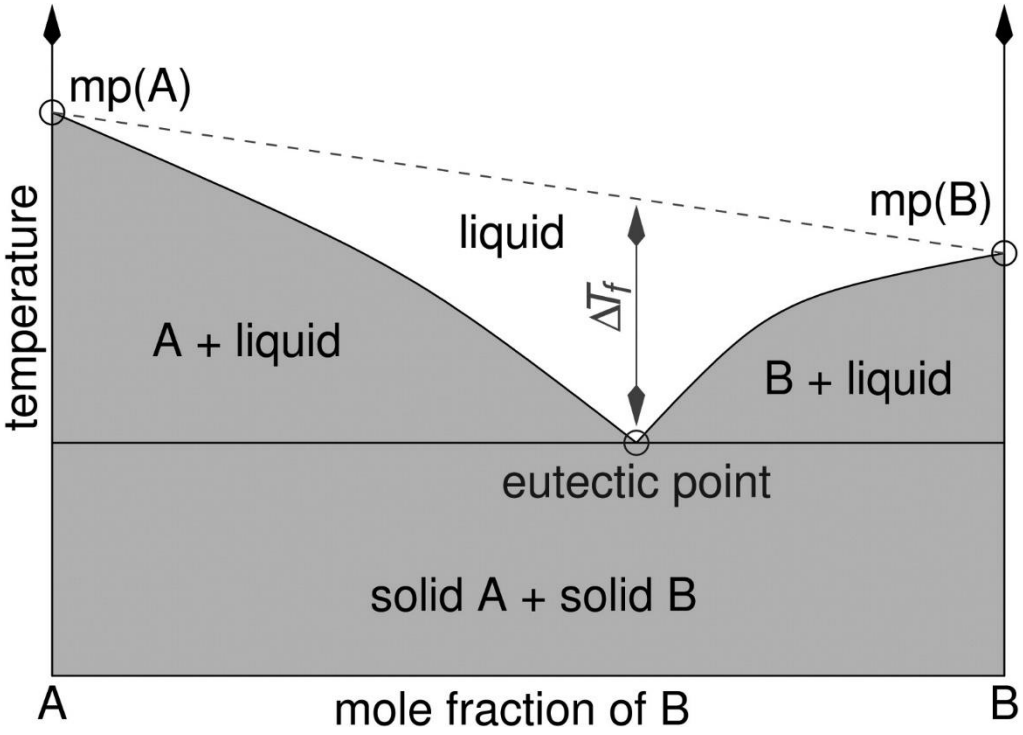

Figure 1.3. Schematic representation of a eutectic point on a two-component phase diagram.[4]

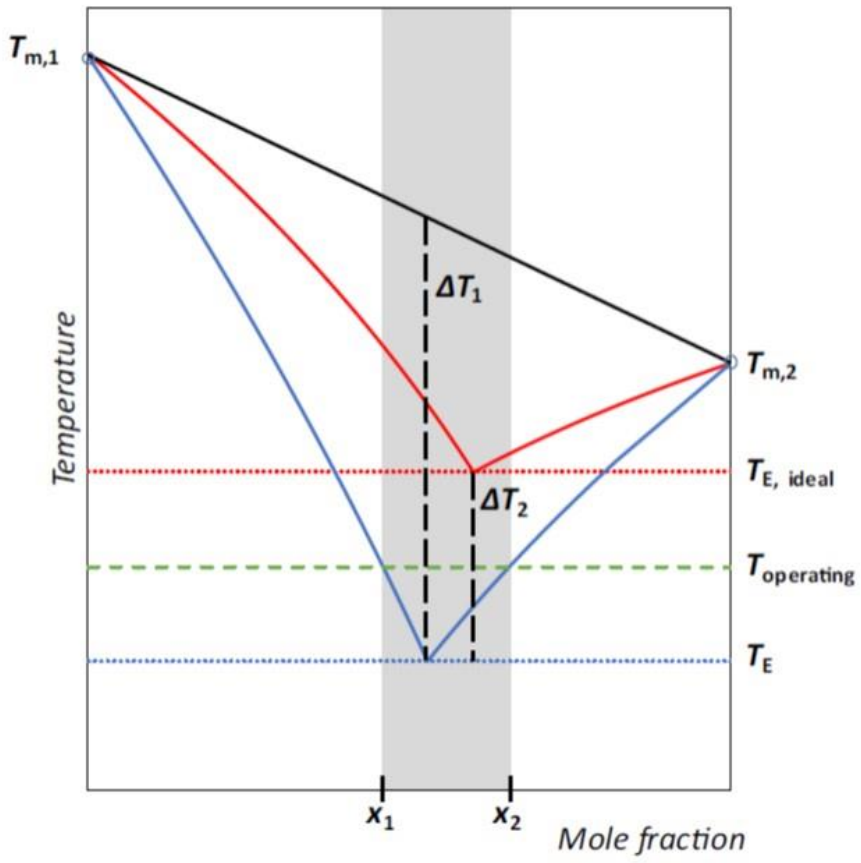

Figure 1.4. Schematic representation of the comparison of the solid-liquid equilibria of a simple ideal eutectic mixture (red line) and a deep eutectic mixture (blue line). T_E is eutectic point.[7]

1.1.3.2 Density, viscosity, conductivity, surface tension and hydrogen bonding

Density. The density is one the most important physical properties for solvent design and applications. Typically, most of DESs exhibit higher densities than that of water, for example, Ethaline has a density of 1.12 g cm^{-3}, and glyceline 1.18 g cm^{-3} at 25 °C. Table 1.2 lists the density data of common DESs at 298 K. However, some hydrophobic DESs [18, 38] show density smaller than water range from 0.88 to 0.99 g cm^{-3}, such as menthol : decanoic acid (molar ratio 1:1), tetraoctylammonium chloride : decanoic acid (molar ratio 1:2).

Mjalli et al. has proposed a method for predicting the DESs' density at different temperatures.[39] The values of measured and predicted densities were compared, and the average of absolute relative percentage error for all the DESs tested was found to be 1.9%.

The salt/HBD molar ratio and composition have obvious consequence on the densities of DESs. Abbott et al. reported densities of different molar ratios of ChCl to glycerol-based DES. They found that as the amount of ChCl increase relatively to glycerol, the density decreased. On the other hand, when increasing glycerol amount, the density increases. DESs densities are also affected by temperature and decreases with increasing temperature[40-43]. Yadav et al. have measured densities of Glyceline from 283 K to 363 K.[41] The temperature dependence of the densities was fitted with a quadratic equation. Other groups have also fitted experimental data to predict DESs densities as a function of temperature which, however, show a linear dependence.

Table 1.2 Physical properties of type III DESs at 298 K.

salt	HBD	Salt:HBD (molar ratio)	Density/g cm^{-3}	Viscosity/ cP	Conductivity/ mS cm^{-1}	Surface tension/ mN m^{-1}	T_f/°C
ChCl	urea	1:2	1.24	632	0.75	52	12
ChCl	Trifluoroacetamide	1:2	1.342				-45
$EtNH_3Cl$	Acetamide	1:1.5	1.041				
ChCl	Ethylene glycol	1:2	1.12	37	7.61	49	
ChCl	Glycerol	1:2	1.18	376	1.05	55.8	-40
ChCl	1,4-Butanediol	1:3	1.052	140 (20°C)	1.65	47.6	
ChCl	1,4-Butanediol	1:4	1.046	88 (20°C)	1.61	47.4	
ChCl	Malonic acid	1:1	1.25	721	0.55	65.7	10

Viscosity. Like ionic liquids, DESs are viscous liquids, their viscosities are 1~3 orders of magnitude higher than those of conventional molecular solvents.[5] This property is an important issue that needs to be addressed in electrochemical studies because it could exert a strong effect on the mass transfer rate of redox in solution and on the conductivity of the DESs. Except for Ethaline (ChCl : ethalene glycol =1:2 molar ratio) and some hydrophobic DESs, most of the DESs exhibit relatively high viscosities (>100cP) at ambient temperature. Table 1.2 lists the viscosities of common DESs at 298 K. The high viscosities of DESs are often attributed to the presence of an extensive hydrogen bond network between each component and the nature of each component, which results in a lower mobility of free species within DESs.[44]

Generally, viscosities of eutectic mixtures are mainly affected by the chemical nature of the DES components, the temperature, and the water content. For binary eutectic mixtures, its viscosity is essentially governed by hydrogen bonds, van der Waals and electrostatic interactions. Table 1.2 lists the viscosity of a series DESs at different emperatures. From the table, we can see that the viscosity of ChCl-based DESs is closely dependent on the nature of the HBD. For example, ChCl/EG (1:2) DES has the lowest viscosity (37 cP at 25 °C). While changing the HBD to glycerol (259 cP at 25 °C), urea (750 cP at 25 °C), or malonic acid (1124 cP at 25 °C) could lead to significant increasing of viscosity. This may due to the presence of more intermolecular hydrogen-bonding. There are also examples showing that viscosity is influenced by the composition of components. For example, in the case of ChCl/glycerol DES, an increase of the ChCl/glycerol molar ratio results in a decrease of the DES viscosity.

Viscosity of DESs is also significantly influenced by the temperature. Viscosity describes the resistance of a fluid in response to a deformation at a given shear rate. Understanding the origin of this critical fluid property is especially important for DESs. Two mostly applied models, the Arrhenius and the VFT model, which best fits the experiments have been used to describe DESs. The Arrhenius equation (eq 2) applies when the liquids at high temperatures or the when the viscosities are measured over a narrow range of temperatures. The Arrhenius equation given as

$$\eta_{\text{Arrhenius}} = \text{A}e^{E/RT} \qquad (2)$$

Where E [kJ mol-1], A, and R are the activation energy for viscous flow, a prefactor, and the molar gas constant, respectively.

The Vogel-Fulcher-Tammann equation (VFT) is often used to describe the temperature dependent viscosity of glass-forming liquids reflecting the contributions of intermolecular interactions such as van der Waals and hydrogen-bonding. The VFT equation could be used in a wide range of temperatures and given by

$$\eta_{VFT} = A'e^{B/(T-T_0)} \qquad (3)$$

Where A', [Pas], the “preexponential factor” that quantifies the viscosity at infinite

temperature, B, [K], the fitting parameter that accounts for the activation energy of viscous flow, and T0, [K], the ideal glass transition temperature.

Several publications have investigated the viscosity as a function of temperature using the two models mentioned above. Cui et al. reported that the viscosity measurements for ChCl-based DESs comprised of acidic HBDs (p-toluenesulfonic acid, trichloroacetic acid, monochloroacetic acid, and propionic acid) were better fit with the VFT model instead of the Arrhenius. Similar results also found by Yadav et al. for choline chloride + glycerol DES.[42] A study by Aroso et al. used rheology to analyze multiple natural DESs formed by combing ChCl or betaine with different sugar molecules. Flow curves were obtained using shear rate ramps from 0.1 to 100 s^{-1} in the temperature range of 283-373 K in steps of 10 K. The results demonstrated Newtonian behavior for all of the NADESs studied and were readily modeled by the Arrhenius equation.

Water content of DESs is another impact of viscosity. The addition of water to a DES leads to considerable decreases of the viscosity. For example, Van Osch et al. studied the impact of water on the viscosity of various hydrophobic DESs of water content from ppm levels to water saturated (approximately 1.64 to 5.1 wt%). The results show that viscosity decreased with increasing water content.

Ionic Conductivity. Ionic conductivity quantifies how easily a material conducts the flow of ions or how easily the material permits a flow of current via the mechanism of ionic conduction. In electrochemistry, the ionic conductivity of solvents is a primary property to conduct electrochemical experiments in it. Owing to their relatively high viscosity, most of DESs exhibit poor ionic conductivities. Table 1.2 show some commonly used DESs' conductivity. The conductivities of DESs generally increase significantly as the temperature increases due to a decrease of the DES viscosity. Hence, Arrhenius-like equation could also be used to predict the conductivity behavior of DESs.

Hashim et al.[45] have reported the electrical conductivity of two classes of DESs based on ammonium and phosphonium salts at different compositions and temperatures. They

found that the electrical conductivities of eighteen DESs have function of temperature, showing that the electrical conductivities of all DESs increase exponentially with an increase in temperature. DES electrical conductivity is also a function of its composition. The electrical conductivity of DESs increased with increasing the salt concentration in the mixture.

Agieienko et al.[46, 47] have investigated the electrical conductivity (κ) of two DESs, Glyceline (choline chloride: glycerol / 1:2 molar ratio), Reline (choline chloride: urea / 1:2 molar ratio), and its mixtures with dimethyl sulfoxide at the temperature range of 278.15-338.15 K. the results show that κ of DESs and its mixtures was best fitted by the empirical Vogel-Fulcher-Tammann equation. Similar trends have also found in Erhaline (choline chloride: ethylene glycol / 1:2 molar ratio)[48].

Lemaoui et al.[49] have predicted the electrical conductivity of DESs using conductor-like screening model for real solvent (COSMO-RS) molecular charge density distributions (Sσ-profiles). The data from literature comprise 236 experimental electrical conductivity measurements for 21 ammonium- and phosphonium-based DESs, covering a wide range of temperatures and molar ratios. The finding showed that the models based on Sσ-profiles as molecular descriptors are excellent at describing the properties of DESs.

The ionic conductivity of choline chloride and oxalic acid DESs have been investigated in anhydrous and hydrated conditions[50]. As expected, ionic conductivity is increasing with increasing temperature. It is noticeable that water plays an important role as an additional component of the DES structure. Ionic conductivity also increases with the increasing water component.

Surface tension. Surface tension is a measure of the energy that is required for increasing the surface area of a material and is related to the tendency of a material to have the smallest surface area possible. Its effects are most prevalent in liquids due to intermolecular interactions among molecules in the liquid and can be measured using several techniques, including a Wilhelmy plate, a Du Nouy ring, and pendant drop.

Surface tension can be measured in DESs alongside density, viscosity, and ionic conductivity as a means of understanding changes in the molecular environment of a DES due to changes in composition and temperature.

Surface tension is a key physicochemical property for the application of DESs in the field of interface and colloid. Surface tension were measured for three choline chloride-based DESs with ethylene glycol, levulinic acid, and phenol HBDs at 298 K and 101.3 kPa[28]. It was reported that the surface tension for Ethaline, 45.66 $mN \bullet m^{-1}$, was lower than that of the pure ethylene glycol, 48.90 $mN \bullet m^{-1}$. Same trend was observed for other ChCl:HBD DESs. The decrease in surface tension from the pure HBD to the formed DES was ascribed to the addition of ChCl which acts as a surfactant and decreasing the cohesive forces at the DESs surface. Chen et al.[51] have systematically investigated the surface tension of 50 typical DESs. The considered parameters include hydrogen-bonding donors, hydrogen-bonding acceptors, addition solvents such as water, water+salt, ethanol, isopropyl alcohol, and ethylacetate, and temperature effects were studied. The temperature dependence and hydrogen bonding effects of surface tension was studied in a range of 298-343 K. By increasing the temperature and quantity of HBDs in DESs, surface tension experienced a decreasing trend in the amount. Hydrogen bonding in DESs has a great effect on the properties. Among all DESs with the same components, the DESs with the strong hydrogen bonding in their structures had the higher viscosity and surface tension. A global and simple model was proposed to estimate the surface tension of DESs[52]. Its correlation is a function of density, acentric factor, and critical properties.

Hydrogen bonding. Hydrogen bonding, as noted in the early publications on DES fundamentals[1, 2] is suspected to be a key intermolecular force responsible of the melting point depression that occurs during the formation of DESs. However, an unambiguous and general definition for the hydrogen bond (H-bond) remains elusive. The IUPAC definition of the H-bond was updated in 2011 which could be a reference.[53, 54] H-bond energies cover two orders of magnitude from 1-170 kJ mol-1 (0.2-40 kcal mol-1).[55] Hydrogen bonds range from the very strong, comparable with covalent

bonds, to moderate, mostly electrostatic, to the very week, comparable with van der Waals forces.[56] H-bonds were detected by using Fourier transform infrared spectroscopy (FTIR)[57, 58], Nuclear magnetic resonance spectroscopy (NMR)[59] or revealed solely from the electron density using density functional theory (DFT)[60]. There are many types of H-bonds, here we show one of the H-bond, ionic H-bond, which could commonly appear in ILs and DESs. The commonly recognized ionic H-bond is formed between a neutral molecule and a charged ion (Figure 1.5).[61]

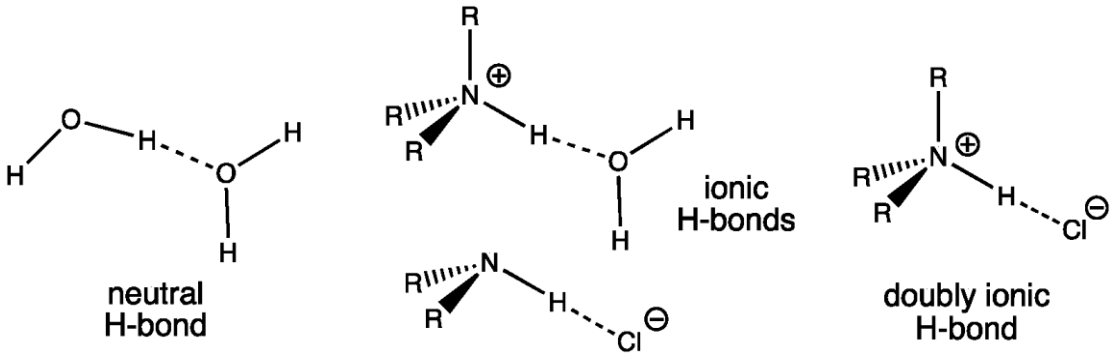

Figure 1.5. Simple exemplars of neutral, ionic and doubly ionic hydrogen bonds.[61]

Hammond et al.[62] have investigated the liquid structure of DES reline (ChCl-urea 1:2 molar ratio) by using neutron diffraction and empirical potential structure refinement (EPSR) model. They report that hydrogen bonding network were present with significant ordering interactions not only between urea and chloride, but between all DES components, including the OH groups of choline anions. Ashworth et al.[63] have studied the effect of different hydrogen bonding types in the ChCl:urea DES via a series of computational simulations. They found that tripodal CH…Cl doubly ionic H-bond motif. Moreover, it is found that the covalency of doubly ionic H-bonds can be greater than, or comparable with, neutral and ionic examples. Unlike traditional solvents, a so-called “alphabet soup” of many different types of H-bond (OH…O＝C, NH…O＝C, OH…Cl, NH…Cl, OH…NH, CH…Cl, CH…O＝C, NH…OH and NH…NH) could exist DESs. These H-bonds exhibit substantial flexibility in terms of number and strength. It is anticipated that H-bonding would have a significant impact on the entropy of the system and thus could play an important role in the formation of the eutectic. H-

bonded complex could be formed in the 2:1 urea: choline-chloride eutectic, such as, [Cl(urea)2]-, urea[choline]+, [Cl(urea)2]-. These two publications illustrate the various hydrogen bonding interaction in DESs that could provide implications for the design of "tunable solvents". Wang et al. investigated the hydrogen bond interactions in DES of choline chloride and polyols by using FTIR, NMR and quantum chemistry calculation.[64] It is shown that ionic hydrogen-bonding interaction between Cl atom of ChCl and H atom of O-H group in the polyols is predominant and its strength decreases with both the increase of carbon number between the two hydroxyl groups in butanediol and the decrease of hydroxyl number in polyols. Hydrogen bonding in DESs between the ions was used to rationalize differences in DES eutectic point temperatures and viscosity.[65] Quantum mechanical molecular dynamics (QM/MD) simulations have been used to probe the three DESs, including Reline (ChCl:urea), Ethaline (ChCl: ethylene glycol), and Glyceline (ChCl: glycerol) all in 1:2 molar ratio.[63] The results show that the structure of the bulk hydrogen bond donor is largely preserved for hydroxyl-based hydrogen bond donors (ChCl: ethylene glycol, ChCl: glycerol), resulting in a smaller melting point depression. By contrast, Reline exhibits a well-established hydrogen bond network between the salt and hydrogen bond donor, leading to a larger melting point depression. While this extensive hydrogen bond network in Reline also exhibits a higher viscosity than in Ethaline and Glyceline.

1.1.3.3 Effect of water content on DESs.

Due to the hygroscopic nature of some DES components like choline chloride, small amount of water is present even in extra-dry DESs that often contain much more water than common organic solvents. The effect of water in DESs has been investigated in many publications from physicochemical properties, solvent structure, and electrochemical behavior.[29, 40, 66-69] Many interesting properties and phenomena found in DESs could be tuned by adjusting the water content, but the reason and consequences of such addition are still a matter of active research. In spite of this, it seems clear that water could play a vital role in the adjustment of DES properties. These makes DESs

very interesting as designer media for their physical, chemical, electrochemical, and spectroscopic properties that are easily and broadly tuned.

Physicochemical properties. Physicochemical properties such as density, viscosity, electrical conductivity considerably vary with water content in DESs. Choline chloride-based DESs has extended investigated as example. The density of choline chloride-based DESs decreases with increasing water concentration over the entire composition range.[40-43, 70] Several publications have investigated the effect of water on viscosity in DESs.[40, 42, 43, 70] Figure 1.6 shown the viscosity as a function of x1 (mole fraction of reline) for aqueous mixtures of reline at different temperatures. As expected, the dynamic viscosity decreases monotonically upon increasing the mole fraction of water at fixed temperature.[43] This is attributed to the much low viscosity of water than that of neat reline at all studied temperatures. Water effects on electrical conductivity [29, 71-74] have been intensively investigated in Reline. The results shown that the conductivity exhibits s smooth but considerable increase before passing through a flat maximum at $x1 \approx 0.18$ and then dropping rapidly in the range $0 < x1 < 0.1$ to the negligible conductivity of water ($< 10^{-6}$ S m^{-1}). These results are not surprising because electrical conductivity is related to ion mobility (i.e. as ion mobility increase, electrical conductivity increases). As the concentration of water increases, the viscosity of the solution decreases causing ion mobility to increase. Similar results are found in ammonium-based DESs[75], glycerol-based DESs,[76] and sodium halides salts-ethylene glycol DES[77] etc.

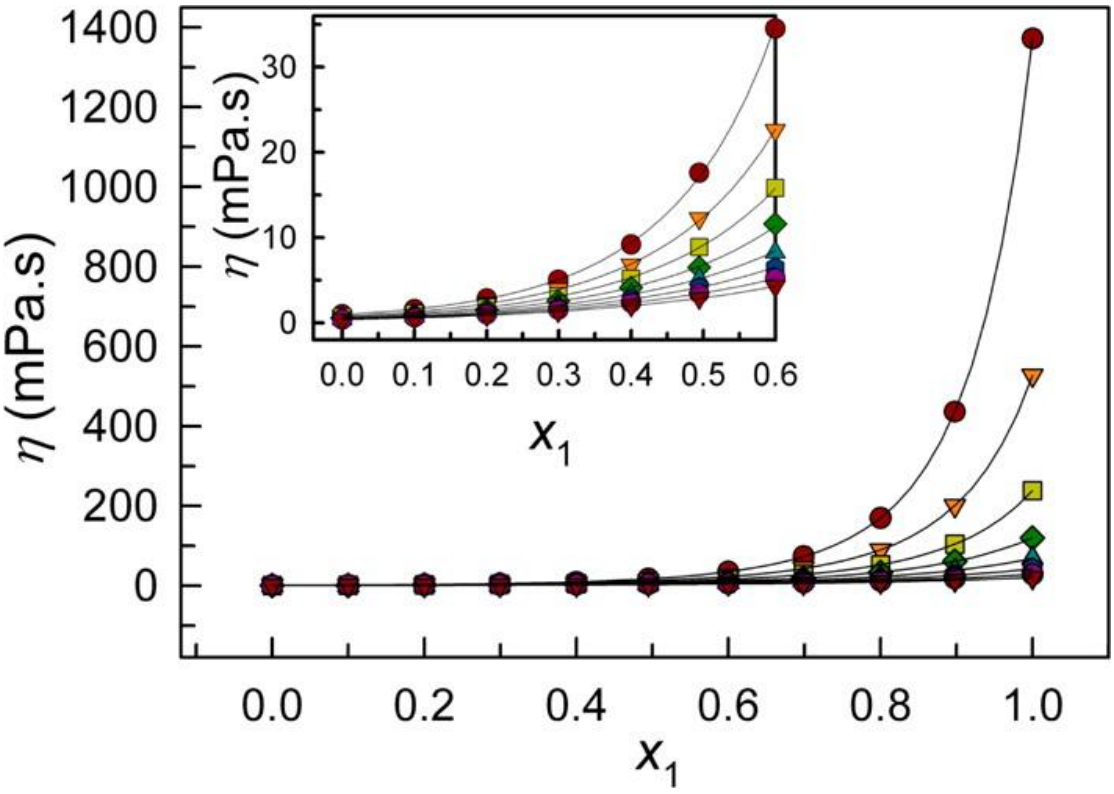

Figure 1.6. Dynamic viscosity (η) as a function of mole fraction of reline (x_1) for (water + reline) mixture at different temperatures. [red ●, 293.15 K; orange ▼, 303.15 K; yellow ■, 313.15 K; green ♦, 323.15 K; blue ▲, 333.15 K; blue ⬢, 343.15 K; purple ●, 353.15 K; red ▼, 363.15 K].[43]

Solvent structure. The water effect on DES nanostructure has been examined across a wide water range in Reline (1ChCl: 2 urea). Hammond et al.[78] reported the nanostructure of a series of choline chloride/urea/water DES mixtures in a wide hydration range using neutron total scattering and empirical potential structure refinement (EPSR). When water amount below 25.0 mol.% (6.48wt.%), water contributes slightly to the hydrogen-bonding network, and strengthens choline-urea bonding. Between 40.0 mol.% (12.18 wt.%) and 76.9 mol.% (40.95 wt.%), the hydrated DES is in a regime where DES clusters exist, but are separated by the diluent. At 83.3 mol.% (50.98 wt.%), a step change in solvation where many of the DES structural motifs stop become dominant as water clusters become favorable. At this point, the system is best described as an aqueous solution of DES components at the molecular level. In summary, with increasing water amount, the mixtures change from ionic mixture to aqueous solution. These analyses support using hydrated DESs as a tool to overcome limitations of DESs, mainly its high viscosity. Ab initio molecular dynamics

simulations were used to investigate the microscopic structure of Ethaline and its mixture with water. Similar results are got in the low range of water (25.0 mol.%) but biased conclusions are due to their narrow water fraction with Ethaline.[67]

The self-diffusion of molecular and ionic species in aqueous mixtures of choline chloride based DESs were investigated in order to elucidate the effect of water on motion and inter-molecular interactions between different species in the mixtures[74, 79]. The results reveal that the hydroxyl proton of Ch+ and the hydrogen bond donor have diffusion coefficients significantly different from those measured for their parent molecules when water is added. The hydroxyl moieties of Ch+ and HBD show a stronger interaction with water for Ethaline as water is added to the system. In aqueous Glyceline, water has little effect on both diffusion of hydroxyl proton of Ch+ and HBD. In Reline, it is likely that water allows the formation of small amounts of ammonium hydroxide. The most surprising observation is from the self-diffusion of water, which is considerably higher expected from a homogeneous liquid. This leads to the conclusion that Reline and Glyceline form mixtures that are inhomogeneous at a microscopic level despite the hydrophilicity of the salt and HBD.

Water effects on relaxation and solvation dynamics of Ethaline were investigated by Alfurayj et al. using various independent experimental methods, such as time-resolved transient absorption laser spectroscopy, broadband dielectric spectroscopy, NMR diffusometry and broadband relaxometry, and molecular dynamics simulations (MDS).[66] Their work demonstrate that even modest amounts of water addition (1-10wt.%) to Ethaline could lead to performance improvements, such as accelerated relaxation and solvation, and provides a more polar solvent environment which is desirable for electrolytes. In contrast, very small amounts of water (<1wt.%) lead to additional slowing of the solvent response.

The presence of water in DESs can also lower their melting points[80, 81] and freezing points[68]. The results show that the freezing points of hydrated Reline decrease when water is added until a minimum is reached for 6 equiv. of water added. As the water amount continues to increase, the freezing point starts increasing[68].

The effect of water content on the electrodeposition of Ni metal on glassy carbon was investigated in Reline.[82] Water content could greatly influence the morphology of Ni deposits. The results show that Ni growth is halted due to water splitting and formation of a mixed layer of Ni/NiOxOH2(1- x) depending on water content. Moreover, the DES components could also be electrochemically reduced at the electrode surface, blocking further three-dimensional growth of the Ni nanoparticles. By careful tuning of the water amount, one could give the ability of controlling self-limiting growth and passivation phenomena.

In summary, the water addition (<10 wt.%) to DESs could remarkably improve its performance and enlarge it practical use by decreasing viscosity, increasing electrical conductivity, decreasing freezing point, accelerated relaxation and solvation with preserving the solvent structures and original properties. In addition, the hydrated DESs have shown great benefits in other fields, such as shape-controlled nanoparticle syntheses and its application in electrocatalysis[83], free radical polymerizations[84, 85], tunable carbon dioxide solubility[86, 87], DNA and protein separation[88, 89], microorganisms in biocatalytic process[90, 91].

1.1.4 Some Applications of DESs

DES has a wide range of applications in all kinds of research field from separation, organic synthesis, electrochemistry to solvent dynamics,…. In this part, we mainly focus on molecular electrochemistry while for other fields we will only provide a brief review.

1.1.4.1 Electrochemistry in DESs

Mass transport, electrochemical potential window, ohmic drop, and diffusion coefficient and kinetics of redox couples in DESs are reviewed in this part. Some are important factors must consider in our experiment and others are significant electrochemical parameters will be measured in the thesis. The general view of our proposal to treat these factors and extract chemical information could be seen in Chapter

2.

1.1.4.1.1 Diffusion of components and electroactive molecules

Wagle et al.[92] have revealed the different microscopic mobilities of components within a DES Glyceline. From macroscopic measurements, the lone-range translational diffusion of the larger cation (choline) is known to be slower compared to that of the smaller hydrogen bond donor (glycerol). However, when the diffusion dynamics are analyzed on the sub-nanometer length scale, a counterintuitive diffusive was found. Indeed, the displacements associated with the localized diffusive motions are actually larger for choline.

Diffusion of redox molecules in DESs is one of the fundamental aspects of electrochemical measurements. The commonly used electrochemical technique to measure diffusion coefficient (D) is cyclic voltammetry and microelectrode chronoamperometry in thin layer cells. Other techniques such as square wave voltammetry, impedance spectroscopy, and polarization measurements, could also be used. Hapiot et al.[93] have investigated the mass transport phenomena and diffusion of redox molecules from bulk DESs to electrode surfaces using cyclic voltammetry method. Derived diffusion coefficients were extracted and found to present some inconsistencies with the classical Stokes-Einstein law established for homogeneous media. They are almost unaffected by the charge present on the diffusing molecules contrarily to observations made for ionic liquids. Diffusion coefficients were determined on the order of 10^{-7} cm^2 s^{-1} which is around 2 orders of magnitude lower than those measured in conventional organic solvents as expected because of the high viscosities of the DES.

1.1.4.1.2 Electrochemical windows

The electrochemical potential window is an important indicator of electrochemical stability when DESs are used as electrolyte for molecular electrochemistry and electrochemical devices.

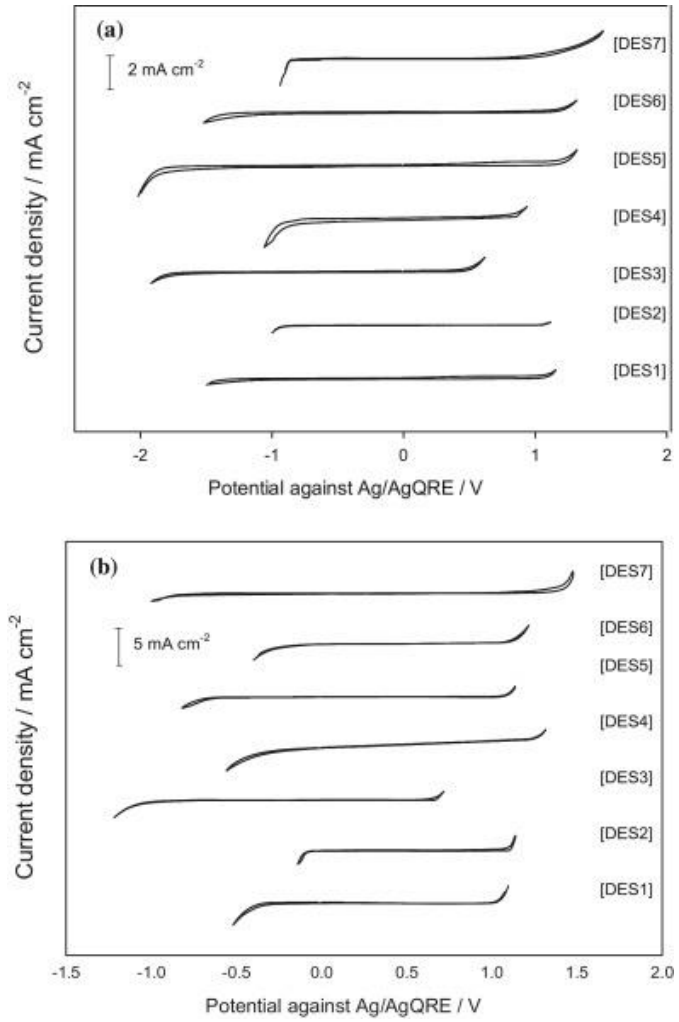

Figure 1.7. (a) Electrochemical potential windows of all seven DESs using GC working electrode; (b) potential windows obtained using Pt microelectrode.[94]

The potential windows of DESs at different electrodes were examined. For example, cyclic voltammograms were recorded at Hg electrode at low scan rate of 50 mV/s and different temperatures for several choline chloride based DESs (1:2 mole ratio).The hydrogen bond donors were 1,2-ethanediol, 1,2-propanediol, 1,3-propanediol, urea, and thiourea.[95] The potential window at Hg electrode in these DESs is around 1.5 V in Reline.

Bahadori et al.[94] have investigated the electrochemical potential window of a series of DESs by means of cyclic voltammetry and chronoamperometry at a scan rate of 0.1 V/s on glassy carbon and Pt microelectrode as shown in Figure 1.7. The potential window lies approximately between 2.0-3.5 V vs. Ag+/Ag QRE for the GC electrode and

between 1.4-2.4 V for the Pt electrode. The choline chloride based-DESs like Ethaline and glyceline display the widest electrochemical potential window. It is discovered that the tested DESs have similar potential windows as compared to some typical ILs.[96] However, some ILs have wider electrochemical window.

1.1.4.1.3 Ohmic drop

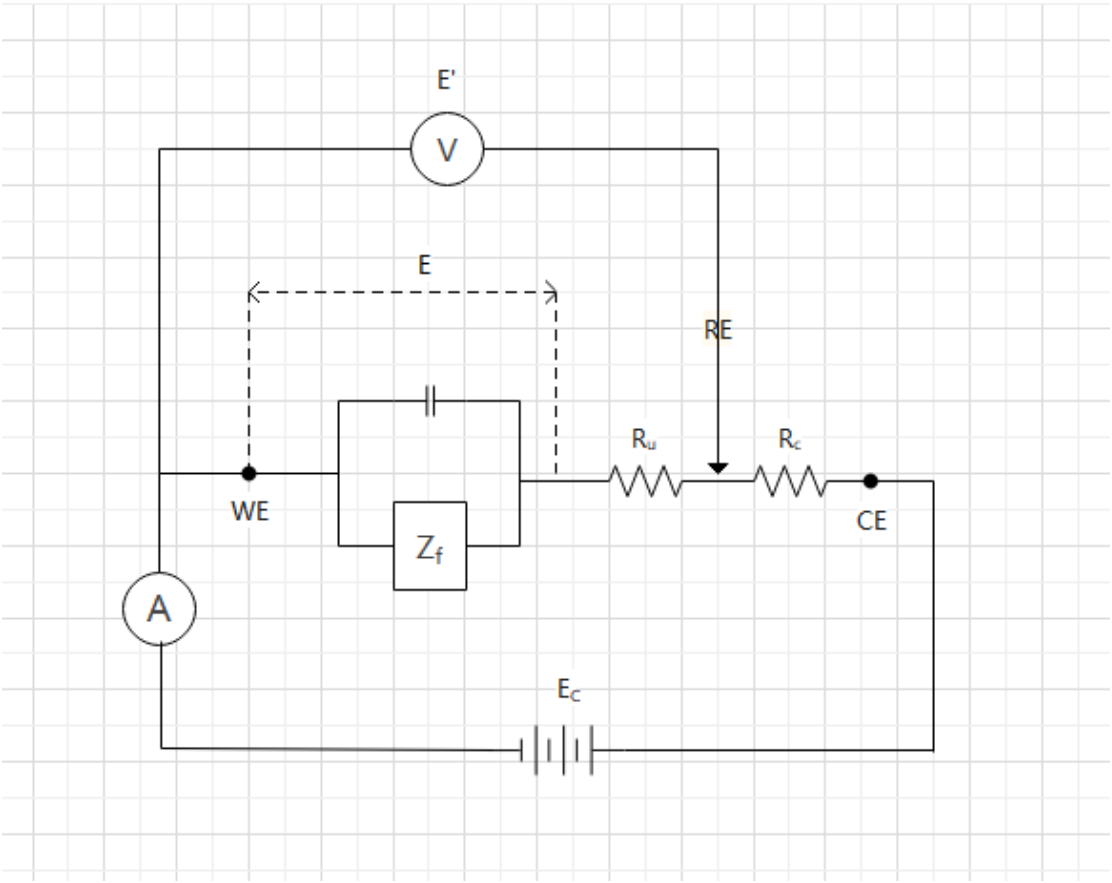

Figure 1.8. General equivalent circuit of a three-electrode electrochemical cell.[97]

Performing a cyclic voltammetry experiment should meet three criteria. First, precise control the electrode potential and measure the current response are required. Second, the current is exclusively the Faradaic component, without double-layer charging currents. Third, the reactants are transported to the working electrode surface exclusively by diffusion. Unfortunately, this could be difficult to achieved in practical situations notably with DESs.

In nonaqueous solutions with low conductivities, a three-electrode system is preferable.

In this arrangement, the electrochemical reactions of interest occur on the working electrode (WE) and the current is flow between the working electrode and the counter electrode (CE). We also need a third electrode to serve as reference electrode (RE) to measure the potential of the working electrode. There has a high input impedance between the WE and RE, so that a negligible current is drawn through the RE. Consequently, its potential remains constant and equal to its open-circuit value.

Figure 1.8 shows the equivalent electric scheme of the three electrodes system. Beside the working electrode, the presence of a capacitance, Cd, in parallel with an impedance, Zf, represents the Faradaic reaction on working electrode surface. Between the Cd- Zf parallel circuit and counter electrode, the resistance of the ionic solution consists of two parts, one for the solution between the WE and RE, Ru, and another, Rc, of the cell resistance. It should be noted that the potential across the Cd- Zf parallel circuit is equal to the potential imposed between WE and RE only if the ohmic drop in the uncompensated resistance, Ru, (uncompensated by the potentiostat), can be neglected. Then, the two potentials E and E' in figure 1.8 are the same. This is not true, especially at high scan rates when the currents are higher.

In voltammetry, the term of importance with respect to Ohmic drop is the uncompensated resistance (Ru) which is the sum of the resistance been the tip of the reference electrode and the working electrode plus the resistance of the working electrode and electronic circuitry. This is why there is a medium dependence on IR drop. It should be noted that any resistances in the working electrode itself, such as in thin wires used to make ultramicroelectrodes, in semiconductor electrodes, or in resistive films on the electrode surface, will also appear in Ru.

The ohmic drop effect is due to the resistance of solution between the WE and RE, of the cell resistance is the main problem with solvent with low conductivities like DESs. Ohmic drop through the uncompensated resistance, Ru, may be large enough, especially at high scan rates. It causes a significant distortion of the Faradaic component (see Figure 1.9), resulting from the fact that the potential E' imposed between WE and RE differs from the potential E across the Cd-Z_f parallel circuit according to $E'=E- R_u i$. The ohmic drop between CE and RE that corresponds to the resistance RC is taken care

of by the potentiostat. It should be noted that even when the tip of the RE is designed for a very close placement near the WE, some uncompensated resistance will remain because the resistance in solution is located very close to the electrode surface.

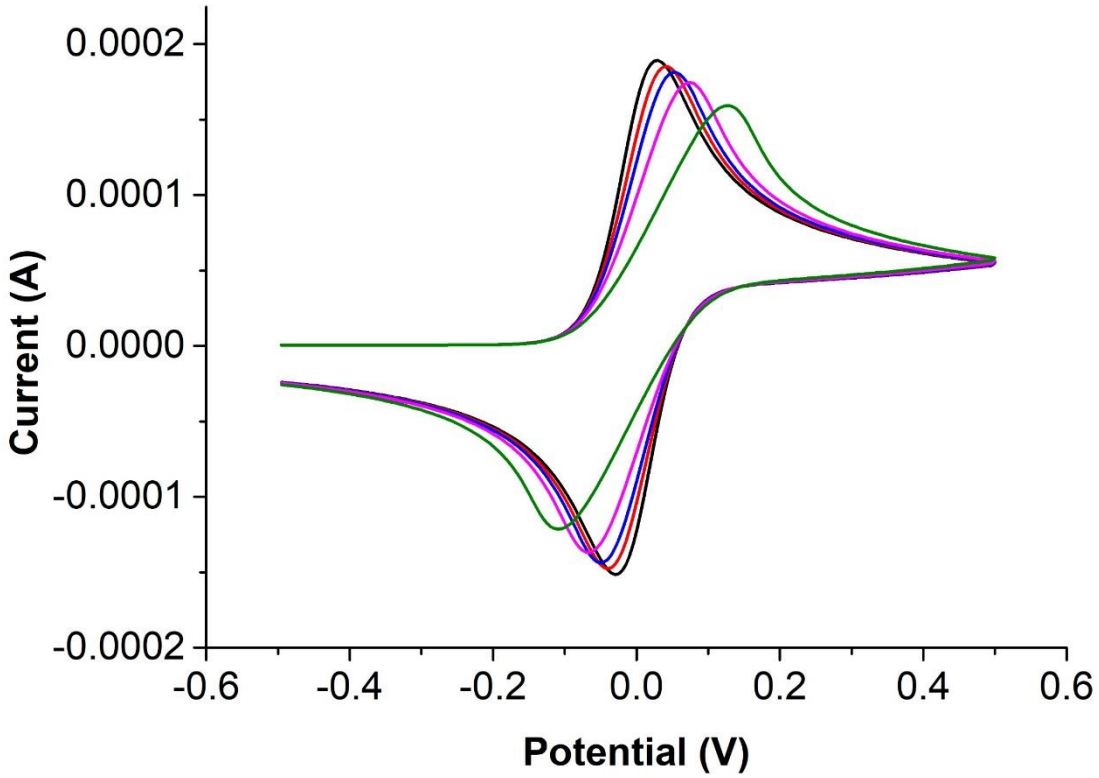

Figure 1.9. Simulation curves of ohmic drop effects on cyclic voltammogram at 100 V/s. simulation parameters: k_S=100 cm·s^{-1}, C°=2·10^{-3} mol·L^{-1}, d=1 mm, D=2·10^{-5} cm^2·s^{-1}, Ru=0, 50, 100, 200, 500, 1000 Ω, Rc=6.7·10^{-9}.

There are two ways to consider the ohmic drop. One consists of equipping the instrument with a positive feedback loop that correct from E'a tension, thus eliminating, at least partially, the ohmic drop effect (electronic compensation). Another approach to minimize ohmic drop is to use ultra-microelectrodes (UME).

Potentiostat which enables an ohmic drop compensation via positive feedback was investigated by J.-M. Saveant and precise the conditions for making the instrumentation and its use. Ionic liquid and deep eutectic solvents have much lower conductivity than traditional solvents with supporting electrolyte. So they present larger uncompensated ohmic drop.[32] Investigation of kinetics in ILs and DESs must take particular care to ohmic drop compensation. Otherwise, one would make wrong conclusion from

distorted signals.

1.1.4.1.4 Fundamental electrochemical analysis

Mass transport and electron transfer in DESs are fundamental electrochemical processes to study. The diffusion coefficients (D) and heterogeneous constant rates (k°) are the corresponding parameters to evaluated the two processes at the electrode surface. However, the determination of D and k° using the traditional electrochemical approach could mask some properties because of the high viscosity and limited conductivity in these media. Sakita et al.[98] reported that semi-integrative approach is an efficient tool to determine such parameters that significantly influenced by the electrolyte viscosity and conductivity. The D value they got is 2.8 $\times 10^{-8}$ cm^2 s^{-1} and k° value around 2 $\times 10^{-4}$ cm s^{-1}. This method is based on a post-treatment approach which corrects the ohmic drop after recording CV in one scan rate or a narrow range of scan rates, that could introduce a big deviation of the result electron transfer rate constants. We have also reported the D and k° values in Ethaline but using direct electronic compensation method and on a millimetric electrode. The D values are in the order of 10^{-7} and k° data are in the order of 10^{-1} for ferrocene and 10^{-2} for ferrocyanide in Ethaline, which is much higher than the previous literature reported without ohmic drop compensation[99]. Renjith et al.[100] has investigated the electrochemical behavior of five redox couples ($Fe(CN)_6^{4-/3-}$, $Ru(NH_3)_6^{2+/3+}$, $FcMeOH^{0/+}$, methyl viologen, and ferrocene) including cationic, anionic and neutral in deep eutectic solvents. Only methyl viologen show a two electron transfer reversible process. Others redox species shown simple one electron transfer reversible process. The diffusion coefficient they got by EIS and CV method is in the range of 10^{-7} to 10^{-9} cm^2/s in different DESs.

Nkuku and LeSuer have reported the cyclic voltammetry, chronoamperometry, and scanning electrochemical microscopy (SECM) of ferrocene in two choline chloride based DESs.[101] Linear diffusion behavior was observed in CV experiments even using ultramicroelectrodes. Diffusion coefficient of ferrocene in DES was found to be 2.7 $\times$ 10^{-8} cm^2 s^{-1} due to the DES high viscosity. Because of the difficulties in achieving

steady-state conditions, SECM approach curves remain tip velocity dependent. Under certain conditions, SECM approach curves to an insulating substrate displays a positive-feedback response which could be described in terms of a dimensionless parameter, the Peclet number Pe, which is the ratio of the convections and diffusive timescales.

1.1.4.2 Application of DES in other fields

Except the examples shown above, DESs also has a wide application in the range of electrodeposition, extraction, energy storage battery technology, catalysis and synthesis media et al.

Electrodeposition. Electrodeposition is a common way for preparing solid metal or alloys coatings on different electrode surface (substrates). They process is based on reducing metal cations that are dispersed in certain electrolytes under an electrical potential. Functionalized surfaces with required properties, such as hardness, corrosion and wear resistances, brightness, and electro-catalysts, could be obtained by electrodeposition. DESs has a relatively high solubility and wider potential window than water which make it a promising electrolyte for electrodeposition.

The electrodeposition of a large range of metal or metal alloys electrodeposition have been tested in DESs, such as Zn[102, 103], Sn, Zn-Sn[104], Ni[82], Al[105, 106], Cu[107], Co, Sm, Sm-Co[108], Ag[109, 110], Cr[111], In[112], Ni-Co[113, 114],Ni-Cr[115], Cu-Sn[116]. Metal deposition can be obtained under either constant current or constant voltage regimes. The morphology and adhesion of the deposit are strongly dependent on current density, as observed in aqueous electrolytes. The morphology of metal deposits can also be tuned by varying DES composition, adding additives, and adjusting water amount.

Separation and CO_2 capture. Separations are industrial relevant processes that involve the physical separation of two or more components from one another. Recently, a sizable portion of research in the field of DES applications has been focused on separations.[117-122] One example is the liquid-liquid extraction of azeotropic mixtures using DES.[123] In their study, a series choline chloride based DESs were studied for

their ability to separate an ethanol-heptane azeotropic mixture. Their results show that the chemical nature of the HBD influences the separation performance. Other examples show that hydrophobic DESs are promissing for the liquid-liquid recovery of various species, including volatile fatty acids,[18] transition metal ions,[124] and radioactive ions from diluted aqueous solutions.[125] Extraction of a wide variety of metal salts and oxides and specifically for phosphates from incinerated sewage sludge ash[126] were investigated in DESs.

Carbon dioxide capture have applications in many scientific disciplines. DES have demonstrated interesting aspects of carbon capture. Some DESs show promising properties as they have high CO_2 solubility, low vapor pressures, and high thermal stabilities compared to conventional media.[127] The mechanism and key factors affecting CO_2 solubility in DES has been investigated.[87, 120, 122, 128-130]

Energy storage. In the electrochemical energy storage, DES appears as a green alternative electrolyte in these electrochemical devices, including redox flow batteries, metal-based rechargeable batteries, super-capacitors,[131] and Li-ion batteries[132, 133], showing a promising future.

Synthesis media and catalysis. As an emerging solvent, many kinds of syntheses have been conducted with success in DESs, such as, organic synthesis, nanomaterial and polymers synthesis etc.

In the field of organic synthesis, the search for a green solvent is of great interest and aims at reducing the use of toxic chemicals. Solvent selection is a delicate issue that affects the chemical behavior of reagents and catalytic platform. Therefore, the correct choice of an appropriate solvent is of crucial importance for successful syntheses that allow for superior selectivity and reactivity. Due to the unique physicochemical properties of DESs, a wide range of organic reactions has been performed in DESs from asymmetric synthesis[134], Diels-Alder reactions[135, 136], multicomponent reactions[137], enzyme bio-transformations[138], and oxidation/reduction processes[139, 140] to C-C coupling reactions[141, 142].

DESs could play a triple role in organic synthesis, as the solvent, as an active catalyst, and as a substrate. Some of the inherent characteristics of DESs could influence the

reaction conditions, mechanistic pathway, the rate of the reaction, product yields and formation of the byproducts due to their specific properties, such as viscosity, water content, density, polarity, pH, molar ratio, concentration, conductivity, and thermal stability. Interestingly, by tuning the inherent nature and molar ratio of the DES components, its physicochemical properties, ability to dissolve solutes and the overall phase behavior, the DES could specifically be transformed and designed to match the specific reaction conditions.

1.2 Electron transfer kinetics

Electron transfer (ET) processes are of considerable importance in both fundamental and applied chemistry. ET include homogeneous (in solutions) and heterogeneous processes which across a phase boundary, such as electrode/electrolyte interface and liquid-liquid interface. The full electrochemical process across an electrode/electrolyte interface, includes three consecutive steps: the diffusion of a reactant to the electrode surface, the heterogeneous ET, and the diffusion of the product into the bulk solution. Quantitative analysis of the ET is possible in the framework of the electron transfer theory developed in 1960s'. Major contributions in this area have been made by Marcus, Hush, Levich, Dogonadze, and many others.

1.2.1 Theory

1.2.1.1 Butler-Volmer model

The potential of an electrode affects the kinetics of reaction occurring on its surface. For a one-step, one-electron process, the current-potential characteristic is given by the following equation:

$$\mathrm{i} = \mathrm{FA}k^0 \left[C_O(0,t) e^{-\alpha f(E-E^{0'})} - C_R(0,t) e^{(1-\alpha) f(E-E^{0'})} \right]$$

where k^0 is the standard rate constant, $C_O(0,t)$ and $C_R(0,t)$ is the concentration of reductant and oxidant respectively and α is the transfer coefficient. This semi-empirical

relation is known as Butler-Volmer formulation of electrode kinetics. It is used in the treatment of almost every problem requiring an account of heterogeneous kinetics. However, while useful in helping to organize the results of experimental studies and in providing information about reaction mechanisms, such an approach cannot predict how the kinetics are affected by such factors as the nature and structure of the reacting species, the solvent, the electrode material and adsorbed layers on the electrode. To obtain such information, one needs a microscopic theory that describes how molecular structure and environment affect the electron-transfer process. Even though BV model has significant limitations, it is very widely used in the electrochemical literature.

1.2.1.2 Marcus theory

$$\mathrm{O} + \mathrm{e} \rightarrow \mathrm{R}$$
$$\mathrm{O} + \mathrm{R}' \rightarrow \mathrm{R} + \mathrm{O}'$$

For simplicity, we consider an outer-sphere, single electron transfer from an electrode to species O, to form the product R. This heterogeneous electrode reaction is equivalent to a homogeneous reduction of O to R by replacing electrode to a suitable reductant R'. We start from a formula which similar to the Arrhenius equation but with more careful examination of the pre-exponential factor as,

$$k_f = K_{P,O} \nu_n \kappa_{el} \exp(-\Delta G_f^{\ddagger}/RT)$$

Where $\Delta G_f^{\ddagger}$ is the activation energy for reduction of O; $K_{P,O}$ is a precursor equilibrium constant, representing the ratio of the reactant concentration in the reactive position at the electrode (the precursor state) to the concentration in bulk solution; ν_n is the nuclear frequency factor (s^{-1}), which represents the frequency of attempts on the energy barrier (generally associated with bond vibrations and solvent motion); κ_{el} is the electronic transmission coefficient, which is related to the probability of electron tunneling.

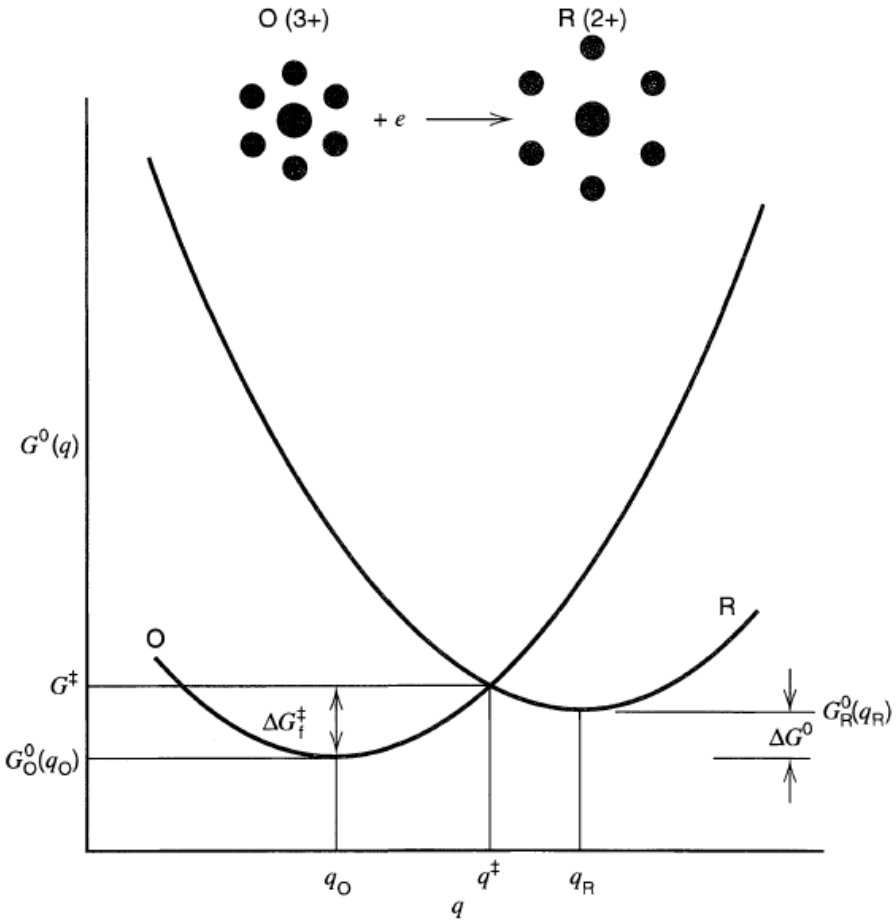

Figure 1.10. Standard free energy, G^0, as a function of reaction coordinate, q, for an electron transfer reaction. The picture at the top is a general representation of structural changes that might accompany electron transfer. Reprinted from Electrochemical Method- Fundamentals and Applications, section 3.6.[143]

We imagine the reaction as occurring on a multidimensional surface defining the standard free energy of the system in terms of the nuclear coordinates of the reactant, product and solvent (Figure 1.10). Changes in nuclear coordinates come from vibrational and rotational motions in O and R, and from fluctuations in the position and orientation of the solvent molecules. Two assumptions are given as that (1) the reactant, O, is centered at some fixed position with respect to the electrode, or in a homogeneous reaction, that the reactants are at a fixed distance from each other and (2) the standard free energies of O and R, G_O^0 and G_R^0, depend quadratically on the reaction coordinate, q. The free energy of activation for reduction of O is $\Delta G_f^{\ddagger}$,

$$\Delta G_f^{\ddagger} = \frac{\lambda}{4}(1 + \frac{\Delta G^0}{\lambda})^2$$

Where λ is the reorganization energy, ΔG^0 is the difference of standard free energy for the reaction.

For an electrode reaction

$$\Delta G_f^{\ddagger} = \frac{\lambda}{4}(1 + \frac{F(E - E^0)}{\lambda})^2$$

When double layer effect is carefully considered, the driving force, ΔG^0 or $F(E\text{-}E^0)$, will become more complexed by introducing work terms. This is because there has a potential difference between the electrode and the reaction site, which lies between the electrode surface and outer Helmoltz plane (OHP). Thus, there are energy changes involved in bringing the reactants and products from the average environment in the medium to the reaction site, where the electron transfer occurs. So the new driving force $\Delta G^{0'}$ could written as for homogeneous or electrode reaction as:

$$\Delta G^{0'} = \Delta G^0 - w_O + w_R = F(E - E^0) - w_O + w_R$$

The critical parameter is λ, the reorganization energy, which represents the energy necessary to transform the nuclear configurations in the reactant and the solvent to those of the product state. It is usually separated into inner, λ_i, and outer, λ_o, components.

$$\lambda = \lambda_i + \lambda_o$$

where λ_i represents the contribution from reorganization of species O, and λ_o that from reorganization of the solvent. Typically, λ_o is computed by assuming that the solvent is a dielectric continuum and the reactant is a sphere of radius a_O for an electrode reaction,

$$\lambda_O = \frac{e^2}{8\pi\varepsilon_0}\left(\frac{1}{a_O} - \frac{1}{R}\right)\left(\frac{1}{\varepsilon_{op}} - \frac{1}{\varepsilon_s}\right)$$

Where ε_{op} and ε_s are the optical and static dielectric constants, respectively, and R is taken as twice the distance from the center of the molecule to the electrode. For a homogeneous electron-transfer reaction:

$$\lambda_O = \frac{e^2}{4\pi\varepsilon_0}\left(\frac{1}{2a_1} + \frac{1}{2a_2} - \frac{1}{d}\right)\left(\frac{1}{\varepsilon_{op}} - \frac{1}{\varepsilon_s}\right)$$

Where a_1 and a_2 are the radii of the reactants and $d=a_1+a_2$. Typical values of λ are in the

range of 0.5 to 1 eV.

Most electron-transfer reactions are considered to be adiabatic. In such cases, variation of the rate constant from one system to another can be treated to changes in the reorganization energies and often the reorganization energy is dominated by the outer reorganization, the changes in the internal structure of the reactant being of a minor factor.

Predictions from Marcus theory

In principle, it is possible to estimate the rate constant for an electrode reaction by computing the pre-exponential terms and reorganization energy values, this is rarely done in practice. The theory's greater value is the chemical and physical insights that could be afforded from this model and arises from its capacity for prediction and generalization about electron transfer reactions:[143]

1. Prediction of transfer coefficient value variations, α:

$$\alpha = \frac{1}{F}\frac{\partial \Delta G_f^{\ddagger}}{\partial E} = \frac{1}{2} + \frac{F(E - E^0)}{2\lambda}$$

   thus, the Marcus theory predicts not only that α ≈ 0.5, but also that it depends on potential in a particular way.
2. Predictions about the relation between the rate constants for homogeneous and heterogeneous reactions of the same reactant.
3. Marcus theory leads to useful qualitative predictions about reaction kinetics.

   For example, when $E = E^0$, $\Delta G^{\ddagger} \approx \lambda/4$, where $k_f = k_b = k^0$. Based on previous relations, k^0 will be larger when the internal reorganization, λ_i, is smaller, that means in reactions where O and R have similar structures. On the other hand, electron transfer involving large structural alterations (such as large changes in bond lengths or bond angles) tend to be slower.

   Solvation also has an important role through its contribution on λ. Large molecules which have bigger a_O tend to show lower solvation energies, and smaller changes in solvation upon reaction, by comparison with smaller species. On this basis, one could expect electron transfers to small molecules will be slower than large ones.

For example, the reduction of O_2 to $O_2^{-\bullet}$ in aprotic solvents is slower than the reduction of Ar to $Ar^{-\bullet}$, where Ar is a large aromatic molecule like anthracene.

The effect of solvent on an electron transfer is larger than simply through its energetic contribution to outer reorganization, λ_o. Previous literature[144] have shown strong evidence that the dynamics of solvent reorganization (usually represented by a solvent longitudinal relaxation time, τ_L) contribute to the pre-exponential factor，for example, $\nu_n \propto \tau_L^{-1}$.

$$\nu_n = (2\pi\tau_{rot})^{-1}$$

Since τ_L is roughly proportional to the viscosity, such inverse proportionality implies that the heterogeneous rate constant would decrease as the solution viscosity increases, or, in other works, as the diffusion coefficient of the reactant decreases.

4. A particularly interesting prediction from this theory is the existence of an "inverted region" for homogeneous electron-transfer reactions arising from the quadratic variation introduced in the Marcus Model.

1.2.2 Measurement methods

1.2.2.1 Fast scan rate cyclic voltammetry

Extraction of electron transfer kinetics from cyclic voltametric signals considering an outer-sphere one electron-transfer reaction on electrode surface with redox species freely moving in solution:

$$A + e \rightarrow B$$

We are focused here on how to use cyclic voltammetry technique to characterize the kinetics of a reaction. Let's take the reduction of A, which is the only reactant and produce B as an example. In an unstirred solution, the reactants move to the electrode surface only by diffusion, and then receives an electron from the electrode to form products. Finally, the products diffuse to bulk solution from the electrode surface. The electrochemical responses depend on both the rate of electron transfer and the rate of diffusion for redox species in solution. In this case, the important point is not the electron transfer being fast or slow in absolute but being fast or slow relative to

diffusion. This reference to diffusion entails the introduction of dimensionless parameters Λ:

$$\Lambda = k\sqrt{\frac{RT}{FvD}}$$

Where *k* is the rate constant and D is the diffusion coefficient of redox species.

To extract rate constant from cyclic voltammogram, we first start from the equation of current at equilibrium:

$$\frac{i}{FS} = k_f(C_A)_{x=0} - k_b(C_B)_{x=0}$$
$$= k_f\left\{(C_A)_{x=0} - (C_B)_{x=0}exp\left[\frac{F}{RT}(E - E^0)\right]\right\}$$

By replacing $(C_A)_{x=0}$, $(C_B)_{x=0}$ by their expressions as a function of the current and then introduce the normalized dimensionless parameters, we obtain the following normalized expression of the cyclic voltammograms:[97]

$$\frac{\psi exp(-\alpha\xi)}{\Lambda} + \frac{1 + exp(-\xi)}{\sqrt{\pi}}\int_0^\tau \frac{\psi}{\sqrt{\tau - \eta}}d\eta = 1$$

Where ψ, ξ, τ are normalized current, potential, and time functions.

The normalized current-potential curves are thus a function of the two parameters Λ and α. Considering a common situation of α=0.5 which means the cathodic and anodic curves are symmetric around the standard potential, we could calculate the different cyclic voltammograms as function of the parameter Λ. As mentioned above, the dimensionless parameter Λ is inversely proportional to the square root of scan rates, so we could adjust the cyclic voltammogram by simply varying the scan rate. In the reversible domain, the peak potential which is close to the formal potential is independent to the scan rate. As soon as the redox system is not reversible, the cathodic peak shifts to negative potentials, the higher the scan rates are, the larger are the shifts while the anodic potential varies in the opposite direction, see Figure 1.11. The peak potential of cathodic and anodic vary as the following equations:[97]

$$E_{p,c} = E^0 - 0.78\frac{RT}{\alpha F} + \frac{RT}{\alpha F}\ln\left(k^0\sqrt{\frac{RT}{\alpha FvD}}\right)$$

$$E_{p,a} = E^0 + 0.78\frac{RT}{\alpha F} - \frac{RT}{(1-\alpha)F}\ln\left(k^0\sqrt{\frac{RT}{(1-\alpha)FvD}}\right)$$

As the formal potential is known, the peak potential offers an easy access to the standard rate of electron transfer by application of the equations above. The measurable range of rate constant is thus dependent on the maximal available scan rates. High scan rates without the influence of the ohmic drop on the electrochemical response could be reach by using a potentiostat equipped with a positive electronic compensation or using an ultra-microelectrode.

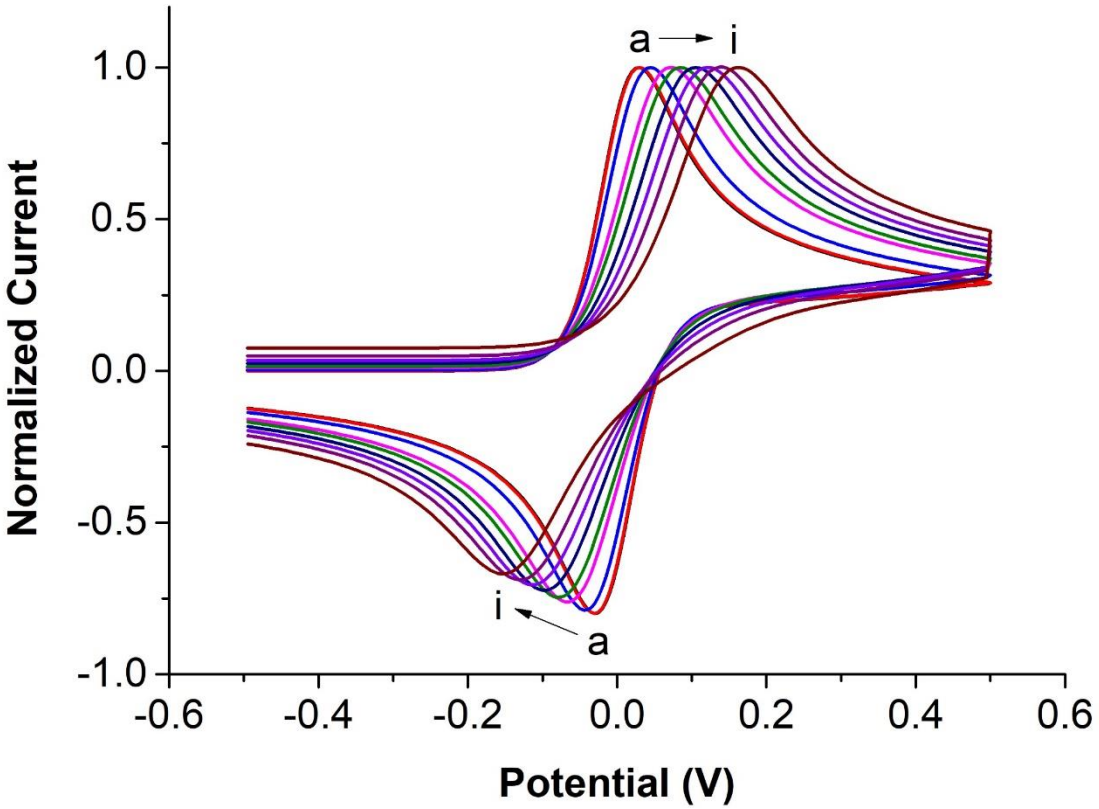

Figure 1.11. Simulation cyclic voltammogram of one-electron transfer process. simulation parameters: k_S=0.5 cm·s^{-1}, C°=2·10^{-3} mol·L^{-1}, d=1 mm, D=3·10^{-5} cm^2·s^{-1}, Ru=0 Ω, Rc=6.7·10^{-9}, T=298.15 K. Scan rate (a) 0.1 (b) 1 (c) 100 (d) 1000 (e) 2000 (f) 5000 (g) 10000 (h) 20000 (i) 50000 V/s.

Although the precise equation could be obtained in limiting kinetics situations, it is difficult, or seems impossible, to get the analytical solution of this equations and people rarely do like this. In practice, digital simulations are the easiest methods to solve this kind of problem in the general case. Commercial computer programs, such as, DigiSim,

ELSIM, CVSIM, and KISSA, are available for some methods.

The main strategy adopted in studying a reaction is to systematically change the experimental variable controlling the characteristic time of the technique (e.g., scan rate, rotation rate, or applied current) and then to determine how the characteristic potentials vary. Here, we changed the scan rate (v) and then measured the peak potential difference ($\Delta E_p = E_{p,a} - E_{p,c}$) of the reversible reaction and make the curves of $\Delta E_p \sim \log(v)$. By fitting of the experimental curves to the theoretical one $\Delta E_p \sim -2\ log_{10}(\Lambda)$, one could get the standard electron transfer rate constants. This method will be used to extract standard rate constant in the thesis.

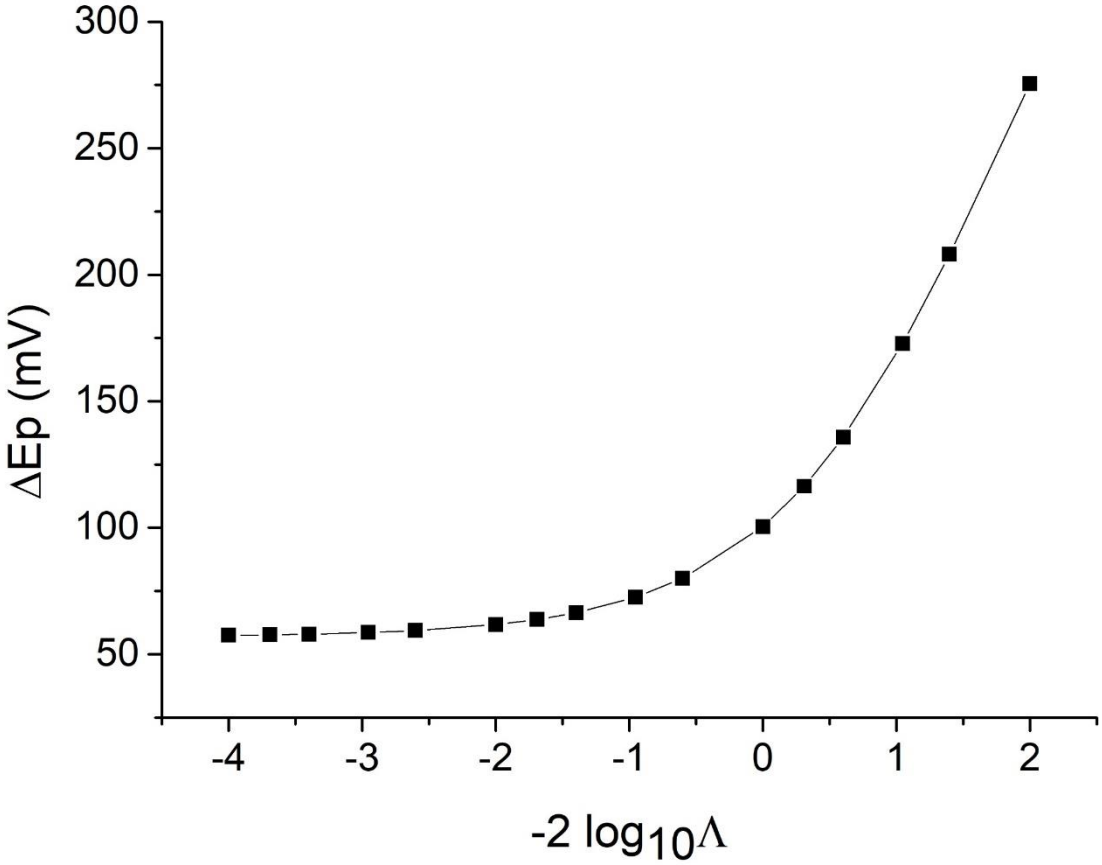

Figure 1.12. Theoretical curve of peak to peak separation ΔEp as a function of longitudinal dimensionless parameter, Λ.

1.2.2.2 Other methods

Other methods or techniques, such as Nicholson approach[145], scanning electrochemical microscopy (SECM)[146], large-amplitude Fourier transformed

alternating current (FTAC) voltammetry[147], and semi-integrative voltammetry[98], could also be used to extract rate constant from heterogeneous electron transfer reaction. Nicholson approach extracts the rate constant from cyclic voltammetry by peak potential separation and frequency. This is a rapid and simple way to get electrode kinetics but failure to take into account the uncompensated ohmic potential drop in the theory, results in a large underestimate of the electrode kinetics.[148] SECM, like fast scan rate cyclic voltammetry, also use simulation methods to get the value of rate constant of a reaction. But unlike transient cyclic voltametric techniques, it is generally used as a steady-state technique. This method could be well used in molecular solvents as Acetonitrile[149, 150] but it remains difficult to approach a true steady state behavior in high viscosity solvents, such as, a ionic liquid[151] or a deep eutectic solvent. Indeed, an electrode with very small radius (in nm scale) would be required to reach a full steady-state. In these cases, mass transfer rates could be highly enhanced by creating nanometer-size gaps or nano-electrodes, thereby fast ET kinetics could be reliably studied.

Large-amplitude Fourier transform alternating current (FTAC) voltammetry[152] provides a powerful technique for the quantitative investigation of both diffusional and surface-confined electrochemical processes. In this ac method, the nonlinear higher harmonic components are enhanced by the use of a large-amplitude as perturbation added to the dc waveform and are highly sensitive to the electrode kinetics, but relatively insensitive to the background charging process. Literatures using this technique to measure electrode kinetics rate constant is available [153-155]

Semi-integrative voltammetry is a robust analytical method that involves transforming a transient peak-shaped voltammogram which obtained under conditions where mass transport occurs by semi-infinite planar diffusion into a form which closely resembles a steady-state voltammogram. This technique shares the same advantages as the directly experimentally based steady-state techniques, but it based on data recorded under transient conditions.

1.2.3 Dynamical solvent effects

As we explained in section 1.2.1.3, variation of the rate constant from one system to another can be treated by considering the changes in the reorganization energies which consist of two parts: the solvent (i.e., outer-shell) reorganization and the reactant intramolecular (i.e., inner-shell) distortion reorganization. When the changes in the internal structure of the reactant are minor factor, the solvent dynamics properties become the main factor to the electron transfer kinetics. That is the so-called solvent-controlled kinetics. This type of reactants is most on metallocene redox couples in the form of $Cp_2M^{+/0}$ (where Cp = cyclopentadienyl and M = Fe, Co, or Mn) that present small inner-shell barriers and often small double-layer effects upon the electrochemical rate constants.[156-158]

When both the outer-shell and inner-shell reorganizations are not negligible, the solvent dynamics can also create important influences on the rate constant. The anticipated nature of the effects are often quite different from the solvent- controlled kinetics. An excellent review of this case can be found.[159] The author gives some instructive comments on the unresolved issues and future directions. Here we don't try to use theoretical aspects of dynamical solvents effects to describe and elucidate the experimental one, but give some examples that using experimental data to test the specific aspects of the theoretical framework.

One simple approach involves correlating solvent-dependent rate data for electron exchange with the solvent viscosity. One study found that the rate constants of two different electrode reactions $Fe(CN)_6^{3-/4-}$ and ferrocene/ferrocenium increased with decreasing the viscosity by dissolving electrochemically inactive materials in the solvents (dextrose in water and sucrose in Me_2SO).[160] Similar result was found in the heterogeneous electron transfer kinetics of Ferrocene-methanol in Me_2SO-water mixtures.[161] These examples indicate that the heterogeneous rate constant would decrease as the solution viscosity increases.

A general limitation of experimental studies is that often the range of explored ET reaction types remains relatively narrow, being restricted almost entirely to out-sphere

electron exchange processes.[159] It would be of particular interest to examine inner-sphere ET and intramolecular ET processes with regard to solvent dynamical effects.[159, 162] The study of solvent dynamics effects on electron transfer in DES are rare now, but the solvent dynamics of wet Ethaline was investigated recently.[66, 163] The relaxation time constants at different water contents shown that very small amounts water (< 1 wt%) actually slow the solvent down and only when water amounts > 1 wt% the relaxation time can decrease. We could found the solvent dynamics effects on the out-sphere reaction and the Non-Marcus behavior for $Fe(CN)_6^{3-/4-}$ couples in Chapter 3.

1.2.4 The influence of hydrogen-bonding to electron transfer

In electrochemistry, the influence of hydrogen-bonding to electron transfer often makes the standard formal potential lower[164] and the electron transfer easier.[165-167] The hydrogen-bonding effect on electron transfer in organic solvents was initially investigated by Smith and her colleagues[168] and then, Gupta and Linschitz show that intermolecular hydrogen bonding can have a significant effect on electron transfer (ET) in organic solvents.[169] In their paper, the authors investigated the cyclic voltametric (CV) behavior of a series of quinones of increasing basicity in the presence of H-donors of varying strength in organic solvents of different polarity. With increasing concentrations of additives, three clearly different types of electrochemical behavior are observed for weakly, moderately, and strongly interacting quinone-additive pairs. With the weak H-donor, they observed a large shift in the second reduction wave towards more positive potentials but with small positive shift in the potential of the first peak. This behavior indicates a degree of stabilization of the radical anion by ethanol, making the first electron transfer slightly easier, and strong stabilization of the dianion, making the second electron transfer considerably easier. Similar behavior can be seen in Figure 1.13 with the reduction of duroquinone in methanol/acetonitrile mixtures.[170]

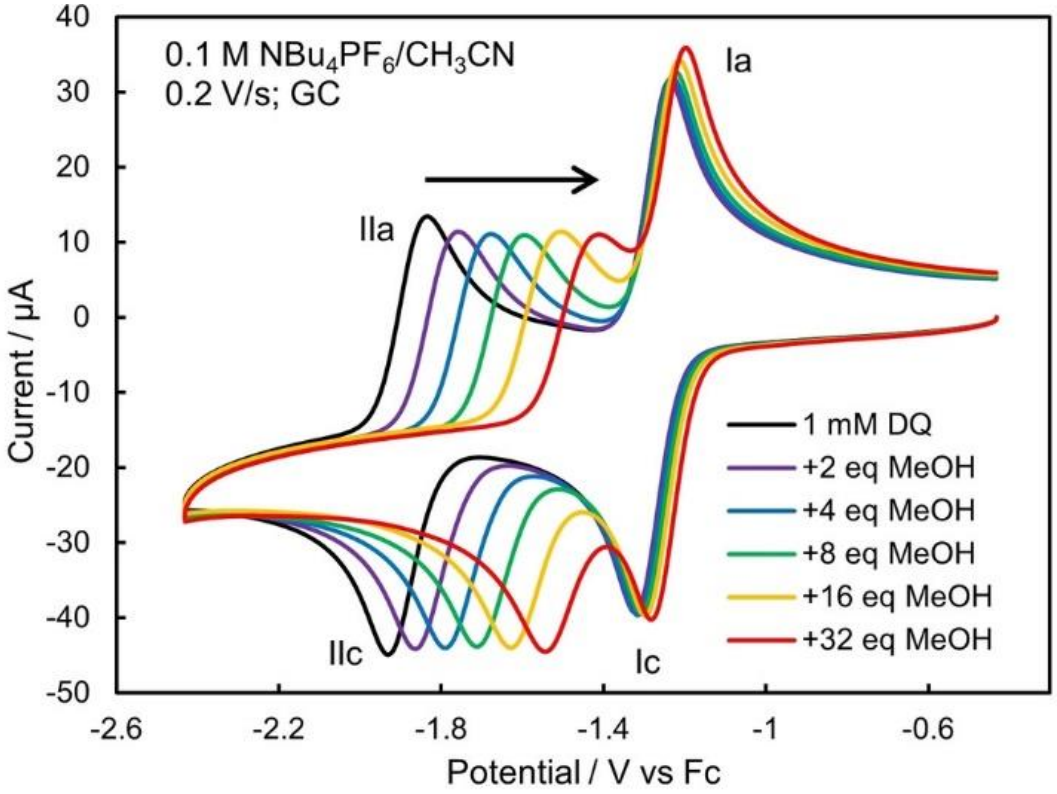

Figure 1.13. Background-substracted CV's of 1 mM duroquinone, DQ, in 0.1 M NBu_4PF_6/CH_3CN with additions of methanol.[170]

The hydrogen-bonding effects on the shift of formal potential[164, 171-178] and ET rate constant[165] has widely investigated. Webster et al.[164] have investigated the hydrogen bonding effects on the electrochemical properties of Phenols and Quinones in organic solvents with increasing water amount. The results show that small changes in what is often considered "trace" amounts of water, were sufficient to considerably change the potential and in some cases the appearance of the voltametric waves observed during the oxidation of the phenols/hydroquinones and reduction of the quinones. Another article from the same group also found the hydrogen bonding effects on tuning the reduction potential of quinones by addition of varies amount of organic acid.[171]

Having established that hydrogen bonding donors (HBD) could exert a strong influence on the thermodynamics of ET, HBD can similarly affect ET kinetics.[165-167] Electron transfer between ortho-chloranil and ferrocene (Fc) derivatives was promoted in the presence of HBDs and further demonstrate that these HBDs can be used as catalysts in a quinone-mediated model synthetic transformation.[165] electron transfer reduction of p-benzoquionesby cobalt tetraphenylporphyrin is enhanced significantly by the

presence of hydrogen bond donor due to the hydrogen bond formation between the semiquinone radical anions and hydrogen bond donor.[167]

Except quinones, other organic molecule like p-phenylenediamine, were also used for investigating the hydrogen-bonding effects on electron transfer and intermolecular proton-coupled electron transfer (PCET).[172, 173, 179]

These effects can be found in the reduction of quinones and dinitroaromatics in Chapter 4 and Chapter 5, respectively.

1.2.5 Potential inversion

For a given molecule, the heterogeneous electron transfer from electrode to the molecule can be simply one electron, the simplest example is the oxidation of ferrocene. But it could also accept/remove two or more electrons depending on the molecular structure and the functional groups that are present. There can be a system containing two identical functional groups that will give rise to reduction/oxidation steps occurring at two resolvable potentials. For example, p-dinitrobenzene has stepwise two electron transfer in acetonitrile due to its two nitro groups.[180] For molecules of appropriate structure, the insertion (or removal) of three-, four-, five, or six-electrons can be detected. For example, C_{60} and C_{70} have the stepwise six-electron reduction.[181]

Electrochemical reduction of neutral compounds in nonaqueous media generally proceeds in successive steps, the first forming the anion radical, the second the dianion, etc. For example, in reduction, the individual standard potentials occur at increasingly negative values as it becomes energetically more and more costly to insert electrons into already negatively charged species. Two steps of reduction are defined for electron acceptor A in the equation below:

$$\mathrm{A} + e^- \rightleftharpoons A^{-\bullet} \qquad E_1^{0\prime}, k_{s,1}, \alpha_1$$

$$A^{-\bullet} + e^- \rightleftharpoons A^{2-} \qquad E_2^{0\prime}, k_{s,2}, \alpha_2$$

$$2A^{-\bullet} \rightleftharpoons A + A^{2-} \qquad \Delta G_{disp}^0, K_{disp}, k_{f,3}, k_{b,3}$$

$$\ln K_{dist} = -\frac{\Delta G_{dist}^0}{RT} = -\frac{F}{RT}(E_1^0 - E_2^0)$$

where $E^{0'}{}_j$, $k_{s,j}$, and α_j are the formal potential, standard heterogeneous electron-transfer

rate constant, and transfer coefficient of step *j*. Reaction 3 is the disproportionation of the anion radical, a process that could affect the electrochemical response under some conditions. The formal potential, $E^{0'}_j$, is defined for a given ionic strength and solvent. The effect of solvation is mainly seen in the energetics of disproportionation reaction, whose equilibrium constant, K_{dist}, and standard Gibbs energy, ΔG^0_{dist}, changes are related to the difference in standard potentials. The situation in which $E^0_1 - E^0_2$ is positive for reduction or negative for oxidations has been called normal ordering of potentials. It is characterized by the addition or removal of the second electron occurring with more difficulty than the first. The separation in standard potentials is quite variable, ranging from about 0.1 V to over 1 V. By contrast, there are many examples where $E^{0'}_1 - E^{0'}_2 < 0$, i.e., insertion of the second electron occurs with greater ease than the first, a situation that has been called "potential inversion".

The underlying causes of potential inversion can be traced to structural changes that accompany one or both electron transfer steps. In some cases, the structural changes that accompanied the electron transfer have been characterized. It has been found that, for reductions, the structural changes have the effect of lowering the LUMO energy thus aiding the insertion of the second electron. Calculations indicate that the planar form in the neutral compounds is converted to a boat form in the dianions.[182] Another example of structure changes derived potential inversion from calculation is trans-2,3-dinitro-2-butene.[183]

In addition to structure changes, there are also other factors that could be dominant, for example the medium (solvent and electrolyte) both by changes in solvation energies of ionic partners in the redox couples and by ion pairing, the interaction of an ion of the electrolyte with substrate ions. The example of this kind is the oxidation of $Rh_2(TM4)_4^{2+}$ (TM4 presents 2,5-diisocyano-2,5-dimethylhexane) in CH_2Cl_2 with 0.1 M tetrabutylammonium salts with various common electrolyte anions.[184] The potentials for the overall two-electron oxidation show normal ordering with PF_6^- < SbF_6^- < $TFPB^-$ (tetrakis[3,5-bis(trifluoromethyl)phenyl)]borate). However, inversion occurs with BF_4^- (+172 mV), ClO_4^- (+191 mV) and a very strong value with Cl^- (+354 mV). Other examples can be find from ref[185] and ref therein. A more recent publication from

Evans et al. shows that the effects of ion pairing are rather modest, 100 mV or less, for 1,4-dinitrobenzene and 2,5-dimethyl-1,4-dinitrobenzene in aprotic solvents.[186] Hydrogen-bonding can also play a crucial role in the observation of potential inversion. Chung et al.[187] reported an important example of hydrogen-bonding derived potential inversion of N,N,N'-triphenylphenylenediamine (PD-1). As shown in Figure 1.14, when 2,4,6-trimethylpyridine is added to the solution of PD-1, the CV exhibits a transform from two oxidation process to one which has different formal potential to both the initial two oxidation peaks. And the value of $E^0_1 - E^0_2$ change from negative to positive, which means potential inversion occurs. We could found these factors, such as, structure, ion-pairing, and hydrogen-bonding, in the reduction of 1,4-dinitrobenzene in Chapter 5.

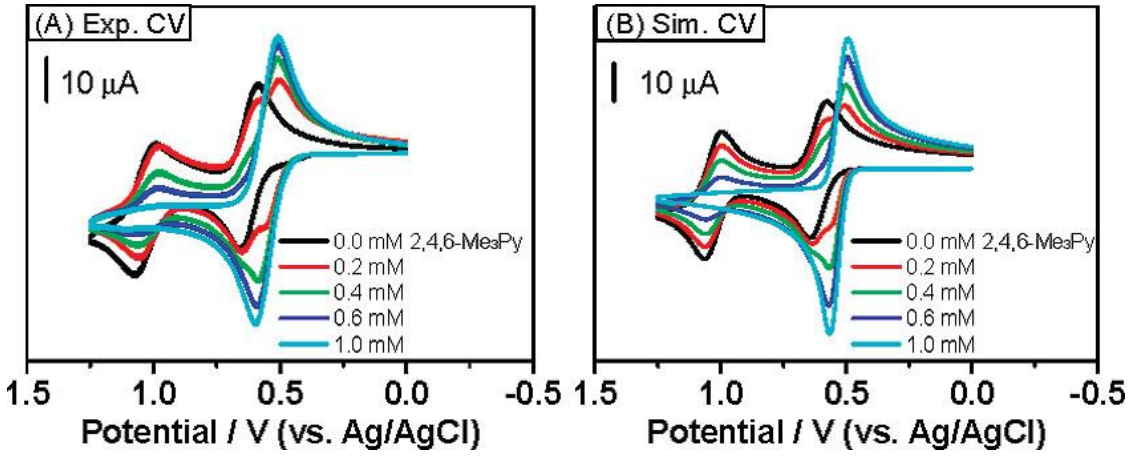

Figure 1.14. (A) experimental and (B) simulated CVs of 1 mM PD-1 in acetonitrile containing 0.1 M TBAP and various concentrations of 2,4,6-trimethylpyridine. Scan rate 0.1 V/s.[187]

Concerted two-electron transfers. For a two-electron process with potential inversion, the inverted potential, $E^0_1 - E^0_2$, is could be as high than a few hundred millivolts (0 to about 0.3 V). Thus, the reaction of the second electron transfer must be fast, so fast that one may wonder if the two electrons are added concertedly rather than sequentially. The possibility of concerted two-electron transfer reactions has been widely considered in the literature, both in theoretical treatments[188-190] and in more phenomenological discussions[191] and it is generally agreed that such reactions are possible. Detailed discussion can be found in the review of Evan[192]. The author concludes that for mild

inversion, the intermediate can often be detected by independent methods ruling out a concerted two-electron transfer. Only in a stronger potential inversion situation, the concerted process becomes more likely.[192]

1.3 Objectives

While DESs are more complex in nature than single-component solvents due to the interactions between the DES components, they present tunable properties, such as physicochemical characteristics including viscosity, density, hydrophilicity and solubility, and their hydrogen-bonding and ionic solvent environment, thermal stability. They possibility as electrolyte in energy storage and specific electrochemical properties are attracting increasing interest in this field. How such special class of solvent could influence the thermodynamics and kinetics of electron transfer are not clear?

This thesis in the framework of fundamental researches contributes to the exploration of electron transfer kinetics and thermodynamics in DES which including single electron transfer and successive two electron transfers.

The continuing interest in electron transfer has many factors: first, to get fundamental kinetics data in a new solvent or trying to obtain more reliable measurements by minimize the uncompensated ohmic drop in solution; secondly, to examine various electron transfer theory[193, 194] and investigate the effects of solvent dynamics[159, 195] and finally, to get the mechanism or elucidate more complexed electron transfer process, such as, multi-electron transfers and proton coupled electron transfer.

As discussed above, the thermodynamics and the kinetics of a single electron transfer reaction could be different when changing from one solvent to another.[32] However, what are the factors that govern the variations of the standard potential ? What are the parameters that determine the rates of heterogeneous or homogeneous electron transfer reactions ?[192]

For a two separate electron transfer process, the typical observation is that addition or removal of the second electron occurs with a greater difficulty than the first one. The

potential separation is mainly due to electrostatic factors. For a neutral molecular reduction reaction, the second reduction is more difficult because an electron is being added to a species that already bears a negative charge whereas in the first reduction the reactant is neutral. This situation is called normal ordering of potential. However, there are some instances that the second electron transfer being easier than the first one. These are examples of potential inversion.[182] Although this subject has been extensively investigated, there are new cases appearing continually. One could always wonder what the factors responsible to the potential inversion are.

As we focus on the type 3 DES which consist of hydrogen bond donor and hydrogen bond acceptor. The hydrogen-bonding effect on the electron transfer are particularly considered.

The objective of this thesis is to explore the electron transfers in deep eutectic solvents and answer the fundamental questions mentioned above in this case. Due to the high viscosity of DES, high scan rate cyclic voltammetry will be used to extract the rate constant in it. In this context, solvent dynamics effect on electron transfer were also considered. For a two- electron transfer systems, solvent effects on the formal potential difference will also be examined in this work.

Chapter 2 Electron transfer kinetics in a deep eutectic solvent

Parts of this chapter 2 and main results have been published in J. Phys. Chem. B 2020, 124, 6, 1025-1032.

2.1 Introduction

As discussed in Chapter 1, Electron transfers (ET) rate constant are a key parameter for most of the envisaged electrochemical applications. For example, ET rates strongly influences the response time of sensor or the current density in an energy storage device. Interest of ET studies in DES is not limited to electrochemistry because the analysis of the charge transfer kinetics provides information about the solvation of a solute. In the framework of the Marcus-Hush theory[144, 196-199], the electron transfer kinetics is for a large part driven by the dynamics and solvent reorganization that accompany the electrochemical process[97, 144, 198, 199]. Numerous publications have addressed this question in ionic liquids (see for example references[32, 200-203]) and only recently in DESs.[93, 94, 98, 100, 204, 205] The situation is quite different in the two media. In ionic liquids, ET are considerably decreased when passing from a classical organic solvents to a ionic liquid, generally by a ratio 10-100 depending on the outer-sphere character of the electron transfer.[32, 198, 199, 201-203] Concerning the DES, well-defined cyclic voltammograms in Ethaline or Reline were reported for "outer-sphere redox" couple like ferrocene/ferrocenium[93, 94, 200, 204, 205] but also for highly charged couple like ferro/ferricyanide,[93, 200] suggesting the occurrence of fast electron transfers. Notice that recent reports have reached a different conclusion. The standard electron transfer rates constants k_s were reported to be significantly lower in DES (below 10^{-3} cm s^{-1}) than in molecular solvents and in the same range or below the values reported in ionic liquids.[94, 200, 204, 205] In a recent publication, Akolkar *et al.* have highlighted the possible difficulties and pitfalls in such kinetics measurements performed in DES. They

explained the need of an accurate treatment of the uncompensated ohmic drop. Accurate characterizations of fast electron transfer kinetics require the use of short experimental times, meaning high scan rates in transient cyclic voltammetry.[97, 143, 206] Despite the relatively good conductivity of DES, their inherent conductivities remain lower than those reported in classical organic or aqueous electrolytic solvents and their viscosities are generally higher.[4] A lower conductivity means a higher resistance of the solution and thus larger distortions due to the ohmic drop, R_uI (where R_u is the uncompensated resistance at the working electrode connection that contains all sources of resistances between the working electrode and the tip of the reference electrode and I is the current passing through the working electrode). Because, the current in cyclic voltammetry increases with the scan rate, the ohmic drop becomes a major problem when high scan rates are required.[206] Additionally, the larger viscosity of DES results in lower diffusion coefficients of the solubilized redox couples and in a lower mass transfer rates from the solution to the electrode. For this reason, in chapter 2, we use high scan rates for measuring a large standard electron transfer rate constant, k_s in DES. If we combine all these difficulties due to the low conductivity of DES and the small diffusion coefficients of solute in DES, accurate examination of a fast electron transfer in such media is a challenging task.

Briefly, there are two general approaches for considering the ohmic drop in electrochemical methods.[143, 206] The first ones rely on post-treatment corrections by full simulations of voltammograms or are based on semi-integral and potential scale correction, impedance spectroscopy including the ohmic drop. Post-treatment techniques generally require an independent measurement of R_u and could be long to obtain if multiple parameters are needed in the treatment.[97, 143] The properties of the working and the reference electrodes must remain perfectly stable during the experiments, which could be difficult to achieve in some experimental situations.[98, 207] A second type of approach is based on the direct corrections of the ohmic drop by using a potentiostat equipped with an electronic ohmic drop compensation circuit (positive feedback) or by simply using a microelectrode to decrease the ohmic drop.[208, 209] In similar situation, we used these different approaches that present their own advantages

and inherent difficulties.[206] A large amounts of literature exists about the conditions needed for obtaining an efficient ohmic drop compensation [208, 209] or more specifically about difficulties in DES investigations.[210] We could also emphasize that the influence of the ohmic drop on a recorded voltammograms could be difficult to detect on a single curve. Then, the characteristics of the cyclic voltammograms could incorrectly be ascribed to a slow ET rate, particularly when the measurement is made at a single scan rate or in a too narrow range of scan rates.[206]

In this chapter, we chose the methodology based on direct electronic compensation and a millimetric electrode. This permits an immediate view of the corrected curves and does not required a separate measurement of R_u when the conditions of bandpass of the potentiostat and cell times are respected. Using a millimetric electrode offers more choice of electrode materials than a microelectrode, notably for carbon electrodes. Glassy carbon (GC) electrodes were used in this study. GC is a well-adapted electrode material for electrochemical analysis in DES notably because of the stability of GC and the high electrochemical windows in a medium that could contain high quantity of water.[211] We used a 1-millimeter diameter glassy carbon electrode as a working electrode. Electron transfer kinetics were investigated for two redox couples, ferrocene/ferrocenium and ferrocyanide/ferricyanide in a widely used DES, Ethaline, which is a 1:2 mixture of choline chloride and ethylene glycol. We chose these two common redox couples that are often considered as standard couples. They present different charges, ferrocyanide ion or $[Fe(CN)_6]^{4-}$ is four times negatively charged and prone to specific interactions with the cation of the DES as observed for negatively charged species in the ionic liquids.[201, 212, 213] As discussed in several publications, the presence of chemical moieties on the surface of GC electrode could also influence the ET kinetics notably in the case of $[Fe(CN)_6]^{4-}$. [211]For a better comparison between experiments, all experiments were performed with the same GC electrode that was prepared and cleaned in the same manner.

Residual water could play a major role in the properties of DES even if the effect is not totally understood; so all experiments were made with a careful control of the residual water and after drying the DES as much as possible (typically residual water

measured by Karl-Fischer coulometric technique is less than 0.5 wt % (around 0.31 mol L^{-1}). Effect of water on ET kinetics will be treated in the following chapter (Chapter 3).

2.2 Experimental Section

2.2.1 Electrochemical Measurements

Electrochemical measurements were performed with a home-built potentiostat using a conventional 3-electrode setup and allowing a fast electronic compensation of the ohmic drop.[208, 209] The counter-electrode was a large Pt wire and the working electrode a 1-millimeter diameter glassy carbon disk electrode. The reference electrode was a quasi-reference electrode made with an Ag wire.

Faradaic peak current, I_p was measured after correction of the baseline that was estimated under the faradaic peak by a linear extrapolation of the background current determined at the beginning of the voltammogram. Diffusion coefficients D were derived assuming a reversible electron transfer at low scan rate using $I_p = 0.446\, FSC^{\circ}\sqrt{D}\sqrt{\frac{Fv}{RT}}$ (F is the Faraday constant, S the electrode surface area, C the initial concentration of the redox couple, R the gas constant, v the scan rate and T the absolute temperature).[97, 143] In all experiments, the peak current I_p was found to vary linearly with the square root of the scan rate. Such results demonstrate a linear diffusion process for the mass transport to the electrode. Apparent heterogeneous electron transfer standard rate constants, k_s, were extracted from the variation of ΔE_p versus the scan rate considering the Butler-Volmer law[97] and uncorrected from the double layer effect. Working curves for the variation of the ΔE_p were calculated as a function of the dimensionless parameter $\Lambda = \frac{k_s}{\sqrt{D}}\sqrt{\frac{RT}{aFv}}$ using the Kissa 1D package developed by C. Amatore and I. Svir and taking transfer coefficient α as 0.5 [214] because working curve

just change a little from α = 0.3 to 0.6 when the system is reversible or quasi-reversible, See Figure 2.1.

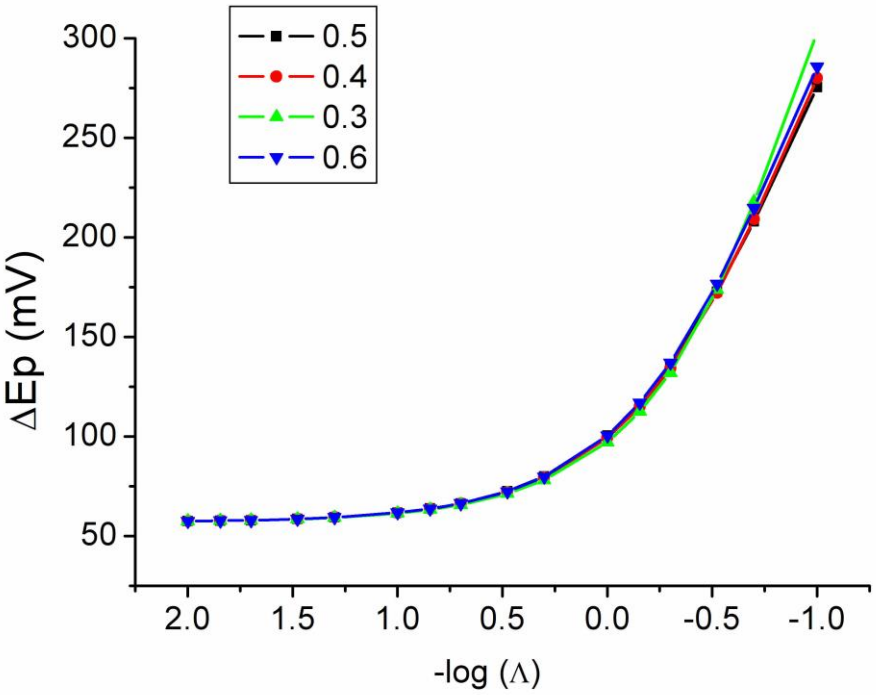

Figure 2.1 Theoretical variation of the peak to peak difference potentials as function of the dimensionless parameter $\Lambda = k_s/D^{1/2}$ $(RT/Fv)^{1/2}$ calculated for different values of the transfer coefficient α assuming a Buttler-Volmer law. Inversion potential is set as 500mV after the E °.

Single parameter adjustment of the theoretical curve with the experimental data provides the value of $\frac{k_s}{\sqrt{D}}$ and then of k_s using the D value derived from the variation of I_p with $v^{1/2}$. We show the original voltammograms with the potential scale versus the quasi-reference electrode on Figures 2.3 and 2.7 to show the quality of the data and for an easier comparison of the data with literature. Notice that the measurement of the rate constant k_s only requires the measure of the peak-to-peak difference ΔE_p and not of the absolute peak potential and that we do not extract $E°$ from this experiments. The procedure is thus almost insensitive to a possible drift of the potential of the Ag quasi-reference electrode but presents the advantage of using a low impedance reference electrode.

As reported and discussed in several publications, the kinetics of the electron transfer for a molecule like ferrocyanide is sensitive to the surface state of the carbon electrode. To maintain a similar surface state on a series of measurements, the working electrode was just cleaned for each series of voltammograms. Each voltammogram was recorded at least 3 times and averaged allowing an estimation of the error on E_p around ± 5mV.

2.2.2 Potentiostat with Ohmic Drop Compensation

We used a homemade potentiostat equipped with a positive feedback electronic compensation following an adder scheme[143, 209] that has been published before and used in several studies. Potentiostat was built with Burr-Brown OPA111AM Low Noise Precision operational amplifiers. Potential scan and signal digitalization were controlled by a PC-computer equipped with a fast National Instruments DAQ card and a SCB-68 block for digital data acquisition. As discussed before, when the band pass of the potentiostat circuit using the ohmic drop compensation is much below than the electrochemical cell-time, over-compensation is not possible as the system oscillates when R_u tends to zero.

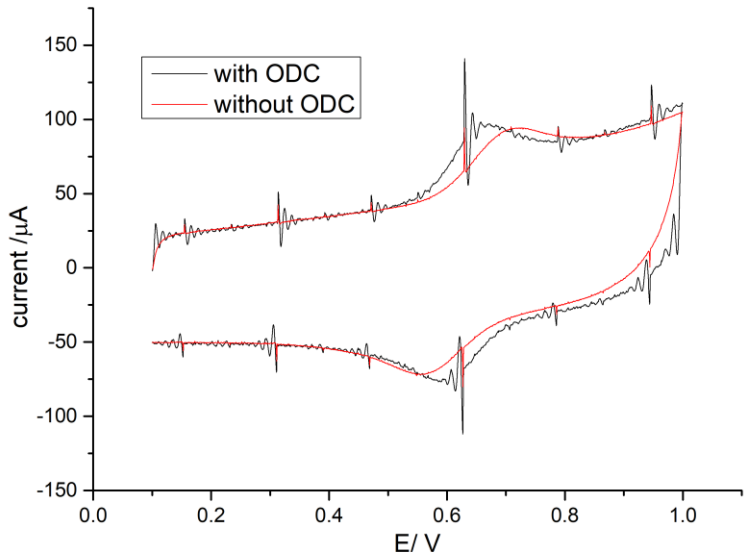

Figure 2.2 Comparison of cyclic voltammograms of 2 mM ferrocene in Ethaline at 100 V/s between with ohmic drop compensation, black line, and without ohmic drop compensation, red line.

Ag wire used as the reference electrode. T= 20 ℃.

This procedure avoids an independent measurement of the uncompensated resistance R_u and allows readjusting the compensation in case where the characteristics of the working electrode have been modified.

Figure 2.2 depict the effect of the ohmic drop on the shape of CV including both peak potential difference ΔE_p and peak current I_p and reveals a higher distortion of ΔE_p and I_p. The displacement of ΔE_p and I_p can disrupt the determination of the kinetic parameters and diffusion coefficient, respectively. This indicate the compensation of the ohmic drop come from solvent resistance and electrode itself is a key factor to extract electron transfer kinetics in deep eutectic solvents and our homemade potentiostat works well for the compensation.

2.2.3 Chemicals

Ferrocene, potassium ferrocyanide and potassium ferricyanide were of the highest available purity grade from commercial source (Aldrich) and used without further purification. Ethaline was prepared separately by mixing the two components of Choline chloride and ethylene glycol in a molar ratio 1:2 and heating at 60 ℃ with a magnetic stirrer until a homogeneous liquid formed.[2] Solutions in Ethaline were prepared by heating the solution with a gradual increase of the temperature up to 60 ℃ in an ultrasonic bath. We found that the redox probes concentrations around 3 x 10^{-3} mol L^{-1} are accessible without the appearance of a precipitate when the solution was cooled down to room temperature. Such concentrations were sufficient to record currents with a good ratio between the signal and background currents and noise.

Potassium ferricyanide or ferrocyanide are not well soluble in ionic liquids and the use of other salts are required like $BMP_3[Fe(CN)_6]$ where BMP is 1-butyl-1-methylpyrrolidinium. $BMP_3[Fe(CN)_6]$ was prepared according to a procedure derived from literature[212, 213] starting from the Ag salt. Briefly, $Ag_3[Fe(CN)_6]$ was prepared by treating $K_3[Fe(CN)_6]$ (1 eq., dissolved with 2-3 mL water) with $AgNO_3$ (3-4 eq.) in methanol and stirred overnight at 30 ℃. $BMP_3[Fe(CN)_6]$ was then obtained by cation

exchange between $Ag_3[Fe(CN)_6]$ and BMP-Br in methanol by stirring overnight. The process was followed by change of the color of the solution from brown to green. Then, the reaction mixture was concentrated under reduced pressure; the resulting precipitate was filtered and dried under vacuum overnight. Ethaline was prepared from commercially available compounds obtained from Aldrich according to general published procedures.[94, 204] Mass fraction of residual water was measured by using a coulometric Karl-Fischer titration (831KF Coulometer – Metrohm and using Hydranal® Coulomat E solution from Fluka) for each sample and after each series of experiments and was found less than 0.5 wt % (around 0.31 mol L^{-1}).

2.3 Results

The ET rate constants of two classical redox couples, ferrocene and ferrocyanide, were extracted from the cyclic voltammograms. The ohmic drop in solution was carefully compensated in this process as discussed above.

2.3.1 Ferrocene Oxidation in Ethaline

The cyclic voltammograms (CVs) of Ferrocene/ferrocenium couple in Ethaline were recorded on a home-made potentiostat which equipped online electronic compensation components from 0.1 to 400 V/s. As seen on Figure 2.3, typical voltammograms of ferrocene oxidation in Ethaline shows a reversible electron transfer process at low (0.5 and 2 V s^{-1}) and high scan rates (25 and 200 V s^{-1}). Experiments at different concentrations (1, 2, and 3 mM) and temperatures were also record to test the stability of our home-made potentiostat and the quality of the whole procedure for correcting of the ohmic drop. Similar values of ΔEp were obtained for all the considered concentrations.

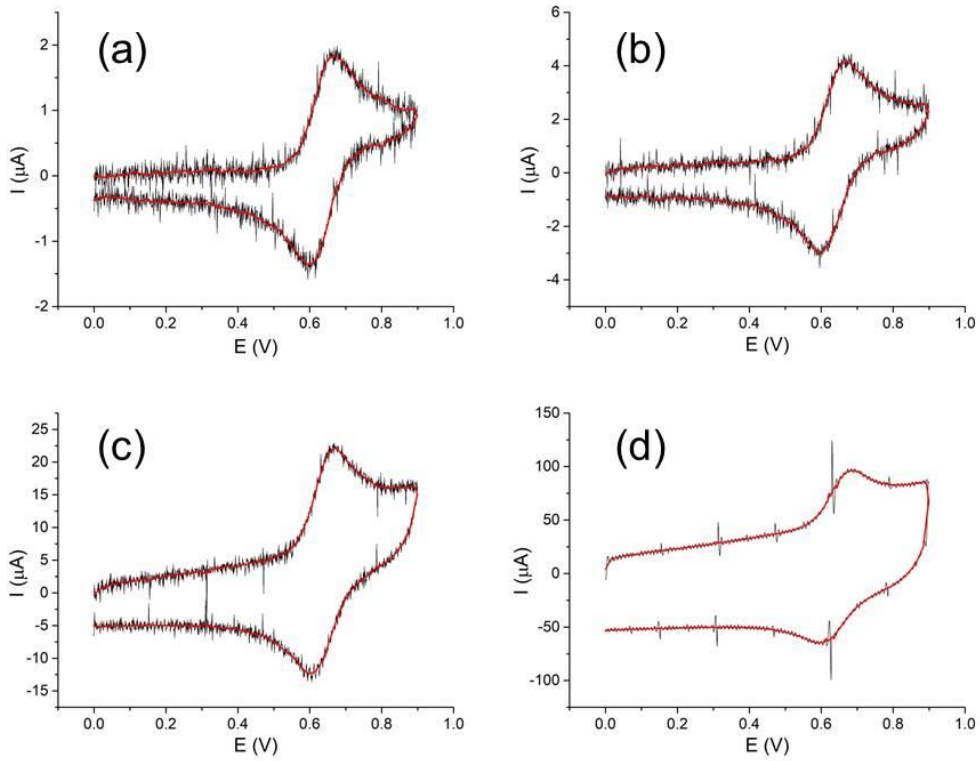

Figure 2.3 Cyclic voltammograms of the oxidation of a solution of ferrocene in Ethaline (C ° = 2 10^{-3} mol L^{-1}) on a 1-mm diameter glassy carbon electrode at 0.5 (a), 2 (b), 25 (c), 200 (d) V s^{-1}. Red lines are smooth lines. T= 298 K.

Variations of the faradaic peak currents (I_p) corrected from the baseline were measured as function of the scan rate (v) and are displayed in Figure 2.4. Linear variations were got in the scan rate range of 0.1 to 200 V/s meaning that the mass-transport of ferrocene from the bulk solution to the electrode surface is controlled by its diffusion and, meanwhile, indicates electron transfer rate constant of ferrocene in Ethaline is rather fast. I_p increases when increasing the temperature as expected for a lower viscosity of Ethaline which is consistent with the previous literature. From the linear slopes of the I_p-$v^{1/2}$ variations, we derived the values of the diffusion coefficients, D, of ferrocene in Ethaline. The D values are shown in table 2.1.

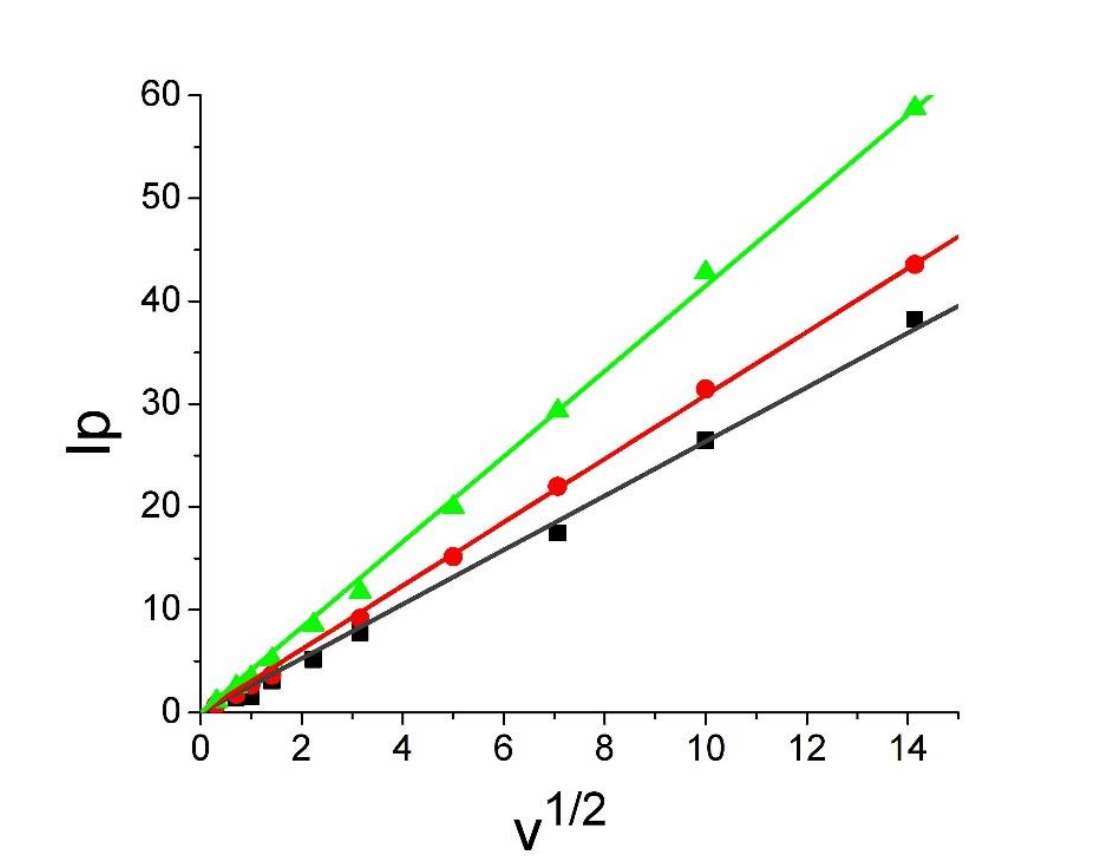

Figure 2.4 Cyclic voltammetry of the oxidation of ferrocene in Ethaline ($C \backsimeq 2\ 10^{-3}$ mol L^{-1}). Variation of the peak current I_p (A) with square root of scan rate v (v in V s^{-1}). T=298 K (Black), 313 K (red), 343 K (red).

As explained above, to determine a value of electron transfer standard rate constant, k_s, we performed the measurement in a large range of scan rates notably to check that the electron transfer controls the electrochemical process without interference of another process and that ohmic drop correction is correctly treated. These experiments were performed for different initial concentrations of ferrocene and found to be similar, see Figure 2.5, confirming the good quality of the ohmic drop compensation.

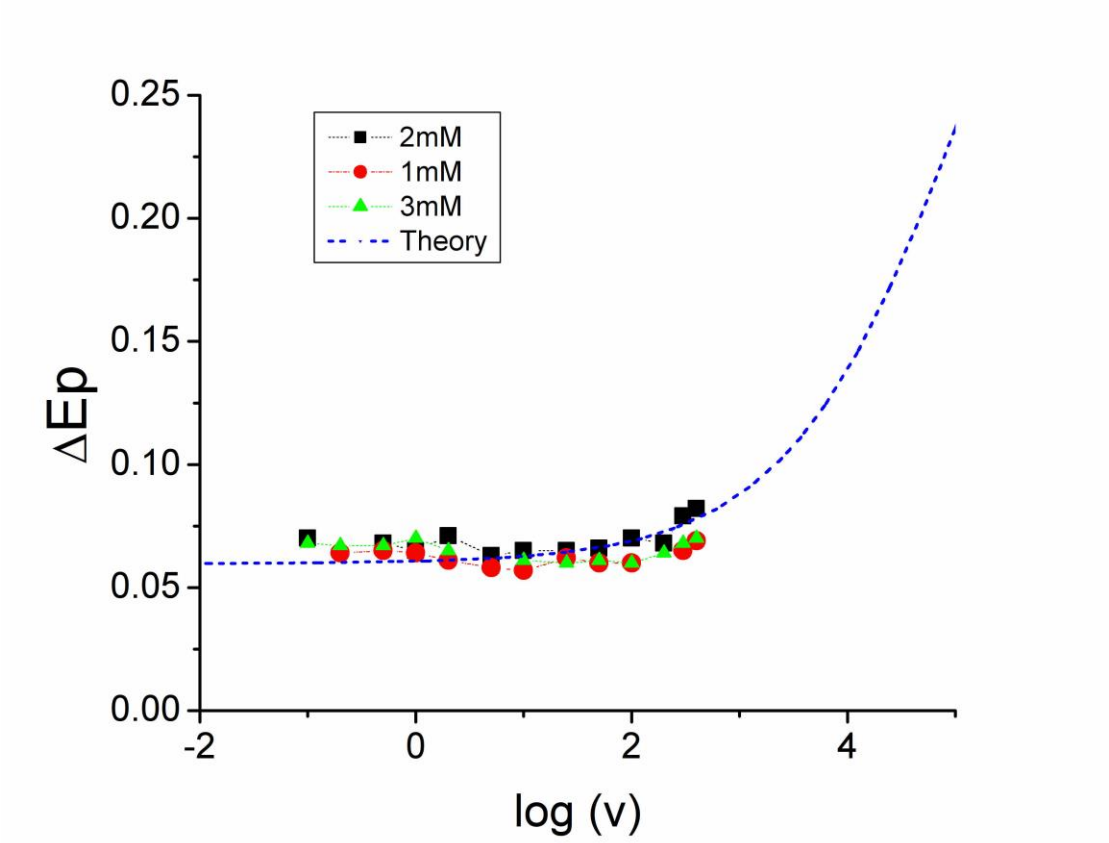

Figure 2.5 Variation of ΔEp in mV with the scan rates in $V.s^{-1}$ for the oxidation of ferrocene in Ethaline at different initial concentrations on a glassy carbon electrode. T = 298K.

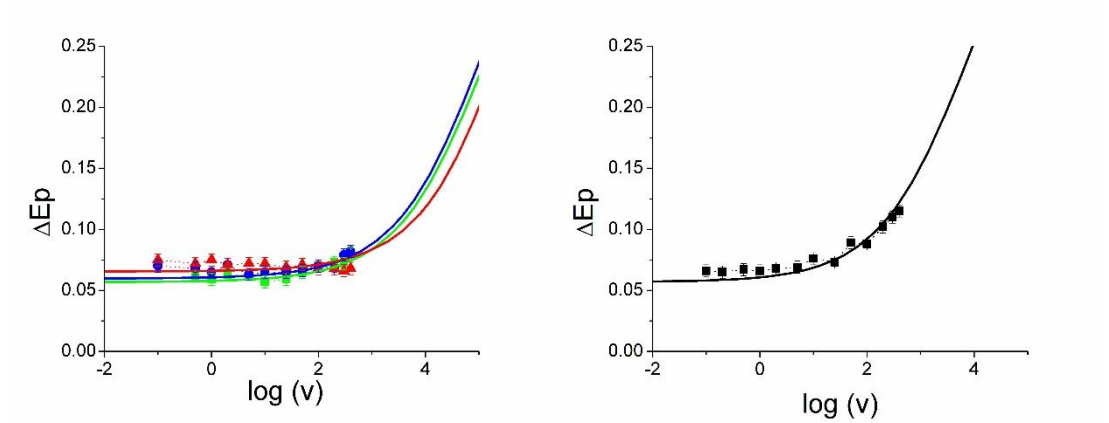

Figure 2.6 Cyclic voltammetry investigations of the oxidation of a 2 10^{-3} mol L^{-1} ferrocene solution in Ethaline (left) and in ACN (+ 0.1 mol L^{-1} nBu_4NPF_6) (right). Variations of Δ*Ep* as function of the log(*v*) (*v*: scan rate in V s^{-1}) at different temperatures: in Ethaline, T= 298 (green), 313 (blue), 343K (red); in acetonitrile at T= 298K. Lines are the theoretical variations assuming a Butler-Volmer law and taking α= 0.5 as transfer coefficient (see text).

Variations of ΔE_p as a function of the scan rates were examined at different temperatures in Ethaline and then compared with the values obtained in Acetonitrile (ACN) using the same glassy carbon electrode (see Figure 2.6).

In ACN, a considerable increase of ΔE_p is observed for scan rates higher than 100 V s^{-1}, which corresponds to a change in the kinetics passing from a diffusion control at low scan rate to an electron transfer control at the higher scan rate.[97, 206] From the fitting of the experimental data with the theoretical curve, it is possible to derive the value of k_s that was found equal to 1.5 cm s^{-1}. This value falls in the range of reported values under similar experimental conditions.[203] In contrast, in Ethaline, ΔE_p displays very little change up to the highest usable scan rates (400 V s^{-1}). It shows that the system is reversible and remains controlled by the diffusion of molecules from the solution to the electrode even at short timescale. A small increase of ΔEp is just visible for the experiments performed at the highest scan rates and temperature. However, it is difficult to clearly conclude that the kinetics is approaching a control by the electron transfer because of the narrow range of the change and we could only derive a lower limit for the heterogeneous electron transfer rate constant as $k_s >> 0.16$ cm s^{-1}. Such estimations of k_s are much higher than reported data which were obtained without taking into account the ohmic drop.[94, 200, 204] As a first remark, we could observe that the k_s values in Ethaline are just slightly slower than the rate constants measured in an organic solvent like ACN. They are also much higher than the values reported in common ionic liquids where k_s around 10^{-2} cm s^{-1} are generally obtained (See discussion below).[32, 202]

2.3.2 Ferrocyanide Oxidation in Ethaline

Cyclic voltammetry was recorded for the oxidation of ferrocyanide in Ethaline using the same experimental conditions (see Figure 2.7). Well-defined voltammograms were obtained at low scan rates as previously reported[93] and also at high scan rates (up to 400 V s^{-1}). Variations of ΔE_p were recorded for two temperatures and compared with the data in aqueous media used as a reference electrolyte (See Figure 2.9). A good

agreement between the experimental and theoretical variations of ΔE_p are observed for all experiments, indicating that the electron transfer controls the kinetics at the highest scan rates. Notice that both slow electron transfer and ohmic drop increases the ΔE_p value, but their relations with the scan rate are different. A good agreement between experiments and the theoretical curve allowing us to validate the quality of the ohmic drop compensation.[206, 207, 209] By adjusting the position of the theoretical curve with the experimental points, we derived the value of $k_s/D^{1/2}$ then the value of k_s after determination of D from the $I_p/v^{1/2}$ variation (See Figure 2.8). The values are then standardized using the values of the diffusion coefficient D for ferrocene and ferrocyanide reported in the literature (see Table 2.1) to limit the error due to the effective area of the working electrode.

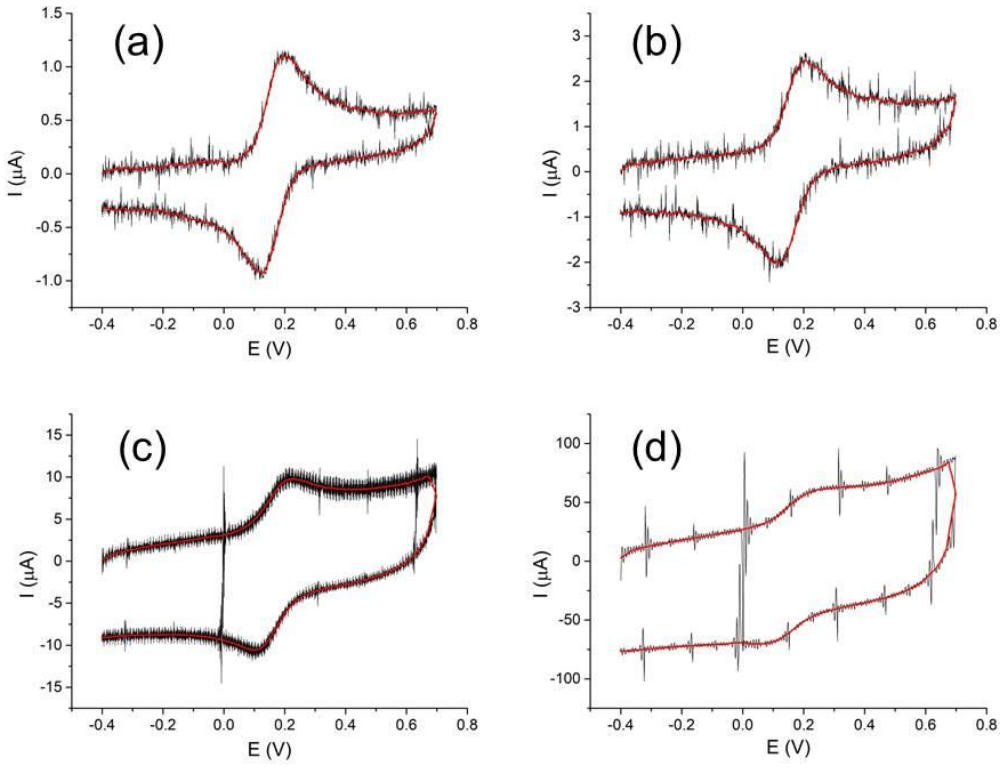

Figure 2.7 Cyclic voltammograms of the oxidation of a 2 10^{-3} mol L^{-1} solution of ferrocyanide in Ethaline on a 1-mm diameter disk glassy carbon at 0.5 (a), 2 (b), 25 (c), 200 (d) V s^{-1}. Red lines are smooth lines.

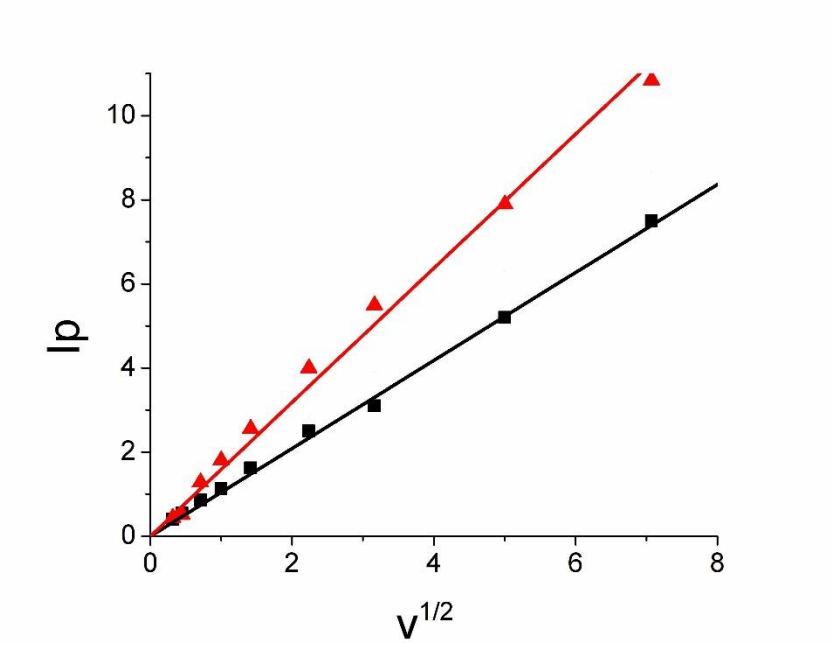

Figure 2.8 Cyclic voltammetry of Ferrocyanide in Ethaline (C ≃ 2 10^{-3} mol L^{-1}). Variation of the peak current I_p (in A) with square root of scan rate v (v in V s^{-1}). T=308 K (black), 333K (Red).

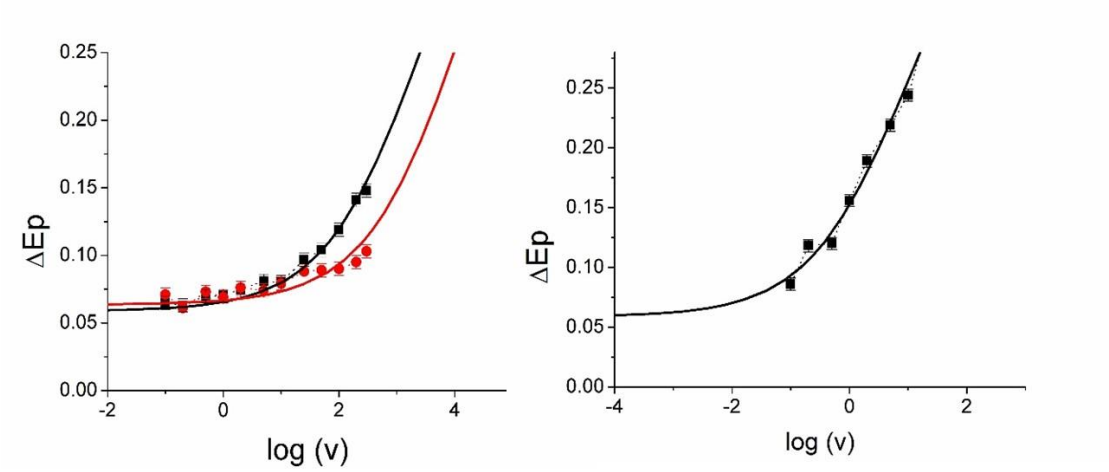

Figure 2.9 Cyclic voltammetry investigations of the oxidation of a 2 10^{-3} mol L^{-1} ferrocyanide solution in Ethaline (left) and in water (+ 0.1 mol L^{-1} KCl) (right) on a 1-mm diameter glassy carbon electrode. Variations of Δ*Ep* (V) as function of the log(*v*) (*v* the scan rate in V s^{-1}) at different temperatures: in Ethaline T= 308 K (black) and 333 K (red); in water at 308 K (right). Lines are the theoretical variations assuming a Butler-Volmer law and taking α = 0.5 as transfer coefficient.

For a final comparison, the behaviors of the ferro/ferricyanide couple were examined and k_s determined in two common ionic liquids 1-Butyl-1-methylpyrrolidinium bis(trifluoromethylsulfonyl)imide (BMP-TFSI) and 1-Ethyl-3-methylimidazolium tetrafluoroborate (EMIM-BF_4) and using the same glassy carbon electrode (See Figure 2.10). In BMP-TFSI, ΔE_p variations follow the curve expected for a simple electron transfer and Butler-Volmer law. ΔE_p values are much larger than those recorded in Ethaline in the same conditions, showing a much slower electron transfer. In EMIM-BF_4, the variations of ΔE_p with the scan rate slightly deviate from the theoretical variations predicted for a simple electron transfer. This suggests that another process is associated to the electron transfer in this ionic liquid, probably a complexation or strong ion pairing association of the ferro/ferricyanide anion with the cation of the ionic liquid.[32, 201] In this work dedicated to DES, we just consider these data to estimate an apparent k_s for an easiest comparison in Table 2.1.

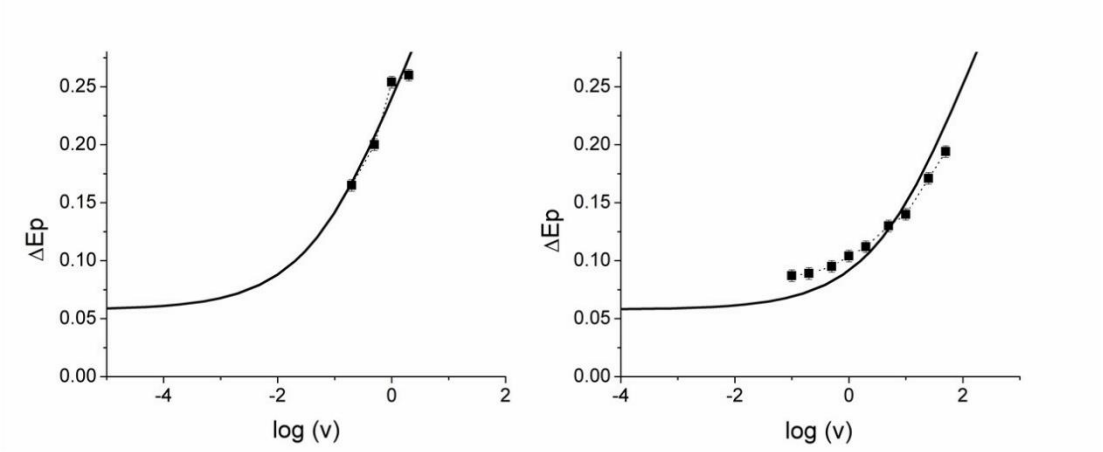

Figure 2.10 Variation of ΔEp with log(v) for the reduction of ferricyanide in BMP-TFSI (left) and EMMI-BF_4 (right). T = 303K

Same observations could be done for the ferrocene/ferrocenium couple. Rate constants could be compared to the numerous studies in common ionic liquids where low k_s values are reported for the oxidation of the ferrocene (0.2-0.01 cm s^{-1} range)[32, 201] in contrast to the large k_s in organic solvents (higher than 1 cm s^{-1}) as measured here in ACN with a carbon electrode. To go further in the analysis, it is useful to use the Marcus

formalism as done in several studies related to electron transfers in molecular solvents but also in ionic liquids. (See, for example, refs[144, 198, 215, 216])

Table 2.1 Calculated parameters and comparison of k_s measured in different media.

Compound/Solvent	T (K)	D ($cm^2\ s^{-1}$)	$k_s/D^{1/2}$ ($s^{-1/2}$)	k_s (cm s^{-1})	k_s [d] (cm s^{-1})	τ_L [e] *(ps)*
Fc/ACN	298	$2.8_5\ 10^{-5}$	300	1.6	$1.4_5 \pm 0.3$	≈ 0.2
Fc/EMIM-TFSI	298	$3.3_5\ 10^{-7}$ [a]	-	-	0.15-0.21[a,b]	6.7
Fc /Ethaline	298	$2.2\ 10^{-7}$	360	> 0.17	$> 0.15_5$	4.0
Fc/Ethaline	313	$4.0_5\ 10^{-7}$	345	> 0.22	> 0.20	-
Fc/Ethaline	343	$8.7\ 10^{-7}$	500	> 0.47	> 0.43	-
Ferrocyanide/Water	308	$8.5\ 10^{-6}$	8.9	$2.6\ 10^{-2}$	$(2.4 \pm 0.5)\ 10^{-2}$	≈ 0.2
Ferrocyanide/Ethaline	308	$1.2\ 10^{-7}$	46	$1.6\ 10^{-2}$	$(1.5 \pm 0.3)\ 10^{-2}$	4.0
Ferrocyanide/Ethaline	333	$2.3\ 10^{-7}$	77	$3.7\ 10^{-2}$	$(3.4 \pm 0.7)\ 10^{-2}$	-
Ferricyanide/BMP-TFSI	303	$1.1\ 10^{-8}$	0.95	$1.0\ 10^{-4}$	$(9.1 \pm 2)\ 10^{-5}$	22
Ferricyanide/EMIM-BF_4	303	$2.7\ 10^{-8}$	8.5	$\approx 1.4\ 10^{-3}$ [c]	$\approx 1.3\ 10^{-3}$	5.0

[a] From Compton et al.[217, 218] [b] From Hapiot et al.[219] [c] *Ep/log(v)* variation does not follow a simple Butler-Volmer Law. Estimation. [d] Values from this work were corrected with D taken from literature. Ferrocene in ACN at 298K: $2.37\ 10^{-5}$ $cm^2\ s^{-1}$.[220] Ferrocyanide in water at 298K: $7.1\ 10^{-6}$ $cm^2\ s^{-1}$.[221] [e] See Table 2.2 for details.

2.4 Discussion

The Marcus theory for electron transfer is based on a dielectric continuum solvent and was originally developed for polar solvent. The applicability of the model to ionic liquids was highly questioned. Based on simulations it was concluded that Marcus Theory is applicable to ET in ionic liquids if specific solvation of the molecules by the ions are neglected. By analogy, we could use the same approach in this chapter for discussing the electron transfer rates in an ionic DES like Ethaline.

In the Marcus theory, the standard rate constant corrected by the effect of the double layer for an adiabatic electron transfer is given by[144, 198]:

$$k_s = \frac{K_p}{\tau_L}\left(\frac{\Delta G_{Os}^{\#}}{4\pi RT}\right)^{1/2} \exp\left[-\left(\frac{\Delta G_{Os}^{\#} + \Delta G_{is}^{\#}}{RT}\right)\right]$$

where K_p is the equilibrium constant for a precursor complex and τ_L is the longitudinal relaxation time that is the relaxation time of the solvent normalized by the ratio of the static ε_s and high frequency ε_{op} relative permittivities, $\Delta G_{Os}^{\#}$, $\Delta G_{is}^{\#}$ are the standard Gibbs activation energy of the outer sphere and inner sphere contributions. According to Marcus theory, $\Delta G_{Os}^{\#}$ could be evaluated considering solvation by a dielectric continuum solvent by the following equation:[144, 198]

$$\Delta G_{Os}^{\#} = \frac{N_{av}e^2}{32\pi\varepsilon_o}\left(\frac{1}{a}-\frac{1}{d}\right)\left(\frac{1}{\varepsilon_{op}}-\frac{1}{\varepsilon_s}\right)$$

where N_{av} is the Avogadro constant, e, the electron charge, ε_o, the permittivity of the vacuum, a, the equivalent radius of the redox molecule and d its distance to its electrical image through the electrode plane. For redox molecules like ferrocene of ferrocyanide, the oxidized and reduced forms of the molecules are very similar and thus the inner-sphere contribution $\Delta G_{is}^{\#}$ to the total activation energy is negligible versus the outer-sphere contribution $\Delta G_{Os}^{\#}$; it means that most of the activation energy comes from the solvent reorganization. In a first approximation, we could neglect for a given molecule the variations of $\left(\frac{1}{a}-\frac{1}{d}\right)$ with the electrolyte as done previously.[198] We could also neglect the variation of the Pekar's factor $\left(\frac{1}{\varepsilon_{op}}-\frac{1}{\varepsilon_s}\right)$ that varies only by a small amount in $\Delta G_{Os}^{\#}$ for the considered polar media (see Table 2.2).

Table 2.2 Estimations of τ_L from dielectric parameters

Solvent	ε_s	ε_{inf}	ε_{op}[a]	*Pekar Factor*[b]	τ_{eff} *(ps)*	τ_L *(ps)*
Acetonitrile [222]	37.5	2	1.8	0.52	3.3	≈ 0.2
Water [223]	80		1.78	0.54	9.3	≈ 0.2
BMPyr-TFSI[224]	11.7	2.42	1.99	0.42	134	≈ 22
EMIM-BF_4 [198, 225]	13.6	6.7	2	0.43	33.7	5.0
EMIN-TFSI [225]	12.3	4.7	2.02	0.41	41	6.7
Ethaline [226]	37	3	2.07 [227]	0.47	71	4.0
Ethylene Glycol[228]	44	3	1.77		114	4.6

[a] Calculated from their refractive indexes n considering $\varepsilon_{op} = n^2$.

[b] When several relaxation processes have reported, an effective harmonic relaxation time, $\tau_{eff,}$ is considered and calculated by averaging the frequencies of the relaxation mode weighted by its relative amplitude following Nakamura et al. approximation in reference 198 and discussed in reference 225.

From this simplification, k_s and $1/\tau_L$ follow a similar trend for a given redox molecule, and correlations have been reported in several publications.[144] The relaxation times τ_L are derived from dielectric loss measured by dielectric spectroscopy techniques.[226, 229] Several studies were dedicated to ionic liquids (see for example for investigation of imidazolium-based ionic salts[225] and reference used for Table 2.2) but Ethaline was only recently investigated by dielectric spectroscopy in a wide range of frequencies and temperatures.[226] Authors have observed that a single relaxation time describes the re-orientational dipolar motions for Ethaline with times close to those of the molecular component.[226, 229] Relaxation times were fitted using a VFT law (Vogel-Fulcher-Tammann) in the whole range of investigated temperatures.[226] Using this correlation, dipolar relaxation time for Ethaline could be estimated to be around 71 ps at 298K leading to τ_L=4 ps. This τ_L is in the range of data reported for ionic liquids with low viscosity like EMIM-TFSI. Similar diffusion coefficients of ferrocene (and thus viscosities) are also reported in EMIM-TFSI and Ethaline. (See Table 2.1) Considering these estimations of τ_L, we could predict that k_s for ferrocene in Ethaline should be larger than k_s in EMIM-TFSI but slower than k_s in acetonitrile. If this prediction remains compatible with our observations, we could emphasize that the ET in Ethaline is relatively fast and faster than in most of the ionic liquids. For the ferro/ferricyanide couple, a better comparison is possible thanks to the larger variations of the in the ΔE_p range of available scan rate. It is remarkable that the rate constant k_s measured in Ethaline ($1.5\ 10^{-2}$ cm s^{-1}) is of the same order as values measured in water ($2.4\ 10^{-2}$ cm s^{-1}) despite totally different media, different diffusion coefficients and relaxation times of the solvent. This value could also be compared with k_s in the two ionic liquids where a large slowdown of the electron transfer is observed with k_s in the range of 10^{-4} - 10^{-3} cm s^{-1}. This is illustrated in Figure 2.11 that shows a plot of k_s with $1/\tau_L$. k_s in Ethaline is more than one order of magnitude larger than its estimation from the longitudinal

relaxation times. A first remark to explain these results concerns the applicability of the Marcus theory to DES and the possibility of a specific solvation by the ions of the DES of the molecule notably by the residual water or the ions of the DES. As mentioned before for ionic liquids, this would result in an additional contribution to the reorganization energy and a smaller rate constant. [198]Another possible explanation is that a faster relaxation process controls the solvation reorganization of the molecule upon electron transfer in DES. From Figure 5, a reorganization with relaxation time around or lower than 0.4 ps is required to explain the data and such process may have not been seen in the dielectric spectroscopy experiments. A better description of the solvation arrangement and the role of the different components (water, ions, Ethylene Glycol) around the redox molecule in DES are necessary. This was predicted by molecular dynamics in ILs (see for example ref[216] and references therein) but not in DES.

Finally, we could remind that the values derived from the Marcus model are uncorrected from the double layer effect. This correction could be different according to the different media especially if a specific adsorption of ions or of the redox molecule occurs on the electrode surface.[198]

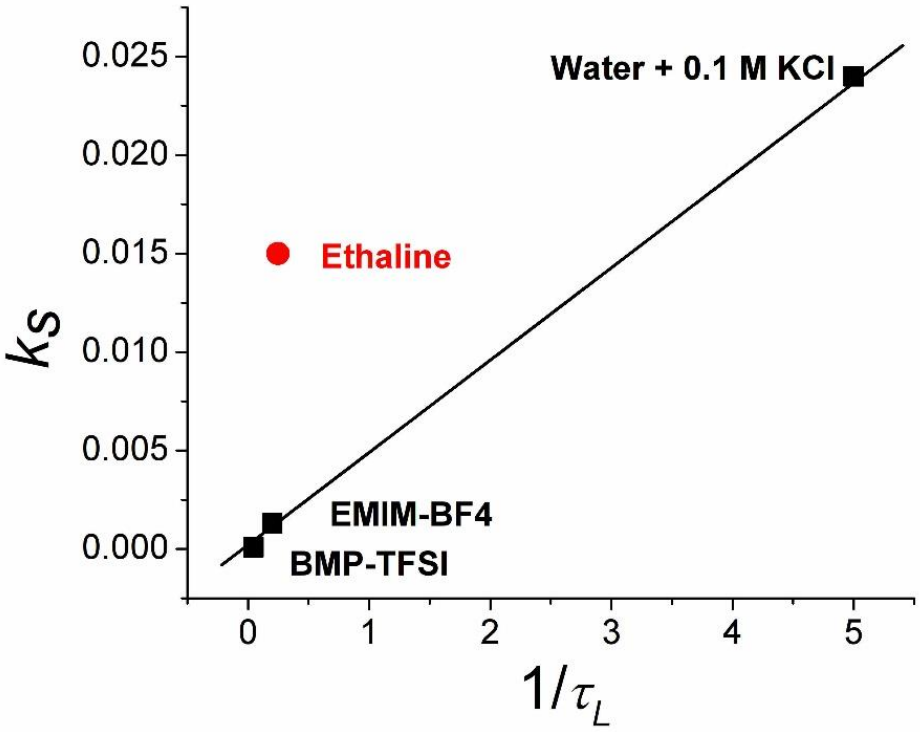

Figure 2.11 Variations of k_s for the ferrocyanide/ferricyanide couple versus $1/\tau_L$, τ_L, being the longitudinal relaxation time of the solvent. k_s in cm s^{-1} and τ_L in ps.

2.5 Conclusions

As a major result, the electron transfer rate constants measured in Ethaline are close to the values reported in organic solvent for ferrocene or in water for ferrocyanide. Ethaline appears more like a molecular solvent than ionic liquid.[32, 201, 202] We could connect this similarity to another observation concerning the small variations of the diffusion coefficients with the charge of the solute as observed previously in Ethaline and in Reline.[93] These behaviors are in sharp contrast to the observations in ionic liquids where diffusion coefficients vary with the charge carried by the solute because of specific interactions between the molecules and the ions of the ionic liquids.[32] These results fall also in line with recent FTIR studies concerning the oxidation of ferrocyanide in Reline where it was observed that the DES components are not considerably affected during the electrochemical process.[100]

This chapter clearly evidences the importance of a careful treatment of the ohmic drop. We found much larger electron transfer rate constant values (sometimes by several orders of magnitude) than recently reported values in ionic liquids and in DES where ohmic drop was not considered.[94, 200, 204] These ohmic drop issues in electrochemical measurements were previously highlighted by other groups.[98, 210] Herein, we have used on-line (or direct) compensation with transient voltammetry on a millimetric electrode in combination of a single-parameter fitting of a working curves with the experimental data. For the present study in DES, the methodology used here is particularly well-adapted since it limits the alteration of the electrode during the recording of the voltammograms, allowing an easy use of different electrode materials and an immediate qualitative view of the experiment.

When considering DES for electrochemical applications, a fast electron transfer is a strong advantage for example in energy storage systems or electrochemical sensors where the current density or time response is a key parameter. From the present results, electrochemical properties in a DES like Ethaline appear more similar to those observed in a molecular solvent than in an ionic liquid.

Chapter 3 Dynamical solvent effects on electron transfer kinetics in deep eutectic solvent-water mixtures. An apparent non-Marcus behavior in deep eutectic solvents.

Part of this chapter has been published in ChemElectroChem, 2022, e202200351.

3.1 Introduction

As discussed above, Ethaline presents a strong hydrophilic character. Without special care during its preparation, storage or use, its rapidly absorbs large quantity of water as simply as humidity coming from the atmosphere.[3] It is well known that the presence of water considerably modifies the properties of DES notably by decreasing viscosity, enhancing conductivity,[46-48] and reducing the melting point[80] which could enlarge the operating range of DES. Because it is very difficult to totally avoid the presence of water in a hydrophilic DES like Ethaline in practical situations, it strengthens the recent efforts for describing the consequences of the presence of water on the DES properties.[66, 78, 163, 230-232] Recent published works involve theoretical calculations[66, 67, 231] and/or experimental investigations of the evolution of their microscopic structure[67] and solvent dynamics.[66] Among them detailed spectroscopic studies and thermodynamics are studied.[66, 163, 232] It was concluded that the structures in a water-containing DES mixture are governed by a subtle balance of hydrogen bond networks, which water mainly competes for associations with the anions but it doesn't cause marked special behavior at the microscopic level.[67] Besides the variations on basic properties like viscosity or conductivity, spectroscopic studies show the considerable influence of the water amount on the solvation dynamics is notably visible on the solvent dipolar relaxation time.[66] It was found that water addition (>1 wt%) to the DES can even be beneficial in electrochemistry because the presence of water accelerates the relaxation and solvation. In contrast, small amounts of water (< 1 wt%) lead to additional slowing of the solvent response. In this perspective, water addition was

sometimes described a “magic” component in DES and drying a DES could even be counterproductive especially when aiming to achieve effective solvation and electron transport.[66] As example, previous works reported how the controlled addition of water could generate desired results[233, 234] or controlling the strength of the H-Bonding by a third component in the DES.[235]

Molecular electrochemistry methods notably cyclic voltammetry are efficient and a practical tool for probing the basic properties of DES.[101, 236] In the present chapter, we used the cyclic voltammetry for examining the variation of the charge transfer kinetics upon water addition considering two redox couples in two DES of Ethaline and $EtNH_3Cl$-Acetamide: the one-electron oxidation of 1,1’-dimethanolferrocene ($Fc(MeOH)_2$) and the one-electron oxidation of ferrocyanide $[Fe(CN)_6]^{4-}$. We used $Fc(MeOH)_2$ as example of an “outer-sphere” couple passing from neutral to one-positive charge species because it is well soluble both in “dry” Ethaline and in water. About $[Fe(CN)_6]^{4-}$, it was considered in numerous electrochemical studies in DES (see for example the reference[237] and the references therein) and was even proposed as a standard for electrochemical measurements as to prepare stable reference electrode in Ethaline.[237] $[Fe(CN)_6]^{4-}$ is four times negatively charged and thus prone to different interactions with the cation of the DES or water than the ferrocene derivative. Such special effects were reported in ionic liquids for negatively charge species.[212, 213] Glassy carbon (GC) electrode was chosen as the working electrode due to its many inherent properties, such as, chemically stable in these DESs, well-adapted electrode material for electrochemical analysis and high electrochemical windows in medium that contains high quantity of water.[211]

In electrochemistry, charge transfers are largely driven by the solvation reorganization[144] and one could expect strong effects on the charge transfer kinetics in a DES when the water amount is increased. Such concern is not only useful for characterizing the fundamental electrochemical properties of a water/DES mixture but it is central for practical applications where the kinetics of the electron transfer play a role on the current density in the operative of the device.[238]

3.2 Experimental Section.

Electrochemical procedures. Electrochemical equipment and procedures were detailed in the previous chapter. As in chapter 2, we use a home-made potentiostat equipped with a positive feedback electronic compensation following an adder scheme.[208, 209] The counter-electrode was a large Pt wire and the working electrode a 1-millimeter diameter glassy carbon disk electrode. The reference electrode was a polypyrrole (Ppy) quasi-reference electrode.[239] Standard rate constants and diffusion coefficient were extract in the same method as described in Chapter 2. For the measurements of the redox potentials, $E°$, solutions containing both 1,1'-ferrocenedimethanol and ferrocyanide were prepared by dissolving chemicals in Ethaline which initial water amount is 0.2 wt% and then adding the required amounts of water to reach 1 wt%, 10 wt% and 28.5 wt% water, respectively. All experiments were conducted at 300±2 K (27±2 ℃).

Chemicals. 1,1'-Ferrocene-dimethanol, potassium ferrocyanide were of the highest available purity grade from commercial source (Aldrich) and used without further purification. Ethaline was prepared from commercially available compounds obtained from Aldrich according to general published procedures including a special care to limit water contamination as done previously.[28, 29] $EtNH_3Cl$-Acetamide was made by the following process. Ethylammonium chloride ($EtNH_3Cl$) was recrystallized from absolute ethanol and then dried for overnight on Schlenk line under high vacuum at 50 ℃ to remove the water. Acetamide was dried in an oven at 70 ℃ for overnight. The two components are mixed at 1:1.5 mole ration and stirred at 60 ℃ until transparent homogeneous liquid formed. Mass fractions of residual water were measured by using a coulometric Karl-Fischer titration (831KF Coulometer-Metrohm and using Hydranal® Coulomat E solution from Fluka). The initial water amount of Ethaline was found as low as 0.15 wt% and $EtNH_3Cl$-Acetamide is 0.4 wt%. DES/Water mixtures were then prepared by directly adding a define volume of ultrapure water and concentrations were verified by Karl-Fischer titration for the lowest amounts of water.

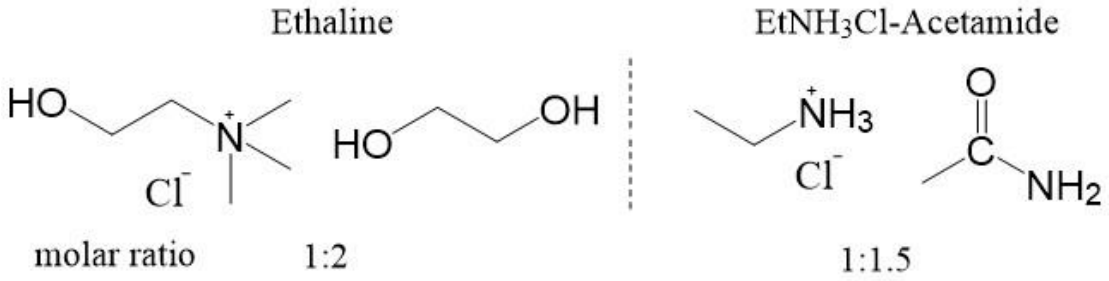

Scheme 3.1 Structure and composition of DESs studied in this chapter.

3.3 Results

3.3.1 Ferrocyanide and 1,1'-dimethanolferrocene Oxidations in Ethaline

Examples of voltammograms of the $[Fe(CN)_6]^{4-}$ and $Fc(MeOH)_2$ oxidations in Ethaline are shown on Figures 3.1 and 3.2 at different scan rates and for the two extreme considered amounts of water: the "dry" Ethaline containing 0.2-0.25 wt% water and one mixture with large amount of water (28.5%).

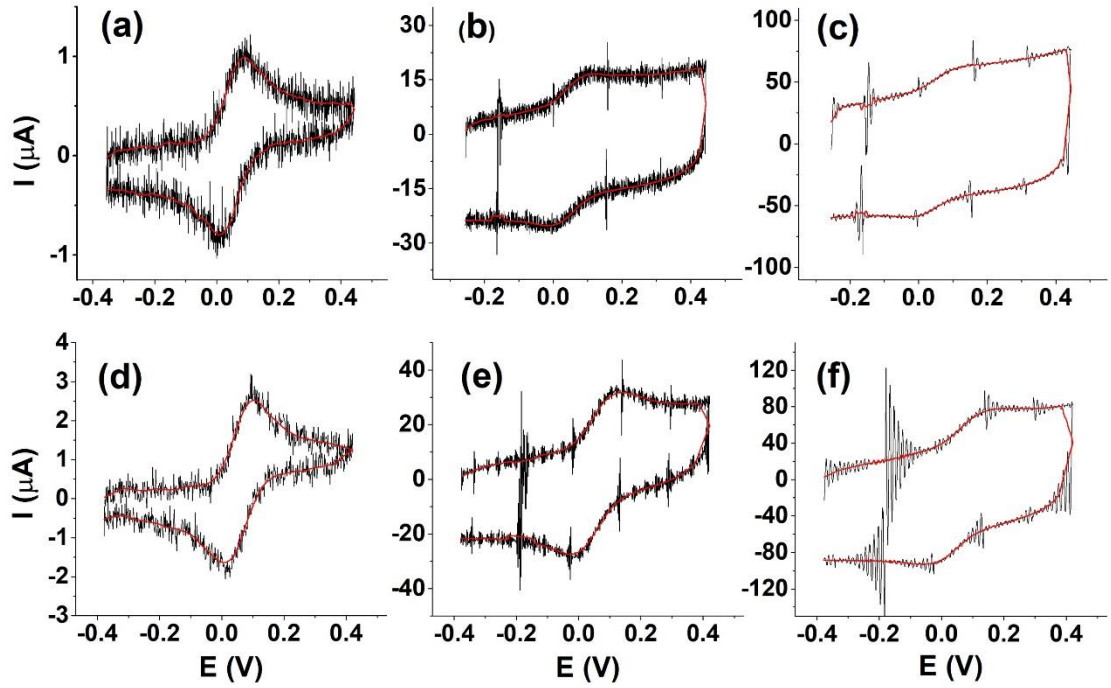

Figure 3.1 Cyclic voltammograms of the oxidation of 2 mM ferrocyanide in Ethaline with two water amounts : 0.25 wt% (a,b,c,), and 28.5 wt% (d,e,f) at scan rates of 0.5 (a,d), 50 (b,e), 200 (c,f) V/s. Red lines are smooth lines.

As observed previously, both redox couples display well-defined cyclic

voltammograms in Ethaline in all the scan rates. When water is added to the DES, the main features of their voltamograms remain and a reversible behavior is always observed like in the "dry" Ethaline.[204, 236]

For measuring the electron transfer standard rate constants, k_s, we used the classical methodology based on the variations of the peak-to-peak potential difference in a large range of scan rates (typically 0.1-500 $V.s^{-1}$).[206, 236] High scan rates are required because these are relatively fast redox couples and the competitive diffusion is lower than in common molecular solvents. Because ohmic drop could be considerable in Ethaline with resistance at the working electrode interface, a careful treatment of the ohmic drop is taken in such analysis. In that purpose, we used a potentiostat equipped with a direct electronic compensation of the ohmic drop which avoids the use of post-corrections of the curves.[206] Limiting the influence of the ohmic drop in fast scan voltammetry would also be possible with using a microelectrode but using a millimetric electrode offers more choice of electrode materials, notably the use of GC carbon electrode.[206]

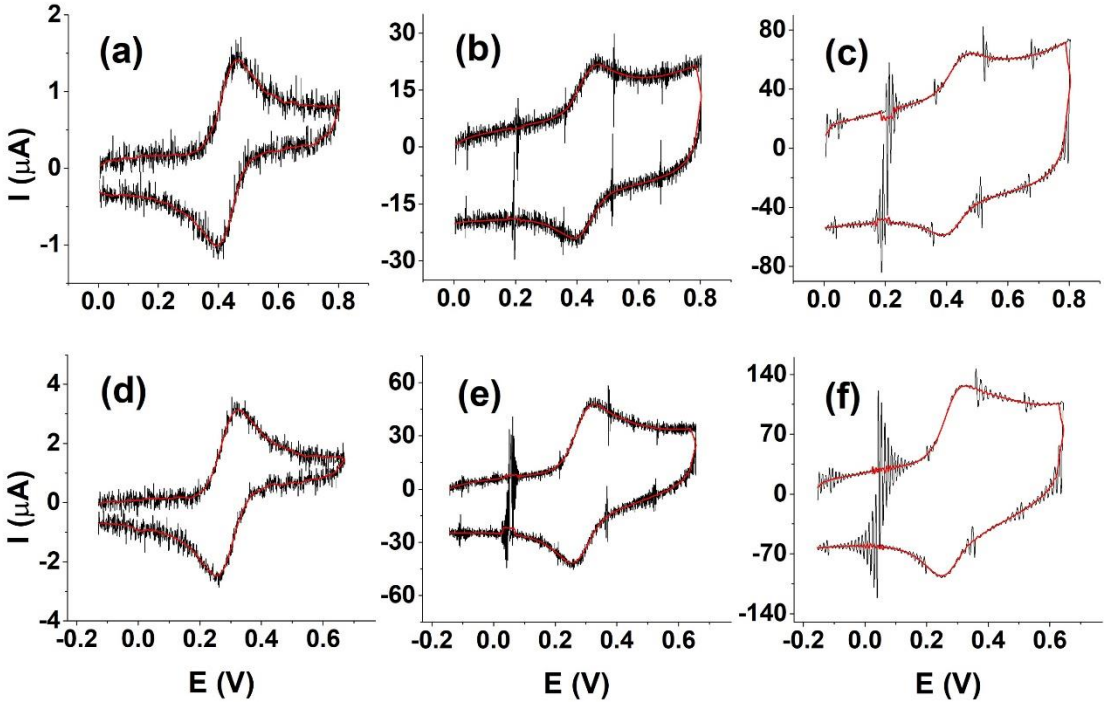

Figure 3.2 Cyclic voltammograms of the oxidation of 2 mM 1,1'-dimethanol-ferrocene in Ethaline for two different water amounts: 0.2 wt% (a, b, c), and 28.3 wt% (d, e, f) at scan rates of 0.5 (a, d), 50 (b, e), 200 (c, f) V/s. Red lines are smooth lines.

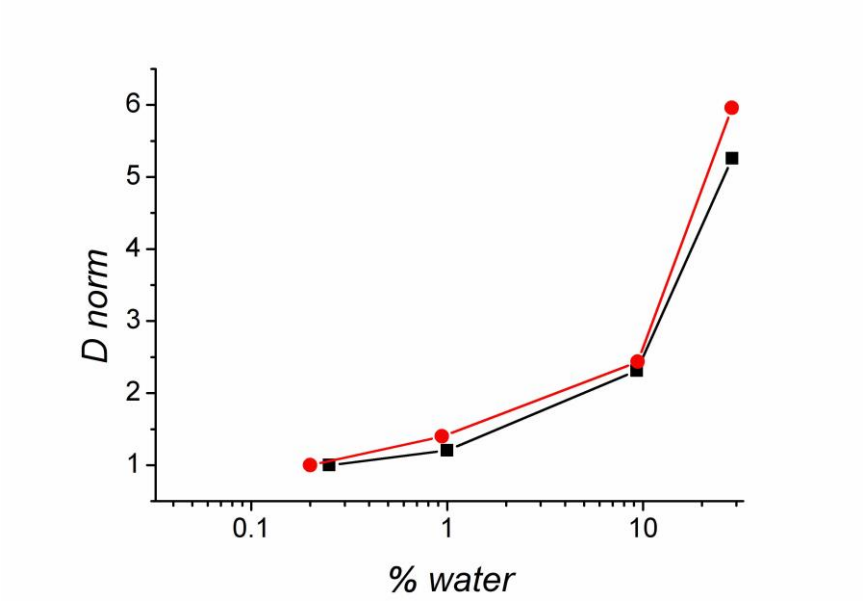

Figure 3.3 Relative variations of the diffusion coefficients $D_{norm}=D_{water}/D_{dry}$ of ferrocyanide (black line) and 1,1'-dimethanolferrocene (red line) in Ethaline with the amounts of added water (Temp: 300K). *wt% water* in Ethaline is shown on a logarithmic scale for an easier reading.

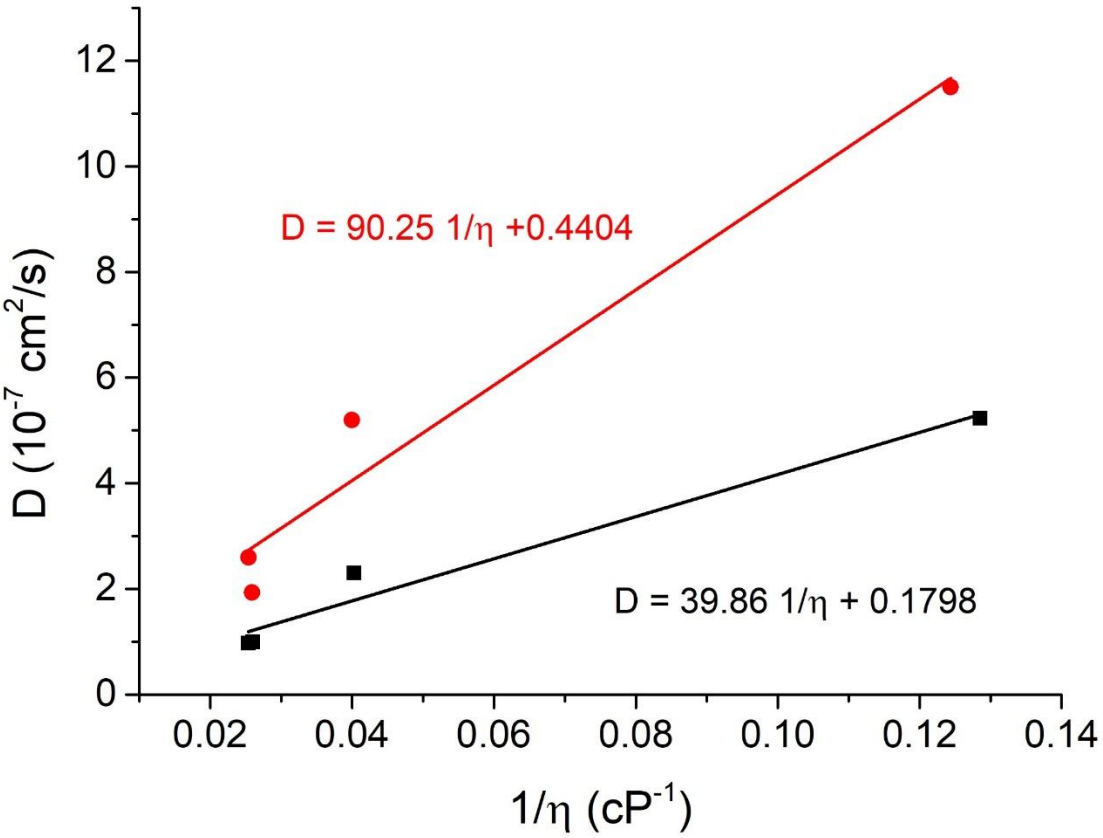

Figure 3.4 Plots of the diffusion coefficient, D, as a function of the reciprocal viscosity, 1/η, for 1,1'-dimethanolferrocene (red line) and ferrocyanide (black line). The viscosity data are from literature, see Table 3.1.

Determination of the electron rate constant, $k_{s,}$ requires an independent measurement of the diffusion coefficients *D* for each redox couple at different water mixtures. *ΔEp* variations with the scan rate provide the value of $\frac{k_s}{\sqrt{D}}$. *D* values were derived from the same set of experiments considering the peak currents measured at the lowest scan rates for which the mass transport controls their electrochemical response and could be considered as reversible. The diffusion coefficients and viscosities of Ethaline/water mixtures are listed in table 3.1. An additional analysis is in the comparison of the diffusion coefficients of the two redox couples. Figure 3.3 shows the relative variations of the normalized diffusion coefficient $D_{norm}=D/D_{dry}$ upon addition of water, the reference D_{dry} value being the data obtained in the "driest" Ethaline. We notice that very similar variations of D_{norm} are obtained for the two couples despite different charges carried on the two molecules. As expected, large increases of *D* with the addition amounts of water are observed for both redox couples which reflects the large decrease of the viscosity with the water quantity.[66] *D* value increases in a range of 5-6 times and viscosity decreases by a ratio around 5 for the whole range of water amounts, see data at Table 3.1. However, the D values of 1,1'-dimethanolferrocene are more than two times higher than ferrocyanide at each viscosity. This observation implies a specific interaction or solvation between $[Fe(CN)_6]^{4-}$ and the components of Ethaline due to its four negative charges and the ionic solvent.

The Stokes-Einstein law predicts that *D* varies linearly as T/η for a sphere diffusing in an ideal liquid at certain temperature (where η is the dynamic viscosity of the DES). The Stokes-Einstein equation:

$$\mathrm{D} = \frac{kT}{6\pi r\eta}$$

Where k is Boltzmann's constant and r is the hydrodynamic radius of the diffusion species. This equation is applicable when the diffusion species is large with respect to the solvent molecules. But as already noticed, this model is probably too simple to account for the diffusion process in DES. As shown in Figure 3.4, the plot of D vs 1/η

shows a correlation which R value equal to 0.954 and 0.945 for ferrocyanide and $Fc(MeOH)_2$, respectively.

Variations of *ΔEp* with the scan rates are displayed on Figures 3.5 and 3.6 for the oxidations of $[Fe(CN)_6]^{4-}$ and $Fc(MeOH)_2$ respectively. Large variations with the scan rates are visible for the oxidation of $[Fe(CN)_6]^{4-}$ contrarily to $Fc(MeOH)_2$ oxidation for which *ΔEp* only slightly increases for the highest scan rates. This confirms a faster electron transfer whatever the water amount in the case of the ferrocene derivative than for $[Fe(CN)_6]^{4-}$. In that case, the small variations observed at the highest scan rate has to be considered with care, as a small defect of the compensation could affect the analysis. We will just consider the small rise as tendencies to obtain limit values as shown in Table 3.2.

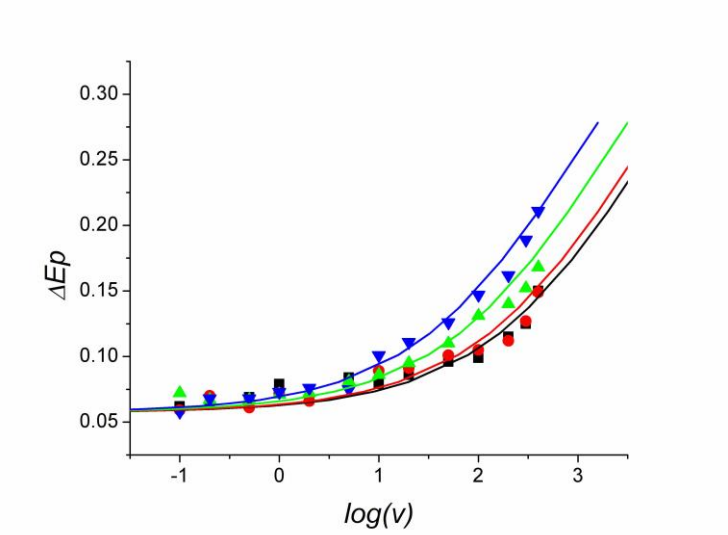

Figure 3.5 Cyclic voltammetry investigations of the oxidation of a 2 x 10^{-3} mol L^{-1} ferrocyanide solution in Ethaline with increasing amount of water. Variations of *ΔEp* as function of the log(*v*) (*v* : scan rate in V s^{-1}) at different concentrations of water: 0.25 (**black**), 1.0 (**red**) , 9.3 (**green**), 28.5 (**blue**) *wt% water* in Ethaline, T= 300 K. Lines are the theoretical variations assuming a Butler-Volmer law and taking $\alpha = 0.5$ as transfer coefficient (see text). From fitting between experiments and data, one could obtain the parameter $\frac{k_s}{\sqrt{D}}$.

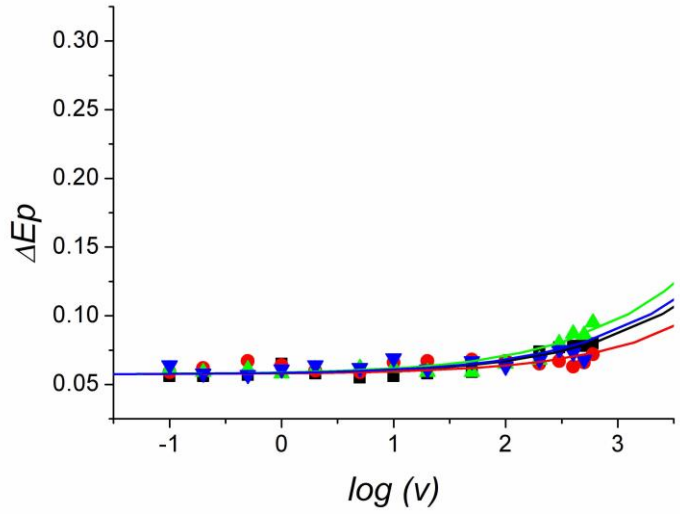

Figure 3.6 Cyclic voltammetry investigations of the oxidation of a 2 x 10^{-3} mol L^{-1} 1,1'-ferrocenedimethanol solution in Ethaline for different concentrations of water. Variations of *ΔEp* as function of the log(*v*) (*v* : scan rate in V s^{-1}) at different concentrations of water: 0.2 (**black**), 0.9 (**red**), 9.4 (**green**), 28.4 (**blue**) *wt% water* in Ethaline, T= 300 K. Lines are the theoretical variations assuming a Butler-Volmer law and taking $\alpha = 0.5$ as transfer coefficient (see text). From fitting between experiments and data, one could obtain the parameter $\frac{k_s}{\sqrt{D}}$.

For $[Fe(CN)_6]^{4-}$ oxidation, a large variation of ΔE_p is observed for scan rates higher than 10 V s^{-1} allowing a more accurate determination of k_s. The amplitude of the variation increases with the quantity of water in the DES which corresponds to a change in the kinetic regime passing from a diffusion control to a control by the electron transfer at high scan rates. Good agreement between the theoretical behavior and experiments are obtained for all the amounts of added water. Because both slow electron transfer and ohmic drop affects the value of *ΔEp* but in a different manner with the scan rates, good agreements between theory and experiments are required to validate the experiments. From the fitting of the experimental data with the theoretical curve, we derived the value of standard electron transfer rate constant k_s as shown in Table 3.1. As a remarkable result, the values of k_s seems remain almost unchanged when adding water to the dry Ethaline making the mixtures water amount rise from 0.25 to 28.5 wt%. We could also observe that k_s values in the water/Ethaline mixture tend to the value measured in pure water (0.025 cm s^{-1}) in similar conditions and using the same glassy carbon electrode.[236] Thus, the larger increase of *ΔEp* and the apparent slowness of the charge transport are not due to a decrease of the charge transfer rate at

the electrode but to an increase of the mass transport. Indeed, the parameter $\frac{k_s}{\sqrt{D}}$ characterizes the competition between the charge transfer and the mass transport and is less favorable.

Table 3.1 Oxidation of ferrocyanide. Calculated parameters in Ethaline with increasing quantities of water at 300 K.

Water (wt%)	$k_s/D^{1/2}$	D (cm s^{-2})	k_s (cm s^{-1})	*E°(V)/Ppy*	*η (cP)*[a]
0.25	58	$9.9_5\ 10^{-8}$	0.018	0.058	38.48
1.0	52	$9.7\ 10^{-8}$	0.016	0.064	39.41
9.3	36	$2.3\ 10^{-7}$	0.017	0.053	24.83
28.5	26	$5.2_3\ 10^{-7}$	0.019	0.053	7.78
100 (308 K)[b]	8.9	$8.5\ 10^{-6}$	0.025	-	1

[a] viscosity interpolated from ref[66] unless otherwise stated. [b] Parameters in water are from ref[236]. The viscosity of water considered as 1 cP.

A noticed before, only small increase of *ΔEp* are visible for the experiments performed at the highest scan rates. We could only derive raw estimate of the rate constant or even only a lower limit for the heterogeneous electron transfer rate constant. Results are gathered in Table 3.2. Examinations of these data show an increase trend for k_s with the amount of the quantity of water, but such variation is not monotonous. It seems that k_s immediately increases when water is added but remains in a narrow range for around 10% and increases again for the large quantity of water.

Table 3.2 Oxidation of $Fc(MeOH)_2$. Calculated parameters in Ethaline with increasing quantities of water.

Water (wt%)	$k_s/D^{1/2}$	D (cm s^{-2})	k_s (cm s^{-1})	*E° (V)/Ppy*	*η (cP)*[a]
0.2	~ 322	$1.9_3\ 10^{-7}$	~ 0.14	0.43_0	38.6
0.94	> 480	$2.6\ 10^{-7}$	> 0.25	0.42_8	39.31
9.4	~ 227	$5.2\ 10^{-7}$	~ 0.16	0.36_4	25
28.4	> 261	$1.1_5\ 10^{-6}$	> 0.28	0.28_9	8.04

[a] viscosity interpolated from ref[66] unless otherwise stated.

In addition to the kinetics measurements, we have also examined the relative variations of redox potential *E°*. For this, we used a mixture of $Fc(MeOH)_2$ and ferrocyanide both dissolving in the same batch of Ethaline and use the Ppy electrode as a reference. As

shown in Figure 3.7, the formal potential of ferrocyanide is at 0.053 V and $Fc(MeOH)_2$ at more positive potential. It is noticeable that the formal potentials differences ($\Delta E°$) of the two species decrease when increasing water amounts in the media. $\Delta E°$ passing from 0.37, 0.36, 0.31, 0.24 V for 0.2, 1, 10, 28.5 wt% water respectively. Some care should be taken about the individual variations as the Ppy reference electrode may also shift when water is added, but it is interesting to notice that most of the $\Delta E°$ variation is due to the $E°$ of $Fc(MeOH)_2$ that becomes less positive[200] while the $E°$ of $[Fe(CN)_6]^{4-}$ seems almost not affected[237] by the water addition. It is also observable that large quantities of water are required to affect the $E°$ of $Fc(MeOH)_2$ to less positive value. It illustrates an easier oxidability of $Fc(MeOH)_2$ probably due to a stabilization of the charged $Fc(MeOH)_2^+$ by water.

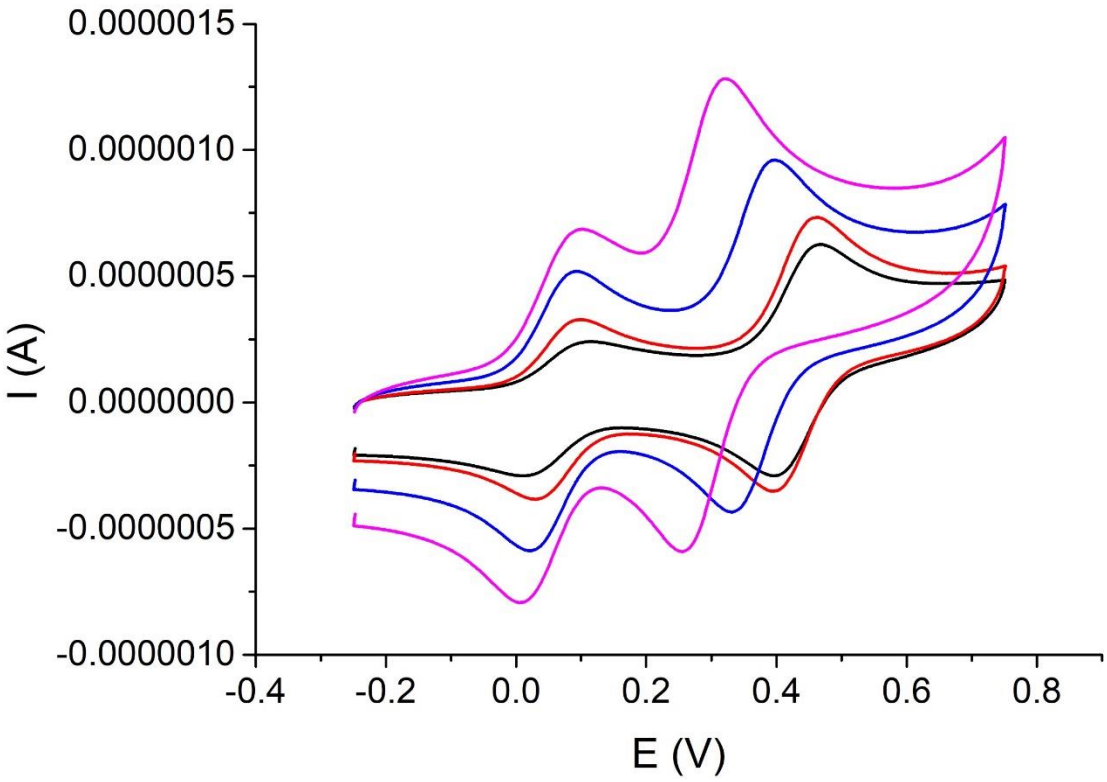

Figure 3.7 CVs of two redox couples, ferrocyanide and 1,1'-dimethanolferrocene, in the same batch of Ethaline on glassy carbon electrode. Ppy@Pt as the reference electrode.

3.3.2 Oxidation of 1,1'-dimethanolferrocene in $EtNH_3Cl$-Acetamide

To get another data about the variations of the rate constant of $Fc(MeOH)_2$ with the water amount, the oxidation of 1,1'-dimethanolferrocene in DES-- $EtNH_3Cl$-Acetamide

(1:1.5 mole ratio) -- was investigated. This DES also shows a relatively low viscosity and good intrinsic conductivity in room temperature.[240] CVs of $Fc(MeOH)_2$ oxidation both at "dry" and "wet" $EtNH_3Cl$-Acetamide are shown in Figure 3.8 which show well-defined shape in both water amounts. The standard potential of $Fc(MeOH)_2$ verses Ppy@Pt reference electrode was also shown in Table 3.3. Unlike in Ethaline, the peak-to-peak separation, ΔE_p, increases significantly with scan rates which indicates a slower electron transfer for $Fc(MeOH)_2$ in $EtNH_3Cl$-Acetamide than in Ethaline. Furthermore, the ΔE_p shifts to negative direction when increasing the water addition while decreasing solvent viscosity.

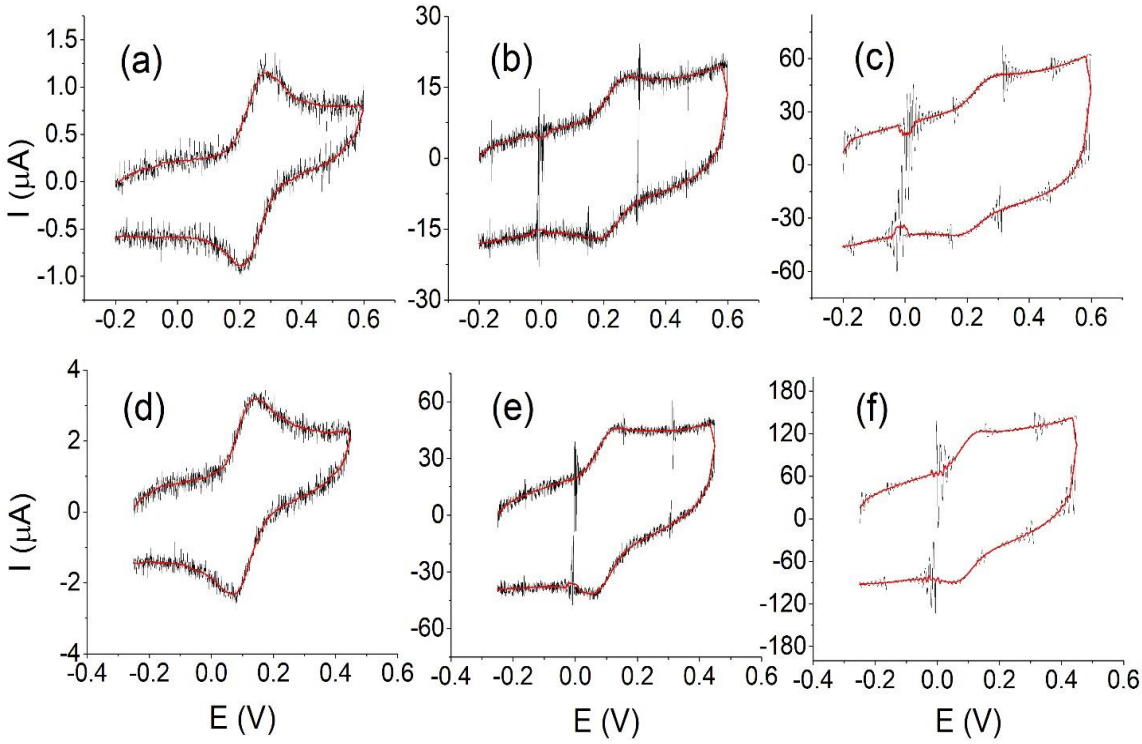

Figure 3.8 Cyclic voltammograms of the oxidation of 2 mM 1,1'-dimethanol-ferrocene in $EtNH_3Cl$-Acetamide for two different water amounts: 0.2 wt% (a, b, c), and 28.3 wt% (d, e, f) at scan rates of 0.5 (a, d), 50 (b, e), 200 (c, f) V/s. Red lines are smooth lines.

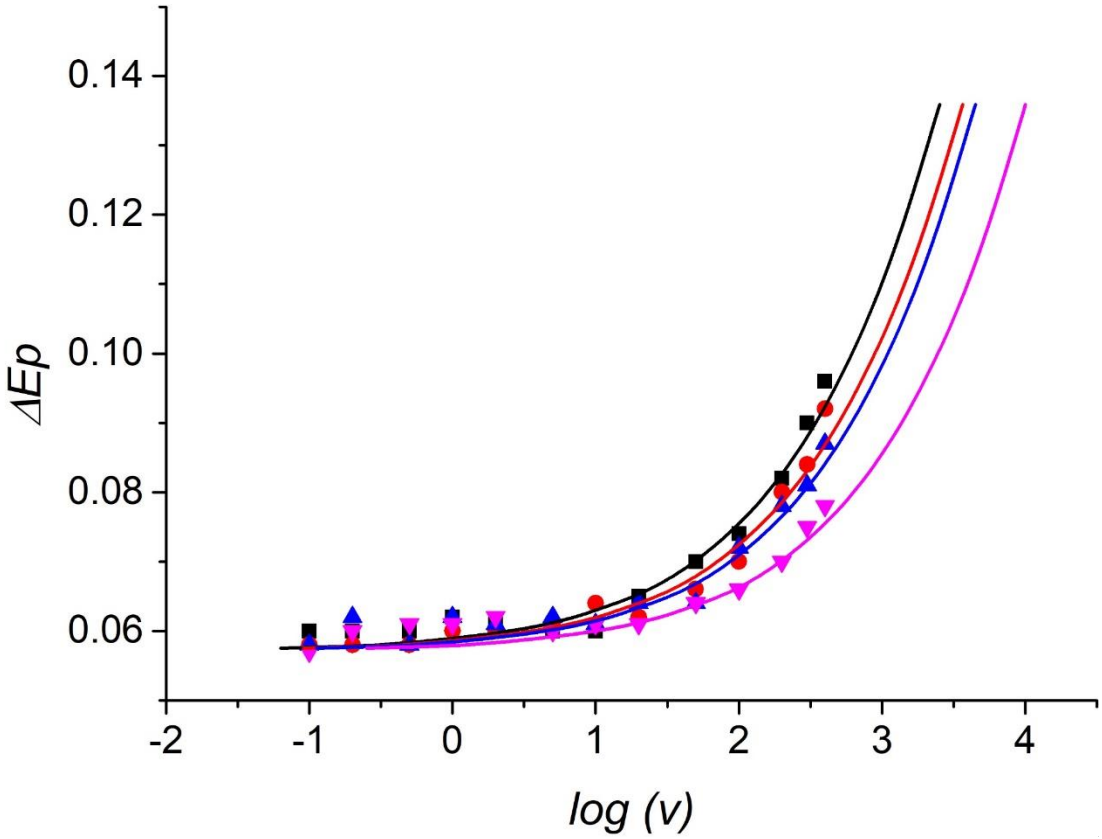

Figure 3.9 Cyclic voltammetry investigations of the oxidation of a 2 x 10^{-3} mol L^{-1} 1,1'-ferrocenedimethanol solution in $EtNH_3Cl$-Acetamide for different concentrations of water. Variations of *ΔEp* (in V) as function of the log(*v*) (*v* : scan rate in V s^{-1}) at different concentrations of water: 0.4 (**black**), 1.1 (**red**), 11 (**blue**), 28.4 (**magenta**) *wt% water* in Ethaline, T= 300 K. Lines are the theoretical variations assuming a Butler-Volmer law and taking $\alpha = 0.5$ as transfer coefficient (see text). From fitting between experiments and data, one could obtain the parameter $\frac{k_s}{\sqrt{D}}$.

The diffusion coefficient, D, and the standard rate constant, k_s, of $Fc(MeOH)_2$ was listed in table 3.3 which are extracted from CVs using the same method as before (Figure 3.9). The previous literature has demonstrated that oxidation of ferrocene in organic solvent is an out-sphere reaction which reorganization energy mainly controlled by the solvent dynamics while the molecular structure not change or could neglect.[144] This behavior fit the Marcus theory very well. As we expected, the rate constant, k_s, of $Fc(MeOH)_2$ increasing with the addition of water in $EtNH_3Cl$-Acetamide resulting decreasing viscosity. This phenomenon seems more like a solvent-controlled process. But the increasing amplitude of k_s is much lower than the increase of D or the decrease of viscosity (see more detail in section 3.4 discussion). We also notice that the rate

constant of $Fc(MeOH)_2$ in this DES is lower than in Ethaline although only a limit value got in it.

Table 3.3 Oxidation of $Fc(MeOH)_2$. Calculated parameters in $EtNH_3Cl$-Acetamide (1:1.5) with increasing quantities of water.

Water (wt%)	$k_s/D^{1/2}$	D (cm s^{-2})	k_s (cm s^{-1})	*E°/Ppy*
0.4	172-230	$8.0\ 10^{-8}$	0.05-0.07	0.242 V
1.1	195-230	$8.4\ 10^{-8}$	0.055-0.07	0.227
11	226	$3.30\ 10^{-7}$	0.13	0.15
28.4	326	$8.4_3\ 10^{-7}$	0.3	0.11

3.4 Discussion

In the framework of the Marcus theory, the standard rate constant k_s corrected by the effect of the double layer for an adiabatic electron transfer is given by:[144, 198]

$$k_s = \frac{K_p}{\tau_L}\left(\frac{\Delta G_{Os}^{\#}}{4\pi RT}\right)^{1/2} \exp\left[-\left(\frac{\Delta G_{Os}^{\#} + \Delta G_{is}^{\#}}{RT}\right)\right]$$

where K_p is the equilibrium constant for a precursor complex and τ_L is the longitudinal relaxation time that is the relaxation time of the solvent normalized by the ratio of the static ε_s and high frequency ε_{op} relative permittivity, $\Delta G_{Os}^{\#}$, $\Delta G_{is}^{\#}$ are the standard Gibbs activation energy of the outer sphere and inner sphere contributions. It is generally admitted that the activation energies do not considerably change for a given redox couple when they are examined in a same class of solvent resulting that k_s and $1/\tau_L$ follow correlate. Additionally, the Stokes-Einstein-Debye relation predicts that τ_L correlates with the dynamic viscosity η and indeed several publications have reported correlations between rate constants k_s and $1/\tau_L$ or η.[159, 160] In a closely-related example, variation of the k_s were reported for the oxidation of ferrocenemethanol in a mixture of DMSO/water when water is added and the corresponding viscosity decreases.[161] This variation is not monotone and a large quantity of water (more than 30%) is required to see a considerable effect and that it supposes that adding water has an effect only on the viscosity and not a specific solvation that could affect the reorganization energy $\Delta G_{Os}^{\#}$. In a recent paper,[66] authors have reported the photoinduced intramolecular charge-

transfer (CT) kinetics of Betaine-30 dye in Ethaline/Water mixture by femtosecond time-resolved absorption spectroscopy (fs-TA). They found very small amounts (< 1 wt% added) of water have a very different effect than larger amounts of water (1 wt% - 28.5 wt% added). When small amounts of water are added (0-1 wt%), an initial slowing of the solvent response is observed. However, in sufficiently wet Ethaline (> 1 wt%) the addition of water contributes to an increase in solvation and relaxation rate.[66] It is noticeable that the full effect between "dry" Ethaline and "wet" Ethaline with the amount of water remains relatively modest (factor of 2.5) as the viscosity changed by 5.4 times. This peculiar behavior was explained by the authors by subtle competitions of the solvation between the different components of the DES/water, the formation of water clusters and water network that could act as a lubricant in the dynamics.[66]

3.4.1 Dependence of CT rate constants on viscosity in Ethaline

Figure 3.10 shows the correlation of $\ln(k_s)$ with $\ln(\eta)$ for the oxidation of $[Fe(CN)_6]^{4-}$ on a glassy carbon electrode from dry Ethaline to pure water. A good linear correlation was found in the same range (red line), but the correlation not as good as before from very dry Ethaline (0.25 wt% of water) to 28.5 wt% because the point of 0.25 wt% are not on the straight line.

From 1 wt% to 28.5 wt% of water and pure water, the $\ln(k_s)$ linearly decrease with $\ln(\eta)$ while increase from 1.0 wt% to 0.25 wt% of water. But, the slope of the correlating line is only -0.12 which is much small value compare to these in organic solvents. The rate constant only changed 1.5 times (from 0.016 to 0.025 cm s^{-1}) in the whole range of solution composition (from dry Ethaline to pure water). In fact, the rate constants k_s are almost unchanged if we compare it with the diffusion coefficient which has increased by a factor of 85 or the viscosity decreased by a factor of 40 (from dry Ethaline to pure water).

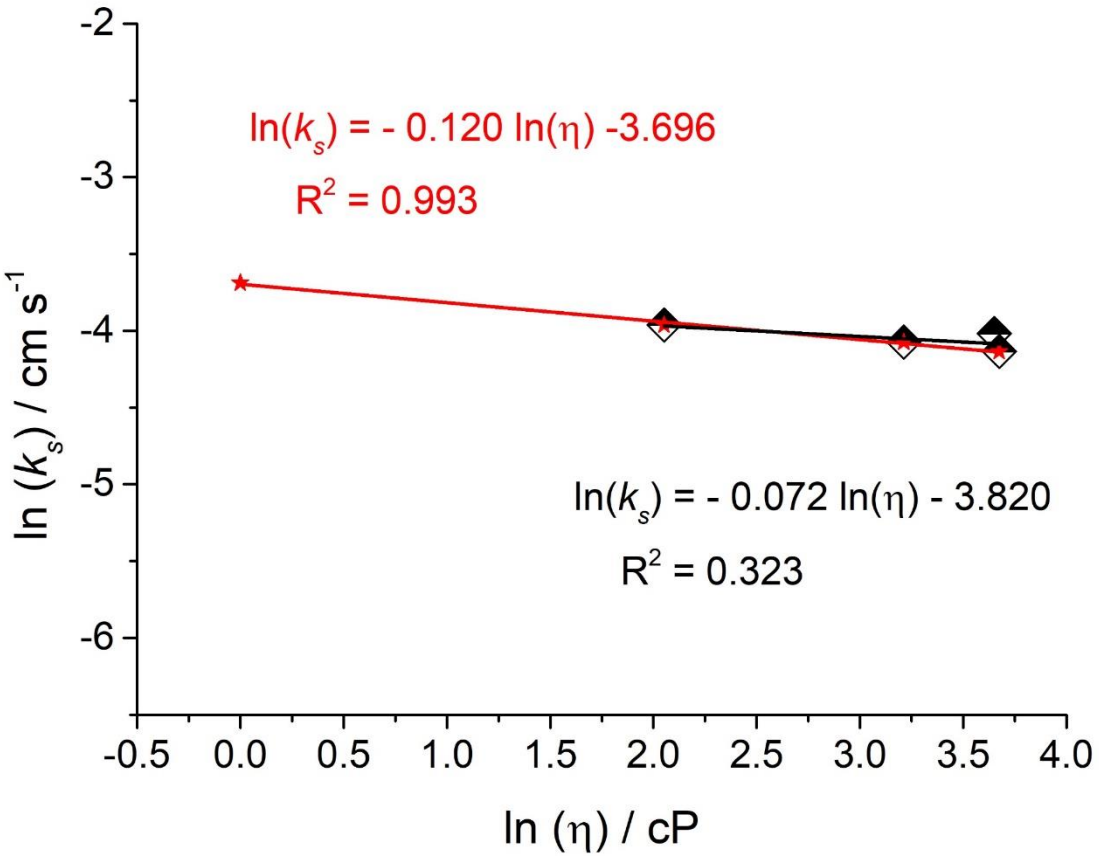

Figure 3.10 Linear correlation of the experimental ET rate constant, ln(k_s) with the viscosity of the solvent used, ln(η), for the oxidation of 2 mM ferrocyanide on a 1 mm diameter glassy carbon electrode from dry Ethaline to pure water. The red line includes the k_s in pure water.

3.4.2 Dependence of CT rate constants on diffusion coefficient in $EtNH_3Cl$-Acetamide

As seen above, it is predicted by the Stokes-Einstein equation that the plot of D vs. 1/η is usually linear at certain temperature. Thus, relating k_s to D is macroscopically equivalent to relating k_s to 1/η. This analysis is useful when the data like viscosity or relaxation time are unknown.

Due to the lack of viscosity data for $EtNH_3Cl$-Acetamide and mixtures with water, the relation between ET rate constants k_s and the diffusion coefficients D for the oxidation of $Fc(MeOH)_2$ were examined at a glassy carbon electrode for the water amounts between 0.4 wt% to 28.4 wt%. As shown in Figure 3.11, good linear relationships between k_s (or $k_{s,norm}$) with D (D_{norm}) were found for the oxidation of ferrocene in this

DES. When increasing the amount of water in $EtNH_3Cl$-Acetamide, the values of D increase by approximately 10 times and the rate constant increases gradually by around 6 times. The solvent effects on kinetics are clearly more pronounced here than we have observed for the oxidation of ferrocyanide but appears to remain lower than the predictions of the outer-sphere Marcus Model.

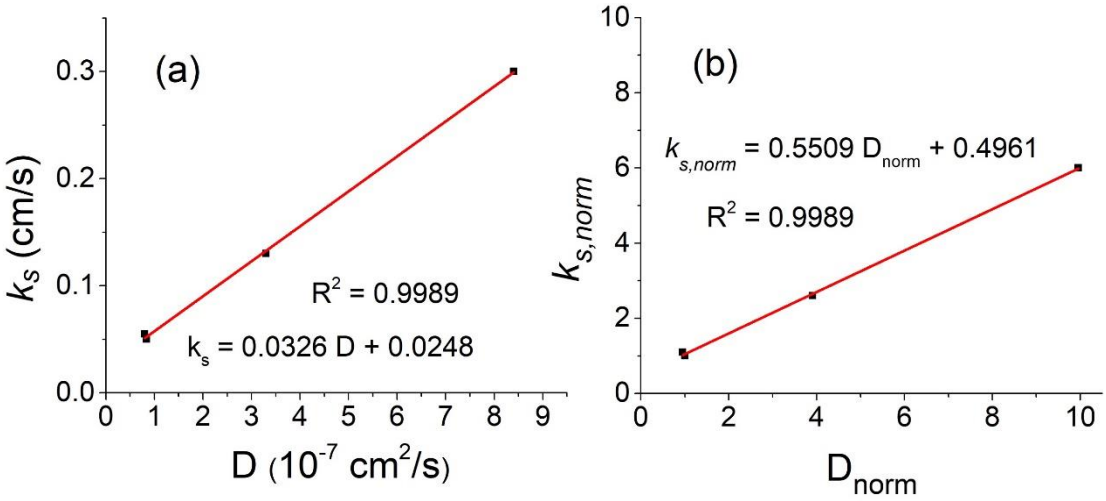

Figure 3.11 Linear correlation of the experimental ET rate constant with the diffusion coefficient. (a) k_s vs. D (b) normalized standard rate constant $k_{s,nom} = k_{s,wet}/k_{s,dry}$ vs. normalized diffusion coefficient $D_{nom} = D_{wet}/D_{dry}$ in EtNH3Cl-Acetamide.

At this point, it is difficult to make a clear conclusion about the origin of the effects on CT rate constants in Ethaline and in $EtNH_3Cl$-Acetamide/water mixture. Besides a different DES, the exact effect with also be function of the molecule and particularly on the charge that is carried by the redox couple that could strongly modifies it solvation environment. This could explain that k_s values of the oxidation of $[Fe(CN)_6]^{4-}$ which is four time negatively charged, are almost not affected by the addition of water while the oxidation of $Fc(MeOH)_2$ indicates a medium increase in $EtNH_3Cl$-Acetamide. In chapter two, we have also reported that the k_s values for $[Fe(CN)_6]^{4-}$ and unsubstituted ferrocene appear to be too high when we considered the viscosity or the relaxation times of the solvents with the ones of "dry" Ethaline and with the determined values of k_s in common solvents.[236] All these observations highlight some anomalies of the CT rate versus the expected Marcus behavior.

3.5 Conclusions

Measurement of the heterogenous charge transfer rate by cyclic voltammetry for the $[Fe(CN)_6]^{4-}$ and $Fc(MeOH)_2$ oxidations in DES/water mixture shown that the CT rate is slightly to medium increase by the addition of water. As a most remarkable observation, the CT rate of the $[Fe(CN)_6]^{4-}$ /$[Fe(CN)_6]^{3-}$ seems unaffected by the change of viscosity when water is added. According to the Marcus theory of charge transfer, standard rate constant, k_s, of a simple outer-sphere electrode reaction is expected to increase when the solvent viscosity decrease. However, the apparently contradictory result observed for $[Fe(CN)_6]^{4-}$ oxidation and a medium rate constant increase for $Fc(MeOH)_2$ oxidation highlight the complexity of the properties of solutes in DES.

Various factors could be considered to explain the differences with a homogeneous solution. First, the use of outer-sphere Marcus model could be problematic. The $[Fe(CN)_6]^{4-/3-}$ redox reaction is more complex than a simple outer-sphere reaction. For $Fc(MeOH)_2$ oxidation, as noticed in Table 3.2, the E^o value vs. Ppy is shift negatively when adding water which emphasizing the impact of solvent structure on the thermodynamics and therefore kinetics. Since the inherent ionic and hydrogen bond characteristic of the considered DES, both ion-pairing[241] and hydrogen-bonding effect between redox couples and DES could play a role on the electrode kinetics. Especially, for $[Fe(CN)_6]^{4-}$ oxidation, due to its negative charged, the ion-pairing effect on its electron transfer kinetics seems more significant than the neutral molecule $Fc(MeOH)_2$. This idea could be demonstrated by studing a negative charged ferrocene derivatives, for example, 1,1'-bis(sulfonate) ferrocene salt.

Another question also remains about the role of the electrode/DES interface in this observation.[242] Our k_s measurements are only apparent rate constants (uncorrected from the Frumkin effect) that thus contains a possible contribution from a change in the electrode/DES interface when water is added. However, the observed behavior could be compared with previous reports coming from totally different methodology. Indeed, similar small changes were also reported for the kinetics of photoinduced CT upon the

addition of water in Ethaline.[66] These spectroscopic measurements that do not imply the use of an electrode support the conclusion that there is not a special effect of the interface on the observed trends. At the end, it is difficult to conclude if this effect is common and will be found for other DES but it clearly reflects the complexity of the mixture of Ethaline that is not a simple solvent.

Nevertheless, the observed behavior is a clear advantage for applications in electrochemistry. Notably, Charge transfer of outer-sphere reaction, like $Fc(MeOH)_2$ oxidation, are enhanced in DES. As concluded previously, presence of water improves the conductivity as it decreases the viscosity of the mixture that could be an advantage for electrochemistry. It justifies the use of DES for improving the solubility of a redox couple without affecting the characteristics of the device. It is also noticeable that macroscopic quantities as viscosity, conductivity or self-diffusion coefficients follow the expected trends when water is added but it also is not surprising that in a complex mixture presenting some organizations, local solvation by water of the electrochemical couples affect the electron transfers in a different manner than for macroscopic quantities. This could explain the apparent disagreement with the Marcus Model.

Chapter 4 Electrochemical reduction of quinones in deep eutectic solvent Ethaline

Work present in this chapter has been published in Electrochem. Sci. Adv., 2022, e2100148.

4.1 Introduction

In this chapter, we focus on redox systems which present more than one electron transfer steps and the electron transfer steps are influenced by hydrogen-bonding interactions or coupled to chemical reactions. Quinones and their substituted derivatives are well adapted for such investigations because they associate the electron transfer to proton transfer and their electrochemical properties are strongly affected by hydrogen bonding[164, 169, 171, 243] as those existing in DES. Theoretical studies have investigated a variety of hydrogen bonds between all components of the DES.[67] This also creates the possibility of numerous combinations between the electrochemical and chemical steps as in the proton-coupled electron transfers (PCET).[244, 245] The electrochemistry of quinones has been studied in aqueous,[246] protic, and aprotic media.[247] The hydrogen bonding and protonation effects on quinones reduction has illustrated in the appearance of proton species in aprotic solvents.[169] Although the redox behavior of quinones has been studied for many decades (see for example the introduction of reference[248] or a review in reference[249]), few studies have been dedicated to their electrochemical properties in solvents like ionic DES. In relation with the present work, some investigations have concerned the reduction of quinone in ionic liquids that have been analyzed in view of the mechanisms reported in molecular solvents taking into account the strength of the hydrogen-bonding characteristics of the ionic liquids.[250-254] Quinones were notably selected as model compounds for evaluating the properties of ionic liquids as electrolytes and compared with molecular solvents.[251] In addition, this also led to electrochemical applications in selected ionic liquids as the CO_2 separation from a gas mixture.[250]

As we already discussed, DES are consists of hydrogen bond donor and hydrogen acceptor and most DESs are containing one ionic component which make it inherently conductive. In this perspective, DES as a solvent can provide both hydrogen-bonding and ionic solvent environments. Due to these specific properties of DES, in the present study, we have examined the quinones reduction in Ethaline which structures shown in Scheme 1 where different substituents are introduced on the ring. This is expected to modify its electric density and basicity and thus the stability of the electrogenerated intermediates.[247]

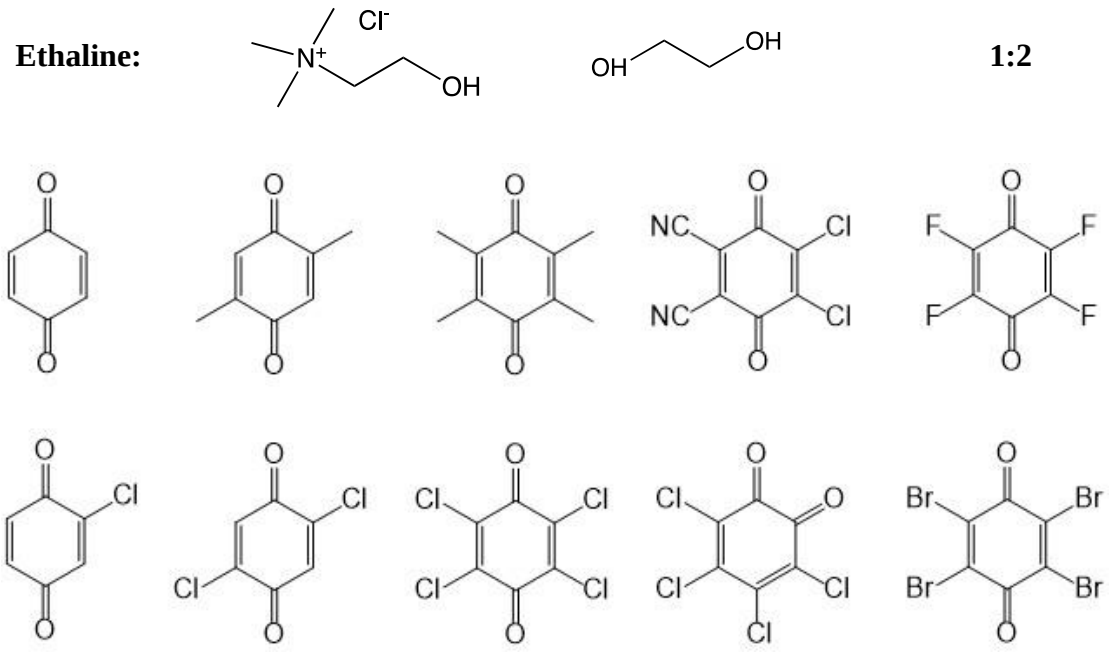

Scheme 4.1 Structures of the quinones and DES (Ethaline) studied in this chapter.

4.2 Experimental section

Chemicals and materials. All quinones were commercially available from Sigma-Aldrich and used as received without further purification unless specified. p-Benzoquinone was purified via reduced pressure sublimation using a cold finger sublimation apparatus before experiments. 2,3-Dichloro-5,6-dicyano-p-benzoquinone (DDQ) was recrystallized from chloroform before use. Ethaline was prepared by mixing the dried choline chloride (ChCl) and anhydrous ethylene glycol (EG)

(ChCl:EG mole ratio 1:2) into a round flask in an argon-filled glovebox and then heated at 333.15 K until a homogeneous liquid was formed. Choline chloride was previously recrystallized from anhydrous ethanol and then dried in a Schlenk line under high vacuum for 90 hours to remove the water.

Electrochemical Measurements. Cyclic voltammetry experiments were done using a conventional three electrode cell, with glassy carbon working electrode (1 mm-diameter disk sealed in a glass tube), platinum grid counter electrode, and Pt/polypyrrole quasi-reference electrode using a SP-50 potentiostat from Biologic Instrument. The Pt/polypyrrole quasi-reference electrode was made according an adaptation of the published procedure.[239] In a solution containing 0.01 mol L^{-1} pyrrole and 0.1 mol L^{-1} NBu_4PF_6 in acetonitrile, PPy film is electropolymerized onto Pt wire with a platinum grid as counter electrode and saturated calomel electrode (SCE) as reference electrode in the condition of sweeping the potential at 0.1 V/s over the potential range -0.6-1.2 V for 50 cycles and stop at 0.4 V.

Solutions of quinones in Ethaline and cyclic voltammetry at low scan rate were made in an argon-filled glovebox, with O_2 and H_2O both below 0.5 ppm. The Pt/PPy reference electrode was immersed no less than 15 min in the solution before measurements at 313±2 K (40 degree centigrade). Ferrocene (Fc) was directly added to the solution at the end of the experiments and used as a calibrating redox couple to provide an absolute potential reference. All potentials in the text are reported versus the half-wave potential of Fc^+/Fc couple. The half-wave potential of Fc^+/Fc couple versus a SCE electrode measured in Ethaline was found to be 0.335 V/SCE. Based on repetitive measurements, errors on potential values are estimated as ± 10 mV. The water amounts were measured using a Karl Fisher Coulometer (831KF Coulometer – Metrohm and using Hydranal® Coulomat E solution from Fluka) before each experiment and are in the range of 330~350 ppm (1.8-1.9 10^{-2} mol L^{-1}).

For fast scan rate cyclic voltammetry in Ethaline (Figures 4.10 and 4.11), cyclic voltammetry experiments were done outside the glovebox at 303K and using a home-made potentiostat equipped with ohmic drop compensation.[236] Ethaline was injected

into a well-sealed cell in glovebox and then taken outside for the experiments. For typical experiments, water amount measured in the cell at the beginning of the experiment was 500 ppm, 2.8 10^{-2} mol L^{-1} of water.

Quinone reductions in acetonitrile (+ 0.1 mol L^{-1} NBu_4PF_6) were studied outside the glovebox at room temperature (293 K) using the same electrodes (excepting the saturated calomel electrode (SCE) as reference electrode) using an Autolab PGSTAT 302N (Metrohm). The water amount measured in acetonitrile, but before adding the supporting electrolyte, was around 500 ppm, 2.8×10^{-2} mol L^{-1}.

All calculations of cyclic voltammetry were done using the Kissa 1D package developed by C. Amatore and I. Svir using the default parameters.[214]

4.3 General observation

4.3.1 Reduction of 1,4-benzoquinone.

Cyclic voltammetry of the reduction of 1,4-benzoquinone in dry Ethaline recorded on a 1 mm-diameter disk glassy carbon electrode which represents the unsubstituted member of the series are presented in Figure 4.1. Experiments were performed in a glove box and Ethaline was specially prepared to limit the presence of water that was around 2.6 10^{-2} mol L^{-1} or lower. A low scan rates (0.05 - 1V s^{-1}), a well-defined electrochemical process is visible at a potential in the range of -0.53 V. The reversibility of the process increases with the scan rate passing from an almost totally irreversible reduction at scan rate of 0.05 V s^{-1} to a partial reversibility around 45-50% at scan rate of 1 V s^{-1}. Another oxidation peak appears an around 0.5 V when the reduction peak of benzoquinone is scanned beforehand. By comparing with an authentic sample studied in Ethaline, this new peak was ascribed to the oxidation of the hydroquinone indicating that protonation of the benzoquinone dianion formed the corresponding hydroquinone. As other general observation, the diffusion coefficient D is estimated around 1.8 10^{-7} cm^2 s^{-1} that is in the range of what we have found for molecules of

similar size in Ethaline.[93, 236]

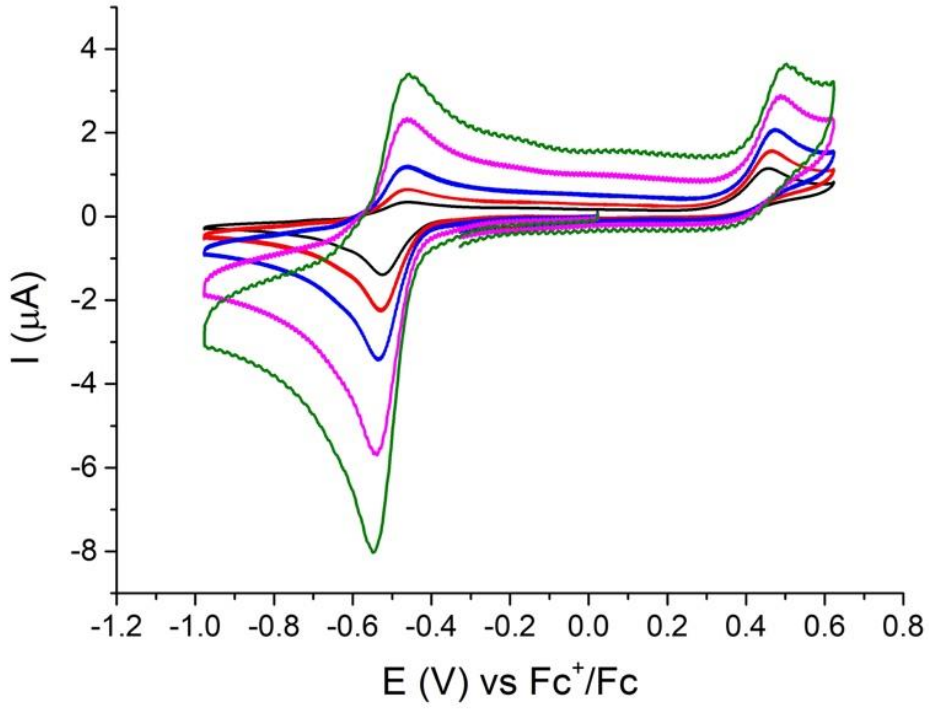

Figure 4.1. Cyclic voltammograms of 3.7 10^{-3} mol L^{-1} of 1,4-benzoquinone in Ethaline on a 1 mm-diameter disk glassy carbon electrode at different scan rates: 0.05, 0.1, 0.2, 0.5 and 1 V s^{-1}. Concentration of water: 2.6×10^{-2} mol L^{-1}. Temp. = 313 K.

The reduction of quinones in presence of a low amount of proton source could be described by an ECE mechanism[244] (electrochemical-chemical-electrochemical) where a radical anion forms at a first step followed by a protonation and a second reduction step leading to a global 2-electron process.[244] The possible mechanism could be:

$$Q + e^- \rightarrow Q^{\bullet-} \qquad E^\circ, k_s$$

$$Q^{\bullet-} + H^+ \rightarrow QH^\bullet \qquad k$$

$$QH^\bullet + e^- \rightarrow \quad QH^-$$

$$QH^- + H^+ \rightarrow QH_2$$

The observed behavior in Ethaline could be analyzed with this mechanism scheme, the initially formed radical anion, $Q^{\bullet-}$ reacts with a proton source to $QH^\bullet$ and then was reduced to QH^- which was finally protonated to form the corresponding hydroquinone

QH_2. Based on simulations using the KISSA 1D software[214] of the ECE mechanism, we could estimate a first order rate constant k for the decay of $Q^{\bullet-}$ around 0.6-0.8 s^{-1} indicating a medium stability of $Q^{\bullet-}$ in this media (simulation not shown here). We could also examine the electron transfer kinetics by considering the peak-to-peak potential difference ΔE_p. At 0.1 V s^{-1}, a value around 60 mV is measured that is indicative of a fast electron transfer. Notice that the measurement of the electron transfer standard rate constant, k_s, is not possible from these few experiments and requires using higher scan rates and a special treatment of the ohmic drop. This will be developed in the following part using a special experimental setup.

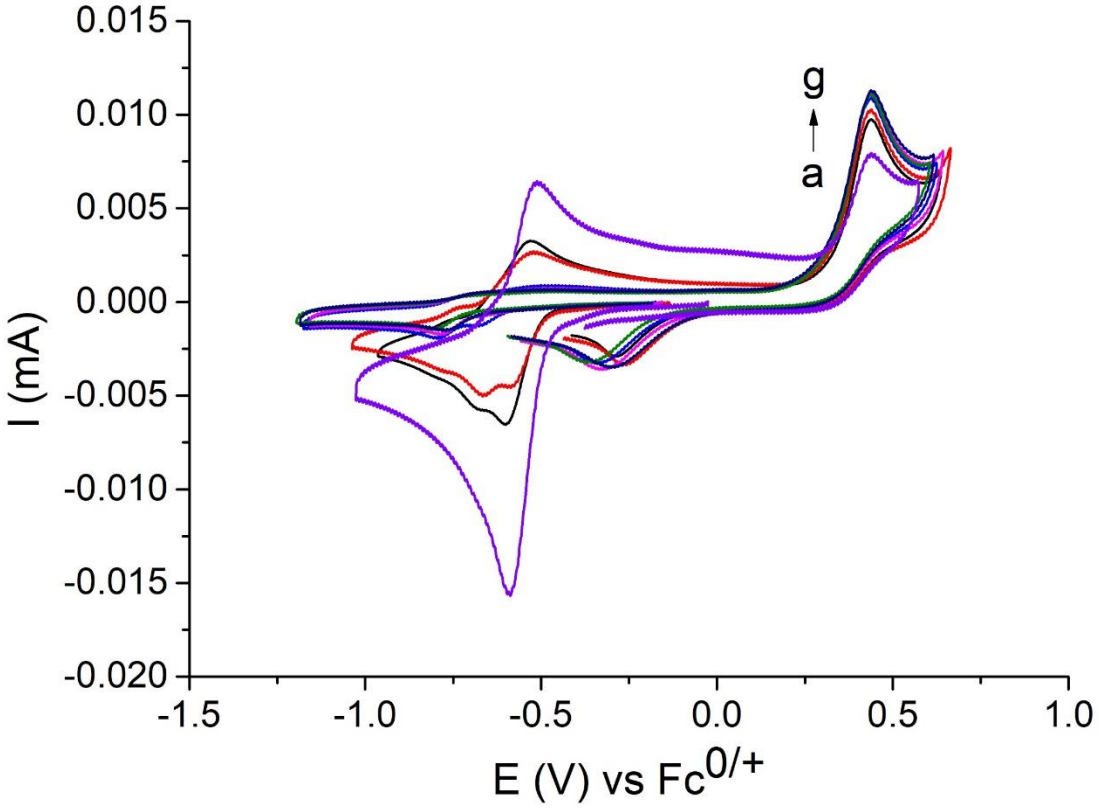

Figure 4.2. Cyclic voltammograms variation of $10.1 \cdot 10^{-3}$ mol L^{-1} of 1,4-benzoquinone in Ethaline on a 1 mm-diameter disk glassy carbon electrode at scan rates 0.5 V s^{-1}. (a) from Fig. 4.1 with current multiply 2.75 (b) initial scan (c) 5 hours later (d) 4 days later (e) 6 days later (f) 10 days later (g) 13 days later. From (b) to (g) was measured in the same solution. Conc of water: 2.6×10^{-2} mol L^{-1}. Temp. = 313 K.

In particular, the CV of p-benzoquinone is change with time. At the initial scan, the CV of p-benzoquinone have the reduction peak at -0.587 V and reverse peak at -0.528 V and another oxidation peak appear at 0.438 V and reverse peak at -0.3 V. The reduction

current of p-benzoquinone decrease with time while the peaks at 0.438 V and -0.3 V increase. To identify the products that is made in this process, the oxidation of hydroquinone in Ethaline was recorded and it showed the same oxidation and return peaks to the p-benzoquinone reduction product. The reduction product could also be extracted from Ethaline by diethyl ether after 13 days standing in glovebox as shown in Figure 4.2 (g). The NMR spectrum confirmed that hydroquinone spontaneously produced (other peaks also appeared). As the p-benzoquinone decays, a new reduction peak at -0.67 V appears, as shown in Figure 4.2 (b) and (c). These reduction peaks could be the intermediate of p-benzoquinone, such as, Q^{2-}, QH^{-}. The first reduction peaks could disappear after 4 days, see Figure 4.2 (d), and a more negative peak appears at around -0.8 V. After 6 days, the second reduction peak also disappeared and only the peak at -0.8 V left. On the contrary, the peak current of hydroquinone continually increase as p-benzoquinone decays. In summary, p-benzoquinone is transformed to hydroquinone in Ethaline at mild conditions. Based on our experimental experience, p-benzoquinone could only be studied in fresh made Ethaline, Figure 4.2 (a), than the one putting for some days, Figure 4.2 (b), for which the transformation has already started during the dissolving process. The reason for this transformation could be that the visible light activated the p-benzoquinone molecules in Ethaline. This also indicates that Ethaline is a kind of protic solvent.

4.3.2 Reduction of halogen-substituted quinones in Ethaline.

Figure 4.3 and 4.4 show the cyclic voltammograms of the reduction of substituted halogenated benzoquinones recorded using the same experimental conditions i.e. glassy carbon electrode and scan rate (0.05 V s^{-1}) for an easier comparison. Two reversible reductions are visible for the tetrasubstituted compounds except tetrafluoro-p-benzoquinone. These observations are similar to those reported in a molecular solvent like acetonitrile but, the potential differences between the first and second electron transfers are much smaller than those in acetonitrile[169] (See data in Table 4.1 and 4.2).

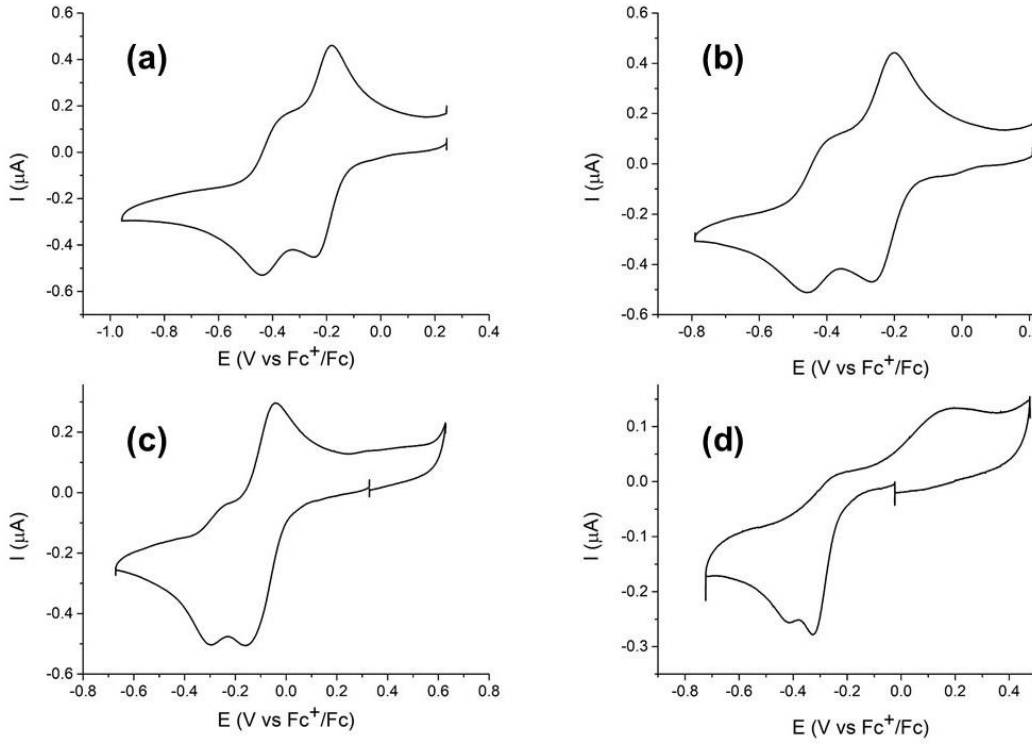

Figure 4.3. Cyclic voltammograms of tetra-substituted-quinones ($C^{\circ}= 2\ 10^{-3}$ mol L^{-1}) in Ethaline on a 1 mm-diameter disk glassy carbon electrode and at a scan rate = 0.05 V s^{-1}. (a) chloranil (tetrachloro-p-benzoquinone); (b) tetrabromo-p-benzoquinone; (c) tetrachloro-o-benzoquinone, (d) tetrafluoro-p-benzoquinone. Water concentration : $1.8\ 10^{-2}$ mol L^{-1}. Temp.= 313K.

Curves recorded for the reductions of mono-choro and dichloro quinones (See Figure 4.4) display similar patterns but with a more negative potential and a slightly lower reversibility indicating a higher reactivity of $Q^{\bullet-}$. As another general observation, the currents at the second reduction are considerably smaller than the current of the first reduction. These phenomena are more impressive when goes from chloranil to 2-chloro-p-benzoquinone. Similar reports have been done in literature regarding the reduction of quinones in molecular aprotic solvent[169, 243] and in ionic liquids[251]. Some explanations have been proposed generally based on the formation of non-electroactive species after the first reduction, but the question remains largely open. (See the discussion in Section 4.4.5).

As seen on Figure 4.3 (d), the case of tetrafluoro-p-benzoquinone is different. The reduction shows two irreversible processes indicating that the stabilization of the radical anion $Q^{\bullet-}$ by fluorine substituent is not sufficient to avoid its rapid decay.

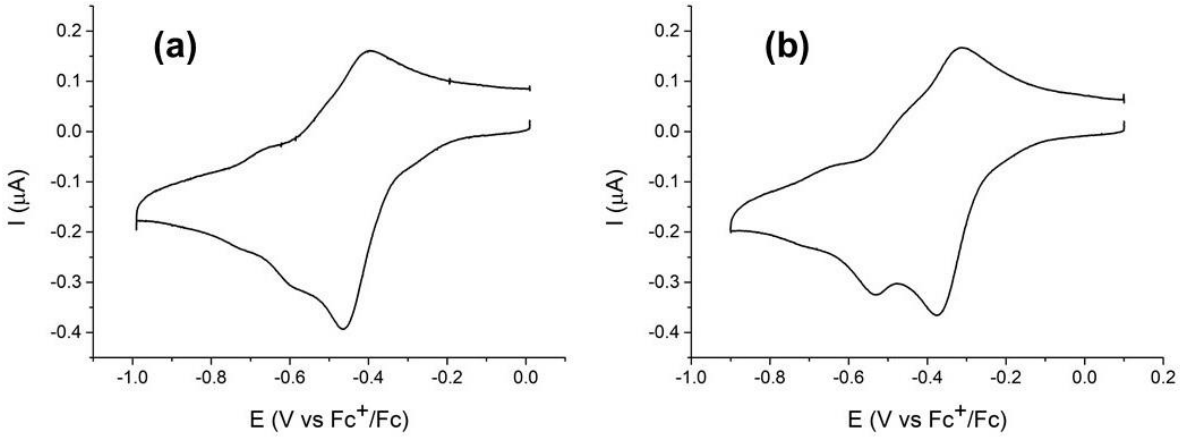

Figure 4.4 Cyclic voltammograms of mono and disubstituted quinones in Ethaline on a 1 mm-diameter disk glassy carbon electrode at a scan rate of 0.05 V s^{-1}. (a) 2-chloro-p-benzoquinone (C° = 2.1 10^{-3} mol L^{-1}); (b) 2,5-dichloro-p-benzoquinone (2.0 10^{-3} mol L^{-1}). Water concentration: 1.8 10^{-2} mol L^{-1}. Temp. = 313 K.

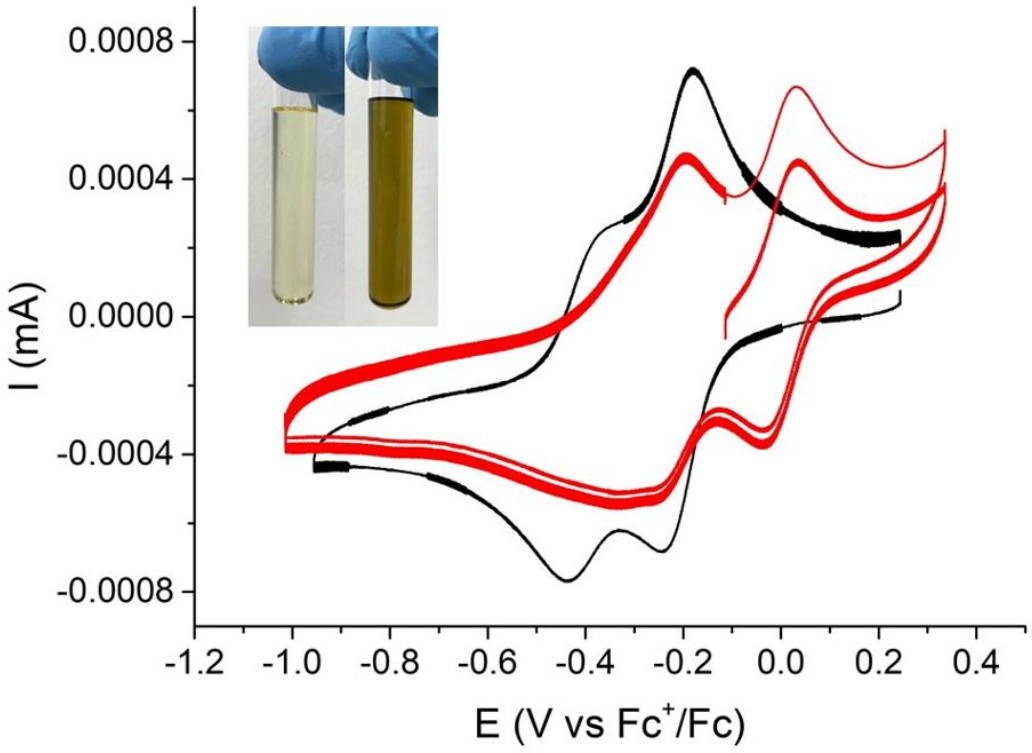

Figure 4.5 Cyclic voltammogram of 2mM chloranil in Ethaline on glassy carbon electrode at a scan rate of 0.1 V/s before (black) and after (red) adding ferrocene. Insert figures are the solution of chloranil in Ethaline before (yellow) and after (green) adding ferrocene. T= 313 K.

An interesting phenomenon was observed when adding ferrocene in chloranil solution in Ethaline, see Figure 4.5, in a temptative of getting an internal standard for potential measurements. After adding ferrocene to the chloranil solution in Ethaline, the mixed

solution changed from yellow to green rapidly which can be seen from the insert picture of Figure 4.5. The CV shows that both anion and dianion of chloranil have changed. The anion's peak current decreases (this can be partly caused by adding ferrocene's Ethaline solution) and the dianion's current disappeared. From the color and CV changing, we could conclude that ferrocene is oxidized to ferrocenium by chloranil. This is due to the solvent effect of Ethaline draws the chloranil reduction potential to much positive with increasing its oxidizing power. But this reaction was not found in other quinones. Spectroscopy methods, such as UV-Vis spectrophotometry, could also be used to monitor this reaction.

Similar phenomenon was reported for the reduction of ortho-chloranil in organic solvent (CH_2Cl_2) with adding hydrogen bond donors (HBD).[165] Pseudo-first-order rate constants were determined at 25 °C by monitoring the reaction between othro-chloranil and the indicated ferrocene in the presence of the indicated HBD. Based on these results, they developed a HBD-coupled electron transfer system which applied as an effective strategy to activate electron-deficient quinones. And this strategy has proved to be potential useful in organic synthesis. From our observation, Ethaline could play a similar role.

4.3.3 Reductions of quinones with strong withdrawing or donor substituents.

To complete the study, we have examined the electrochemistry of some other quinones in Ethaline bearing strong withdrawing substituent or donor substituents. Figure 4.6 shows the cyclic voltammetry of the reduction of 2,3-dichloro-5,6-dicyano-p-benzoquinone (DDQ) in Ethaline at low scan rate. Current analysis demonstrates that DDQ is a mono-electron transfer by taking the first reduction of chloranil as a $1e^-$ standard. It corresponds to the reversible formation of the radical anion in Ethaline as expected from a good stabilization of the electrogenerated $Q^{\bullet -}$ by the two cyano groups. A more surprising observation is the quasi-absence of a second reduction process. In fact, a second process is actually visible around -0.5 V but its peak current is much smaller (it is only 25 % of the first reduction) which similar to the above observations

that second peak currents are considerably smaller in Ethaline. Another broad intermediate process is also visible between the two peaks (in the -0.1-0 V potential zone) that may be due to the carbon electrode as proposed previously.[248]

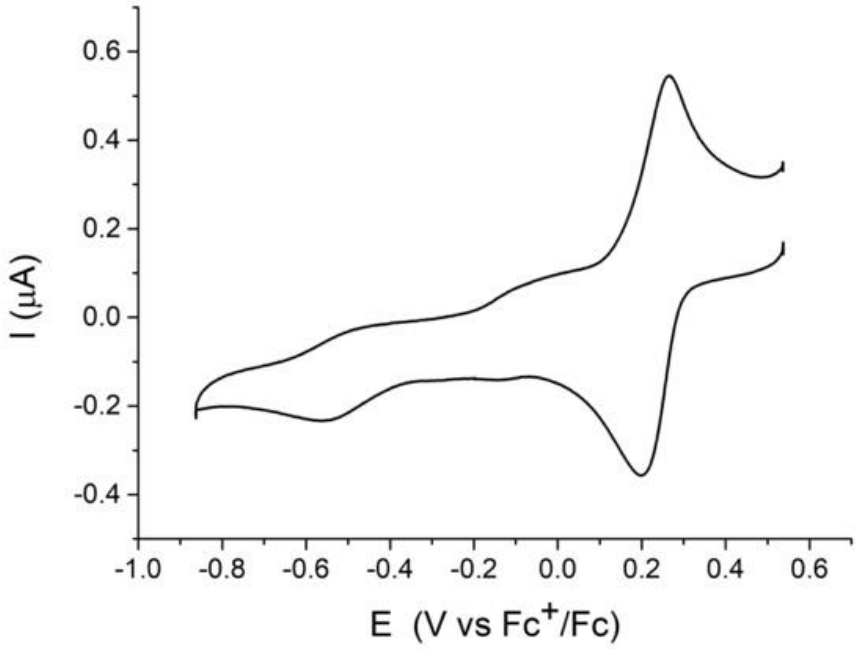

Figure 4.6 Cyclic voltammogram on 1 mm diameter glassy carbon electrode of 2.1 10^{-3} L^{-1} 2,3-dichloro-5,6-dicyano-p-benzoquinone on a 1 mm-diameter disk glassy carbon electrode in Ethaline at 313 K at scan rate of 0.05 V s^{-1}. Water concentration : 1.8 10^{-2} mol L^{-1} .

As seen on Figure 4.7, reductions of dimethyl-substituted and tetramethyl-p-benzoquinone (duroquinone) also display a partially reversible cyclic voltammograms. However, the analysis of the peak current intensity shows a global stoichiometry of $2e^-$ transfer by taking the first reduction peak of chloranil as a $1e^-$ standard. The reduction peak currents characterized by their half peak width (E_p-$E_{p/2}$) are much thinner with E_p-$E_{p/2}$ ≈ 38 mV (corresponding to the simultaneous transfer of 2-electron process, theory 28 mV) than peak currents of the other quinones with E_p-$E_{p/2}$ ≈ 63-65 mV.[255, 256] Contrarily to the reduction of benzoquinone, the reversibility does not increase with the scan rate and the return peaks takes a more plateau shape when the scan rate is increased with the appearance of new peaks (See Figure 4.8).[257] Such behavior could be explained by the same general ECE mechanism when the chemical steps are fast and partially at the equilibrium. In the framework of the $(ECE)_{rev}$ mechanism, increasing

the scan rate makes the equilibrium less reversible and thus the global reversibility of the process decreases. This leads to a more irreversible process and appearance of new peaks due to the direct reoxidation of intermediates in the ECE mechanism.[97] (more detail discussion see Section 4.4.3)

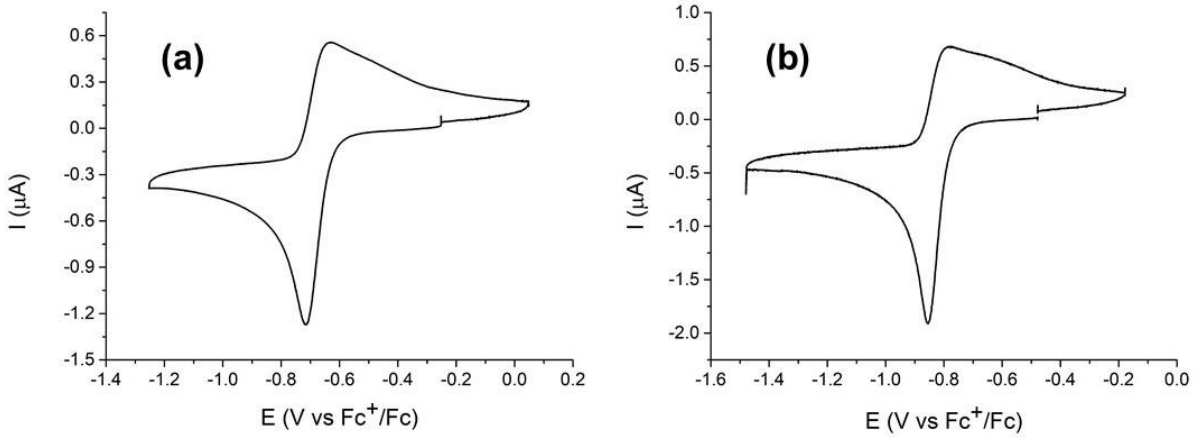

Figure 4.7 Cyclic voltammetry of the reduction of quinones with donor groups in Ethaline on a 1 mm-diameter disk glassy carbon electrode. Solution of (a) 2.3 10^{-3} mol L^{-1} 2,5-dimethyl-p-benzoquinone and (b) 2.1 10^{-3} mol L^{-1} duroquinone in Ethaline. Temp: 313 K. Scan rate 0.05 V s^{-1}. Water concentration: 1.8 10^{-2} mol L^{-1}.

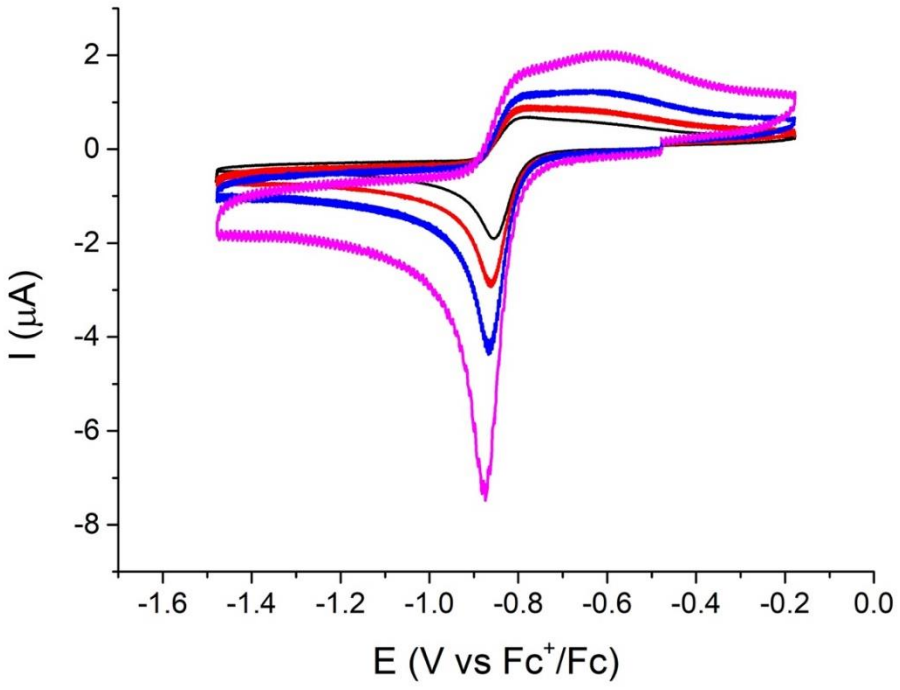

Figure 4.8 Cyclic voltammograms of duroquinone in Ethaline at different scan rates of 0.05, 0.1, 0.2, 0.5 V s^{-1}. Experimental conditions are same to Figure 4.7 (b).

4.4 Discussions

4.4.1 Diffusion coefficient of quinones in Ethaline.

The characteristics of the quinones reductions in Ethaline are reported in Table 4.1. The derived diffusion coefficients, *D*, were calculated from the first reduction peak current I_p considering the prevailing diffusion control.[97, 143, 256]

Table 4.1. Electrochemical parameters for the reduction of quinones in Ethaline at 313K.

Quinone	E^1_p/V	ΔE^1/mV	E^2_p/V	D/cm^2 s^{-1}	**n**
2,3-Dichloro-5,6-dicyano-p-benzoquinone	0.20	60	-0.56	1.7×10^{-7}	1
Tetrachloro-o-benzoquinone	-0.16	83	-0.29	2.2×10^{-7}	1
2,3,5,6-Tetrachloro-p-benzoquinone (Chloranil)	-0.24	58	-0.44	2.0×10^{-7}	1
2,3,5,6-Tetrabromo-p-benzoquinone	-0.26	62	-0.46	1.6×10^{-7}	1
2,3,5,6-Tetrafluoro-p-benzoquinone	-0.33	-	-	1.5×10^{-7}	1
2-chloro-p-benzoquinone	-0.46	65	-	2.0×10^{-7}	1
2,5-Dichloro-p-benzoquinone	-0.38	64	-	1.5×10^{-7}	1
p-Benzoquinone	-0.53	62	-	1.8×10^{-7}	2
2,5-Dimethyl-p-benzoquinone	-0.72	-	-	1.6×10^{-7}	2
2,3,5,6-Tetramethyl-p-benzoquinone (Duroquinone)	-0.85	-	-	2.2×10^{-7}	2

E^1_p :Peak potentials of the first reduction E^2_p : Peak potentials of the second reduction peak. ΔE^1 : Peak to peak difference of the fist reduction measured at 0.05 V s^{-1} from reversible or partially reversible voltammograms. All potentials are measured versus the Fc^+/Fc couple in Ethaline.

For the reversible 1-electron system, they were derived using the relation for a reversible monoelectronic process : $I_p = 0.446\ FSC^\circ\sqrt{D}\sqrt{\frac{Fv}{RT}}$ where *F* is the Faraday constant, *S* the electrode surface area, *C* the initial concentration of the redox couple, *R* the gas constant, *v* the scan rate and *T* the absolute temperature. For the fully bielectronic couple (2,5-dimethyl-p-benzoquinone and duroquinone), to take into

account the thinner peak of an $(ECE)_{rev}$ mechanism we considered the equation for the simultaneous transfer of 2 electrons, n=2 and $I_p = 0.446\ nFSC\sqrt{D}\sqrt{\frac{nFv}{RT}}$. [97, 143] The relation for the $EC_{irr}E$ mechanism, $I_p = 0.496\ nFSC\sqrt{D}\sqrt{\frac{Fv}{RT}}$ was used for the analysis of the benzoquinone voltammogram (n=2).[97, 143] The electron transfer number (n) is determined by taking the chloranil first reduction peak current as $1e^-$ transfer (see Table 4.1). The diffusion coefficients in Ethaline of the different quinones are in the 1.5 - 2 10^{-7} cm^2 s^{-1} range. They are around two orders smaller than those measured in a molecular solvent like acetonitrile in agreement with the higher viscosity of Ethaline.[93, 236] In that sense, the mass transport of quinones in Ethaline does not reveal a special behavior compared to other redox molecules like ferrocene.

4.4.2 Reduction potentials in Ethaline. Comparison with the potential in acetonitrile.

Reduction potentials reflect the interactions of the quinone and of its radical anion with the electrolyte solvent.[169, 171, 243] In this chapter, we have compared the redox potentials of quinones in Ethaline, shown in Table 4.1, with those measured in acetonitrile, shown in Table 4.2, containing 0.1 mol L^{-1} NBu_4PF_6 as supporting electrolyte.

In an ionic liquid or in a DES like Ethaline, the supporting electrolyte that is also the solvent, could participate in ion-pairing or H-bonding interactions with the reduced quinone forms, whereas the polarity of the solvent also affects the solvation energies.[251, 253] Rigorously, such correlation would require the measurement of the thermodynamic data, *i.e*. the standard potentials $E°$ that could only be derived from a reversible voltammogram.[97, 143] The reduction of quinones in acetonitrile presents reversible processes, while only few of the studied quinone reductions were found to be totally reversible in Ethaline. Thus, our comparison in Figure 4.9 was only based on the peak potential variations E_p, but covers a large change in the reduction power that is much higher than 1 V. Considering this large variations of potential, and even if different kinetics controls could prevail in the ECE mechanism that may introduce deviations

between E_p and $E°$, we could detect a general trend from such correlation. Indeed, a good linear variation is observed with a slope of 0.71 (R=0.987) in Figure 4.9. It shows that the reduction potentials vary similarly in both solvents and the effect of the substitution is higher in acetonitrile than in Ethaline. It is also noticeable that the reduction of all studied quinones is easier in Ethaline than in acetonitrile. An easier reduction is indicative of a better stabilization of Q and $Q^{\bullet-}$ by Ethaline than by acetonitrile confirming the occurrence of H-donor associations.[169] Passing from a withdrawing group to a donor group increases the negative charge density on the oxygen atoms of the quinones and thus favors the interaction with the electrolyte/solvent. A better stabilization by the solvent is thus expected to present slope that is smaller than unity as it is observed in our correlation (Figure 4.9). Presence of water is also an important parameter as it could also affect the value of the potential notably by the formation of hydrogen-bonding.[164, 171] However, the quantity of residual water in acetonitrile containing an ammonium salt as electrolyte is comparable or litter higher than in our measurements in Ethaline.

Table 4.2. Reduction potentials of quinones measured in acetonitrile vs. Fc^+/Fc

Quinone	E^1_p/V	E^{2p}/V	ΔE^1_p-ΔE^2_p
2,3-Dichloro-5,6-dicyano-p-benzoquinone	0.10	-0.74	0.84
Tetrachloro-o-benzoquinone	-0.31	-1.08	0.77
Chloranil	-0.40	-1.20	0.80
Tetrabromo-p-benzoquinone	-0.41	-1.17	0.76
Tetrafluoro-p-benzoquinone	-0.41	-1.25	0.84
2,5-Dichloro-p-benzoquinone	-0.60	-1.38	0.78
2-chloro-p-benzoquinone	-0.76	-1.46	0.70
p-Benzoquinone	-0.92	-1.55	0.63
2,5-Dimethyl-p-benzoquinone	-1.09	-1.75	0.66
Duroquinone	-1.27	-1.93	0.66

Peak potentials recorded on a 1 mm diameter disk electrode on a glassy carbon electrode in Acetonitrile (+ 0.1 mol L^{-1} NBu_4PF_6). Data used for Figure 4.9.

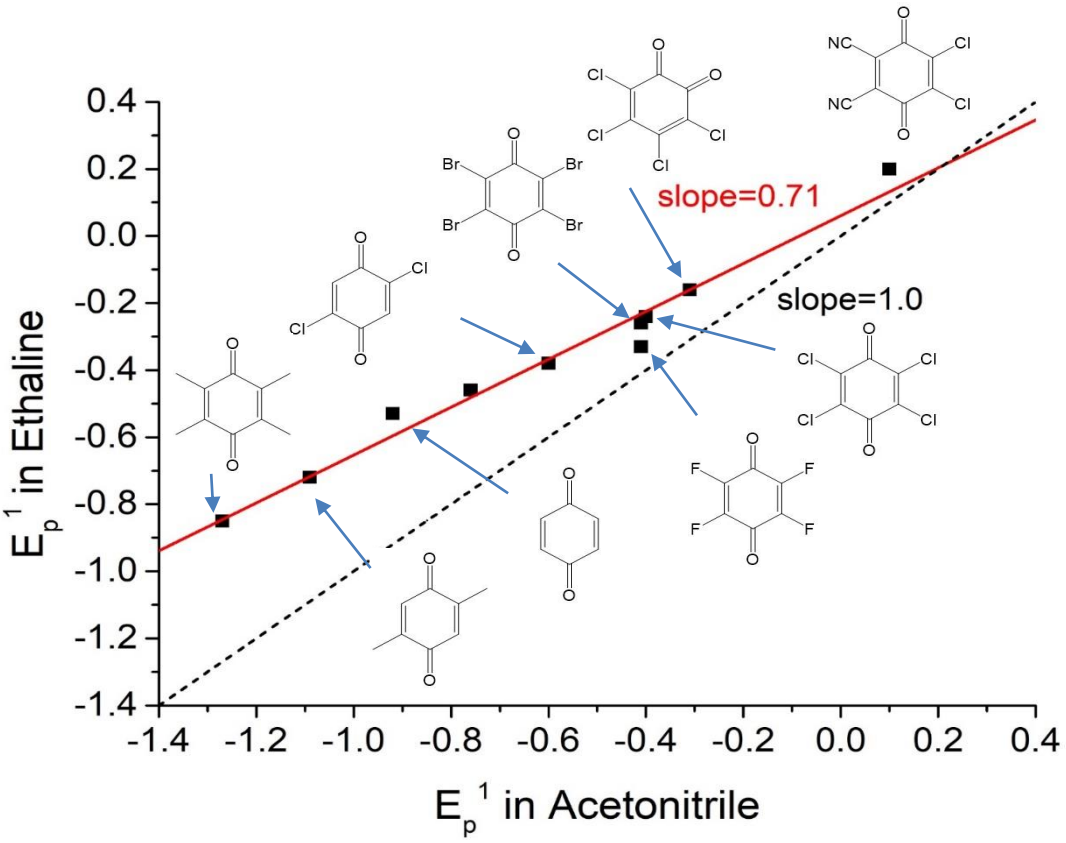

Figure 4.9 Variation of the peak potentials for the first reduction of the quinone in Ethaline versus values in acetonitrile + 0.1 mol L^{-1} NBu_4PF_6). Potentials are measured versus the Ferrocene/Ferrocenium couple at 0.05 V s^{-1}. In Ethaline at 313 K, in acetonitrile 293 K.

We could also consider the potential difference between the first and the second reduction. In a molecular solvent like acetonitrile containing a quaternary ammonium salt as supporting electrolyte, the two reductions of a quinone derivative are generally separated by about 0.7 V (See Table 4.2). As seen in Table 4.1 in Ethaline, with the exception of 2,3-dichloro-5,6-dicyano-p-benzoquinone, the potential differences between the first and the second electron transfers are only or less than 0.2 V. This falls in line with a higher stabilization of the charged species by the solvent and confirms the occurrence of strong H-bonding interactions.[169] This phenomena will be studied in detail in the next chapter with the reduction of dinitrocompounds.

4.4.3 Hydrogen-bonding effect on quinones reduction in Ethaline

The previous literature have studied the hydrogen-bonding effect on quinones

electrochemistry which by adding minor amounts of hydrogen bond donors to aprotic solvent,[166, 167, 169, 258] but few are in a pure hydrogen-bonding environment solvent like DES. We found this solvent can exert special influence on quinones behavior.

The first impressive feature is the reduction potential of quinones in Ethaline are strongly shift to positive position (see Figure 4.9) and for the reversible two electron transfer process, for example chloranil, the separation of formal potentials was largely compressed from 0.8 V in acetonitrile to 0.2 V in Ethaline and for duroquinone, the two electron transfer merged together (see table 4.1 and 4.2). In the previous reports,[169] the results revealed the hydrogen bonding effects on quinone reduction by adding certain amount of hydrogen bond donor and the most impressive potential shifts were seen in the second peak while the first was slightly infected. In Ethaline which possess highly hydrogen-bonding environment, this effect was strongly enhanced for both the first and second peaks.

The other noticeable observation is the easier protonation of quinones in Ethaline. As we know, p-benzoquinone in aprotic solvents, like acetonitrile, show two separate reversible electron transfers. The electrochemistry of p-benzoquinone in unbuffered and buffered aqueous solution shown reversible and quasi-reversible two-electron transfer, respectively.[246] As we observed here, p-benzoquinone could be readily transformed to hydroquinone in Ethaline due to the fast protonation. This makes Ethaline more like an acidic solvent as its reported pH is in the range of 4.7-6.9. The water amount in Ethaline is in the same order of acetonitrile while the protonation was not observed in acetonitrile. This all manifest that the solvent effect of Ethaline, unlike water, does favour p-benzoquinone protonation. On the other hands, p-benzoquinone (BQ) shows a rather high basicity. The pK_a values of the possible proton source of water (14) and ethylene glycol (15.1) are both lower than semiquinone (4.0) and Q^{2-} (11-12) of BQ,[169] this makes the proton transfer unfavorable. A possible explanation is that the hydrogen-bonding between p-benzoquinone and the solvent (hydrogen bond donor, H-D) make the proton transfer easier and faster. The proposed H-bonding effects on proton coupled electron transfer (PCET) can be seen in Scheme 4.2. At the beginning, BQ

formed H-bonding with the solvent which can reduce it first reduction potential. After two electron transfer, the ionic H-bonding complex formed between Q^{2-} and solvent which makes the intermolecular proton transfer occur. This could provide a wider perspective for the proton transfer process. The current plateau in the reverse scan of methyl-substituted quinones could also explained by forming the H-bonding complex which formal potentials are higher than non-H-bonded redox couple.[172] This phenomenon was also found in the oxidation of Phenylenediamines in organic solvent in the presence of weak bases.[179, 259] While for the higher basicity duroquinone and 2,5-dimethyl-p-benzoquinone, corresponding hydroquinone was not formed which could due to the steric hindrance effect.

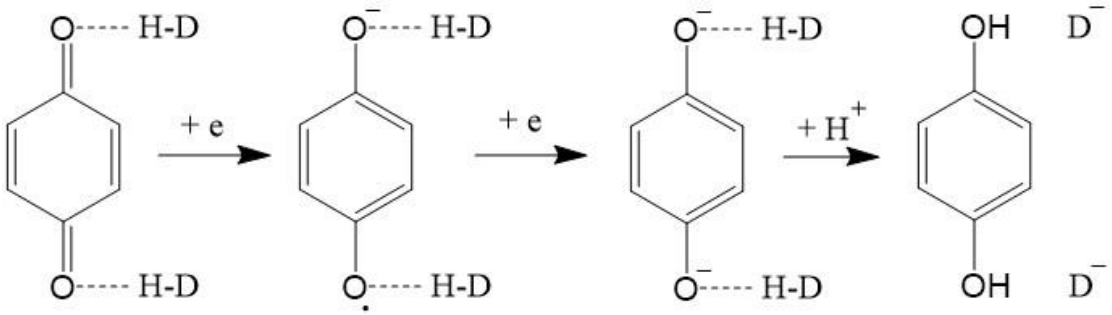

Scheme 4.2 Hydrogen-bonding effects on proton coupled electron transfer of p-benzoquinone.

Finally, the activation of electron-deficient quinones,[167] chloranil, was occasionally found when adding internal standard molecular ferrocene in solution. Quinones as a one-electron oxidants have been used in preparative chemistry including both synthetic applications and generation of species for in situ characterization.[260] As yet, few examples have been reported of the oxidation of organometallics to simple, primary redox products (see reference[260] and therein). As revealed in Figure 4.5, ferrocene was oxidized by chloranil to ferrocenium with the color changing from yellow to green. A possible reason for this reaction is the occurrence of hydrogen-bonding between chloranil and DES solvent facilitated the electron transfer.[165] As shown in scheme 4.3, the oxidizing power increases from electron-donor substituted quinones to electron-withdrawing substituted quinones (the reduction potential from low to high values in Table 4.1). Due to the hydrogen-bonding enhanced positive shifts of formal potential

in Ethaline, the oxidizing power of quinones increase at the same time. The success of this proposal depends both on the HBD strength and quinone's reactivity.

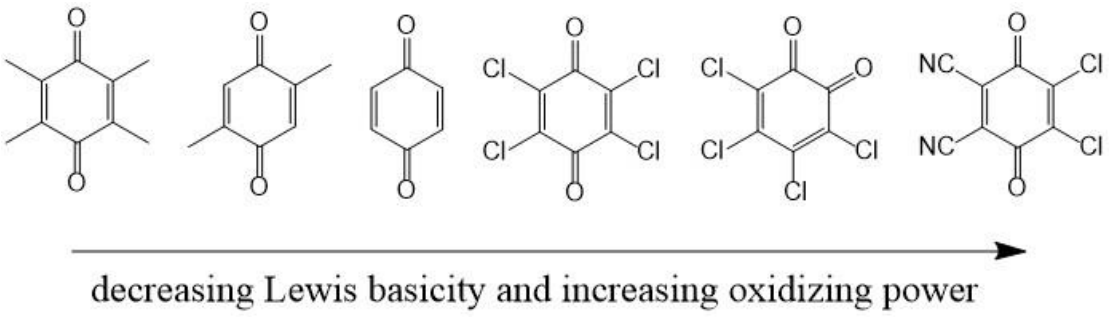

Scheme 4.3 Effect of quinone structure on oxidizing ability and Lewis basicity.

Therefore, the hydrogen-bonding environment of DES has a high influence on the reduction potential, protonation and activity of quinones in Ethaline.

4.4.4 Electron transfer kinetics of the quinone reduction in Ethaline.

Electron transfer rate constant k_s is another important parameter besides the reduction potentials for detecting the presence of a specific solvation. As explained above, in the framework of the Marcus theory, the standard rate constant corrected by the effect of the double layer for an adiabatic electron transfer is given by:[159, 198]

$$k_s = \frac{K_p}{\tau_L}\left(\frac{\Delta G_{Os}^{\#}}{4\pi RT}\right)^{1/2} exp\left[-\left(\frac{\Delta G_{Os}^{\#} + \Delta G_{is}^{\#}}{RT}\right)\right]$$

where K_p is the equilibrium constant for a precursor complex and τ_L is the longitudinal relaxation time that is the relaxation time of the solvent normalized by the ratio of the static ε_s and high frequency ε_{op} relative permittivities, $\Delta G_{Os}^{\#}$, $\Delta G_{is}^{\#}$ are the standard Gibbs activation energy of the outer sphere and inner sphere contributions. $\Delta G_{Os}^{\#}$ reflects the change of solvation between the neutral quinone and the produced radical anion. In this part of chapter 4, we focus on the electrochemical properties of the tetra-bromo and tetra-chloro quinones that present the simplest patterns. Such investigations in a DES are quite challenging as they require using high scan rates.[236] The main difficulties arise both from the higher resistivity and the lower viscosity of a DES like

Ethaline. As for previous measurement, the higher resistivity results in higher residual ohmic drop that make unusable the curves recorded at high scan rates for a quantitative analysis. Experiments in Ethaline require a special setup in which the ohmic drop could be effectively compensated.[208, 209] Fast scan rate voltammograms using a 1 mm-diameter disk glassy carbon electrode are shown on Figures 4.10 and 4.11. Use of the positive feedback compensation explain the extra-noise that is visible on these curves.

Cyclic voltammetry of two reversible reductions of quinones, chloranil and tetrabromo-p-benzoquinone, are shown in Figure 4.10 and 4.11, respectively. Both the low and high scan rates are shown in these pictures. As observed, the both redox couples show reversible reduction peaks at low scan rates but only the first reduction peak are visible at high scan rates.

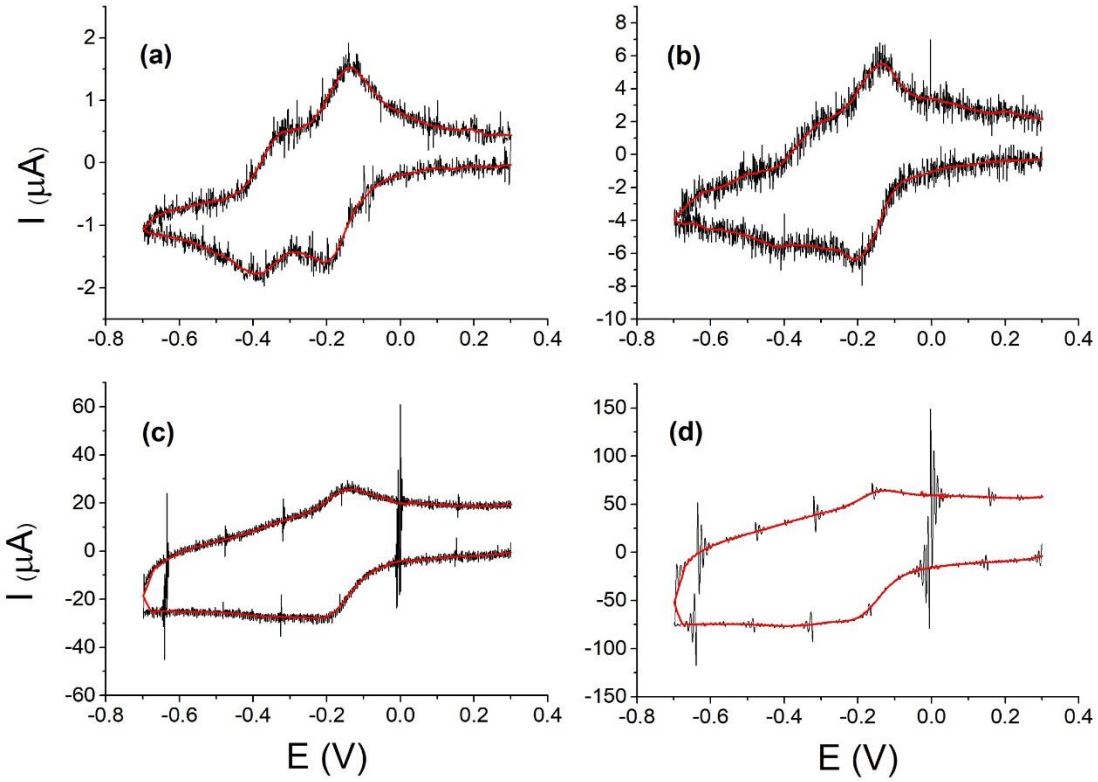

Figure 4.10 High scan rate cyclic Voltammetry of 2 10^{-3} mol L^{-1} chloranil solution in Ethaline on a 1 mm-diameter disk glassy carbon electrode. Scan rates (a) 0.5 (b) 5 (c) 50 (d) 200 V s^{-1}. Temp. = 303 K. Concentration of water: 2.8 10^{-2} mol L^{-1}.

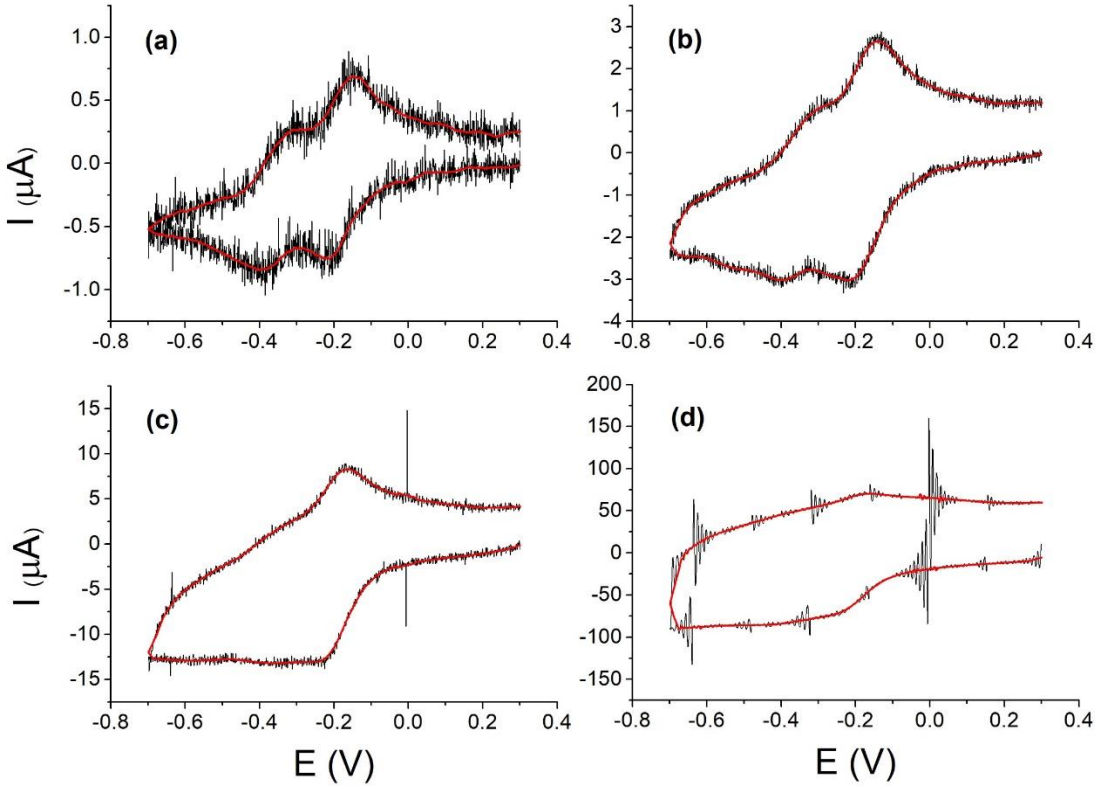

Figure 4.11 High scan rate cyclic voltammetry of 2.0 10^{-3} mol L^{-1} tetrabromo-p-benzoquinone solution in Ethaline on a 1 mm-diameter disk glassy carbon electrode. Scan rates : (a) 0.2 (b) 2 (c) 20 (d) 200 V s^{-1} Temp. = 303 K. Concentration of water: 2.8 10^{-2} mol L^{-1}.

The value of the standard rate charge transfer constant k_s were derived from the variation of the peak-to-peak potential with the scan rate following previously described procedures.[97, 236] Figure 4.12 shows the experimental ΔE_p versus log of the scan rate for the first reduction as the fit with the theoretical variations. The adjustment between experimental and calculated variations provides a unique determination the experimental parameter $k_s/D^{1/2}$. For both quinones, ΔE_p does not considerably vary for most of the low scan rates range and only increases for the highest scan rates. This is indicative of a high value of parameter $k_s/D^{1/2}$ that could be measured as 230 and 295 s^{-1} for the first reduction of chloranil and tetra-bromo-p-benzoquinone respectively. Taking into account the D values, we derived k_s values of 0.12 cm s^{-1} for the reduction of chloranil and 0.14 cm s^{-1} for the reduction of tetra-bromoquinone. These values are higher than the charge transfer rates for a couple like ferri/ferrocyanide in the same conditions (2 10^{-2} cm s^{-1}) (see Chapter 2 and 3) but remain slower than the transfer rate of a fast system like the ferrocene/ferrocenium couple,[236] a ranking that is similar to

what is expected in a classical molecular solvent like acetonitrile.

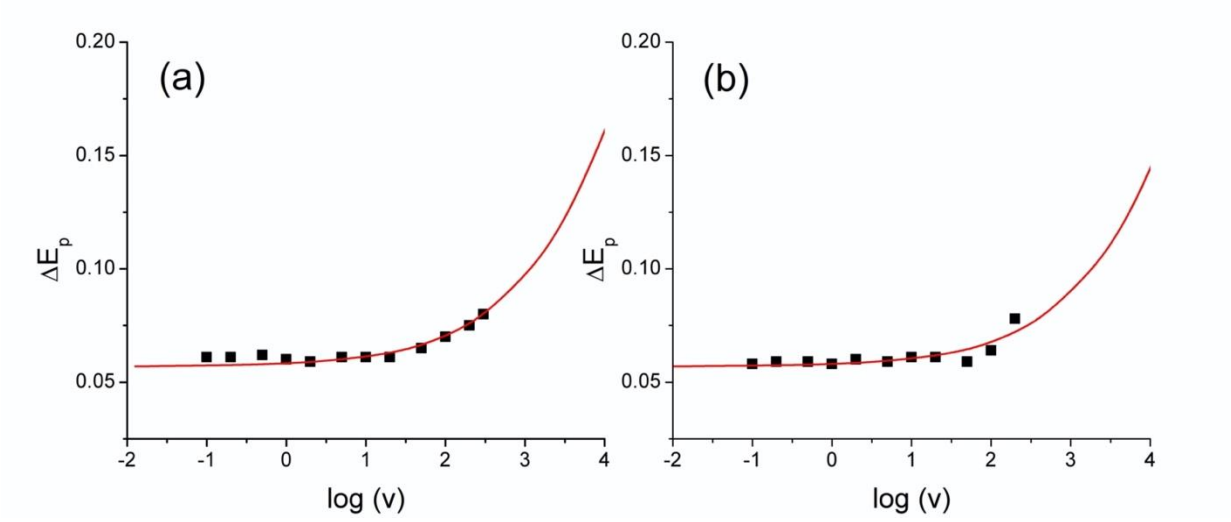

Figure 4.12 Variation of the peak potential ΔE_p with the scan rate. (a) Reduction of chloranil in Ethaline. (b) Reduction of tetrabromo-p-benzoquinone in Ethaline. Temp.: 303 K. Working electrode is a 1 mm-diameter disk glassy carbon electrode. Lines are the theoretical behavior assuming a Buttler-Volmer Law and a transfer coefficient α equal to 0.5.

4.4.5 Second reduction of quinones in Ethaline.

As noticed above, for all the studied quinones, the peak current of the second reduction in Ethaline is considerably smaller than the one of the first reduction, the difference depending on the structure of the quinone and substituents. Similar observations were reported in several publications (see for examples references[169, 243] and the references therein) for the reduction of substituted quinones in molecular solvents and in imidazolium based ionic liquids[251]. A simple explanation could be a difference of diffusion coefficients between the radical anion $Q^{\bullet-}$ and the neutral quinone Q resulting of a second smaller peak. Such explanation does not sound for a molecular solvent or in a DES like Ethaline where the diffusion coefficients present negligible variations with the charge of the molecule.[93, 236] Notice that because of the occurrence of homogeneous electron transfer reactions and the ensuing coupling of diffusional pathways, this will also lead to a loss of reversibility of the voltammogram, which is not visible in our results. Instead, different explanations considering some forms of dimerization of $Q^{\bullet-}$ were proposed in the literature to explain the voltammetry. Among

the possible mechanisms, the reaction between the neutral quinone Q and the dianion Q^{2-} yielding an electro inactive dimeric product $[Q_2]^{2-}$ was proposed for explaining the lower currents.[169, 243] These assumptions were then latter discussed. Some inconsistencies with a proposed dimerization mechanism when changing the concentration of quinone were spotted and a different mechanism involving the association of $Q^{\bullet-}$ with the OH present on the surface of a glassy carbon electrode was proposed.[248] To bring some additional highlights on this puzzling phenomenon, we focus on the evolution of the second process on the voltammograms of Figures 4.10 and 4.11 (reductions of chloranil and tetrabromo-p-benzoquinone in Ethaline). At low scan rate (Figure 4.3 a, b), the second peak is reversible and smaller than the first process as reported before. When the scan rate is increased, the second peak becomes broader and more unsymmetric, the return peak current being larger than the forward peak current. For the highest scan rate, the second peak becomes almost not visible. This observation appears incompatible with the hypothesis of the formation of a non-electroactive species (as a dimer) in a competitive manner as the reverse effect with the scan rate is expected.[243] On the contrary, the behavior observed in Ethaline is understandable in the framework of a CE mechanism where a chemical step precedes the second electron transfer. Based on the above observations, it is likely that such chemical step be a specific interaction with the media notably by hydrogen-bonding or with a low amount of proton donor in the literature leading to the more reducible $Q^{\bullet-}$ (sol).[169, 171] If it is difficult to clearly identify the nature of 'sol', we have not observed considerable changes of the voltammograms when the amount of water was doubled.

The CE mechanism is characterized by a large a variety of possible voltammograms shapes depending on competition between diffusion and the homogeneous preceding reaction that is characterized by its equilibrium constant K, and a kinetics parameter $\lambda = \frac{RT}{F}\frac{(k_+ + k_-)}{v}$ with k_+ and k_- being the forward and return kinetics rate constants of the preceding chemical step:[97]

$$Q + e^- \rightarrow Q^{\bullet-} \qquad E^\circ, k_s$$

$$Q^{\bullet-} \leftrightarrow Q^{\bullet-}(sol) \qquad K, k^+, k^- \quad (1)$$

$$Q^{\bullet -}(sol) + e^- \rightarrow Q^{2-}(sol) \qquad E^\circ, k_s \quad (2)$$

We performed simulations of the voltammograms assuming this mechanism (See Figure 4.13, notice that background currents are not introduced in the simulated curves). These simulations support the hypothesis of a CE mechanism by reproducing the general trend with a kinetics parameter $K(k_+ + k_-)^{1/2}$ in the range of $30\ s^{-1/2}$. To verify the proposed mechanism, KISSA was used to model the cyclic voltammograms for 2 mM quinones at a planar electrode ($0.01\ cm^{-2}$).[214] All the species diffusion coefficients are assumed tha same value of $2\ 10^{-7}\ cm^{-2}$ /s and temperature is 303 K.

ET steps:
A + e = B, k0 = 0.12 cm/s, alpha = 0.5, E0 = -0.17 V
C + e = D, k0 = 0.12 cm/s, alpha = 0.5, E0 = -0.12 V
Homogeneous reactions:
B = C, $k_f = 200000\ s^{-1}$, $k_r = 1 \cdot 10^9\ s^{-1}$
B + C = A + D, $k_f = 3.8922\ M^{-1}\ s^{-1}$, $k_r = 0.573519\ M^{-1}\ s^{-1}$

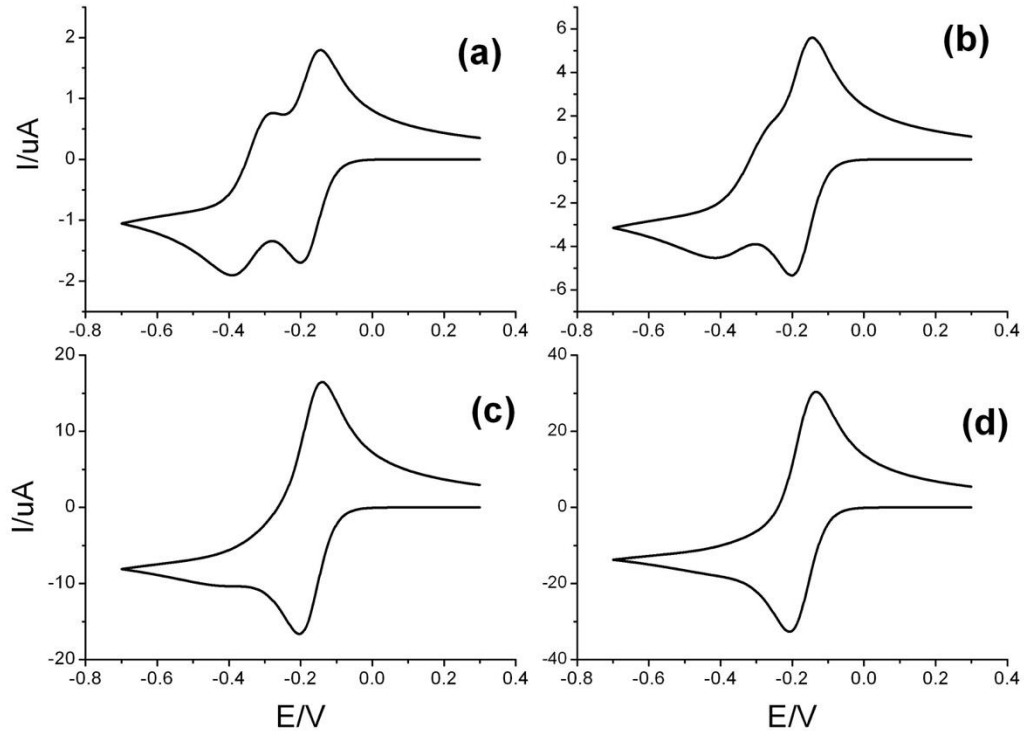

Figure 4.13 High scan rates cyclic Voltammetry of the reduction of chloranil in Ethaline. Simulation of the experiments of Figure 4.10 using KISSA-1D software. Scan rate: (a) 0.5 (b) 5 (c) 50 (d) 200 V/s.

4.5 Conclusions

The electrochemical behavior of quinones in Ethaline are varies with their structure nature and display many similarities with what is observed in a solvent like acetonitrile but shown some notable differences with in organic aprotic solvent, water (buffered and unbuffered water), and ionic liquids. The most impressive characteristics is the large positive potential shifts and the comparison of two reduction peaks of quinones compare with the aprotic solvents mentioned above. This shift shows a linear trend as in aprotic solvents, like acetonitrile. The main reason is due to the special solvent environment of Ehaline which, in particular, the hydrogen-bonding effect between the solvent and quinones and its intermediates are emphasized. The diffusion coefficient of quinones are around $2 \cdot 10^{-7}$ $cm^2 \cdot s^{-1}$ which is two orders slower than in acetonitrile due to its high viscosity. Electron transfer numbers or the mechanisms are properly analyzed. Ethaline shows some kind of protic solvent for the high basicity quinones, such as, methyl-substituted-p-benzoquinones, p-benzoquinone, and one of the electron-withdrawing substituted quinone -- tetrafluoro-p-benzoquinone. This phenomenon of protonation is easily observed from the transformation of p-benzoquinone to hydroquinone. The activation of electron-defficient quinone, chloranil, was found by its reaction with the standard molecular of ferrocene due to the hydrogen-bonding environment. This could provide a new case for chloranil as redox oxidant which has a promising application in organic synthesis. The electron transfer kinetics of some reversible quinones showed that fast kinetics was also found in Ethaline.

We should mention that here we just show one example of DES--Ethaline. As the physicochemical properties could vary much in different DESs due to their very different components[261], such as, the acidity and basicity, the redox behavior of quinones could change from one DES to another. But the hydrogen-bonding effect in DESs could always exert similar influences.

Chapter 5 Electrochemical Reduction of Dinitroaromatics in Deep Eutectic Slovents

5.1 Introduction

Our previous results have shown that electron transfer kinetics in DESs are relatively higher than in ionic liquids (ILs).[236] We also highlighted the effects of hydrogen-bonding that notably result in large potential compression or shift to positive potential are observed in the reduction of quinones in a DES Ethaline.[262] To make a better understanding of these solvent effects on electron transfer, the reduction of dinitroaromatics in DESs is presented in Chapter 5.

The electrochemical reduction of dinitroaromatic, which possess two identical nitro groups and thus two electron transfer, in protic[263-266] and aprotic solvents[183, 267-269] has been extensively studied. The main interests in studying the electrochemistry of successive electron transfers to molecules was related to the indication of the structural and solvent environmental factors that may rise to potential inversion.[180, 270] Dinitro-compounds have been extensively studied in organic solvent which some show successive one electron transfer and others multi-electron transfer. What most interesting is some show potential inversion[182, 192] due to the structure changing.

$$A + e \rightleftharpoons A^{\bullet -},\ E_1^0,\ k_{s1}$$

$$A^{\bullet -} + e \rightleftharpoons A^{2-},\ E_2^0,\ k_{s2}$$

For the molecules with two identical substitutes, the factors controlling the potential difference between the first and second charge transfer ΔE^0 ($\Delta E^0 = E_1^0 - E_2^0$) have been thoroughly studied. Ammar and Saveant have investigated the reduction of dinitro-aromatics in acetonitrile (ACN) and dimethylformamide (DMF).[180] They show that the distance between the nitro groups and the conjugation structure play the main role to decrease the value of $E_1^0 - E_2^0$. Evans *et al.* have investigated the electrochemical reductions of a series of dinitroaromatics at a glassy carbon electrode in DMF.[267] They

found the E_1^0- E_2^0 value of para-substituted derivatives, such as, 1,4-dinitrobenzene, 2,6-dinitronaphthalene, and 2,6-dinitroanthracene are lower than their corresponding meta dinitro-aromatic derivatives due to the resonance of para-substituted compounds which tends to stabilize the dianions.

Besides the structural factors, the solvent environmental also plays considerable role in the potential separation. When water was added as a co-solvent added to the DMF solution in the range of 0-10 %, the ΔE^0 could dramatically decrease even leading to a potential inversion in some situation such as the reduction of 4,4'-dinitrobiphenyl[270]. Ion pairing effects[186, 270, 271] have long been studied in the reduction of redox in organic solvents as the addition of cations, such as, Li^+ [270], K^+ [272], and quaternary ammonium salt[186], could pair with the dianions and dramatically decrease the ΔE^0. Specifically, the electrochemical reductions of dinitroaromatics in acetonitrile were investigated with four quaternary ammonium electrolytes. The results shown that ion pairing effects can be varied with the salt structures and the smaller cations have stronger effect on the separation of standard potential[186].

In addition, the general mechanisms of the electrochemical reduction of dinitroaromatic have been extensively studied in different solutions from aqueous,[264, 273] aprotic solvent[273] to ionic liquid[274]. In aprotic media, the only products of nitrobenzene obtained were the anion radicals which are stable in the time range of cyclic voltammetry and irreversible reduction peaks are observed at more negative potentials, which usually lead to phenylhydroxylamine (PhNHOH). The dianion salt of nitrobenzene has been isolated in liquid ammonia[275] and highly purified DMF.[276] However, in aqueous and more generally in protic solvents, the mechanisms are much complicated. The general accepted proposal is first the generation of nitrosobenzene (PhNO) and then its reduction to the predominant product of phenylhydroxylamine (PhNHOH) or aniline[265] (depending on the strength of the acid medium) via the intermediate N-phenylhydroxylamine. Azo (PhN=NPh) and azoxy (PhN=NOPh) compounds[266, 277] could also be formed at more negative potential of nitrosobenzene. These products could be seen as the coupling of nitrosobenzene anions with its parent molecule. For the dinitro-aromatic compounds, the mechanism in presence of protons

is even more complex because of the presence of the two nitro groups and the numerous possible redox state leading to numerous possible cross reactions between charges and protons transfert states. Only one nitro group transformed was observed in the presence of proton donors[278], which has similar mechanism of mononitroaromatics.

In this chapter, we report the electrochemical reduction of a series dinitrocompounds in DES and some preliminary analysis of the reduction mechanisms in this type solvent. While structure effects were highly emphasized in previous studies, here we show the solvent environments becomes the significant factor in a DES like Ethaline for potential inversion of dinitrocompounds reductions.

The reductions of the following molecules were considered in this chapter:

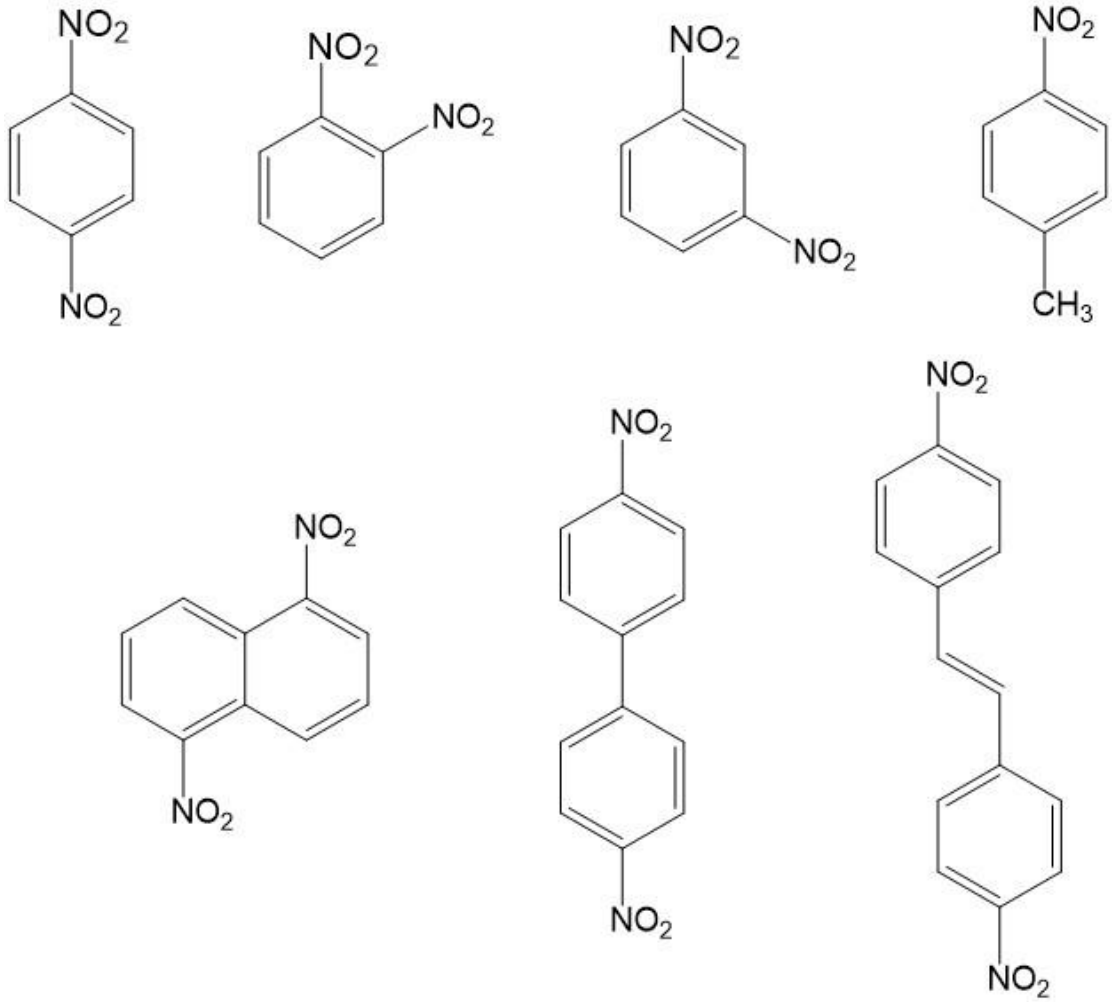

Scheme 1 Structure of dinitroaromatics (including one mononitroaromatics) studied in this chapter.

5.2 Experimental section

Chemicals. 1,5-dinitronaphthalene and 4,4'-dinitrobiphenyl were from TCI. Other dinitro-aromatic compounds were commercially available from Sigma-Aldrich and used as received without further purification. Anhydrous Acetonitrile and the supporting electrolyte Tetrabutylammonium hexafluorophosphate (TBA-PF_6, ≥99.0%) from Sigma-Aldrich. Ethaline was prepared by mixing the dried choline chloride (ChCl) and anhydrous ethylene glycol (EG) (ChCl:EG mole ratio 1:2) into a round flask and then heated in oil bath with stirring at 333.15 K until a homogeneous liquid was formed. Choline chloride was previously recrystallized from anhydrous ethanol and then dried in a Schlenk line under high vacuum for 12 hours to remove the water.

Electrochemical experiments. The cyclic voltammetry experiments were carried out in a three-electrode cell system at 25±1 °C excepted specified. CV of low scan rates (0.05-1 V/s) were record on an Autolab potentiostat and high scan rates on a home-made potentiostat equipped with a positive feedback component which could compensate the ohmic drop between the reference electrode and working electrode. The working electrode is a 1 mm diameter glassy carbon electrode. It was carefully polished before each set of voltammograms with 1 μm diamond paste and rinsed with ultrapure water and acetone. The counter electrode is a big platinum grid and the reference electrode is Ppy@Pt quasi-reference electrode. Solution were prepared freshly before experiments, and oxygen was removed by bubbling argon no less than 5 min which was constantly fed to the cell's free space above the solution surface.

The water amounts in Ethaline were measured using a Karl Fisher Coulometer (831KF Coulometer – Metrohm and using Hydranal® Coulomat E solution from Fluka) before each experiment and are in the range of 0.15-0.2 wt% (mol L^{-1}).

Digital simulations. All calculations of cyclic voltammetry were performed using the Kissa 1D package developed by C. Amatore and I. Svir using the default parameters.

5.3 Results

5.3.1 Electrochemical reduction of 1,4-dinitrobenzene in DESs

The cyclic voltammetry of the reduction of 1,4-dinitrobenzene in Ethaline on a 1mm diameter glassy carbon electrode is shown in Figure 5.1. The first reduction peak is an almost reversible at -0.777 V. Some irreversible reduction peaks are visible at more negative potentials. A corresponding oxidation peak appear at -0.743 V when the reduction peak of the 1,4-dinitrobenzene is scan beforehand.

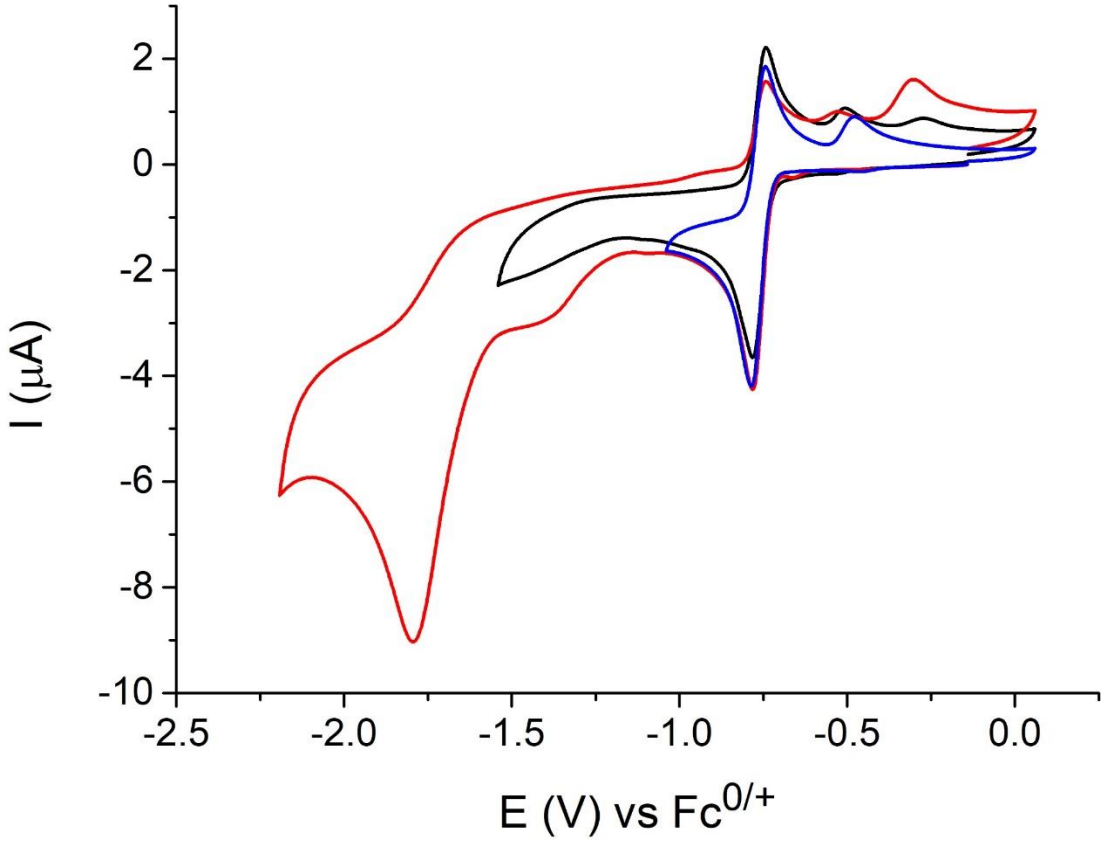

Figure 5.1 Cyclic voltammetry of 3.2 mM 1,4-dinitrobenzene in Ethaline at room temperature 293 K at scan rate of 0.2 V/s.

The first reduction peak could be ascribed to the formation of the dianion which formed after the bi-electronic reduction of 1,4-dinitrobenzene. As examined in aprotic and protic media in many publications, the formal potential of nitroso-benzene is more positive than corresponding nitrobenzene. From this point, the oxidation system at -

0.477 V can be ascribed to the formation of the nitroso-benzene which is produced after the protonation of the dianion and loss of one water molecule. The protons could come from residual water in Ethaline or from Ethaline itself because its components containing OH groups (water being the most probable source of proton in these conditions). When scanning to more negative potentials, a broad and relatively small second reduction peak is observed at -1.464 V and a corresponding oxidation peak at -0.319 V. By comparing with the potential of azobenzene (PhN=NPh) in Ethaline, these peaks possess similar potential separation. Without entering in more details, the possible nature of this peak is the formation of azo or azoxy compounds.[266, 277] When continuing to more negative potential, a third peak appear at -1.768 V which is chemically irreversible. This could suggest that the formed nitroso-benzene be reduced and undergoes rapid protonation and then probably yields phenylhydroxylamine (PhNHOH) and other reductions. It seems that p-phenylenediamine, which possess two reversible oxidation peaks in Ethaline is not formed in this process (not shown).

After examined the whole reduction process of 1,4-dinitrobenzene in Ethaline, a careful investigation was put on the more interesting first reduction peak that is characteristic of the influence of Ethaline on the reduction process. Figure 5.2 shown the CVs of the first reduction peak of 1,4-dinitrobenzene in Ethaline at various scan rates at 25 °C. At a scan rate of 0.1 V/s, the potential peak separation ($\Delta E_p = E_{pa} - E_{pc}$) of the first reduction process is 34 mV. Notice that the nitrosobenzene which visible at a more positive potential also display ΔE_p around 35 mV, see Figure 5.2 (a). These values are much lower than the theoretical potential separation of 58 mV, which means a potential inversion occurs during the reduction of 1,4-dinitrobenzene in Ethaline. In traditional organic solvents, such as acetonitrile (ACN) and dimethylformamide (DMF), 1,4-dinitrobenzene have a normal ordering of potential.

The observation of potential inversion, which the second electron transfer occurs with greater ease than introduce the first, of 1,4-dinitrobenzene in Ethaline should indicates that the solvents environment in DES are particularly different to organic solvents. When increasing the scan rate, the nitrosobenzene peak decrease rapidly and could hardly see for scan rates above 5 V/s, see Figure 5.2 (c). This indicates that the

protonation of the dianion remains relatively slow in Ethaline.

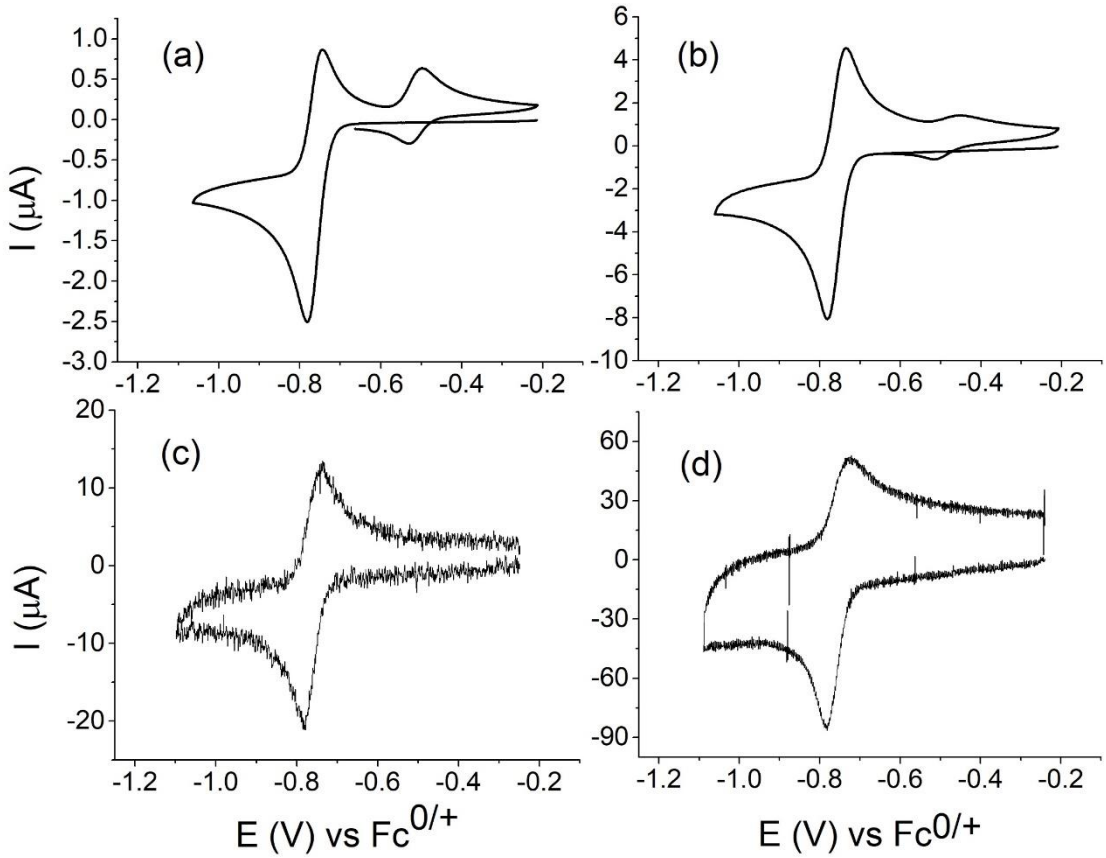

Figure 5.2 Cyclic voltammetry of 2.2 mM 1,4-dinitrobenzene in Ethaline 0.15wt% of water at 298 K at scan rate of (a) 0.1 (b) 1 (c) 5 (d) 50 V/s.

Although the chemical reactions follow to the first reduction process, we could examine the electron transfers processes leading the dianion notably through the standard potential difference $\Delta E^0 = E_1^0 - E_2^0$ (E_1^0, E_2^0 are standard potentials for the first and second electron transfers, respectively) in Ethaline and the difference between the forward and return peak potentials ΔE_p measured at various scan rates. As for the other measurments made in Ethaline, one should take into account the possible influence of the ohmic drop, as the uncompensated ohmic drop tends to increase the ΔE_p values. These experiments were carefully done using the home-made potentiostat which is equipped with an electronic positive feedback component to allow the ohmic drop to be compensated. For a fast two-electron systems (meaning when the two electron transfer are fast), the standard potential difference ΔE^0 is directly related to the value of ΔE_p value and thus ΔE^0 can be extracted from a simple theoretical curve (so called

thermodynamic control) of ΔE_p verses ΔE^0. In practice, this ideal situation is rarely encountered for all scan rates and ΔE_p is also function of the two individual charge transfer constants k_{s1}, and k_{s2}. Figure 5.3 shows the experimental variations of ΔE_p *versus* log (scan rates). The standard potential difference ΔE^0 value could be estimated from the low scan rates values which are supposed to be under the thermodynamic control range.[255, 279] For 1,4-dinitrobenzene, the standard potential difference ΔE^0 value is -34 mV at 0.1 V/s. Assuming that k_{s1}, and k_{s2} are similar, the rising part of Figure 5.3 allows and estimation of the charge transfer rate constants which can be estimated as 0.3 cm s^{-1}.[255, 279]

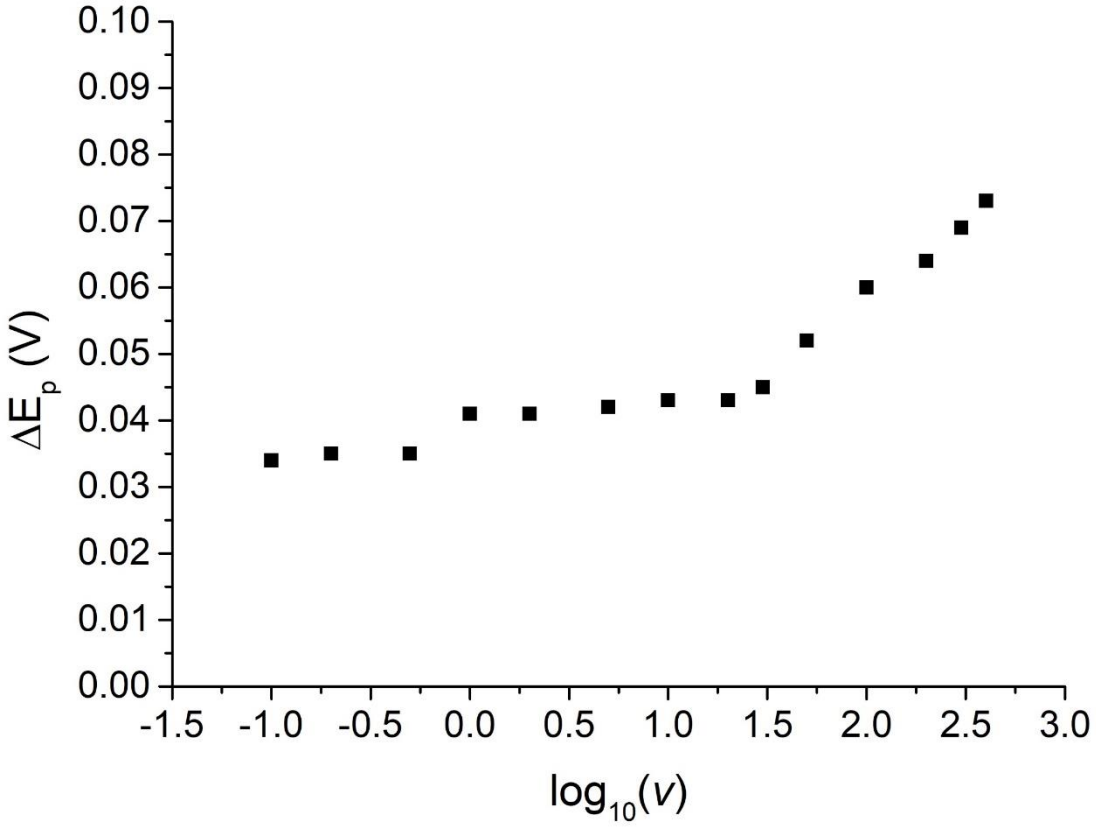

Figure 5.3 Peak potential separation of 1,4-dinitrobenzene in Ethaline variation with scan rates at 298 K.

We tried the same analysis for the reduction of 1,4 dinitro benzene in another DES that is composed of Ethylammonium chloride-Acetamide in 1:1.5 mole ratio. Unfortunately, the reduction of 1,4-dinitrobenzene displays an irreversible process and for all the available scan rates up to 100 V/s. As Ethylammonium chloride possess a much higher acidity than the Ethaline, the protonation of the dianion appears much faster and the

same treatment is not possible as this is only feasible on reversible voltammograms.

To make a comparison with the reduction of dinitrobenzene, the cyclic voltammograms of a mononitrobenzene, 4-nitrotoluene, in Ethaline were also recorded. As it shown in Figure 5.4, it has two chemically irreversible reduction processes. The first reduction peak is at -1.243 V and the second at -1.304 V at scan rate of 0.1 V/s. This voltammogram is rather similar to the ones reported in protic media as already extensively studied. The first reduction peak produces the radical anion or the dianion of nitrotoluene which could then couple with protons producing nitrosotoluene as evidences by the presence of more positive peak at -0.662 V and corresponding reduction peak at -0.768 V. The same features are observed for the reductions of the other dinitro-compounds which are shown below. Notice that the second reduction processes are also very close to the first one.

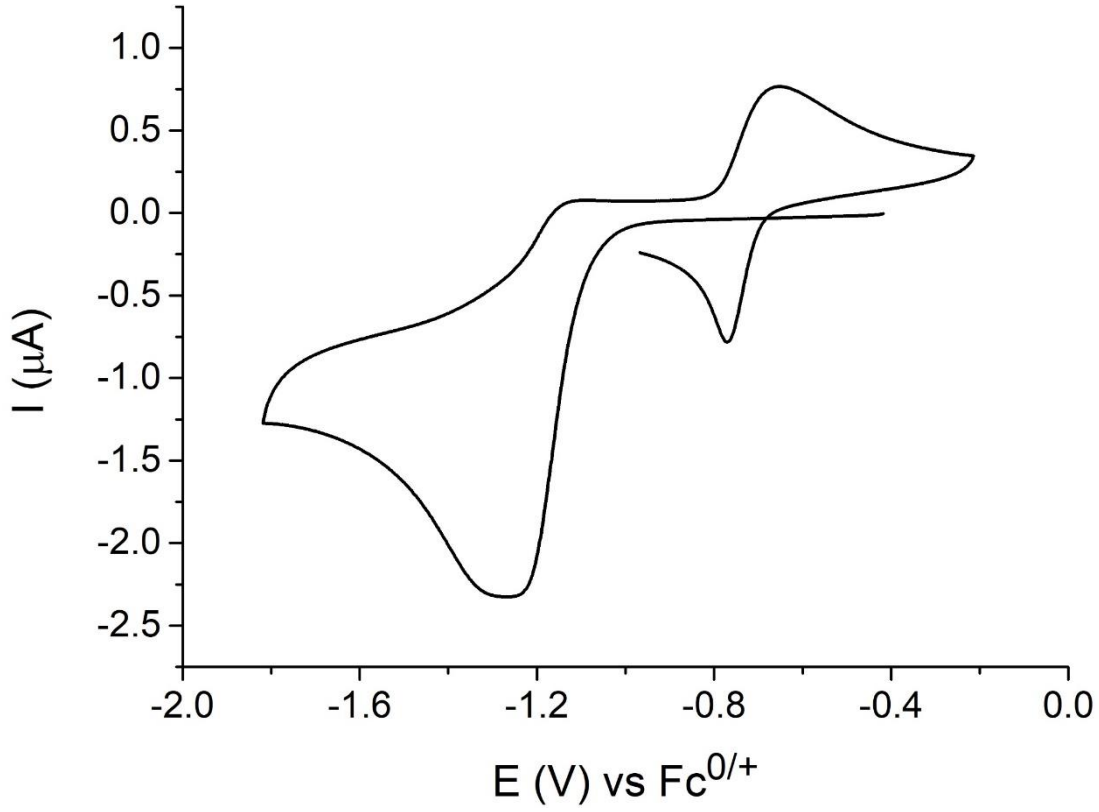

Figure 5.4 Cyclic voltammetry of 2.6 mM 4-nitrotoluene in Ethaline at scan rate of 0.1 V/s at 293 K.

5.3.2 Electrochemical reduction of other dinitroaromatics in Ethaline

1,2- and 1,3-Dinitrobenzene. To evaluate how the structure factors influence the electrochemical behavior in Ethaline, the reduction of isomers of 1,4-dinitrobenzene, 1,2-dinitrobenzene and 1,3-dinitrobenzene were also investigated in Ethaline. Figure 5.5 (a) shows the stepwise reduction of 1,2-dinitrobenzene in Ethaline. Unlike the para-dinitrobenzene, the reduction of 1,2-dinitrobenzene displays irreversible voltamograms under scan rates of 5 V/s. The first reduction peak was at -0.890 V. The reversibility of the first reduction process increases up to around 45% (I_{pa}/I_{pc}) at 200 V/s, but no potential inversion was evidenced. At more positive potential, the nitrosobenzene characteristic peak was found at -0.470 V. When the potential was scanned at more negative potentials, the second and third irreversible reduction peaks at -1.333 V, -1.403 V appeared. This could be ascribed to the two-step reduction of nitrosobenzene coupled with proton transfer reaction producing the corresponding phenylhydroxylamine.

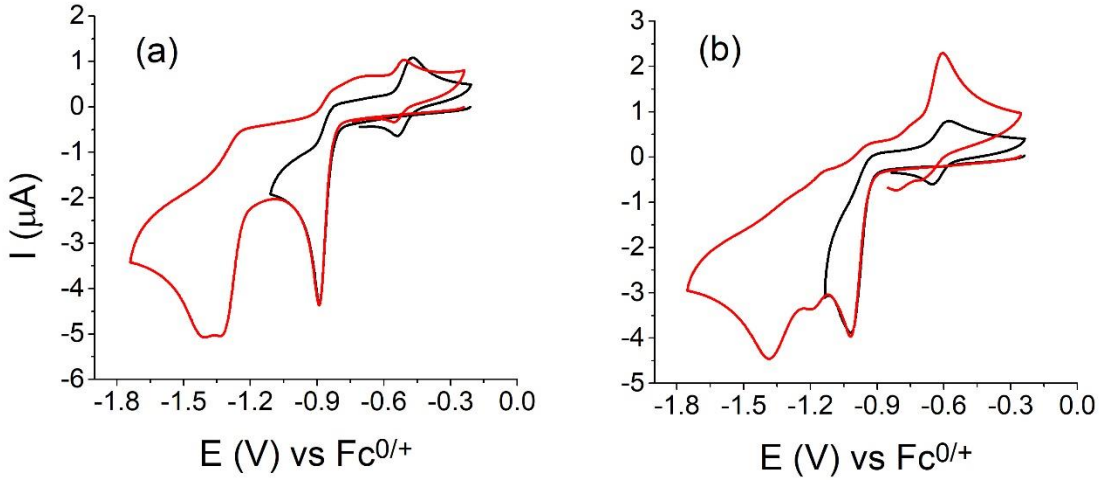

Figure 5.5 cyclic voltammogram of 2.2 mM 1,2-dinitrobenzene (a) and 2 mM 1,3-dinitrobenzene (b) in Ethaline at scan rate of 0.1 V/s. T=298 K.

Figure 5.5 (b) shows the CVs of 1,3-dinitrobenzene and its first irreversible reduction peak at -1.018 V which more negative than 1,2-dinitrobenzene and 1,4-dinitrobenzene. Like its isomers, nitroso-compound was produced at more positive potential of -0.578 V. The second and third reduction peaks are at -1.194 V and -1.386 V, respectively. The phenylhydroxylamine could still be the main product but the reverse oxidation peak

current appears larger than the one of the nitroso-benzene, suggesting the formation of other species. The mechanism of productions for these new species was not elucidated at this level of the work.

1,5-Dinitronaphthalene. Figure 5.6 shows the CVs of 1,5-dinitronaphthalene in Ethaline at 25 °C. As 1,2- and 1,3-dinitrobenzene, the first reduction peak of 1,5-dinitronaphthalene in Ethaline is an irreversible multi-electron transfer process followed by proton transfer leading to the formation of the corresponding nitroso-compounds that is visible at a more positive potential of -0.530 V. When scanning to more negative potential, a second reduction peak at -1.260 V and the reverse oxidation peak at -0.605 V are visible. This oxidation peak has a close but different potential to dinitroso-compounds and its peak current is larger. All these observations indicate that this peak is the oxidation of the species formed at the second reduction process. A likely species is the corresponding phenylhydroxylamine which is formed after electron transfer and proton transfer reaction of dinitrosonaphthalene. When the reverse scan covers the oxidation peak at -0.605 V, two reduction peaks appear which indicates that the oxidation of phenylhydroxylamine could not transfer to corresponding dinitroso-compound and that another new species formed. It could also be mentioned that the first reduction peak is much sharper than the second one. This suggests a stoichiometry of more than one electron (the potential of two electron transfer are close). Noticed that the reversible redox process at 0 V is the added standard reference ferrocene.

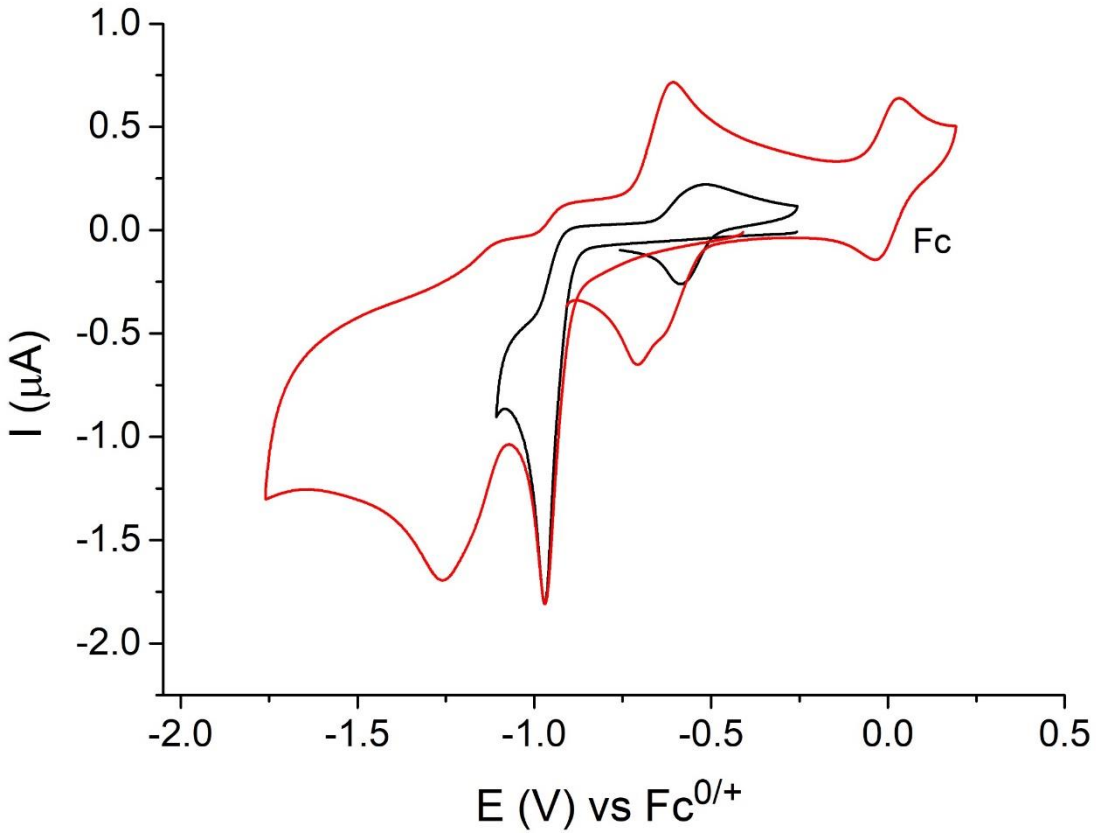

Figure 5.6 cyclic voltammogram of 1.0 mM 1,5-dinitronaphthalene in Ethaline on a 3 mm diameter glassy carbon electrode at scan rate of 0.1 V/s. T=298 K.

4,4'-Dinitrobiphenyl and 4,4'-dinitrostilbene. The $\Delta E^0 = (E_1{}^0 - E_2{}^0)$ of 4,4'-dinitrobiphenyl and 4,4'-dinitrostilbene are 21 mV and > -46 mV, respectively, in acetonitrile at 20 °C and 67 mV and 2 mV, respectively, in DMF at 25 °C. This relatively low standard potential separation or even potential inversion means that the second electron transfer are close or easier than the first one. Encourage by the potential inversion of 1,4-dintrobenzene in Ethaline, we expect the potential inversion could also occur in these two dinitro-compounds in DESs. Figure 5.7 shows the CVs of 4,4'-dinitrobiphenyl and 4,4'-dinitrostilbene in Ethaline at 25 °C. Unexpectedly, the two dinitro-aromatics display chemically irreversible reduction processes. This can due to the electron transfer coupled proton reaction in Ethaline. The CVs of the two molecules show similar behavior to the one of 1,5-dinitronaphthalene in Ethaline which both formed nitrosocompound after first reduction and corresponding phenylhydroxylamine at the second reduction process. As 4,4'-dinitrostilbene has a low solubility in Ethaline, its reduction current is small and the background are relatively large. The first reduction

peak of 4,4'-dinitrobiphenyl is at -1.017 V, and the second at -1.275 V. For 4,4'-dinitrostilbene, the first reduction peak is at -1.027 V, and the second at -1.236 V. The reduction potential of these two dinitro-aromatics are more negative than others dinitro-aromatics. The possible reasons of no potential inversion happen will discuss in the following part.

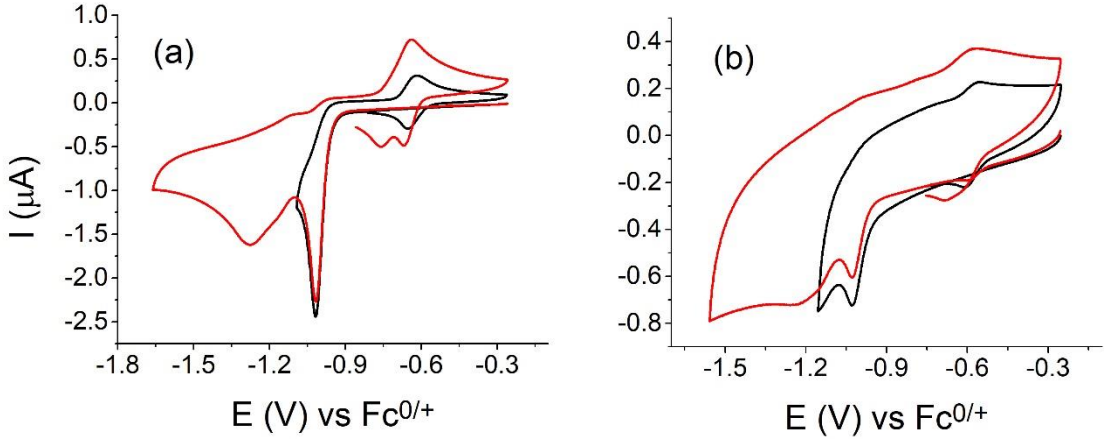

Figure 5.7 cyclic voltammogram of 0.93 mM 4,4'-dinitrobiphenyl (a) and 0.25 mM 4,4'-dinitrostilbene (b) in Ethaline at scan rate of 0.1 V/s. T=298 K

5.4 Discussion

5.4.1 Thermodynamics of dinitroaromatics in Ethaline

The characteristics of the dinitro-aromatic compounds reductions in Ethaline are gathered in Table 5.1. The derived diffusion coefficients, *D*, were calculated from the first reduction peak current I_p in the diffusion-controlled range of scan rates.[97, 143] For the four-electron transfer couple (for example 1,2-dinitrobenzene), to take into account the thinner peak of an $(ECE)_{rev}$ mechanism we considered the equation for the simultaneous transfer of 4 electrons, n ≥ 2 and $I_p = 0.446\, nFSC\sqrt{D}\sqrt{\frac{nFv}{RT}}$, where *n* is electron transfer numbers, *F* is the Faraday constant, *S* the electrode surface area, *C* the initial concentration of the redox couple, *R* the gas constant, *v* the scan rate and *T* the absolute temperature. Finally, the relation for the $EC_{irr}E$ mechanism, $I_p = 0.496$

$nFSC\sqrt{D}\sqrt{\frac{Fv}{RT}}$ was used to calculate the D values (n=2 or 4). The diffusion coefficients of the dinitro-aromatic compounds in Ethaline are all in the range of $2.0 – 9.0\times10^{-7}$ cm^2 s^{-1}. They are around two orders smaller than those in a molecular solvent like acetonitrile and one order smaller than in DMF reflecting the higher viscosity of Ethaline versus the molecular solvents.

Another important thermodynamic parameter is the redox potential of dinitro-aromatic compounds in Ethaline. The reduction potential of dinitro-aromatics has been reported in literature in several organic solvents. As shown in table 5.1, the first reduction peak potential of the dinitro-aromatic compounds examined here are no less than 0.30 V positive in Ethaline than their values in DMF.[267] This relative low reduction potential of could be ascribed to its special solvent environment and the occurrence of hydrogen-bonding in Ethaline. As DESs are composed of hydrogen donor and hydrogen acceptor, these components could also interact with the nitro groups by forming hydrogen-bonding resulting in a stabilization of the electro-generated species and thus lower reduction potentials.

Table 5.1 Electrochemical parameters for the reduction of Dinitrocompounds in Ethaline at 298K.

Dinitrocompounds	E^1_p/V	ΔE^0/mV	D/cm^2 s^{-1}	**n**
1,4-dinitrobenzene	-0.777	-30	3.2×10^{-7}	2
1,2-dinitrobenzene	-0.890		2.9×10^{-7}	4
1,3-dinitrobenzene	-1.018		3.0×10^{-7}	4
1,5-dinitronaphthalene	-0.970		3.4×10^{-7}	4
4,4’-dinitrobiphenyl	-1.017		8.6×10^{-7}	4
4,4’-dinitrostilbene	-1.027		3.2×10^{-7}	4
4-nitrotoluene (at 293K)	-1.243		2.3×10^{-7}	2

E^1_p :Peak potentials of the first reduction E^2_p : Peak potentials of the second reduction peak. ΔE^1 : Peak to peak difference of the fist reduction measured at 0.1 V s^{-1} from reversible voltammograms. All potentials are measured versus the Fc^+/Fc couple in Ethaline. n: the first reduction peak electron transfer numbers.

5.4.2 Potential inversion in Ethaline

The first reduction peak of a series dinitro-aromatic molecules exhibits widely different electrochemical behavior. The standard potential separation ΔE^0 of 1,4-dinitrobenzene is around -30 mV as shown before while other molecules shown irreversible behavior. This phenomenon illustrates that the electron transfer in a hydrogen-bonding and ionic solvent environment depends strongly on the structure of the dinitro-compounds. On the other hand, the changing of 1,4-dinitrobenzene from successive electron transfers in acetonitrile[180] to potential inversion in Ethaline also indicate the special properties of a DES like Ethaline.

The solvent and structure effects in Ethaline combined together can create a potential inversion which not happen in acetonitrile and DMF.[180, 267, 270] There are several reasons for this phenomenon. First, the dianion of para-dinitrobenzene could be form a quinonoid resonance structure and substantially delocalized the electrons over the entire molecule as shown below (scheme 4.2).[280, 281] While other dinitro-aromatic compounds, such as nitrotoluene and ortho-dinitroaromatics could steric inhibited to form the resonance structure.[281]

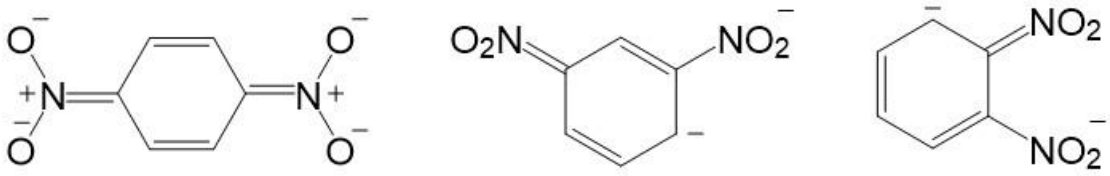

Scheme 2 Quinonoid resonance structure of 1,4-dinitrobenzene dianion and inhibition resonance of other dinitrobenzenes dianion.

Another reason is the solvation effects including both hydrogen-bonding and ion pairing effect. The standard potential separation ΔE^0 of 1,4-dinitrobenzene in acetonitrile and DMF is + 212 and + 321 mV, respectively.[180] So the potential inversion of 1,4-dinitrobenzene in Ethaline is clearly ascribed to a solvent effect.

Electrochemical behavior in Ethaline-acetonitrile mixture. To investigate in more detail the solvent effect in Ethaline, electrochemical behavior of 1,4-dinitrobenzene

(DNB) were examined in a series of Ethaline/acetonitrile mixtures. As shown in Figure 5.8, 1,4-dinitrobenzene shows two separate reversible electron transfer process in pure acetonitrile. When adding only 1.3 % of Ethaline, the second electron transfer process merges into the first one giving rise to a single reversible wave. With increasing the amounts of Ethaline, the CVs of 1,4-dinitrobenzene are gradually compressed. This could be clearly seen from the insert plot of ΔEp versus Ethaline's mole fraction. ΔE_p values considerably decrease with the increasing amount of Ethaline from 55 mV to 42 mV. This effect was much more pronounced in 0 - 10% of Ethaline but gradually decrease from 10% to 40%. The observed compression of ΔE^0 ($\Delta E^0 = E_1^0 - E_2^0$) turns to potential inversion in pure Ethaline as shown in Figure 5.2. At low Ethaline percentage where viscosity change could be depressed, the reduction peaks current of the multi-electron transfer process is about two times of the one electron transfer process in acetonitrile, 2.2 and 2.3 times for 1.3% and 3.8% of Ethaline, respectively. This corresponds to an electron stoichiometry of two for the first reduction peak when Ethaline is added and proves that the dianion of 1,4-dinitrobenzene is formed in one step. The decreasing of the reduction peak current is due to the increasing solution viscosity by adding Ethaline. In addition, a small peak at more positive potential appeared when adding Ethaline ascribed to the presence of the corresponding nitrosobenzene which is formed by protonation of 1,4-dinitrobenzene's dianion.

Besides the ΔE^0 compression observed above, another trend is also seen that the potential of the two-electron transfer reduction peak turns to a lower position when increasing the Ethaline amounts, see the trends of Figure 5.8 (a) to (g). This phenomenon indicates that Ethaline as a hydrogen-bonding donor could also affect the potentials and mechanisms of 1,4-dinitrobenzene in acetonitrile which confirmed our proposal of hydrogen-bonding effects on the potential inversion of 1,4-dinitrobenzene. The observation here parallels the behavior reported by Gupta and Linschitz who observed positive shifts of quinones reduction potential when a hydrogen bond donor appears.[169] . Similar effects are reported for Phenylenediamines with Pyridines[187, 282] for which the second electron transfer becomes more negative potential or merged with the first one or even turns to potential inversion.

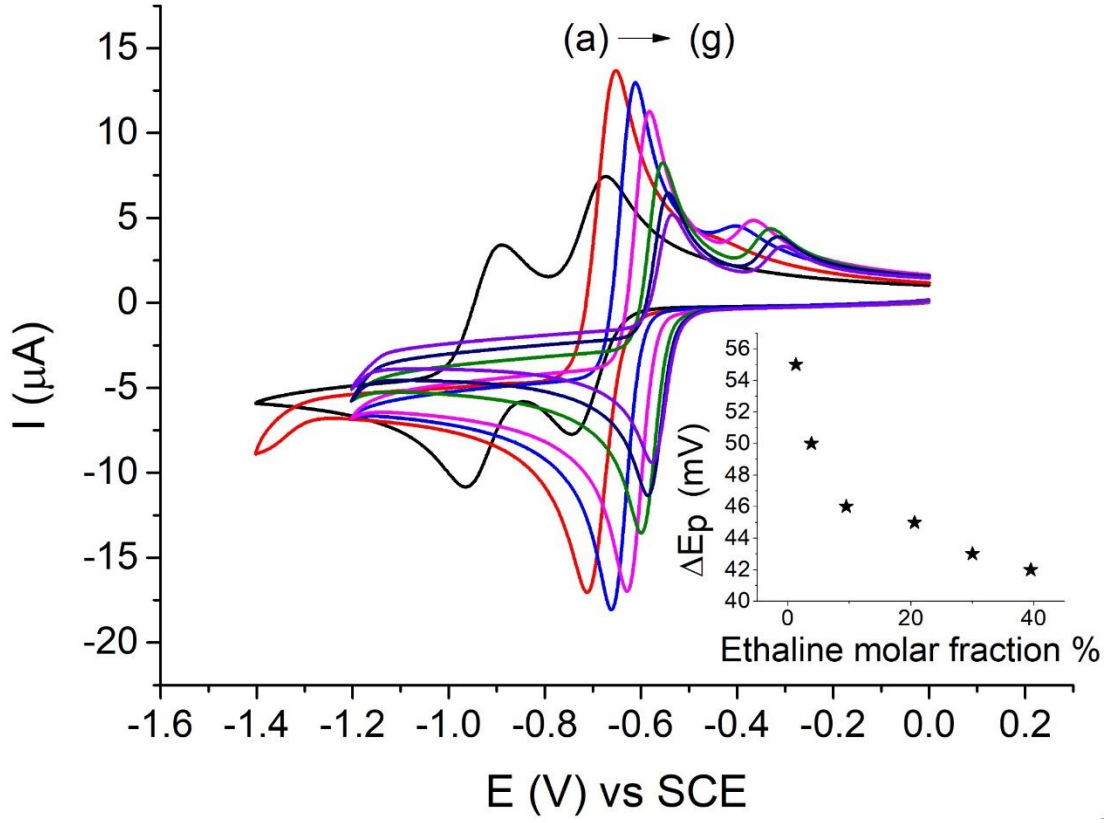

Figure 5.8 CVs of 1,4-dinitrobenzene in (a) acetonitrile (with 0.1 M Bu_4N^+ PF_6^-) and Ethaline-acetonitrile mixture at varies mole fraction (b) 1.3 %, (c) 3.8 %, (d) 9.5 %, (e) 20.6 %, (f) 30 %, (g) 39.5 %. The insert plot is the delta Ep of DNB vs Ethaline mole fraction. T=293 K.

By comparison, the electrochemical behavior of 1,4-dinitrobenzene in Ethylene glycol (EG) was also investigated, see Figure 5.9. The first reduction peak potential of 1,4-dinitrobenzene in EG is -0.767 V at 0.1 V/s which is a little positive (+10 mV) than in Ethaline. The CVs of 1,4-dinitrobenzene shows irreversible reduction at low scan rate, and turn to partially reversible when increasing the scan rate. The oxidation peak at reverse scan indicates that nitroso derivatives are formed which was similarly seen in Ethaline showing that EG alone could be the proton source.

However, no potential inversion was found and for all the scan rates (see Figure 5.9). This significant difference let us consider that ion pairing as in Ethaline must play a vital role in the potential inversion of 1,4-dinitrobenzene. In Ethaline, choline cations could be paired with the dianions of 1,4-dinitrobenzene and the ion-pair formation gives an additional stabilization of the dianion. The ion pairing effect on ΔE^0 in the reduction of dinitro-aromatics has been studied in organic solvents.[186, 270, 271] In particular, Evan

and colleagues[186] have investigated the ion pairing effect of a series of quaternary ammonium salt (R_4N^+) on 1,4-dinitrobenzene and 2,5-dimethyl-1,4-dinitrobenzene in acetonitrile and DMF. Although ion pairing between the dianion and R_4N^+ was found for $(CH_3)_4N^+$ with the two dinitro-benzene, the effects remain rather modest and no potential inversion occurred in pure organic solvent until water added.[186] The combination of hydrogen bonding between water and dianion and the ion pairing effect results potential inversion. In our system, choline cation has a similar structure with $(CH_3)_4N^+$ And its concentration in Ethaline is 4.21 mol/L which is much higher than the supporting electrolyte concentration of 0.1 mol/L in normal electrochemical system. In summary, the two components of Ethaline combined the hydrogen-bonding and ion pairing effects together resulting the potential inversion of 1,4-dinitrobenzene in Ethaline.

The complexity in our system is that the potential inversion of 1,4-dinitrobenzene is coupled with proton transfer reactions. For other dinitroaromatics, the proton transfer reaction results irreversible electrochemical behavior due to localized system[280] or no resonance structure formed. To evaluate the source of the proton, we performed another experiment of 1,4-dinitrobenzene in acetonitrile with pure water added to the solution. We found that nitrosobenzene peak was not observed up to 2 wt% of water in acetonitrile as the two successive electron transfer merged into one reversible two-electron reduction peak. As the water amounts in Ethaline is much lower than 2 wt%, the possible proton source should come from Ethaline itself. This conclusion makes sound when compare the CVs between Ethaline and ethylene glycol which shown more significant proton transfer than in Ethaline (Figure 5.9). In chapter 4, we also talked about the H-bonding effects on the protonation of quinones in Ethaline. The reason found in there could also suitable to dinitroaromatics.

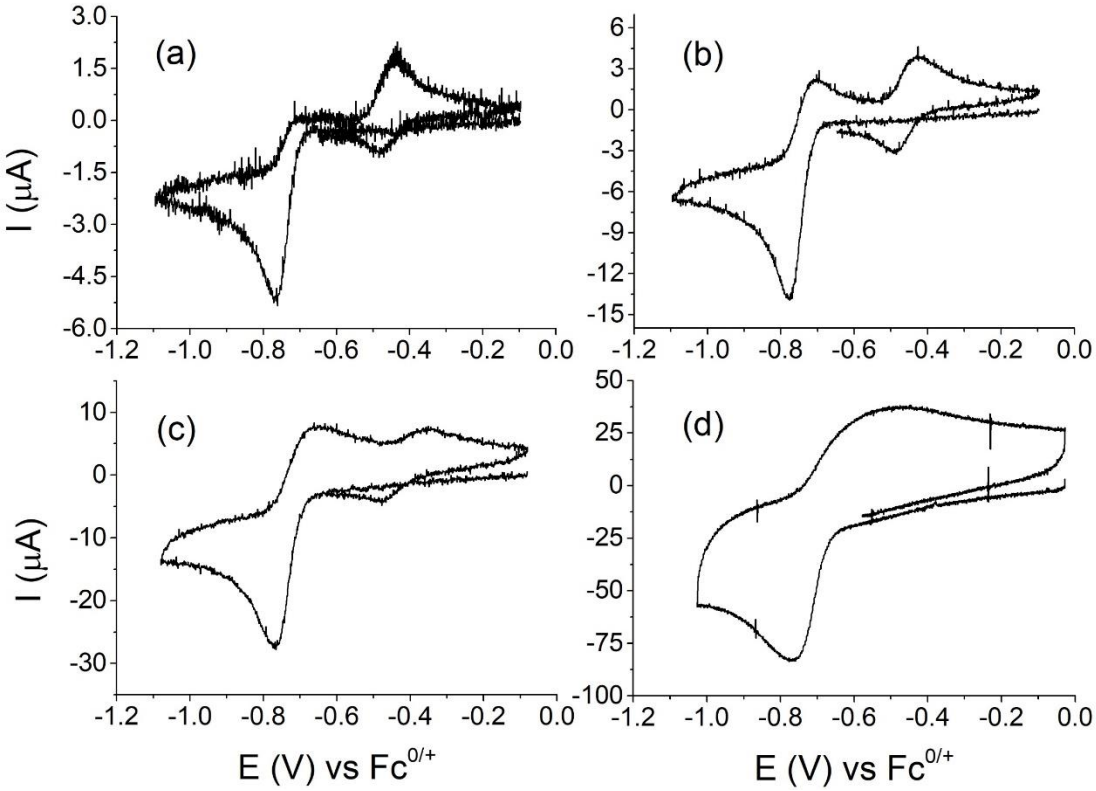

Figure 5.9 CVs of 1,4-dinitrobenzene in ethylene glycol (with 0.2 M Et_4N^+ Cl^-) at varies scan rate (a) 0.1, (b) 1, (c) 5, (d) 50 V/s at 294 K.

In theory, 4,4'-dinitrobiphenyl and 4,4'-dinitrostilbene could also form the delocalized system, but no potential inversion observed in Ethaline. This could due the distance effect of the two nitro group, the longer the distance, the less stable of the dinitroaromatics' dianion.[280]

5.4.3 Mechanism of dinitrocompounds in DES

5.4.3.1 Mechanism of 1,4-dinitrobenzene in Ethaline

From the discussion of sections 5.3.1 and 5.4.2, we have got the primary information of 1,4-dinitrobenzene reduction in Ethaline that the first reduction peak is two-electron transfer and the nitrosocompounds formed at more positive potential and azo or azoxy compounds are formed at more negative potential.

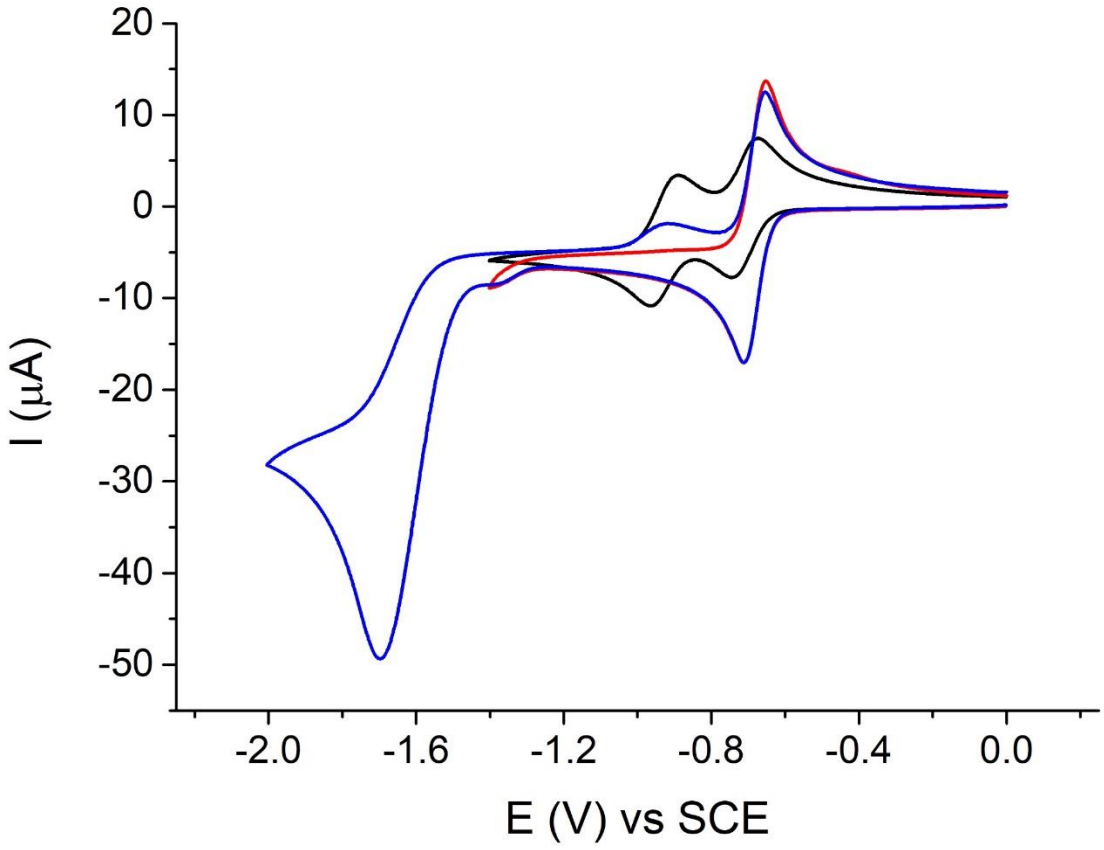

Figure 5.10 CVs of 1,4-dinitrobenzene in acetonitrile (5 mL) with adding 100 µl Ethaline at 0.1 V/s on a glassy carbon electrode.

To further understanding the final products of the 1,4-dinitrobenzene reduction in Ethaline, the experiments of 1,4-dinitrobenzene in acetonitrile with adding small amounts Ethaline was conduct. As seen in Figure 5.10, an irreversible peak appears at -1.69 V which peak current after deduct baseline is 2.43 times of the first one and an oxidation peak of reverse scan appears at -0.91 V. This means it undergoes 4-5 electron transfers after the formation of the dianion. This multi-electron transfer suggests the products are not phenylhydroxylamine but continued reduced to another product which most possible product is 4-nitroaniline. The possible mechanism of 1,4-dinitrobenzene is shown in Scheme 3 path 1.

5.4.3.2 Mechanism of other dinitroaromatics

All the other dinitroaromatics undergoes similar mechanism but different with 1,4-dinitrobenzene. To explore the mechanism of this type dinitroaromatics in Ethaline,

cyclic voltammetry (CV) of 1,2-dinitrobenzene in aprotic solvent was conducted in the appearance of Ethaline. As shown in the Figure 5.11 (a), the CV of 1,2-dinitrobenzene in acetonitrile has two reversible reduction peaks which indicate two step one electron transfer and formed anion radical and dianion, respectively. When only 10 μL Ethaline added in the 5 mL solution, the CV of 1,2-dinitrobenzene was distorted to irreversible and protonation occurred. A more negative irreversible reduction peak appeared at around -1.6 V and another reverse peak at more positive potential of -0.54 V. With more Ethaline added, the two step electron transfer in acetonitrile merged into one and the reduction current increasing steadily. The reduction current reached to maximum when adding 200 μL Ethaline. In this case, the reduction peak is four times of the 1,2-dinitrobenzene's first reduction peak in acetonitrile, see Figure 5.11 (d). This changing indicates that electron transfer number changed from 1 to 4 in the first reduction peak after adding Ethaline. Meanwhile, the second reduction peak also have the same electron transfer number to the first one. When more Ethaline was added, see Figure 5.11 (e), both the first and second reduction peaks are start to decrease which due to the adding Ethaline increased the solution viscosity. In this process, the reduction potential moved to more positive direction with increasing amount of Ethaline. The same experiments were also done for other dinitroaromatics, such as 4,4'-dinitrobiphenyl and 1,5-dinitronaphthalene which have the same results. In general, the first reduction peak of all the other dinitroaromatics examined here, unlike the para-dinitrobenzene, undergoes four electron transfer which means two nitro groups was reduced simultaneously.

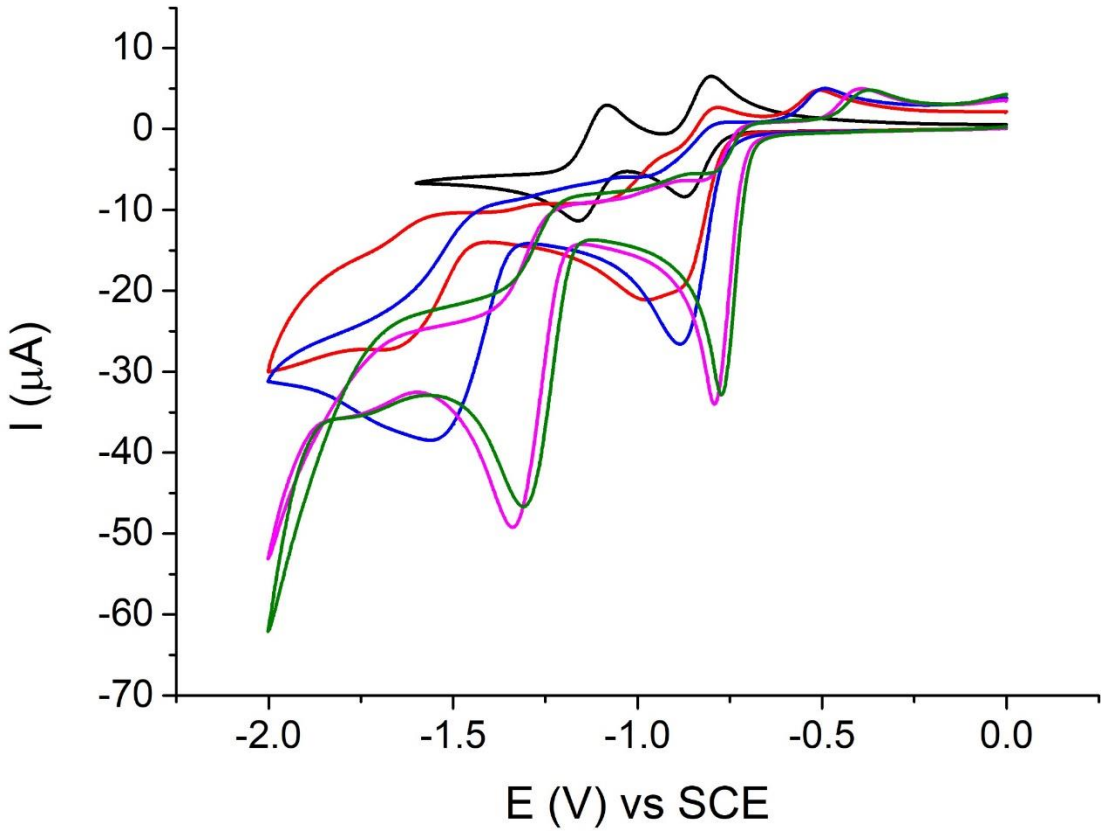

Figure 5.11 1,2-dinitrobenzene in acetonitrile with various amount Ethaline (a) in pure acetonitrile, black (b) 10 μL, red (c) 100 μL, blue (d) 200 μL, purple (e) 300 μL, green.

Base on the above analysis, we proposed the possible mechanism for the reduction of dinitrobenzene in Ethaline, see Scheme 3. Two types of mechanism could exist. For 1,4-dinitrobenzene, the first reduction peak is a 2-electron transfer process which produce dianion, and then the dianion coupled with a proton reaction producing nitrosonitrobenzene (NNB). The NNB was reduced to anion radical which part undergoes a radical-radical dimerization[283] to form azo or azoxy compounds and most reduced to aniline via the intermediate N-phenylhydroxylamine. In this way, the transformation of only one nitro group[278] is observe in the reduction of 1,4-dinitrobenzene in Ethaline (see Scheme 3 path 1).

For other dinitroaromatics, the first reduction undergoes an irreversible 4-electron transfer, then followed by proton transfer reaction yield corresponding dinitrosocompounds. The dinitrosocopound could be further irreversibly reduced via a 4-electron transfer or two steps of 2-electron transfer which generally yield phenylhydroxylamine. But no azo or azoxy compounds formed (see Scheme 3 path 2).

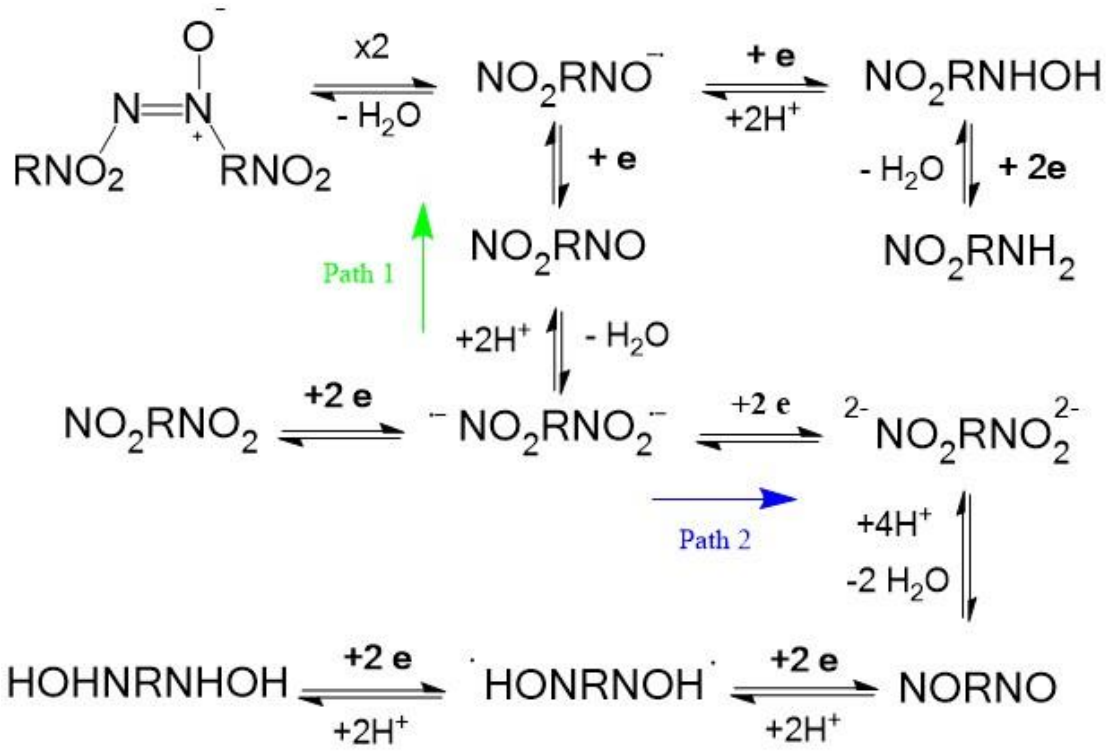

Scheme 3 General mechanism for the reduction of dinitroaromatics in Ethaline.

5.5 Conclusions and Perspectives

Electrochemical reduction of a series dinitrocompounds was investigated in a DES Ethaline. The redox behavior is dependent on both the natural structure and the solvation environment. A very interesting phenomenon of potential inversion was found for 1,4-dinitrobenzene in Ethaline. The reasons for the inverted potential are thoroughly examined and the formation of quinonoid resonance structure and the special solvation environment in Ethaline including both the hydrogen-bonding and ion-pairing effect is responsible for it. These combined effects provide a broad view of the study of potential inversion. The electron transfer of the potential inversion process was coupled with a proton transfer making it transformed into the corresponding nitrosoaromatics. The protonation extension depends on the acidity of the DES and the structure of dinitroaromatics. The potential inversion and protonation are thus competing with each

other. Other para-dinitroaromatics, such as 2,6-dinitronaphthalene and 2,6-dinitroanthracene, are promising alternatives as they also could form resonance structures. Another interesting finding is that the reduction potential of dinitrocompounds in Ethaline are relatively lower than in organic solvent. This is attribute to the hydrogen-bonding effect as we found in the reduction of quinones in Ethaline. Except 1,4-dinitrobenzene, all the other dinitrocompounds examined showed irreversible behavior. This is due to their localized electronic structure (ortho- or meta-dinitro) or weak resonance (4,4'-dinitrobiphenyl and 4,4'-dinitrostilbene).

Two mechanisms that correspond to only one nitro group and both two are reduced are found. 1,4-Dintrobenzene undergoes only one nitro group reduction mechanism while the others two nitro groups are reduced. The main final products of the two mechanisms are different. For 1,4-dinitrobenzene, the main products could be aniline while others could mainly produce phenylhydroxylamine.

Acknowledgements

I would like to express my appreciation to the following people who have been involved, offering technical help, friendship, and support, in the work of my thesis.

The first and most I would like to thank is my supervisor Prof. Philippe Hapiot. He has in-depth knowledge of electrochemistry and is one of the best electrochemists. Philippe offers me great help in life and research. When I came from China, he gave me a nice reception and helped me reserve a room in INSA. Philippe teach me a lot in the experiments and during our discussions. His logic and meticulous research impressed me. In the preparation of my thesis, Philippe offered great help in writing and revising the thesis. I am very appreciative of his patience and valuable instruction during my PhD. in Rennes.

Prof. Corinne Lagrost are heartfelt thanked for her help in introducing me to all the equipment and experimental skills in the lab. We have together made ionic liquids and deep eutectic solvents. I am very appreciative of her valuable time and we have collaborated on our first research project.

I would also like to express my gratitude to Dr. Yann R. Leroux for his supporting and helpful advice in my experiments and Dr. Jean-Francois Bergamini for his support in building a potentiostat with ohmic drop compensation and other technique support. Dr. Quentin Lenne was thanked for his supporting in the lab and advice on life in Rennes. Thanks also go to Dr. Ludovic Paquin, Dr. Emmanuelle Limanton, and Dr. Lucie Percevault for their offering our DESs in the beginning and giving me access to Karl-Fischer titration. In the end, I also appreciate all the members in MaCSE (Rennes) for their share in the lab and for friendly treatment.

I am especially thankful to my family, my mother, old brother, and sisters for their great support in my study.

In the end, I would like to thank the China Scholarship Council (CSC) for granting my PhD. in Rennes.

Conclusions and perspectives

In this manuscript, we have examined different aspects of the electrochemistry of classical molecules in DES that could be classified into four general categories. First, the standard potential and diffusion coefficient for both one- and two successive electron transfer reactions were extracted from the cyclic voltammetry of redox species. Secondly, electron transfer rate constants were measured by the fast scan rate cyclic voltammetry method and compared with the prediction of the classical model like the Marcus Theory. Third, differences in standard potential, normal ordering, and potential inversion, for two-electron transfer reactions and their mechanisms in DESs were examined. Finally, we obtained some indications about reactions that coupled electron transfer and proton transfers like quinones or dinitro aromatics compounds.

In the second chapter, the rate constants of two common redox couples, Fe(CN)63-/4- and ferrocene/ferrocenium, were measured in a DES Ethaline and compared with ionic liquid and organic solvent or water. The results show that the charge transfer kinetics in Ethaline is much faster than in ionic liquid and in the same order as the rates reported in organic solvents or water despite the large differences in viscosities between these media.

To test the validity of Marcus theory in DES, the rate constants as a function of water addition, therefore viscosity or solvent relaxation time, were examined in two types of redox couples in Chapter 3. Surprisingly, two types of responses are observed. For the 1,1'-dimethanol-ferrocene, outer-sphere electron transfer reaction, the correlation of rate constants with solvent reorganization are close to the Marcus theory or rather smaller depending on the DES. While for the oxidation of ferrocyanide, the inner-sphere electron transfer reaction, the rate constants are almost kept constant with water addition leading to an apparently non-Marcus behavior.

In the following chapters, the electrochemical behavior of two types of redox species which both possess two identical groups, quinones and dinitro-aromatics, were investigated in DESs. First, we have considered the behaviors of electrochemical reduction of quinones in Ethaline in Chapter 4. Both the first and second formal potentials of quinones is much lower than in organic solvents, like acetonitrile, and the formal potential difference are largely compressed. Charge transfer kinetics and mechanisms of some reversible quinones are then examined in detail. Some specific phenomena are observed in this special solvent environment. For example, the high basicity quinone, 1,4-benzoequinone, is quite easily protonated to hydroquinone in Ethaline and another electron-deficient quinone, chloranil, are activated by the solvent hydrogen-bonding. It results that the electron transfer between chloranil and ferrocene is quite easy in Ethaline which is a very promising reaction system in organic synthesis.

Electrochemical reductions of dinitro-aromatics in DES are treated in Chapter 5. Potential inversion was observed for 1,4-dinitrobenzene in Ethaline due to their resonance structure, hydrogen-bonding, and ionic pairing effects. Meanwhile, the protonation of the dianion is competed with this process. All the other dinitro-aromatics undergo irreversible electron transfer. Two different mechanisms of dinitro-aromatic compounds in Ethaline are observed. Only one nitro group is reduced for 1,4-dinitrobenzene and its final product is most possible to be aniline. While for other dinitro-aromatics, two nitro groups are both reduced and the final products are phenylhydroxylamine. The common is nitroso-compounds was produced in both types of mechanism.

All those observations in DES illustrate the special solvent environment and the special effects on the electrochemical properties due to hydrogen-bonding and ionic solvent existing in a DES like Ethaline. However, our results remain limited to a small variety of DES. In a future extension of this work, it would be necessary to extend this study to other DESs that could also lead to a sort of classification of the DES according to their properties. Additionally, the classical model as Marcus theory has difficulties to

describe the observations as exemplified by the variation of the charge transfer kinetics with viscosity or relation time of the solvents. These apparent discrepancies are not totally surprising as they compare phenomena that found their origin at a different scale. For example, solvation is a very localized phenomenon as diffusion or viscosity are macroscopic parameters. This also illustrates the need for theoretical calculations and modeling of a DES environment and solubilization of a molecule in DES in combination with experiments. Nevertheless, our results illustrate all the interest in these media for electrochemical applications.

References

[1] Abbott A. P., Boothby D., Capper G., et al. Deep eutectic solvents formed between choline chloride and carboxylic acids: Versatile alternatives to ionic liquids[J]. Journal of the American Chemical Society, 2004,126:9142-9147.

[2] Abbott A. P., Capper G., Davies D. L., et al. Novel solvent properties of choline chloride/urea mixtures[J]. Chem Commun (Camb), 2002:70-71.

[3] Hansen B. B., Spittle S., Chen B., et al. Deep Eutectic Solvents: A Review of Fundamentals and Applications[J]. Chem Rev, 2021,121:1232-1285.

[4] Smith E. L., Abbott A. P., Ryder K. S. Deep Eutectic Solvents (DESs) and Their Applications[J]. Chem Rev, 2014,114:11060-11082.

[5] Zhang Q. H., Vigier K. D., Royer S., et al. Deep eutectic solvents: syntheses, properties and applications[J]. Chemical Society Reviews, 2012,41:7108-7146.

[6] Abbott A. P., Capper G., Davies D. L., et al. Preparation of novel, moisture-stable, Lewis-acidic ionic liquids containing quaternary ammonium salts with functional side chains[J]. Chem Commun (Camb), 2001:2010-2011.

[7] Martins M. A. R., Pinho S. P., Coutinho J. A. P. Insights into the Nature of Eutectic and Deep Eutectic Mixtures[J]. Journal of Solution Chemistry, 2018,48:962-982.

[8] Kollau L. J. B. M., Vis M., van den Bruinhorst A., et al. Quantification of the liquid window of deep eutectic solvents[J]. Chem Commun (Camb), 2018,54:13351-13354.

[9] Marcus Y. Unconventional Deep Eutectic Solvents: Aqueous Salt Hydrates[J]. Acs Sustainable Chemistry & Engineering, 2017,5:11780-11787.

[10] Sitze M. S., Schreiter E. R., Patterson E. V., et al. Ionic liquids based on FeCl3 and FeCl2. Raman scattering and ab initio calculations[J]. Inorganic Chemistry, 2001,40:2298-2304.

[11] Abbott A. P., Capper G., Davies D. L., et al. Solubility of metal oxides in deep eutectic solvents based on choline chloride[J]. Journal of Chemical and Engineering Data, 2006,51:1280-1282.

[12] Gambino M., Bros J. P. Capacite calorifique de l'uree et de quelques melanges eutectiques a base d'uree entre 30 et 140° C[J]. Thermochimica Acta, 1988,127:223-236.

[13] Abbott A. P., Barron J. C., Ryder K. S., et al. Eutectic-based ionic liquids with metal-containing anions and cations[J]. Chemistry-a European Journal, 2007,13:6495-6501.

[14] Abranches D. O., Martins M. A. R., Silva L. P., et al. Phenolic hydrogen bond donors in the formation of non-ionic deep eutectic solvents: the quest for type V DES[J]. Chem Commun (Camb), 2019,55:10253-10256.

[15] van Osch D. J. G. P., Dietz C. H. J. T., van Spronsen J., et al. A Search for Natural Hydrophobic Deep Eutectic Solvents Based on Natural Components[J]. Acs Sustainable Chemistry & Engineering, 2019,7:2933-2942.

[16] Paiva A., Craveiro R., Aroso I., et al. Natural Deep Eutectic Solvents - Solvents for the 21st Century[J]. Acs Sustainable Chemistry & Engineering, 2014,2:1063-1071.

[17] Liu Y., Friesen J. B., McAlpine J. B., et al. Natural Deep Eutectic Solvents: Properties, Applications, and Perspectives[J]. Journal of Natural Products, 2018,81:679-690.

[18] van Osch D. J. G. P., Zubeir L. F., van den Bruinhorst A., et al. Hydrophobic deep eutectic solvents as water-immiscible extractants[J]. Green Chemistry, 2015,17:4518-4521.

[19] Ribeiro B. D., Florindo C., Iff L. C., et al. Menthol-based Eutectic Mixtures: Hydrophobic Low

Viscosity Solvents[J]. Acs Sustainable Chemistry & Engineering, 2015,3:2469-2477.
[20] Cao J., Yang M., Cao F. L., et al. Well-Designed Hydrophobic Deep Eutectic Solvents As Green and Efficient Media for the Extraction of Artemisinin from Artemisia annua Leaves[J]. Acs Sustainable Chemistry & Engineering, 2017,5:3270-3278.
[21] Yang M. Y., Hong K., Li X. Q., et al. Freezing temperature controlled deep eutectic solvent dispersive liquid-liquid microextraction based on solidification of floating organic droplets for rapid determination of benzoylureas residual in water samples with assistance of metallic salt[J]. Rsc Advances, 2017,7:56528-56536.
[22] Murakami Y., Das S. K., Himuro Y., et al. Triplet-sensitized photon upconversion in deep eutectic solvents[J]. Physical Chemistry Chemical Physics, 2017,19:30603-30615.
[23] Dietz C. H. J. T., Kroon M. C., Di Stefano M., et al. Selective separation of furfural and hydroxymethylfurfural from an aqueous solution using a supported hydrophobic deep eutectic solvent liquid membrane[J]. Faraday Discussions, 2018,206:77-92.
[24] Florindo C., Romero L., Rintoul I., et al. From Phase Change Materials to Green Solvents: Hydrophobic Low Viscous Fatty Acid Based Deep Eutectic Solvents[J]. Acs Sustainable Chemistry & Engineering, 2018,6:3888-3895.
[25] Bezold F., Minceva M. A water-free solvent system containing an L-menthol-based deep eutectic solvent for centrifugal partition chromatography applications[J]. Journal of Chromatography A, 2019,1587:166-171.
[26] Farooq M. Q., Abbasi N. M., Anderson J. L. Deep eutectic solvents in separations: Methods of preparation, polarity, and applications in extractions and capillary electrochromatography[J]. Journal of Chromatography A, 2020,1633.
[27] Crawford D. E., Wright L. A., James S. L., et al. Efficient continuous synthesis of high purity deep eutectic solvents by twin screw extrusion[J]. Chem Commun (Camb), 2016,52:4215-4218.
[28] Gajardo-Parra N. F., Lubben M. J., Winnert J. M., et al. Physicochemical properties of choline chloride-based deep eutectic solvents and excess properties of their pseudo-binary mixtures with 1-butanol[J]. Journal of Chemical Thermodynamics, 2019,133:272-284.
[29] Agieienko V., Buchner R. Densities, Viscosities, and Electrical Conductivities of Pure Anhydrous Reline and Its Mixtures with Water in the Temperature Range (293.15 to 338.15) K[J]. Journal of Chemical and Engineering Data, 2019,64:4763-4774.
[30] Hallett J. P., Welton T. Room-Temperature Ionic Liquids: Solvents for Synthesis and Catalysis. 2[J]. Chem Rev, 2011,111:3508-3576.
[31] Welton T. Room-temperature ionic liquids. Solvents for synthesis and catalysis[J]. Chem Rev, 1999,99:2071-2083.
[32] Hapiot P., Lagrost C. Electrochemical reactivity in room-temperature ionic liquids[J]. Chem Rev, 2008,108:2238-2264.
[33] Wilkes J. S., Zaworotko M. J. Air and Water Stable 1-Ethyl-3-Methylimidazolium Based Ionic Liquids[J]. Journal of the Chemical Society-Chemical Communications, 1992:965-967.
[34] Endres F., El Abedin S. Z. Air and water stable ionic liquids in physical chemistry[J]. Physical Chemistry Chemical Physics, 2006,8:2101-2116.
[35] MacFarlane D. R., Meakin P., Sun J., et al. Pyrrolidinium imides: A new family of molten salts and conductive plastic crystal phases[J]. Journal of Physical Chemistry B, 1999,103:4164-4170.
[36] Bonhote P., Dias A. P., Papageorgiou N., et al. Hydrophobic, highly conductive ambient-temperature molten salts[J]. Inorganic Chemistry, 1996,35:1168-1178.

[37] Scammells P. J., Scott J. L., Singer R. D. Ionic liquids: The neglected issues[J]. Australian Journal of Chemistry, 2005,58:155-169.

[38] van Osch D. J. G. P., Dietz C. H. J. T., Warrag S. E. E., et al. The Curious Case of Hydrophobic Deep Eutectic Solvents: A Story on the Discovery, Design, and Applications[J]. Acs Sustainable Chemistry & Engineering, 2020,8:10591-10612.

[39] Mjalli F. S., Vakili-Nezhaad G., Shahbaz K., et al. Application of the Eotvos and Guggenheim empirical rules for predicting the density and surface tension of ionic liquids analogues[J]. Thermochimica Acta, 2014,575:40-44.

[40] Kuddushi M., Nangala G. S., Rajput S., et al. Understanding the peculiar effect of water on the physicochemical properties of choline chloride based deep eutectic solvents theoretically and experimentally[J]. Journal of Molecular Liquids, 2019,278:607-615.

[41] Yadav A., Kar J. R., Verma M., et al. Densities of aqueous mixtures of (choline chloride plus ethylene glycol) and (choline chloride plus malonic acid) deep eutectic solvents in temperature range 283.15-363.15 K[J]. Thermochimica Acta, 2015,600:95-101.

[42] Yadav A., Trivedi S., Rai R., et al. Densities and dynamic viscosities of (choline chloride plus glycerol) deep eutectic solvent and its aqueous mixtures in the temperature range (283.15-363.15) K[J]. Fluid Phase Equilibria, 2014,367:135-142.

[43] Yadav A., Pandey S. Densities and Viscosities of (Choline Chloride plus Urea) Deep Eutectic Solvent and Its Aqueous Mixtures in the Temperature Range 293.15 K to 363.15 K[J]. Journal of Chemical and Engineering Data, 2014,59:2221-2229.

[44] Ghaedi H., Ayoub M., Sufian S., et al. The study on temperature dependence of viscosity and surface tension of several Phosphonium-based deep eutectic solvents[J]. Journal of Molecular Liquids, 2017,241:500-510.

[45] Bagh F. S. G., Shahbaz K., Mjalli F. S., et al. Electrical conductivity of ammonium and phosphonium based deep eutectic solvents: Measurements and artificial intelligence-based prediction[J]. Fluid Phase Equilibria, 2013,356:30-37.

[46] Agieienko V., Buchner R. A Comprehensive Study of Density, Viscosity, and Electrical Conductivity of (Choline Chloride plus Glycerol) Deep Eutectic Solvent and Its Mixtures with Dimethyl Sulfoxide[J]. Journal of Chemical and Engineering Data, 2021,66:780-792.

[47] Agieienko V., Buchner R. Variation of Density, Viscosity, and Electrical Conductivity of the Deep Eutectic Solvent Reline, Composed of Choline Chloride and Urea at a Molar Ratio of 1:2, Mixed with Dimethylsulfoxide as a Cosolvent[J]. Journal of Chemical and Engineering Data, 2020,65:1900-1910.

[48] Harifi-Mood A. R., Buchner R. Density, viscosity, and conductivity of choline chloride plus ethylene glycol as a deep eutectic solvent and its binary mixtures with dimethyl sulfoxide[J]. Journal of Molecular Liquids, 2017,225:689-695.

[49] Lemaoui T., Darwish A. S., Hammoudi N. E., et al. Prediction of Electrical Conductivity of Deep Eutectic Solvents Using COSMO-RS Sigma Profiles as Molecular Descriptors: A Quantitative Structure-Property Relationship Study[J]. Industrial & Engineering Chemistry Research, 2020,59:13343-13354.

[50] Gontrani L., Bonomo M., Plechkova N. V., et al. X-Ray structure and ionic conductivity studies of anhydrous and hydrated choline chloride and oxalic acid deep eutectic solvents[J]. Physical Chemistry Chemical Physics, 2018,20:30120-30124.

[51] Chen Y., Chen W. J., Fu L., et al. Surface Tension of 50 Deep Eutectic Solvents: Effect of Hydrogen-

Bonding Donors, Hydrogen-Bonding Acceptors, Other Solvents, and Temperature[J]. Industrial & Engineering Chemistry Research, 2019,58:12741-12750.

[52] Haghbakhsh R., Taherzadeh M., Duarte A. R. C., et al. A general model for the surface tensions of deep eutectic solvents[J]. Journal of Molecular Liquids, 2020,307.

[53] Desiraju G. R. IUPAC definition of the hydrogen bond. Terminology and nomenclature[J]. Acta Crystallographica a-Foundation and Advances, 2017,73:C308-C308.

[54] Arunan E., Desiraju G. R., Klein R. A., et al. Definition of the hydrogen bond (IUPAC Recommendations 2011)[J]. Pure and Applied Chemistry, 2011,83:1637-1641.

[55] Steiner T. The hydrogen bond in the solid state[J]. Angewandte Chemie-International Edition, 2002,41:48-76.

[56] Jeffrey G. A. An introduction to hydrogen bonding. USA: Oxford University Press; 1997.

[57] Wulf A., Fumino K., Ludwig R. Spectroscopic evidence for an enhanced anion-cation interaction from hydrogen bonding in pure imidazolium ionic liquids[J]. Angew Chem Int Ed Engl, 2010,49:449-53.

[58] Fumino K., Wulf A., Ludwig R. Hydrogen bonding in protic ionic liquids: reminiscent of water[J]. Angew Chem Int Ed Engl, 2009,48:3184-6.

[59] Lu J., Hung I., Brinkmann A., et al. Solid-State (17) O NMR Reveals Hydrogen-Bonding Energetics: Not All Low-Barrier Hydrogen Bonds Are Strong[J]. Angew Chem Int Ed Engl, 2017,56:6166-6170.

[60] Johnson E. R., Keinan S., Mori-Sanchez P., et al. Revealing noncovalent interactions[J]. Journal of the American Chemical Society, 2010,132:6498-506.

[61] Hunt P. A., Ashworth C. R., Matthews R. P. Hydrogen bonding in ionic liquids[J]. Chemical Society Reviews, 2015,44:1257-1288.

[62] Hammond O. S., Bowron D. T., Edler K. J. Liquid structure of the choline chloride-urea deep eutectic solvent (reline) from neutron diffraction and atomistic modelling[J]. Green Chemistry, 2016,18:2736-2744.

[63] Ashworth C. R., Matthews R. P., Welton T., et al. Doubly ionic hydrogen bond interactions within the choline chloride-urea deep eutectic solvent[J]. Physical Chemistry Chemical Physics, 2016,18:18145-18160.

[64] Wang H. Y., Liu S. Y., Zhao Y. L., et al. Insights into the Hydrogen Bond Interactions in Deep Eutectic Solvents Composed of Choline Chloride and Polyols[J]. Acs Sustainable Chemistry & Engineering, 2019,7:7760-7767.

[65] Stefanovic R., Ludwig M., Webber G. B., et al. Nanostructure, hydrogen bonding and rheology in choline chloride deep eutectic solvents as a function of the hydrogen bond donor[J]. Physical Chemistry Chemical Physics, 2017,19:3297-3306.

[66] Alfurayj I., Fraenza C. C., Zhang Y., et al. Solvation Dynamics of Wet Ethaline: Water is the Magic Component[J]. Journal of Physical Chemistry B, 2021,125:8888-8901.

[67] Alizadeh V., Malberg F., Padua A. A. H., et al. Are There Magic Compositions in Deep Eutectic Solvents? Effects of Composition and Water Content in Choline Chloride/Ethylene Glycol from Ab Initio Molecular Dynamics[J]. Journal of Physical Chemistry B, 2020,124:7433-7443.

[68] Smith P. J., Arroyo C. B., Hernandez F. L., et al. Ternary Deep Eutectic Solvent Behavior of Water and Urea-Choline Chloride Mixtures[J]. Journal of Physical Chemistry B, 2019,123:5302-5306.

[69] Zhekenov T., Toksanbayev N., Kazakbayeva Z., et al. Formation of type III Deep Eutectic Solvents and effect of water on their intermolecular interactions[J]. Fluid Phase Equilibria, 2017,441:43-48.

[70] Siongco K. R., Leron R. B., Li M. H. Densities, refractive indices, and viscosities of N,N-diethylethanol

ammonium chloride-glycerol or -ethylene glycol deep eutectic solvents and their aqueous solutions[J]. Journal of Chemical Thermodynamics, 2013,65:65-72.

[71] Lapena D., Bergua F., Lomba L., et al. A comprehensive study of the thermophysical properties of reline and hydrated reline[J]. Journal of Molecular Liquids, 2020,303.

[72] Du C. L., Zhao B. Y., Chen X. B., et al. Effect of water presence on choline chloride-2urea ionic liquid and coating platings from the hydrated ionic liquid[J]. Scientific Reports, 2016,6.

[73] Shah D., Mjalli F. S. Effect of water on the thermo-physical properties of Reline: An experimental and molecular simulation based approach[J]. Physical Chemistry Chemical Physics, 2014,16:23900-7.

[74] D'Agostino C., Gladden L. F., Mantle M. D., et al. Molecular and ionic diffusion in aqueous - deep eutectic solvent mixtures: probing inter-molecular interactions using PFG NMR[J]. Physical Chemistry Chemical Physics, 2015,17:15297-15304.

[75] Siongco K. R., Leron R. B., Caparanga A. R., et al. Molar heat capacities and electrical conductivities of two ammonium-based deep eutectic solvents and their aqueous solutions[J]. Thermochimica Acta, 2013,566:50-56.

[76] Rashid S. N., Hayyan A., Hayyan M., et al. Ternary glycerol-based deep eutectic solvents: Physicochemical properties and enzymatic activity[J]. Chemical Engineering Research & Design, 2021,169:77-85.

[77] Sedghamiz M. A., Raeissi S. Physical properties of deep eutectic solvents formed by the sodium halide salts and ethylene glycol, and their mixtures with water[J]. Journal of Molecular Liquids, 2018,269:694-702.

[78] Hammond O. S., Bowron D. T., Edler K. J. The Effect of Water upon Deep Eutectic Solvent Nanostructure: An Unusual Transition from Ionic Mixture to Aqueous Solution[J]. Angewandte Chemie-International Edition, 2017,56:9782-9785.

[79] D'Agostino C., Gladden L. F., Mantle M. D., et al. Correction: Molecular and ionic diffusion in aqueous - deep eutectic solvent mixtures: probing inter-molecular interactions using PFG NMR[J]. Physical Chemistry Chemical Physics, 2017,19:1686.

[80] Meng X. Q., Ballerat-Busserolles K., Husson P., et al. Impact of water on the melting temperature of urea plus choline chloride deep eutectic solvent[J]. New Journal of Chemistry, 2016,40:4492-4499.

[81] Lopez-Salas N., Vicent-Luna J. M., Imberti S., et al. Looking at the "Water-in-Deep-Eutectic-Solvent" System: A Dilution Range for High Performance Eutectics[J]. Acs Sustainable Chemistry & Engineering, 2019,7:17565-17573.

[82] Cherigui E. M., Sentosun K., Mamme M. H., et al. On the Control and Effect of Water Content during the Electrodeposition of Ni Nanostructures from Deep Eutectic Solvents[J]. Journal of Physical Chemistry C, 2018,122:23129-23142.

[83] Liao H. G., Jiang Y. X., Zhou Z. Y., et al. Shape-Controlled Synthesis of Gold Nanoparticles in Deep Eutectic Solvents for Studies of Structure-Functionality Relationships in Electrocatalysis[J]. Angewandte Chemie-International Edition, 2008,47:9100-9103.

[84] Mota-Morales J. D., Sanchez-Leija R. J., Carranza A., et al. Free-radical polymerizations of and in deep eutectic solvents: Green synthesis of functional materials[J]. Progress in Polymer Science, 2018,78:139-153.

[85] Sanchez-Leija R. J., Torres-Lubian J. R., Resendiz-Rubio A., et al. Enzyme-mediated free radical polymerization of acrylamide in deep eutectic solvents[J]. Rsc Advances, 2016,6:13072-13079.

[86] Garcia G., Atilhan M., Aparicio S. Interfacial Properties of Deep Eutectic Solvents Regarding to CO2

Capture[J]. Journal of Physical Chemistry C, 2015,119:21413-21425.
[87] Su W. C., Wong D. S. H., Li M. H. Effect of Water on Solubility of Carbon Dioxide in (Aminomethanamide+2-Hydroxy-N,N,N-trimethylethanaminium Chloride)[J]. Journal of Chemical and Engineering Data, 2009,54:1951-1955.
[88] Xu K. J., Wang Y. Z., Huang Y. H., et al. A green deep eutectic solvent-based aqueous two-phase system for protein extracting[J]. Analytica Chimica Acta, 2015,864:9-20.
[89] Mondal D., Mahto A., Veerababu P., et al. Deep eutectic solvents as a new class of draw agent to enrich low abundance DNA and proteins using forward osmosis[J]. Rsc Advances, 2015,5:89539-89544.
[90] Maugeri Z., de Maria P. D. Whole-Cell Biocatalysis in Deep-Eutectic-Solvents/Aqueous Mixtures[J]. ChemCatChem, 2014,6:1535-1537.
[91] Gutierrez M. C., Ferrer M. L., Yuste L., et al. Bacteria Incorporation in Deep-eutectic Solvents through Freeze-Drying[J]. Angewandte Chemie-International Edition, 2010,49:2158-2162.
[92] Wagle D. V., Baker G. A., Mamontov E. Differential Microscopic Mobility of Components within a Deep Eutectic Solvent[J]. J Phys Chem Lett, 2015,6:2924-8.
[93] Fryars S., Limanton E., Gauffre F., et al. Diffusion of redox active molecules in deep eutectic solvents[J]. Journal of Electroanalytical Chemistry, 2018,819:214-219.
[94] Bahadori L., Chakrabarti M. H., Mjalli F. S., et al. Physicochemical properties of ammonium-based deep eutectic solvents and their electrochemical evaluation using organometallic reference redox systems[J]. Electrochimica Acta, 2013,113:205-211.
[95] Costa R., Figueiredo M., Pereira C. M., et al. Electrochemical double layer at the interfaces of Hg/choline chloride based solvents[J]. Electrochimica Acta, 2010,55:8916-8920.
[96] Lu X., Burrell G., Separovic F., et al. Electrochemistry of room temperature protic ionic liquids: a critical assessment for use as electrolytes in electrochemical applications[J]. Journal of Physical Chemistry B, 2012,116:9160-70.
[97] Savéant J.-M., Costentin C. Elements of Molecular and Biomolecular Electrochemistry: An Electrochemical Approach to Electron Transfer Chemistry. 2nd ed. Hoboken, NJ: John Wiley and Sons Inc.; 2019.
[98] Sakita A. M. P., Della Noce R., Fugivara C. S., et al. Semi-integrative Voltammetry as an Efficient Tool To Study Simple Electrochemical Systems in Deep Eutectic Solvents[J]. Analytical Chemistry, 2017,89:8296-8303.
[99] Bahadori L., Manan N. S., Chakrabarti M. H., et al. The electrochemical behaviour of ferrocene in deep eutectic solvents based on quaternary ammonium and phosphonium salts[J]. Physical Chemistry Chemical Physics, 2013,15:1707-14.
[100] Renjith A., Lakshminarayanan V. Electron-Transfer Studies of Model Redox-Active Species (Cationic, Anionic, and Neutral) in Deep Eutectic Solvents[J]. Journal of Physical Chemistry C, 2018,122:25411-25421.
[101] Nkuku C. A., LeSuer R. J. Electrochemistry in deep eutectic solvents[J]. Journal of Physical Chemistry B, 2007,111:13271-7.
[102] Alesary H. F., Cihangir S., Ballantyne A. D., et al. Influence of additives on the electrodeposition of zinc from a deep eutectic solvent[J]. Electrochimica Acta, 2019,304:118-130.
[103] Abbott A. P., Barron J. C., Frisch G., et al. The effect of additives on zinc electrodeposition from deep eutectic solvents[J]. Electrochimica Acta, 2011,56:5272-5279.
[104] Abbott A. P., Capper G., McKenzie K. J., et al. Electrodeposition of zinc-tin alloys from deep eutectic

solvents based on choline chloride[J]. Journal of Electroanalytical Chemistry, 2007,599:288-294.
[105] Cvetkovic V. S., Vukicevic N. M., Jovicevic N., et al. Aluminium electrodeposition under novel conditions from AlCl3-urea deep eutectic solvent at room temperature[J]. Transactions of Nonferrous Metals Society of China, 2020,30:823-834.
[106] Abood H. M. A., Abbott A. P., Ballantyne A. D., et al. Do all ionic liquids need organic cations? Characterisation of [AlCl2 center dot nAmide](+) AlCl4- and comparison with imidazolium based systems[J]. Chem Commun (Camb), 2011,47:3523-3525.
[107] Abbott A. P., El Ttaib K., Frisch G., et al. Electrodeposition of copper composites from deep eutectic solvents based on choline chloride[J]. Physical Chemistry Chemical Physics, 2009,11:4269-4277.
[108] Gomez E., Cojocaru P., Magagnin L., et al. Electrodeposition of Co, Sm and SmCo from a Deep Eutectic Solvent[J]. Journal of Electroanalytical Chemistry, 2011,658:18-24.
[109] Abbott A. P., Azam M., Ryder K. S., et al. Study of silver electrodeposition in deep eutectic solvents using atomic force microscopy[J]. Transactions of the Institute of Metal Finishing, 2018,96:297-303.
[110] Abbott A. P., El Ttaib K., Frisch G., et al. The electrodeposition of silver composites using deep eutectic solvents[J]. Physical Chemistry Chemical Physics, 2012,14:2443-2449.
[111] Abbott A. P., Capper G., Davies D. L., et al. Ionic liquid analogues formed from hydrated metal salts[J]. Chemistry-a European Journal, 2004,10:3769-3774.
[112] Alcanfor A. A. C., dos Santos L. P. M., Dias D. F., et al. Electrodeposition of indium on copper from deep eutectic solvents based on choline chloride and ethylene glycol[J]. Electrochimica Acta, 2017,235:553-560.
[113] Li W. R., Hao J. J., Mu S. H., et al. Electrochemical behavior and electrodeposition of Ni-Co alloy from choline chloride-ethylene glycol deep eutectic solvent[J]. Applied Surface Science, 2020,507.
[114] You Y. H., Gu C. D., Wang X. L., et al. Electrodeposition of Ni-Co alloys from a deep eutectic solvent[J]. Surface & Coatings Technology, 2012,206:3632-3638.
[115] Ren X. Y., Zhu X. L., Xu C. Y., et al. The Electrodeposition of Amorphous/Nanocrystalline Ni-Cr Alloys from ChCl-EG Deep Eutectic Solvent[J]. Journal of the Electrochemical Society, 2020,167.
[116] Abbott A. P., Alhaji A. I., Ryder K. S., et al. Electrodeposition of copper-tin alloys using deep eutectic solvents[J]. Transactions of the Institute of Metal Finishing, 2016,94:104-113.
[117] Ruggeri S., Poletti F., Zanardi C., et al. Chemical and electrochemical properties of a hydrophobic deep eutectic solvent[J]. Electrochimica Acta, 2019,295:124-129.
[118] Liu X. W., Xu D. M., Diao B. T., et al. Choline chloride based deep eutectic solvents selection and liquid-liquid equilibrium for separation of dimethyl carbonate and ethanol[J]. Journal of Molecular Liquids, 2019,275:347-353.
[119] Altunay N., Elik A., Gurkan R. Monitoring of some trace metals in honeys by flame atomic absorption spectrometry after ultrasound assisted-dispersive liquid liquid microextraction using natural deep eutectic solvent[J]. Microchemical Journal, 2019,147:49-59.
[120] Hou Y. C., Yao C. F., Wu W. Z. Deep Eutectic Solvents: Green Solvents for Separation Applications[J]. Acta Physico-Chimica Sinica, 2018,34:873-885.
[121] Verevkin S. P., Sazonova A. Y., Frolkova A. K., et al. Separation Performance of BioRenewable Deep Eutectic Solvents[J]. Industrial & Engineering Chemistry Research, 2015,54:3498-3504.
[122] Garcia G., Aparicio S., Ullah R., et al. Deep Eutectic Solvents: Physicochemical Properties and Gas Separation Applications[J]. Energy & Fuels, 2015,29:2616-2644.
[123] Oliveira F. S., Pereiro A. B., Rebelo L. P. N., et al. Deep eutectic solvents as extraction media for

azeotropic mixtures[J]. Green Chemistry, 2013,15:1326-1330.
[124] Schaeffer N., Martins M. A. R., Neves C. M. S. S., et al. Sustainable hydrophobic terpene-based eutectic solvents for the extraction and separation of metals[J]. Chem Commun (Camb), 2018,54:8104-8107.
[125] Phelps T. E., Bhawawet N., Jurisson S. S., et al. Efficient and Selective Extraction of (TcO4-)-Tc-99m from Aqueous Media Using Hydrophobic Deep Eutectic Solvents[J]. Acs Sustainable Chemistry & Engineering, 2018,6:13656-13661.
[126] Soldner A., Zach J., Konig B. Deep eutectic solvents as extraction media for metal salts and oxides exemplarily shown for phosphates from incinerated sewage sludge ash[J]. Green Chemistry, 2019,21:321-328.
[127] Sarmad S., Mikkola J. P., Ji X. Y. Carbon Dioxide Capture with Ionic Liquids and Deep Eutectic Solvents: A New Generation of Sorbents[J]. ChemSusChem, 2017,10:324-352.
[128] Zubeir L. F., van Osch D. J. G. P., Rocha M. A. A., et al. Carbon Dioxide Solubilities in Decanoic Acid-Based Hydrophobic Deep Eutectic Solvents[J]. Journal of Chemical and Engineering Data, 2018,63:913-919.
[129] Kamgar A., Mohsenpour S., Esmaeilzadeh F. Solubility prediction of CO2, CH4, H-2, CO and N-2 in Choline Chloride/Urea as a eutectic solvent using NRTL and COSMO-RS models[J]. Journal of Molecular Liquids, 2017,247:70-74.
[130] Leron R. B., Li M. H. Solubility of carbon dioxide in a choline chloride-ethylene glycol based deep eutectic solvent[J]. Thermochimica Acta, 2013,551:14-19.
[131] Zhang C. K., Zhang L. Y., Yu G. H. Eutectic Electrolytes as a Promising Platform for Next-Generation Electrochemical Energy Storage[J]. Acc Chem Res, 2020,53:1648-1659.
[132] Padwal C., Pham H. D., Jadhav S., et al. Deep Eutectic Solvents: Green Approach for Cathode Recycling of Li-Ion Batteries[J]. Advanced Energy and Sustainability Research, 2022,3.
[133] Tran M. K., Rodrigues M. T. F., Kato K., et al. Deep eutectic solvents for cathode recycling of Li-ion batteries[J]. Nature Energy, 2019,4:339-345.
[134] Martinez R., Berbegal L., Guillena G., et al. Bio-renewable enantioselective aldol reaction in natural deep eutectic solvents[J]. Green Chemistry, 2016,18:1724-1730.
[135] Vidal C., Merz L., Garcia-Alvarez J. Deep eutectic solvents: biorenewable reaction media for Au(I)-catalysed cycloisomerisations and one-pot tandem cycloisomerisation/Diels-Alder reactions[J]. Green Chemistry, 2015,17:3870-3878.
[136] Marullo S., Meli A., D'Anna F. A Joint Action of Deep Eutectic Solvents and Ultrasound to Promote Diels-Alder Reaction in a Sustainable Way[J]. Acs Sustainable Chemistry & Engineering, 2020,8:4889-4899.
[137] Shaabani A., Hooshmand S. E., Tabatabaei A. T. Synthesis of fully substituted naphthyridines: a novel domino four-component reaction in a deep eutectic solvent system based on choline chloride/urea[J]. Tetrahedron Letters, 2016,57:351-353.
[138] Gorke J. T., Srienc F., Kazlauskas R. J. Hydrolase-catalyzed biotransformations in deep eutectic solvents[J]. Chem Commun (Camb), 2008:1235-1237.
[139] Cicco L., Rios-Lombardia N., Rodriguez-Alvarez M. J., et al. Programming cascade reactions interfacing biocatalysis with transition-metal catalysis in Deep Eutectic Solvents as biorenewable reaction media[J]. Green Chemistry, 2018,20:3468-3475.
[140] Yin J. M., Wang J. P., Li Z., et al. Deep desulfurization of fuels based on an oxidation/extraction process with acidic deep eutectic solvents[J]. Green Chemistry, 2015,17:4552-4559.

[141] Hooshmand S. E., Afshari R., Ramon D. J., et al. Deep eutectic solvents: cutting-edge applications in cross-coupling reactions[J]. Green Chemistry, 2020,22:3668-3692.

[142] Dilauro G., Garcia S. M., Tagarelli D., et al. Ligand-Free Bioinspired Suzuki-Miyaura Coupling Reactions using Aryltrifluoroborates as Effective Partners in Deep Eutectic Solvents[J]. ChemSusChem, 2018,11:3495-3501.

[143] Bard A. J., Faulkner L. R. Electrochemical methods: fundamentals and applications. 2nd ed. New York: John Wiley and Sons; 2000.

[144] Weaver M. J. Dynamic Solvent Effects on Activated Electron-Transfer Reactions - Principles, Pitfalls, and Progress[J]. Chem Rev, 1992,92:463-480.

[145] Nicholson R. S. Theory and application of cyclic voltammetry for measurement of electrode reaction kinetics[J]. Analytical Chemistry, 1965,37:1351-1355.

[146] Bard A. J., Mirkin M. V., Unwin P. R., et al. Scanning Electrochemical Microscopy .12. Theory and Experiment of the Feedback Mode with Finite Heterogeneous Electron-Transfer Kinetics and Arbitrary Substrate Size[J]. Journal of Physical Chemistry, 1992,96:1861-1868.

[147] Zhang J., Guo S. X., Bond A. M., et al. Large-amplitude Fourier transformed high-harmonic alternating current cyclic voltammetry: Kinetic discrimination of interfering faradaic processes at glassy carbon and at boron-doped diamond electrodes[J]. Analytical Chemistry, 2004,76:3619-3629.

[148] Zhang J., Guo S. X., Bond A. M. Discrimination and evaluation of the effects of uncompensated resistance and slow electrode kinetics from the higher harmonic components of a Fourier transformed large-amplitude alternating current voltammogram[J]. Analytical Chemistry, 2007,79:2276-2288.

[149] Sun Y. Y. T., Mirkin M. V. Toward More Reliable Measurements of Electron-Transfer Kinetics at Nanoelectrodes: Next Approximation[J]. Analytical Chemistry, 2016,88:11758-11766.

[150] Kim J., Bard A. J. Electrodeposition of Single Nanometer-Size Pt Nanoparticles at a Tunneling Ultramicroelectrode and Determination of Fast Heterogeneous Kinetics for Ru(NH3)(6)(3+) Reduction[J]. Journal of the American Chemical Society, 2016,138:975-979.

[151] Lovelock K. R. J., Cowling F. N., Taylor A. W., et al. Effect of Viscosity on Steady-State Voltammetry and Scanning Electrochemical Microscopy in Room Temperature Ionic Liquids[J]. Journal of Physical Chemistry B, 2010,114:4442-4450.

[152] Bond A. M., Duffy N. W., Guo S. X., et al. Changing the look of voltammetry[J]. Analytical Chemistry, 2005,77:186a-195a.

[153] Li J. Z., Kennedy G. F., Gundry L., et al. Application of Bayesian Inference in Fourier-Transformed Alternating Current Voltammetry for Electrode Kinetic Mechanism Distinction[J]. Analytical Chemistry, 2019,91:5303-5309.

[154] Li J. Z., Kennedy G. F., Bond A. M., et al. Demonstration of Superiority of the Marcus-Hush Electrode Kinetic Model in the Electrochemistry of Dissolved Decamethylferrocene at a Gold-Modified Electrode by Fourier-Transformed Alternating Current Voltammetry[J]. Journal of Physical Chemistry C, 2018,122:9009-9014.

[155] Tan S. Y., Lazenby R. A., Bano K., et al. Comparison of fast electron transfer kinetics at platinum, gold, glassy carbon and diamond electrodes using Fourier-transformed AC voltammetry and scanning electrochemical microscopy[J]. Physical Chemistry Chemical Physics, 2017,19:8726-8734.

[156] Opało M., Kapturkiewicz A. Solvent effect on the kinetics of the electrooxidation of

phenothiazine[J]. Electrochimica Acta, 1985,30:1301-1306.
[157] Gennett T., Milner D. F., Weaver M. J. Role of solvent reorganization dynamics in electron transfer processes. Theory-experiment comparisons for electrochemical and homogeneous electron exchange involving metallocene redox couples[J]. J. Phys. Chem., 1985,89:2787-2794.
[158] McManis G. E., Golovin M. N., Weaver M. J. Role of solvent reorganization dynamics in electron-transfer processes. Anomalous kinetic behavior in alcohol solvents[J]. J. Phys. Chem., 1986,1986:6563-6570.
[159] Weaver M. J. Dynamical solvent effects on activated electron-transfer reactions: principles, pitfalls, and progress[J]. Chem. Rev, 1992,92:463-480.
[160] Zhang X., Leddy J., Bard A. J. Dependence of rate constants of heterogeneous electron transfer reactions on viscosity[J]. J. Am. Chem. Soc., 1985,107:3719-3721.
[161] Miao W. J., Ding Z. F., Bard A. J. Solution viscosity effects on the heterogeneous electron transfer kinetics of ferrocenemethanol in dimethyl sulfoxide-water mixtures[J]. Journal of Physical Chemistry B, 2002,106:1392-1398.
[162] Bard A. J. Inner-Sphere Heterogeneous Electrode Reactions. Electrocatalysis and Photocatalysis: The Challenge[J]. Journal of the American Chemical Society, 2010,132:7559-7567.
[163] Jani A., Malfait B., Morineau D. On the coupling between ionic conduction and dipolar relaxation in deep eutectic solvents: Influence of hydration and glassy dynamics[J]. Journal of Chemical Physics, 2021,154.
[164] Tessensohn M. E., Hirao H., Webster R. D. Electrochemical Properties of Phenols and Quinones in Organic Solvents are Strongly Influenced by Hydrogen-Bonding with Water[J]. Journal of Physical Chemistry C, 2013,117:1081-1090.
[165] Turek A. K., Hardee D. J., Ullman A. M., et al. Activation of Electron-Deficient Quinones through Hydrogen-Bond-Donor-Coupled Electron Transfer[J]. Angewandte Chemie-International Edition, 2016,55:539-544.
[166] Okamoto K., Ohkubo K., Kadish K. M., et al. Remarkable accelerating effects of ammonium cations on electron-transfer reactions of quinones by hydrogen bonding with semiquinone radical anions[J]. Journal of Physical Chemistry A, 2004,108:10405-10413.
[167] Fukuzumi S., Kitaguchi H., Suenobu T., et al. Activation of electron transfer reduction of p-benzoquinone derivatives by intermolecular regioselective hydrogen bond formation[J]. Chem Commun (Camb), 2002:1984-1985.
[168] Ge Y., Lilienthal R. R., Smith D. K. Electrochemically-controlled hydrogen bonding. Selective recognition of urea and amide derivatives by simple redox-dependent receptors[J]. Journal of the American Chemical Society, 1996,118:3976-3977.
[169] Gupta N., Linschitz H. Hydrogen-bonding and protonation effects in electrochemistry of quinones in aprotic solvents[J]. Journal of the American Chemical Society, 1997,119:6384-6391.
[170] Smith D. K. Exploring the Role of H-Bonding in Organic Electrochemistry - From Supramolecular Applications to Mechanistic Investigations[J]. Chemical Record, 2021,21:2488-2501.
[171] Shi R. R. S., Tessensohn M. E., Lauw S. J. L., et al. Tuning the reduction potential of quinones by controlling the effects of hydrogen bonding, protonation and proton-coupled electron transfer reactions[J]. Chem Commun (Camb), 2019,55:2277-2280.
[172] Clare L. A., Pham T. D., Rafou L. A., et al. The Role of H-Bonding in Nonconcerted Proton-Coupled Electron Transfer: Explaining the Voltammetry of Phenylenediamines in the Presence of Weak Bases in Acetonitrile[J]. Journal of Physical Chemistry C, 2019,123:23390-23402.

[173] Tessensohn M. E., Lim S., Miechie, et al. The Dual Roles of Phenylenediamines: Using their Voltammetric Behavior to Measure the Hydrogen Donor and Acceptor Abilities of Alcohols in Acetonitrile[J]. Chemphyschem, 2017,18:3562-3569.

[174] Gamboa-Valero N., Astudillo P. D., Gonzalez-Fuentes M. A., et al. Hydrogen bonding complexes in the quinone-hydroquinone system and the transition to a reversible two-electron transfer mechanism[J]. Electrochimica Acta, 2016,188:602-610.

[175] Galano A., Gomez M., Gonzalez F. J., et al. Correlation between Hydrogen Bonding Association Constants in Solution with Quantum Chemistry Indexes: The Case of Successive Association between Reduced Species of Quinones and Methanol[J]. Journal of Physical Chemistry A, 2012,116:10638-10645.

[176] Hui Y. L., Chng E. L. K., Chua L. P. L., et al. Voltammetric Method for Determining the Trace Moisture Content of Organic Solvents Based on Hydrogen-Bonding Interactions with Quinones[J]. Analytical Chemistry, 2010,82:1928-1934.

[177] Bu J. J., Lilienthal N. D., Woods J. E., et al. Electrochemically controlled hydrogen bonding. Nitrobenzenes as simple redox-dependent receptors for arylureas[J]. Journal of the American Chemical Society, 2005,127:6423-6429.

[178] Uno B., Okumura N., Goto M., et al. n-sigma charge-transfer interaction and molecular and electronic structural properties in the hydrogen-bonding systems consisting of p-quinone dianions and methyl alcohol[J]. Journal of Organic Chemistry, 2000,65:1448-1455.

[179] Tamashiro B. T., Cedano M. R., Pham A. T., et al. Use of a Wedge Scheme to Describe Intermolecular Proton-Coupled Electron Transfer through the H-bond Complex Formed Between a Phenylenediamine-Based Urea and 1,8-Naphthyridine[J]. Journal of Physical Chemistry C, 2015,119:12865-12874.

[180] Ammar F., Savéant J. M. Thermodynamics of successive electron transfers. Internal and solvation enthalpy and entropy variations in a series of polynitro compounds[J]. Electroanalytical Chemistry and Interfacial Electrochemistry, 1973,47:115-125.

[181] Xie Q. S., Perezcordero E., Echegoyen L. Electrochemical Detection of C-60(6-) and C-70(6-) - Enhanced Stability of Fullerides in Solution[J]. Journal of the American Chemical Society, 1992,114:3978-3980.

[182] Evans D. H., Hu K. Inverted potentials in two-electron processes in organic electrochemistry[J]. Journal of the Chemical Society-Faraday Transactions, 1996,92:3983-3990.

[183] Lehmann M. W., Singh P., Evans D. H. Potential inversion in the reduction of trans-2,3-dinitro-2-butene[J]. Journal of Electroanalytical Chemistry, 2003,549:137-143.

[184] Hill M. G., Lamanna W. M., Mann K. R. Tetrabutylammonium Tetrakis[3,5-Bis(Trifluoromethyl)Phenyl]Borate as a Noncoordinating Electrolyte - Reversible 1e- Oxidations of Ruthenocene, Osmocene, and Rh2(Tm4)42+ (Tm4 = 2,5-Diisocyano-2,5-Dimethylhexane)[J]. Inorganic Chemistry, 1991,30:4687-4690.

[185] Hill M. G., Rosenhein L. D., Mann K. R., et al. Ir Spectroelectrochemical Investigation of the Disproportionation of W2(Sbz)2(Co)8-[J]. Inorganic Chemistry, 1992,31:4108-4111.

[186] Macias-Ruvalcaba N. A., Evans D. H. Study of the effects of ion pairing and activity coefficients on the separation in standard potentials for two-step reduction of dinitroaromatics[J]. Journal of Physical Chemistry B, 2005,109:14642-14647.

[187] Chung Y. C., Tu Y. J., Lu S. H., et al. Redox Potential Inversion by Ionic Hydrogen Bonding between Phenylenediamines and Pyridines[J]. Organic Letters, 2011,13:2826-2829.

[188] Zusman L. D., Beratan D. N. Two-electron transfer reactions in polar solvents[J]. Journal of Chemical Physics, 1996,105:165-176.

[189] Zusman L. D., Beratan D. N. Three-state model for two-electron transfer reactions[J]. Journal of Physical Chemistry A, 1997,101:4136-4141.

[190] Medvedev I. G. Electron correlations for adiabatic electrochemical electron transfer reactions in a model for an electrode with an infinitely wide conduction band[J]. Russian Journal of Electrochemistry, 2003,39:44-52.

[191] Gileadi E. Simultaneous two-electron transfer in electrode kinetics[J]. Journal of Electroanalytical Chemistry, 2002,532:181-189.

[192] Evans D. H. One-electron and two-electron transfers in electrochemistry and homogeneous solution reactions[J]. Chem Rev, 2008,108:2113-2144.

[193] Marcus R. A. On the Theory of ElectronTransfer Reactions. VI. Unified Treatment for Homogeneous and Electrode Reactions[J]. j. Chem. Phys., 1965,43:679-701.

[194] Hush N. S. Adiabatic theory of outer sphere electron transfer reactions in solution[J]. Trans. Faraday. Soc., 1961,57:557-580.

[195] Fawcett W. R., Blum L. Estimation of the outer-sphere contribution to the activation parameters for homogeneous electron-transfer reactions using the mean spherical approximation[J]. Chemical Physics Letters, 1991,187:173-179.

[196] Marcus R. A. On the theory of oxidation-reduction reactions involving electron transfer[J]. Journal of Physical Chemistry, 1955,24:966-978.

[197] Hush N. S. Adiabatic rate processes at electrodes 1. Energy-charge relationships[J]. Journal of Chemical Physics, 1958,28:962-972.

[198] Fawcett W. R., Gaal A., Misicak D. Estimation of the rate constant for electron transfer in room temperature ionic liquids[J]. Journal of Electroanalytical Chemistry, 2011,660:230-233.

[199] Lynden-Bell R. M. Does Marcus theory apply to redox processes in ionic liquids? A simulation study[J]. Electrochemistry Communications, 2007,9:1857-1861.

[200] Frenzel N., Hartley J., Frisch G. Voltammetric and spectroscopic study of ferrocene and hexacyanoferrate and the suitability of their redox couples as internal standards in ionic liquids[J]. Physical Chemistry Chemical Physics, 2017,19:28841-28852.

[201] Barrosse-Antle L. E., Bond A. M., Compton R. G., et al. Voltammetry in Room Temperature Ionic Liquids: Comparisons and Contrasts with Conventional Electrochemical Solvents.[J]. Chemistry-an Asian Journal, 2010,5:202-230.

[202] Lagrost C., Preda L., Volanschi E., et al. Heterogeneous electron-transfer kinetics of nitro compounds in room-temperature ionic liquids[J]. Journal of Electroanalytical Chemistry, 2005,585:1-7.

[203] Zhang J., Bond A. M. Conditions required to achieve the apparent equivalence of adhered solid- and solution-phase voltammetry for ferrocene and other redox-active solids in ionic liquids[J]. Analytical Chemistry, 2003,75:2694-2702.

[204] Bahadori L., Manan N. S. A., Chakrabarti M. H., et al. The electrochemical behaviour of ferrocene in deep eutectic solvents based on quaternary ammonium and phosphonium salts[J]. Physical Chemistry Chemical Physics, 2013,15:1707-1714.

[205] Nkuku C. A., LeSuer R. J. Electrochemistry in deep eutectic solvents[J]. Journal of Physical Chemistry B, 2007,111:13271-13277.

[206] Andrieux C. P., Hapiot P., Saveant J. M. Fast Kinetics by Means of Direct and Indirect

Electrochemical Techniques[J]. Chem Rev, 1990,90:723-738.
[207] Imbeaux J. C., Savéant J.-M. Convolutive Potential Sweep Voltammetry: I. Introduction[J]. Journal of Electroanalytical Chemistry, 1973,44:169-187.
[208] Garreau D., Hapiot P., Savéant J.-M. Instrumentation for Fast Voltammetry at Ultramicroelectrodes - Stability and Bandpass Limitations[J]. Journal of Electroanalytical Chemistry, 1989,272:1-16.
[209] Garreau D., Savéant J.-M. Linear Sweep Voltammetry -compensation of cell resistance and stability[J]. Journal of Electroanalytical Chemistry, 1972,35:309-331.
[210] Shen D., Steinberg K., Akolkar R. Avoiding Pitfalls in the Determination of Reliable Electrochemical Kinetics Parameters for the Cu2+-> Cu1+ Reduction Reaction in Deep Eutectic Solvents[J]. Journal of the Electrochemical Society, 2018,165:E808-E815.
[211] McCreery R. L. Advanced carbon electrode materials for molecular electrochemistry[J]. Chem Rev, 2008,108:2646-2687.
[212] Yamagata M., Tachikawa N., Katayama Y., et al. Electrochemical behavior of several iron complexes in hydrophobic room-temperature ionic liquids[J]. Electrochimica Acta, 2007,52:3317-3322.
[213] Tachikawa N., Katayama Y., Miura T. Electrode kinetics of some iron complexes in an imide-type room-temperature ionic liquid[J]. Journal of the Electrochemical Society, 2007,154:F211-F216.
[214] Klymenko O. V., Oleinick A., Svir I., et al. KISSA - Software for Simulation of Electrochemical Reaction Mechanisms of Any Complexity[J]. https://www.kissagroup.com/, 2019.
[215] Matyushov D. V., Newton M. D. Electrode reactions in slowly relaxing media[J]. Journal of Chemical Physics, 2017,147.
[216] Nikitina V. A., Kislenko S. A., Nazinutdinov R. R., et al. Ferrocene/Ferrocenium Redox Couple at Au(111)/Ionic Liquid and Au(111)/Acetonitrile Interfaces: A Molecular-Level View at the Elementary Act[J]. Journal of Physical Chemistry C, 2014,118:6151-6164.
[217] Barnes A. S., Rogers E. I., Streeter I., et al. Extraction of electrode kinetic parameters from microdisc voltammetric data measured under transport conditions intermediate between steady-state convergent and transient linear diffusion as typically applies to room temperature ionic liquids[J]. Journal of Physical Chemistry B, 2008,112:7560-7565.
[218] Fietkau N., Clegg A. D., Evans R. G., et al. Electrochemical rate constants in room temperature ionic liquids: The oxidation of a series of ferrocene derivatives[J]. Chemphyschem, 2006,7:1041-1045.
[219] Lagrost C., Carrie D., Vaultier M., et al. Reactivities of some electrogenerated organic cation radicals in room-temperature ionic liquids: Toward an alternative to volatile organic solvents?[J]. Journal of Physical Chemistry A, 2003,107:745-752.
[220] Wang Y. J., Rogers E. I., Compton R. G. The measurement of the diffusion coefficients of ferrocene and ferrocenium and their temperature dependence in acetonitrile using double potential step microdisk electrode chronoamperometry[J]. Journal of Electroanalytical Chemistry, 2010,648:15-19.
[221] Konopka S. J., McDuffie B. Diffusion Coefficients of Ferri- and Ferrocyanide Ions in Aqueous Media, Using Twin-Electrode Thin-Layer Electrochemistry[J]. Analytical Chemistry, 1970,42:1741-1746.
[222] E. M. M. G., N. N. G. M., Weaver M. J. Role of solvent reorganization dynamics in electron transfer processes. Anomalous kinetics behavior in acohol solvents.[J]. Journal of Physical Chemistry, 1986,90.
[223] Popov I., Ben Ishai P., Khamzin A., et al. The mechanism of the dielectric relaxation in water[J]. Physical Chemistry Chemical Physics, 2016,18:13941-13953.
[224] Weingartner H., Sasisanker P., Daguenet C., et al. The dielectric response of room-temperature

ionic liquids: Effect of cation variation[J]. Journal of Physical Chemistry B, 2007,111:4775-4780.
[225] Nakamura K., Shikata T. Systematic Dielectric and NMR Study of the Ionic Liquid 1-Alkyl-3-Methyl Imidazolium[J]. Chemphyschem, 2010,11:285-294.
[226] Reuter D., Binder C., Lunkenheimer P., et al. Ionic conductivity of deep eutectic solvents: the role of orientational dynamics and glassy freezing[J]. Physical Chemistry Chemical Physics, 2019,21:6801-6809.
[227] Leron R. B., Soriano A. N., Li M. H. Densities and refractive indices of the deep eutectic solvents (choline chloride plus ethylene glycol or glycerol) and their aqueous mixtures at the temperature ranging from 298.15 to 333.15 K[J]. Journal of the Taiwan Institute of Chemical Engineers, 2012,43:551-557.
[228] Undre P. B., Khirade P. W., Rajenimbalkar V. S., et al. Dielectric relaxation in Ethylene Glycol - Dimethyl Sulfoxide mixtures as a function of composition and temperature.[J]. Journal of the Korean Chemical Society, 2012,56:416-423.
[229] Faraone A., Wagel D. V., Baker G. A., et al. Glycerol Hydrogen-Bonding Network Dominates Structure and Collective Dynamics in a Deep Eutectic Solvent[J]. Journal of Physical Chemistry B, 2018,122:1261-1267.
[230] Rozas S., Benito C., Alcalde R., et al. Insights on the water effect on deep eutectic solvents properties and structuring: The archetypical case of choline chloride plus ethylene glycol[J]. Journal of Molecular Liquids, 2021,344.
[231] Sapir L., Harries D. Restructuring a Deep Eutectic Solvent by Water: The Nanostructure of Hydrated Choline Chloride/Urea[J]. Journal of Chemical Theory and Computation, 2020,16:3335-3342.
[232] Jani A., Sohier T., Morineau D. Phase behavior of aqueous solutions of ethaline deep eutectic solvent[J]. Journal of Molecular Liquids, 2020,304.
[233] Ge X., Gu C. D., Wang X. L., et al. Deep eutectic solvents (DESs)-derived advanced functional materials for energy and environmental applications: challenges, opportunities, and future vision[J]. Journal of Materials Chemistry A, 2017,5:8209-8229.
[234] Ge X., Gu C. D., Wang X. L., et al. Ionothermal synthesis of cobalt iron layered double hydroxides (LDHs) with expanded interlayer spacing as advanced electrochemical materials[J]. Journal of Materials Chemistry A, 2014,2:17066-17076.
[235] Huang F. Y., Li T. B., Yan X. H., et al. Ternary Deep Eutectic Solvent (DES) with a Regulated Rate-Determining Step for Efficient Recycling of Lithium Cobalt Oxide[J]. Acs Omega, 2022,7:11452-11459.
[236] Zhen F. C., Peracevult L., Paquin L., et al. Electron Transfer Kinetics in a Deep Eutectic Solvent '[J]. Journal of Physical Chemistry B, 2020,124:1025-1032.
[237] Shen X., Sinclair N., Wainright J., et al. Evaluating and Developing a Reliable Reference Electrode for Choline Chloride Based Deep Eutectic Solvents[J]. Journal of the Electrochemical Society, 2020,167.
[238] Weber A. Z., Mench M. M., Meyers J. P., et al. Redox flow batteries: a review[J]. Journal of Applied Electrochemistry, 2011,41:1137-1164.
[239] Ghilane J., Hapiot P., Bard A. J. Metal/polypyrrole quasi-reference electrode for voltammetry in nonaqueous and aqueous solutions[J]. Analytical Chemistry, 2006,78:6868-6872.
[240] Abbott A. P., Capper G., Gray S. Design of Improved Deep Eutectic Solvents Using Hole Theory[J]. Chemphyschem, 2006,7:803-806.
[241] Sharma A., Li J. Z., Guo S. X., et al. Modeling the Influence of Low Concentrations of Water on the

Thermodynamics, Electron Transfer Kinetics, and Diffusivity of the [Ru(CN)(6)](4-/3-) Process in Propylene Carbonate[J]. Journal of Physical Chemistry C, 2020,124:13726-13738.

[242] Ghosh S., Soudackov A. V., Hammes-Schiffer S. Electrochemical Electron Transfer and Proton-Coupled Electron Transfer: Effects of Double Layer and Ionic Environment on Solvent Reorganization Energies[J]. Journal of Chemical Theory and Computation, 2016,12:2917-2925.

[243] Lehmann M. W., Evans D. H. Anomalous behavior in the two-step reduction of quinones in acetonitrile[J]. Journal of Electroanalytical Chemistry, 2001,500:12-20.

[244] Costentin C., Robert M., Saveant J. M. Update 1 of: Electrochemical Approach to the Mechanistic Study of Proton-Coupled Electron Transfer[J]. Chem Rev, 2010,110:Pr1-Pr40.

[245] Costentin C., Robert M., Saveant J. M. Concerted Proton-Electron Transfers: Electrochemical and Related Approaches[J]. Acc Chem Res, 2010,43:1019-1029.

[246] Quan M., Sanchez D., Wasylkiw M. F., et al. Voltammetry of quinones in unbuffered aqueous solution: Reassessing the roles of proton transfer and hydrogen bonding in the aqueous Electrochemistry of Quinones[J]. Journal of the American Chemical Society, 2007,129:12847-12856.

[247] Huynh M. T., Anson C. W., Cavell A. C., et al. Quinone 1 e(-) and 2 e(-)/2 H+ Reduction Potentials: Identification and Analysis of Deviations from Systematic Scaling Relationships[J]. Journal of the American Chemical Society, 2016,138:15903-15910.

[248] Staley P. A., Newell C. M., Pullman D. P., et al. The Effect of Glassy Carbon Surface Oxides in Non-Aqueous Voltammetry: The Case of Quinones in Acetonitrile[J]. Analytical Chemistry, 2014,86:10917-10924.

[249] Kim R. S., Chung T. D. The Electrochemical Reaction Mechanism and Applications of Quinones[J]. Bulletin of the Korean Chemical Society, 2014,35:3143-3155.

[250] Gurkan B., Simeon F., Hatton T. A. Quinone Reduction in Ionic Liquids for Electrochemical CO2 Separation[J]. Acs Sustainable Chemistry & Engineering, 2015,3:1394-1405.

[251] Nikitina V. A., Nazmutdinov R. R., Tsirlina G. A. Quinones Electrochemistry in Room-Temperature Ionic Liquids[J]. Journal of Physical Chemistry B, 2011,115:668-677.

[252] Ernst S., Aldous L., Compton R. G. The voltammetry of surface bound 2-anthraquinonyl groups in room temperature ionic liquids: Cation size effects[J]. Chemical Physics Letters, 2011,511:461-465.

[253] Wang Y. J., Rogers E. I., Belding S. R., et al. The electrochemical reduction of 1,4-benzoquinone in 1-ethyl-3-methylimidazolium bis(trifluoromethane-sulfonyl)-imide, [C(2)mim][NTf2]: A voltammetric study of the comproportionation between benzoquinone and the benzoquinone dianion[J]. Journal of Electroanalytical Chemistry, 2010,648:134-142.

[254] Carter M. T., Osteryoung R. A. Interaction of 9,10-Anthraquinone with Tetrachloroaluminate and Proton in Basic Aluminum-Chloride - 1-Ethyl-3-Methylimidazolium Chloride Room-Temperature Molten-Salts[J]. Journal of the Electrochemical Society, 1992,139:1795-1802.

[255] Hapiot P. F., Kispert L. D., Konovalov V. V., et al. Single two-electron transfers vs successive one-electron transfers in polyconjugated systems illustrated by the electrochemical oxidation and reduction of carotenoids[J]. Journal of the American Chemical Society, 2001,123:6669-6677.

[256] Savéant J. M., Andrieux C. P., Nadjo L. Disproportionation and e.c.e. mechanisms: IV. Reversible e.c.e. process[J]. Journal of Electroanalytical Chemistry and Interfacial Electrochemistry, 1973,41:137-141.

[257] Cobb S. J., Ayres Z. J., Newton M. E., et al. Deconvoluting Surface-Bound Quinone Proton Coupled Electron Transfer in Unbuffered Solutions: Toward a Universal Voltammetric pH Electrode[J].

Journal of the American Chemical Society, 2019,141:1035-1044.
[258] Yuasa J., Yamada S., Fukuzumi S. One-step versus stepwise mechanism in protonated amino acid-promoted electron-transfer reduction of a quinone by electron donors and two-electron reduction by a dihydronicotinamide adenine dinucleotide analogue. Interplay between electron transfer and hydrogen bonding[J]. Journal of the American Chemical Society, 2008,130:5808-5820.
[259] Clare L. A., Pham A. T., Magdaleno F., et al. Electrochemical Evidence for Intermolecular Proton-Coupled Electron Transfer through a Hydrogen Bond Complex in a p-Phenylenediamine-Based Urea. Introduction of the "Wedge Scheme" as a Useful Means To Describe Reactions of This Type[J]. Journal of the American Chemical Society, 2013,135:18930-18941.
[260] Connelly N. G., Geiger W. E. Chemical redox agents for organometallic chemistry[J]. Chem Rev, 1996,96:877-910.
[261] Abbasi N. M., Farooq M. Q., Anderson J. L. Investigating the Variation in Solvation Interactions of Choline Chloride-Based Deep Eutectic Solvents Formed Using Different Hydrogen Bond Donors[J]. Acs Sustainable Chemistry & Engineering, 2021,9:11970-11980.
[262] Zhen F., Hapiot P. Electrochemical reduction of quinones in Ethaline chosen as an example of deep eutectic solvent.[J]. Electrochemical Science Advances, 2022,e2100148.
[263] Sun Y. P., Xu W. L., Scott K. A Study of the Electrochemical Reduction of Nitrobenzene to P-Aminophenol in a Packed-Bed Electrode Reactor[J]. Electrochimica Acta, 1993,38:1753-1759.
[264] Cyr A., Huot P., Belot G., et al. The Efficient Electrochemical Reduction of Nitrobenzene and Azoxybenzene to Aniline in Neutral and Basic Aqueous Methanolic Solutions at Devarda Copper and Raney-Nickel Electrodes - Electrocatalytic Hydrogenolysis of N-O and N-N Bonds[J]. Electrochimica Acta, 1990,35:147-152.
[265] Marquez J., Pletcher D. A study of the electrochemical reduction of nitrobenzene to p-aminophenol[J]. Journal of Applied Electrochemistry, 1980,10:567-573.
[266] Asirvatham M. R., Hawley M. D. Electron-transfer processes: The electrochemical and chemical behavior of nitrosobenzene[J]. Journal of Electroanalytical Chemistry, 1974,57:179-190.
[267] Macias-Ruvalcaba N. A., Telo J. P., Evans D. H. Studies of the electrochemical reduction of some dinitro aromatics[J]. Journal of Electroanalytical Chemistry, 2007,600:294-302.
[268] Macias-Ruvalcaba N. A., Evans D. H. Studies of potential inversion in the electrochemical reduction of 11,11,12,12-tetracyano-9,10-anthraquinodimethane and 2,3,5,6-tetramethyl-7,7,8,8-tetracyano-1,4-benzoquinodimethane[J]. Journal of Physical Chemistry B, 2006,110:5155-5160.
[269] Kraiya C., Evans D. H. Investigation of potential inversion in the reduction of 9,10-dinitroanthracene and 3,6-dinitrodurene[J]. Journal of Electroanalytical Chemistry, 2004,565:29-35.
[270] Andrieux C. P., Savéant J. M. Effect of solvent and ion-pairing on the entropy and enthalpy factors in successive reductions of dinitro compounds[J]. Journal of Electroanalytical Chemistry and Interfacial Electrochemistry, 1974,57:27-33.
[271] Baik M. H., Schauer C. K., Ziegler T. Density functional theory study of redox pairs: 2. Influence of solvation and ion-pair formation on the redox Behavior of cyclooctatetraene and nitrobenzene[J]. Journal of the American Chemical Society, 2002,124:11167-11181.
[272] Smith W. H., Bard A. J. Electrochemical reactions of organic compounds in liquid ammonia: Part IV. Reduction of cyclooctatetraene[J]. Journal of Electroanalytical Chemistry and Interfacial Electrochemistry, 1977,76:19-26.
[273] Zuman P., Fijalek Z. Contribution to the Understanding of the Reduction-Mechanism of

Nitrobenzene[J]. Journal of Electroanalytical Chemistry, 1990,296:583-588.
[274] Silvester D. S., Wain A. J., Aldous L., et al. Electrochemical reduction of nitrobenzene and 4-nitrophenol in the room temperature ionic liquid [C(4)dmim][N(Tf)(2)][J]. Journal of Electroanalytical Chemistry, 2006,596:131-140.
[275] Smith W. H., Bard A. J. Electrochemical reactions of organic compounds in liquid ammonia. II nitrobenzene and nitrosobenzene[J]. Journal of the American Chemical Society, 1974,97:5203-5210.
[276] Jensen B. S., Parker V. D. Reversible anion radical-dianion redox equilibria involving ions of simple aromatic compounds[J]. Chem. Commun., 1974:367-368.
[277] Steudel E., Posdorfer J., Schindler R. N. Intermediates and Products in the Electrochemical Reduction of Nitrosobenzene - a Spectroelectrochemical Investigation[J]. Electrochimica Acta, 1995,40:1587-1594.
[278] Mendkovich A. S., Syroeshkin M. A., Mikhalchenko L. V., et al. Integrated Study of the Dinitrobenzene Electroreduction Mechanism by Electroanalytical and Computational Methods[J]. International Journal of Electrochemistry, 2011,2011:346043.
[279] Guerro M., Carlier R., Boubekeur K., et al. Cyclic vinylogous TTF: a potential molecular clip triggered by electron transfer[J]. Journal of the American Chemical Society, 2003,125:3159-3167.
[280] Nelsen S. F., Konradsson A. E., Weaver M. N., et al. Intervalence near-IR spectra of delocalized dinitroaromatic radical anions[J]. Journal of the American Chemical Society, 2003,125:12493-12501.
[281] Maki A. H., Geske D. H. Electron-spin resonance of electrochemically generated free radicals. Isomeric dinitrobenzene mononegative ions[J]. The Journal of Chemical Physics, 1960,33:825-832.
[282] Tessensohn M. E., Koh Y. R., Lim S., et al. Using Voltammetry to Measure the Relative Hydrogen-Bonding Strengths of Pyridine and Its Derivatives in Acetonitrile[J]. Chemphyschem, 2017,18:2250-2257.
[283] Costentin C., Saveant J. M. Dimerization of electrochemically generated ion radicals: mechanisms and reactivity factors[J]. Journal of Electroanalytical Chemistry, 2004,564:99-113.

Résumé en Français

Dans ce manuscrit, nous avons examiné différents aspects de l'électrochimie de molécules classiques dans les solvent eutectiques profonds (DES) qui peuvent être résumés sous quatre catégories générales. Tout d'abord, le potentiel standard et les coefficients de diffusion pour une ou deux réactions successives de transfert d'électrons ont été extraits de la voltamétrie cyclique des espèces redox. Deuxièmement, les constantes de vitesse de transfert d'électrons ont été mesurées par voltamétrie cyclique à vitesse de balayage rapide et comparées aux prédictions du modèle classique de la théorie de Marcus pour le transfert électronique hétérogène. Troisièmement, les différences de potentiel standard, inversion de potentiel pour les réactions de transfert à deux électrons et leurs mécanismes dans les DES ont été examinées. Enfin, nous avons obtenu de nouvelles indications sur les réactions couplant transfert d'électron et transfert de proton comme les quinones ou les composés aromatiques dinitrés.

Comme premier résultat marquant, les constantes de vitesse de transfert d'électrons mesurées dans l'Ethaline sont proches des valeurs rapportées dans un solvant organique pour le ferrocène ou dans l'eau pour le ferrocyanure. L'Ethaline apparaît plus comme un solvant moléculaire que comme un liquide ionique On pourrait relier cette similitude à d'autres observations concernant les faibles variations des coefficients de diffusion avec la charge du soluté comme celles observées précédemment dans l'Ethaline et dans la Reline Ces comportements contrastent les observations dans les liquides ioniques où les coefficients de diffusion varient avec la charge portée par le soluté en raison d'interactions spécifiques entre les molécules et les ions des liquides ioniques. Ces résultats sont conformes aux récentes études FTIR publiées concernant l'oxydation du ferrocyanure dans la Reline où il a été observé que les composants DES ne sont pas considérablement affectés pendant le processus électrochimique. Ce travail met clairement en évidence l'importance d'un traitement soigneux de la chute ohmique. Nous avons trouvé des valeurs constantes de taux de transfert d'électrons beaucoup plus grandes (parfois de plusieurs ordres de grandeur) que les valeurs récemment rapportées dans les liquides ioniques et dans le DES où la chute ohmique n'était pas prise en compte. Ces problèmes de chute ohmique dans les mesures électrochimiques ont déjà été

mis en évidence par d'autres groupes. Ici, nous avons utilisé une compensation en ligne (ou directe) avec une voltamétrie transitoire sur une électrode millimétrique en combinaison d'un ajustement à un seul paramètre d'une courbe de travail avec les données expérimentales. Pour la présente étude en DES, la méthodologie utilisée ici est particulièrement bien adaptée puisqu'elle limite l'altération de l'électrode lors de l'enregistrement des voltammogrammes, permettant une utilisation aisée de différents matériaux d'électrode et une vision qualitative immédiate de l'expérience. Lorsque l'on considère le DES pour des applications électrochimiques, un transfert rapide d'électrons est un avantage important, par exemple dans les systèmes de stockage d'énergie ou les capteurs électrochimiques où la densité de courant ou la réponse temporelle est un paramètre clé. D'après les présents résultats, les propriétés électrochimiques dans un DES comme l'Ethaline semblent plus similaires à celles observées dans un solvant moléculaire que dans un liquide ionique.

La mesure de la vitesse de transfert de charge hétérogène par voltamétrie cyclique pour les oxydations $[Fe(CN)_6]^{4-}$ et $Fc(MeOH)_2$ dans le mélange DES/eau montre que le taux de CT est légèrement augmenté par l'ajout d'eau. Comme observation la plus remarquable, le taux de CT du $[Fe(CN)_6]^{4-}/[Fe(CN)_6]^{3-}$ ne semble pas affecté par le changement de viscosité lors de l'ajout d'eau. Selon la théorie de Marcus du transfert de charge, la constante de vitesse standard, ks, d'une simple réaction d'électrode à sphère externe devrait augmenter lorsque la viscosité du solvant diminue. Cependant, les résultats apparemment contradictoires observés pour la constante de vitesse d'oxydation de $[Fe(CN)_6]^{4-}$ et une légère augmentation pour l'oxydation de $Fc(MeOH)_2$ mettent en évidence la complexité des propriétés des solutés dans un DES. Divers facteurs pourraient être considérés pour expliquer les différences avec une solution homogène. Premièrement, l'utilisation du modèle de Marcus de la sphère externe pourrait être difficile à utiliser pour certains couples car la réaction redox $[Fe(CN)_6]^{4-/3-}$ est plus complexe qu'une simple réaction de la sphère externe. Pour l'oxydation de $Fc(MeOH)_2$, comme on l'a remarqué, la valeur E_o par rapport à Ppy est décalée négativement lors de l'ajout d'eau, ce qui accentue l'impact de la structure du solvant sur la thermodynamique et donc la cinétique. Étant donné les caractéristiques inhérentes aux liaisons ioniques et hydrogène du DES considéré, les effets d'appariement d'ions et de liaison hydrogène entre les couples redox et le DES pourraient jouer un rôle sur la cinétique de l'électrode.

Une dernière question demeure sur le rôle de l'interface électrode/DES dans cette observation. Nos mesures de k_s ne sont que des constantes de vitesse apparentes (non corrigées de l'effet Frumkin) qui contiennent donc une contribution possible d'un changement de l'interface électrode/DES lorsque de l'eau est ajoutée. Cependant, le comportement observé pourrait être comparé aux rapports précédents provenant d'une méthodologie totalement différente. En effet, de petits changements similaires ont également été signalés pour la cinétique de la CT photoinduite lors de l'ajout d'eau dans l'Ethaline. Ces mesures spectroscopiques qui n'impliquent pas l'utilisation d'une électrode permettent de conclure qu'il n'y a pas d'effet particulier de l'interface sur les tendances observées. Au final, il est difficile de conclure si cet effet est général et se retrouvera pour d'autres DES mais il reflète bien la complexité du mélange d'un DES qui n'est pas un simple solvant. Néanmoins, le comportement observé est un avantage certain pour beaucoup applications en électrochimie. Le transfert de charge de la réaction de l'oxydation du $Fc(MeOH)_2$ est accélérée dans les DES. Comme conclu précédemment, la présence d'eau améliore considérablement la conductivité car elle diminue la viscosité du mélange, ce qui est un avantage pour l'électrochimie. Elle justifie l'utilisation d'un DES pour améliorer la solubilité d'un couple redox sans affecter les caractéristiques du dispositif. On remarque également que les grandeurs macroscopiques comme la viscosité, la conductivité ou les coefficients d'autodiffusion suivent les tendances attendues lors de l'ajout d'eau mais il n'est pas non plus surprenant que dans un mélange complexe présentant certaines organisations, la solvatation locale par l'eau des couples électrochimiques affecte l'électron transferts d'une manière différente que pour les grandeurs macroscopiques. Cela pourrait expliquer le désaccord apparent avec le modèle Marcus pour le transfert électronique.

Le comportement électrochimique des quinones dans l'Ethaline varie en fonction de leur nature structurelle et présente de nombreuses similitudes avec ce qui est observé dans un solvant comme l'acétonitrile, mais présente aussi des différences notables avec les solvants aprotiques organique, l'eau et les liquides ioniques. Les caractéristiques les plus impressionnantes sont les grands décalages de potentiel positifs et la comparaison de deux pics de réduction des quinones par rapport aux solvants aprotiques mentionnés ci-dessus. Ce déplacement montre une variation linéaire comme dans les solvants aprotiques, comme l'acétonitrile. La raison principale est due à l'environnement solvant spécial d'Ethaline qui, en particulier, l'effet de liaison hydrogène entre le solvant et les

quinones et ses intermédiaires sont accentués. Le coefficient de diffusion des quinones est d'environ $2 \cdot 10^{-7}$ $cm^2 \cdot s^{-1}$, soit deux ordres de grandeurs de moins que dans l'acétonitrile en raison de sa viscosité élevée. Les stœchiométries de transfert d'électrons ou les mécanismes sont correctement analysés. L'Ethaline apparaît comme une sorte de solvant protique pour les quinones à haute basicité, telles que les p-benzoquinones substituées par des groupes méthyle, la p-benzoquinone et l'une des quinones substituées attirant les électrons - la tétrafluoro-p-benzoquinone. Ce phénomène de protonation est observé dès la transformation de la p-benzoquinone en hydroquinone. L'activation d'une quinone déficiente en électrons, tel le chloranil, a été trouvée par sa réaction avec le ferrocène moléculaire standard en raison de l'environnement de liaison hydrogène. Cela pourrait fournir un nouvel outil pour utiliser la chloranil comme oxydant redox qui a une application prometteuse en synthèse organique. La cinétique de transfert d'électrons de certaines quinones réversibles a montré qu'une cinétique rapide a également été trouvée dans l'Ethaline. Nous signalons ici que nous montrons juste un exemple de DES avec l'Ethaline. Comme les propriétés physicochimiques peuvent varier considérablement entre les DES en raison de leurs composants très différents, tels que l'acidité et la basicité, le comportement redox des quinones peut changer d'un DES à l'autre. Mais l'effet de liaison hydrogène dans les DES pourrait toujours exercer des influences similaires.

Dans la dernière partie du manuscrit, les réductions électrochimiques d'une série de composés dinitrés ont été étudiées dans un DES Ethaline. Le comportement redox dépend à la fois de la structure naturelle et de l'environnement de solvatation. Un phénomène très intéressant d'inversion de potentiel a été trouvé pour le 1,4-dinitrobenzène dans l'Ethaline. Les raisons du potentiel inversé sont soigneusement examinées et la formation de la structure de résonance quinonoïde et l'environnement de solvatation spécial dans l'Ethaline, y compris l'effet de liaison hydrogène et d'appariement d'ions, en sont responsables. Ces effets combinés offrent une vision large de l'étude de l'inversion de potentiel. Le transfert d'électrons du processus d'inversion de potentiel a été couplé à un transfert de protons le transformant en les nitroso-aromatiques correspondants. L'extension de protonation dépend de l'acidité du DES et de la structure des dinitro-aromatiques. L'inversion potentielle et la protonation sont donc en concurrence. D'autres para-dinitro-aromatiques, tels que le 2,6-dinitronaphtalène et le 2,6-dinitroanthracène, sont des alternatives prometteuses car ils pourraient également former des structures de résonance. Un autre résultat intéressant est que le

potentiel de réduction des composés dinitrés dans l'Ethaline est plus faible que dans un solvant organique. Ceci est attribué à l'effet de liaison hydrogène comme nous l'avons trouvé dans la réduction des quinones dans l'Ethaline. A l'exception du 1,4-dinitrobenzène, tous les autres composés dinitrés examinés présentent un comportement irréversible. Cela est dû à leur structure électronique localisée (ortho- ou méta-dinitré) ou à faible résonance (4,4'-dinitrobiphényle et 4,4'-dinitrostilbène).

Deux mécanismes qui correspondent à un seul groupe nitro et les deux sont réduits sont trouvés. Le 1,4-ditrobenzène ne subit qu'un seul mécanisme de réduction du groupe nitro tandis que les deux autres groupes nitro sont réduits. Les principaux produits finaux des deux mécanismes sont différents. Pour le 1,4-dinitrobenzène, le principal produit pourrait être l'aniline tandis que la réduction des autres composés conduirait principalement à la phényl-hydroxylamine.

The End

UNIVERSITÉ DE RENNES 1

Titre : Transfert d'Électrons dans les Eutectiques Profonds. De la Cinétique aux Effets de Liaisons Hydrogène et de Paires d'Ions.

Mots clés : Électrochimie, Transferts d'Électron, Eutectiques Profonds, Mécanismes Réactionnels.

Résumé : Les Solvants Eutectiques Profonds (DES) sont une nouvelle classe de solvants qui présentent des propriétés très intéressantes pour les applications en Électrochimie. Dans ce contexte, les objectifs de cette thèse sont d'obtenir une meilleure connaissance des propriétés fondamentales de ces solvants pour l'électrochimie. Une première partie est consacrée à l'étude des cinétiques de transfert de charge dans l'Ethaline. Les constantes standards, k_s sont mesurées pour des couples redox courants et comparées aux cinétiques dans les liquides ioniques et les solvants organiques classiques. Les valeurs de k_s mesurées ne sont que très légèrement inférieures à celles mesurées dans un solvant classique. Ces données sont discutées en fonction du temps de relaxation du solvant et Comparée à la théorie de Marcus pour un transfert d'électron adiabatique.

L'effet de la présence d'eau est ensuite examiné. D'une manière surprenante, les valeurs de k_s pour l'oxydation du ferrocyanure ne varient pratiquement pas avec la quantité d'eau ou la viscosité du DES contrairement aux prédictions théoriques.

Les deux chapitres suivants sont consacrés à l'étude de systèmes redox où le transfert d'électron est couplé à des transferts de protons avec les exemples de la réduction des quinones et de dérivés aromatiques nitrés. Les données sont discutées en fonction de l'existence de paires d'ion et de liaisons hydrogène entre le soluté et les composants du DES permettant ainsi un contrôle des propriétés redox.

Title : Electron Transfer in Deep Eutectic Solvents: from Kinetics to the Hydrogen-bonding and Ion Pairing Effects.

Keywords : Electrochemistry, Electron Transfers, Deep Eutectics, Reaction Mechanisms.

Abstract : Deep Eutectic Solvents (DES) are a new class of solvents displaying very interesting properties for applications in Electrochemistry. In this context, the objectives of this thesis are to obtain a better knowledge and description of the fundamental properties of DES for electrochemistry. A first part of the thesis concerns the study of charge transfer kinetics in Ethaline. Standard rate constants, k_s are measured for common redox couples and compared to data in conventional ionic liquids and organic solvents. The measured values of k_s are only a little lower than those measured in conventional solvents. The data are discussed in view of the solvent relaxation times using Marcus theory for an adiabatic electron transfer. Effects of the presence of water are then examined. Surprisingly, k_s values that are measured for the ferrocyanide oxidation do not considerably vary with the amount of water or the viscosity of Ethaline contrary to theoretical predictions and behavior in common solvents.

The next two chapters are devoted to the studies of redox systems where the electron transfers are coupled to proton transfers with the examples of the reductions of quinones and aromatic nitro derivatives. Results are discussed according to the existence of ions pairs and hydrogen bonding between the solute and the components of the DES opening a route to a control of the redox properties by an appropriate choice of the DES.